Mapping aquifer stress, groundwater abstraction, recharge, and groundwater's contribution to environmental flows in British Columbia

by

Tara Forstner
B.Sc., Dalhousie University, 2013

A Thesis Submitted in Partial Fulfillment
of the Requirements for the Degree of

MASTER OF SCIENCE

in the School of Earth and Ocean Sciences

Mapping aquifer stress, groundwater abstraction, recharge, and groundwater's contribution to environmental flows in British Columbia

by

Tara Forstner
B.Sc., Dalhousie University, 2013

Supervisory Committee

Dr. Tom Gleeson (School of Earth and Ocean Sciences)
Supervisor

Dr. Jon Husson (School of Earth and Ocean Sciences)
Department Member

Dr. Yonas B. Dibike (Department of Geography)
Outside Member

Abstract

Groundwater is considered a reliable resource, relatively insensitive to seasonal or even multi-year climatic variation, however quantifying aquifer-scale estimates of stress in diverse hydrologic environments is particularly difficult due to data scarcity and the limited number of techniques in deriving stress parameters, such as use and availability, which can be applied over a large spatial area. The scope of this project is to derive aquifer-scale estimates of annual volumes for groundwater withdrawal, recharge, and groundwater's contribution to environmental flows as a means to provide screening level estimates of aquifer-scale stress using the groundwater footprint. British Columbia (BC) has mapped and classified more than 1100 aquifers, but the level of development for each aquifer has always been subjectively based on well density or the anecdotal knowledge of groundwater use.

Sectoral groundwater use is critical for local regions and aquifer-scale groundwater stress studies which are significantly impacted by changes in the groundwater use nominator. Results suggest that BC uses a total of ~562 million cubic meters of groundwater annually. The largest annual groundwater use by major sectors is agriculture (38%), finfish aquaculture (21%), industrial (16%), municipal water distribution systems (15%), and domestic private well users (11%).

Estimating recharge uses multi-scale methods to examine the recharge mechanisms and provide a more reliable recharge estimate in complex mountainous terrain. Local-scale recharge was estimated using the water table fluctuation (WTF) method outlined by Cuthbert (2014). Aquifer-scale recharge was quantified using a quasi-2D water balance model and generalized aquifer parameters of soil and aquifer material, regional climate, and water table depth. Regional scale aquifer recharge was attributed the areal average recharge flux modelled by the global hydrologic model, PCR-GLOBWB. Results show that generally recharge predictably varies with precipitation and that the average recharge is 791 mm for the local-scale method, 462 mm (32% of precipitation) for the aquifer-scale and 393 mm (33%) for the global hydrologic model.

This study estimates groundwater's contribution to environmental flows across the province for this first time using two separate approaches. The first approach uses the groundwater presumptive standard, which is a general standard for managing groundwater pumping. The second method introduces a novel approach for estimating the contribution of groundwater to environmental flows using the existing environmental flow needs framework and an understanding of low flow zone hydrology. In general, both methods show larger contributions from groundwater to environmental flows in the Lower Mainland and southern Vancouver Island compared to the Interior.

For each aquifer, the groundwater footprint (expressed as the unitless ratio of groundwater footprint to aquifer area) is calculated four times; using results from each of the two methods used to estimate recharge and each of the two methods used to estimate the groundwater contribution to environmental flows. Of the unconfined aquifers (n = 404) in the province, 43 aquifers (11%) are stressed with high certainty, 32 aquifers (8%) are stressed with low certainty, 296 aquifers (70%) are less stressed, and 29 aquifers (11%) were not included due to missing parameters or issues where modelled recharge was less than environmental flows.

Table of Contents

List of Tables

List of Figures

Author Contributions

The core of this thesis is composed of three chapters that will be submitted as peer-reviewed manuscripts. Below the preliminary author list, title and author contributions are clarified.

Forstner, T., Gleeson, T. Unseen and overlooked: methods for quantifying groundwater abstraction from different sectors in a data-scarce region, British Columbia, Canada.

> T.F. developed methodology and performed analysis and wrote manuscript. TG supervised and contributed to methodology, interpretation and presentation of results.

Forstner, T., Gleeson, T., Allen, D.M., Cuthbert, M., Borrett, L. Multi-scale, multi-method recharge estimation for diverse mountainous environments: quantifying recharge for unconfined aquifers in British Columbia.

> T.F., LB and TG developed methodology (TF leading for WTF; TG leading for HELP). TF performed analysis and wrote manuscript. TG supervised and contributed to interpretation and presentation of results. DMA and MC contributed to interpretation and presentation of results.

Gleeson, T., Forstner, T., and de Graaf, I. Quantifying a crucial yet missing flux: groundwater's contribution to environmental flows in aquifer stress analysis.

> TF and TG developed methodology with TG leading. TF performed analysis and wrote manuscript. TG supervised and contributed to interpretation and presentation of results, and will expand the introduction, implications and conclusions after the thesis is submitted.

Additionally, an earlier version of this thesis was submitted as a project report and published online as follows:

Forstner, T., Gleeson, T., Borrett, L., Allen, D.M., Wei, M., and Baye, A. 2018. Mapping aquifer stress, groundwater recharge, groundwater use, and the contribution of groundwater to environmental flows for unconfined aquifers across British Columbia. Water Science Series, WSS2018-04. Province of British Columbia.

The author contributions are outlined above except MW and AB who contributed to the general methodology development and interpretation of results during project meetings.

Acknowledgements

First and foremost, I would like to acknowledge the support and patience of my supervisor Dr. Tom Gleeson. Not only in his guidance through research, but also through encouraging self-confidence in my work and teaching me how to ask questions.

I would also like to thank Mike Wei, Christine Bieber, and Andarge Baye for their experience and their constant support throughout my thesis. Thanks as well, to my research group at University of Victoria, who put up with my "stupid questions" and provided many moments of comedic relief over the last couple years.

Finally, the completion of this thesis would not have been possible without my partner, Matt and my Canadian and kiwi families, who provided "writing havens". A special shout out to my mom, Suzanne – my pillar in all adventures, a constant whisper of "you got this".

CHAPTER 1:
Introduction

Groundwater is a critical source of freshwater supporting residential, commercial, industrial and agricultural sectors within British Columbia (BC), accounting for approximately 23% of the national volume of water used (Rivera 2003; Hess 1986). The province of BC has mapped and classified more than 1100 aquifers but the level of development for each aquifer has always been subjectively based on well density or the mapper's knowledge of groundwater use (Berardinucci and Ronneseth 2002). This thesis focuses on the spatial and statistical analysis of existing data to map aquifer stress across the province and develop an aquifer-scale decision support tool for water managers.

This research is motivated by some of these key questions:

- Given that the overlying stream already has a water allocation restriction that indicates the surface water supply is reaching its limit (e.g., fully recorded; fully recorded except for domestic; fully recorded except with storage), how much more can we allocate from the underlying aquifer, if it is connected? Where are those aquifers in the province?
- How much water is available from this specific aquifer? How firm or uncertain is that number? What are the indicators that availability limits for this specific aquifer has been reached? Which specific aquifers do we need to most work on?

Where groundwater abstraction exceeds aquifer availability for prolonged periods, the declining storage of aquifer groundwater leads to persistent groundwater depletion (Wada et al. 2010; Famiglietti 2014a). Quantifying groundwater stress promotes the sustainable management of groundwater resources and groundwater supported ecosystems (Barlow and Leake 2012; Gleeson et al. 2012; Gleeson and Richter 2017). Water stress studies provide a framework to understand the dynamics

for evaluating changes in groundwater resources by comparing water availability to human water use (van Beek L. P. H. et al. 2011; Wada et al. 2011; Richey et al. 2015; Mehran et al. 2017) and can promote sustainable practices in stressed regions through management and policy changes (Tringali et al. 2017; Bhanja et al. 2017). Groundwater quantity stress is often approached as a comparison between use and availability where availability is often represented as the mean annual groundwater recharge (van Beek L. P. H. et al. 2011; Wada et al. 2011; Richey et al. 2015).

Gleeson et al. (2012) proposed the novel approach of considering groundwater's contribution to environmental flows within the framework of defining availability. Scientific literature supports environmental flow regimes as essential to sustain freshwater and estuarine ecosystems and the human livelihood and well-being that depend on the ecosystems' (Zektser et al. 2005; Acreman et al. 2014; Harwood et al. 2014; Gleeson and Richter 2017). However, few methods have been proposed in the literature to quantify groundwater's contribution to environmental flows (Gleeson and Richter 2017).

The scope of this thesis is to derive aquifer-scale estimates of annual volumes for groundwater withdrawal, recharge, and groundwater's contribution to environmental flows as a means to provide screening level estimates of aquifer-scale stress quantified using the groundwater footprint (GF), which is often expressed as a unitless measure of GF normalized by aquifer area (GF/A). The GF is a ratio of use to availability, where availability is the difference between aquifer recharge and the aquifer's contribution to environmental flows. When the GF/A > 1, the aquifer is considered stressed, whereas, when the GF/A < 1, the aquifer is less stressed. Aquifers are not considered 'unstressed' as all mapped aquifers in BC are assumed to be under some phase of development, based on historical metrics of aquifer mapping in the province, such as well density (Kreye et al. 2001; Wei et al. 2007).

The GF is considered a critical tool providing measurements for aquifers as a tool for water analysis and policy which builds on other common hydrological methods, such as the ecological footprint or virtual water analyses (Gleeson et al. 2012). Unlike other methods such as GRACE, which explicitly measure volumetric observations

of groundwater storage depletion (Richey et al. 2015), the GF is a potential indicator aquifer stress (Gleeson and Wada 2013; Esnault et al. 2014). In addition, the GF considers aquifers as a hydrologically grounded scale of analysis which is more intuitive to water managers and the general public than depletion volumes. Typically, groundwater depletion is characterized using several water level observations, however data is often scarce leading to knowledge gaps in mapping aquifer stress analyses (Konikow and Kendy 2005).

A major part of this thesis included a synthesis of varying scales of data. Where possible, local-scale data was used; however, in many cases, due to lack of spatially distributed data, national or global-scale data was used. This brings inherent uncertainty and limitations considering the resolution of global models is approximately 100 km^2, whereas the average area of aquifers in BC is ~30 km^2. No new field data was collected, and deriving these parameters relies on data previously collected for this desktop data synthesis, analysis and modelling study. The main challenges in this study for deriving aquifer-scale estimates of stress for unconfined aquifers in BC include (i) spatial distribution of aquifers in a province of diverse hydrologic environments, and (ii) local scale data sparsity and coverage.

In addition to addressing the urgent gaps in provincial groundwater knowledge, the following research questions and deliverables motivate this thesis:

1. What is the spatial distribution of groundwater use in BC? (Chapter 2)

   Groundwater use has been previously unrecorded in BC, however, with the new provincial Water Sustainability Act (WSA), groundwater use is licensed for all but private domestic wells. As a result, the current status of groundwater use from aquifers is critical in order to mitigate over allocation of groundwater resources. This thesis develops methods for estimating sectoral groundwater use in data sparse regions in an effort to produce the first spatially distributed map of groundwater use in BC.

2. What is the spatial distribution of aquifer recharge in BC? (Chapter 3)

Estimating aquifer recharge is difficult in diverse hydrological environments due to the spatial and temporal variability of recharge processes. In addition, data sparsity across the majority of aquifers attributes to difficulties in choosing the appropriate method which captures annual fluxes of aquifer-scale recharge and the various recharge processes. Chapter 3 offers a comparison of three methods at different spatial scales for deriving recharge and results in the first spatially distributed estimates of recharge for unconfined aquifers in BC.

3. What is the contribution of groundwater to environmental flow needs (EFN) across BC? (Chapter 4)

Groundwater's contribution to environmental flows is a critical attribute in aquifer availability analysis, however few methods exists to quantify the flux. Chapter 4 develops a new method for quantifying groundwater's contribution to environmental flows based on surface water data and compares this method to the first application of the peer-reviewed groundwater presumptive standard. This chapter results in the first spatially distributed map of groundwater's contribution to environmental flows for BC.

4. What is the groundwater footprint of aquifers across BC? (Chapter 4)

Using the results from the spatial distribution of aquifer withdrawal, recharge, and groundwater's contribution to environmental flows, we then estimate aquifer stress using the groundwater footprint. Chapter 4 is the culmination of the previous three chapters and results in the first spatially distributed map of first order estimates of aquifer stress.

The 'Introduction' section of Chapters 2-4 includes a literature review so to reduce repetition, a separate literature review chapter is not included.

CHAPTER 2:
Unseen and overlooked: methods for quantifying groundwater abstraction from different sectors in a data-scarce region British Columbia, Canada

1. INTRODUCTION

Groundwater is considered a reliable resource, relatively insensitive to seasonal or even multi-year climatic variation (Manga 1999; Kundzewicz and Doell 2009; Pavelic et al. 2012; Lapworth et al. 2013), often favorable over surface water especially in rural regions, dry regions with limited surface water or during periods of drought (Bredehoeft and Young 1983; Rutulis 1989; Tsur 1990; Siebert et al. 2010). However, in some regions the risk of overexploitation is large (Llamas 1998; Changming et al. 2001; Konikow and Kendy 2005; Aeschbach-Hertig and Gleeson 2012; Scanlon et al. 2012; Famiglietti 2014b). Groundwater depletion occurs when groundwater use is greater than recharge or decreased discharge due to pumping and is indicated by substantial head declines (Konikow and Kendy 2005). Groundwater depletion is widespread in both developed and developing countries (Wada et al. 2010; Aeschbach-Hertig and Gleeson 2012; Barlow and Leake 2012; Scanlon et al. 2012; Dalin et al. 2017) and tracking and estimating the magnitude of depletion is challenging in a large part due to a sparsity of data on subsurface conditions and uncertainty in interpreting available data (Konikow and Kendy 2005). Water stress studies provide frameworks to mitigate groundwater depletion and stress (Gleeson et al. 2012; Gleeson and Wada 2013; Richey et al. 2015), however, groundwater use is a critical flux in these equations and often pumping data is unavailable.

Quantifying groundwater can be especially challenging as direct measurements require pumping data which is often unreported. Therefore, we rely on indirect methods of quantification (Ireson et al. 2006; Richey et al. 2015; Srinivasan et al. 2015). On a global scale, most methods focus on one major sector (Castaño et al. 2010; Siebert et al. 2010; Wada et al. 2014), which could be misleading on a local or regional scale. For example, studies which only identified groundwater use for irrigated agriculture sector – which accounts for a substantial portion of groundwater use on a global-scale – may misrepresent groundwater abstractions in regions significantly impacted by other sectors on a local-scale (Howard and Gelo 2002). Furthermore, while global or regional studies are useful for identifying global-scale trends, global analysis using low-resolution models are limited in drawing conclusions about individual aquifers, watersheds, or communities (Alley et al. 2018).

The objective of this chapter is quantifying groundwater use through a novel multi-method sectoral approach for regions where groundwater abstraction data is scarce. We face two key challenges. Firstly, the lack of established peer reviewed methods for sectoral groundwater use for quantification of aquifers <1 km^2. And secondly, most reported groundwater use data is at the national or provincial scale. As aquifer stress studies are very sensitive to the "use" component, groundwater use estimation at an aquifer-scale or local-scale is critical. Sectoral methods are developed for the annual volumetric quantification and spatial distribution of groundwater use for municipal water distribution systems, private domestic well users in municipal and rural regions, industrial use for manufacturing, mining, and oil and gas industries, irrigated agriculture, and finfish aquaculture. The methods presented here are ideal for aquifer-scale estimates for the use in aquifer stress and management studies. The developed methods are applied to British Columbia, a province of diverse hydrologic environments, representative of humid to semi-arid climates where groundwater use is derived locally based on demand from various sectors. For example, the Interior has a semi-arid climate supporting economically significant agriculture, whereas, in coastal regions, island aquifers sustain small urban populations. The major sectors were identified based on current reporting

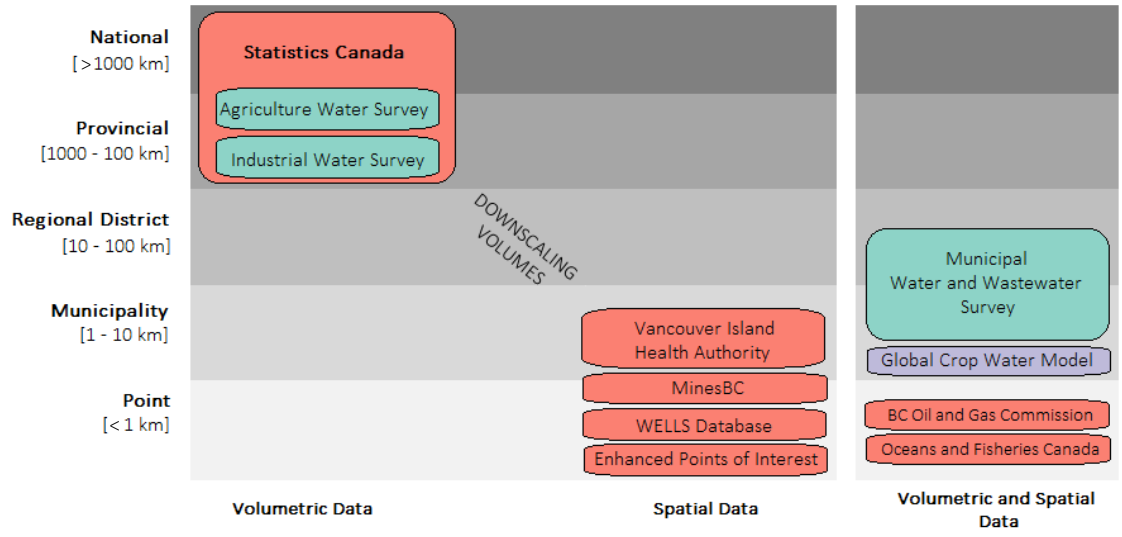

Figure 2.1. Scales of data. The majority of volumetric data is reported on the national and provincial scale. Spatial data on the scale of regional district, municipal, and point scale is used to downscale volumetric values. The color of the box indicated the type of data: model data (purple), federal survey data (green), other (pink).

categories outlined in the *Water Sustainability Act* (Province of British Columbia 2016a), provincial and federal surveys, and previous studies (Hess 1986; Rutherford 2004).

This chapter first describes the region of interest, British Columbia, and introduces the motivation, local challenges, and scope and then following sections describes the individual methods for the major sectors of use and subsequently, the results and concluding discussion. Since terminology can be confusing, it is important to clarify the technical terms used herein to discuss water availability. *Groundwater use* is a general term for the utilization of groundwater. *Groundwater abstraction* is the volume of water removed from an aquifer without considering return flows or leakage. *Groundwater consumption* is the difference between water abstraction and the quantity of water returned to the aquifer, for example, via leakage or over irrigation.

2. GROUNDWATER USE IN BRITISH COLUMBIA

Several issues arise in deriving spatially distributed groundwater consumptive data for the province of British Columbia, Canada. The primary challenge in this study is the historical lack of reporting standards and provincial groundwater regulation

under the *Water Act* (Province of British Columbia 1909) which has since been replaced by the *Water Sustainability Act* (WSA - Province of British Columbia 2016) which came into effect February 29, 2016. Most groundwater data in BC is disseminated across many sources, and the data is often reported on a range of spatial scales from municipal-scale data to single representative provincial values. If the reported scale is greater than the aquifer scale a proxy is required to spatially distribute and downscale the volumes of groundwater consumed. To be useful in quantifying groundwater use, data needs both the volume of groundwater used (volumetric data) as well as the location (spatial data). Most regional-scale data do not have refined spatial data. Very little of the data has both volumetric and spatial data at the scale of aquifers in BC (Figure 2.1).

Groundwater and surface water sources supply the population via water distribution systems, self-supplied via private wells or diverted from streams/reservoirs. Major and minor sectors were based on a previous groundwater use study by (Hess 1986), which identified main sectors as domestic, commercial, industrial, agriculture, and finfish aquaculture (Figure 2.2). Two major methods of water supply were

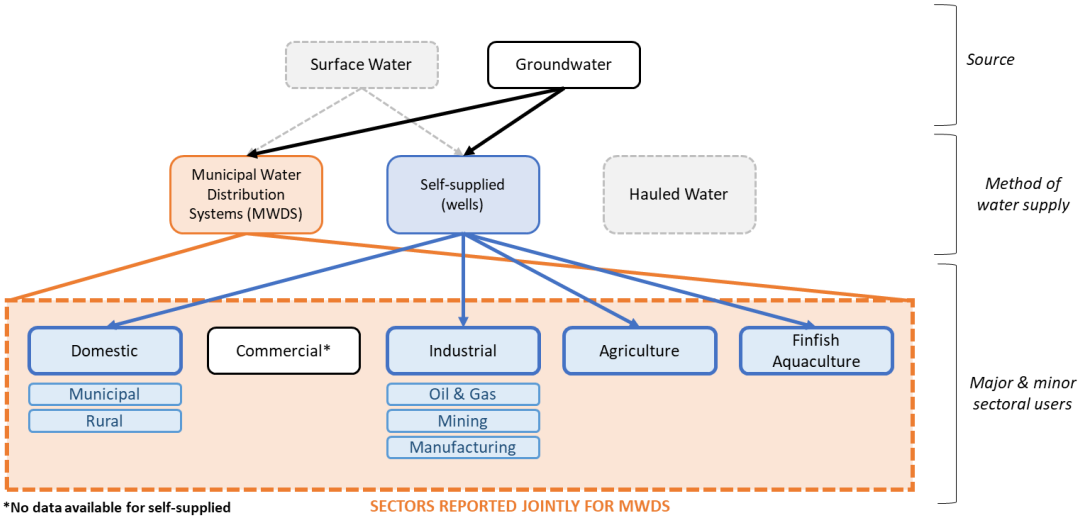

Figure 2.2 Classification scheme of source water, method of water supply, and the major and minor sectoral users in this study. The grey dashed boxes indicate sources (surface water) or water supply methods (hauled water) not considered in this study. Derived volumes for the self-supplied commercial volumes are not reported due to lack of available data.

considered in this study, municipal water distribution systems, and self-supplied by wells. Due to the classification of historically reported data, some sectors were lumped. For example, municipal water distribution systems (MWDS) supply water to a diverse network of sectors where partitioning volumes was not possible. As a result, MWDS was considered its own sector of use supplying to all major sectors. Where possible, major sectors were partitioned into minor sectors such as with the domestic and industrial groundwater use sectors. Private water purveyors (ex. improvement districts) were not included in this analysis for lack of data. Improvement districts are common in rural areas of BC, where local authorities provide specific water services at the request of landowners. They vary in size from small subdivisions to larger communities.

3. DATA AND METHODS

The following section contains the methods for each of the major sectors. Regional or global models are used to supplement regions with little to no local coverage for the agricultural sector (Figure 2.3). Before discussing the methodology for each sector we describe the three steps in attributing aquifer groundwater volumes since this is common to all sectors. Firstly, for each sector, groundwater volumes are categorically derived, for example by city or by type of manufacturing. Secondly, derived volumes are subsequently spatially distributed to wells or locations. The final step is attributing the well location to a source aquifer, which is either reported or estimated.

3.1. VOLUME ATTRIBUTION TO AQUIFERS

The following sections describe methods used to derive annual groundwater volumes which are then attributed to either reported wells from the provincial database, attributed to locations, or directly attributed to the aquifer. When a volume is associated with a well, the method of aquifer attribution is based on the following priorities:

1. If an aquifer is associated with the reported well, abstracted groundwater volumes are attributed to this aquifer.

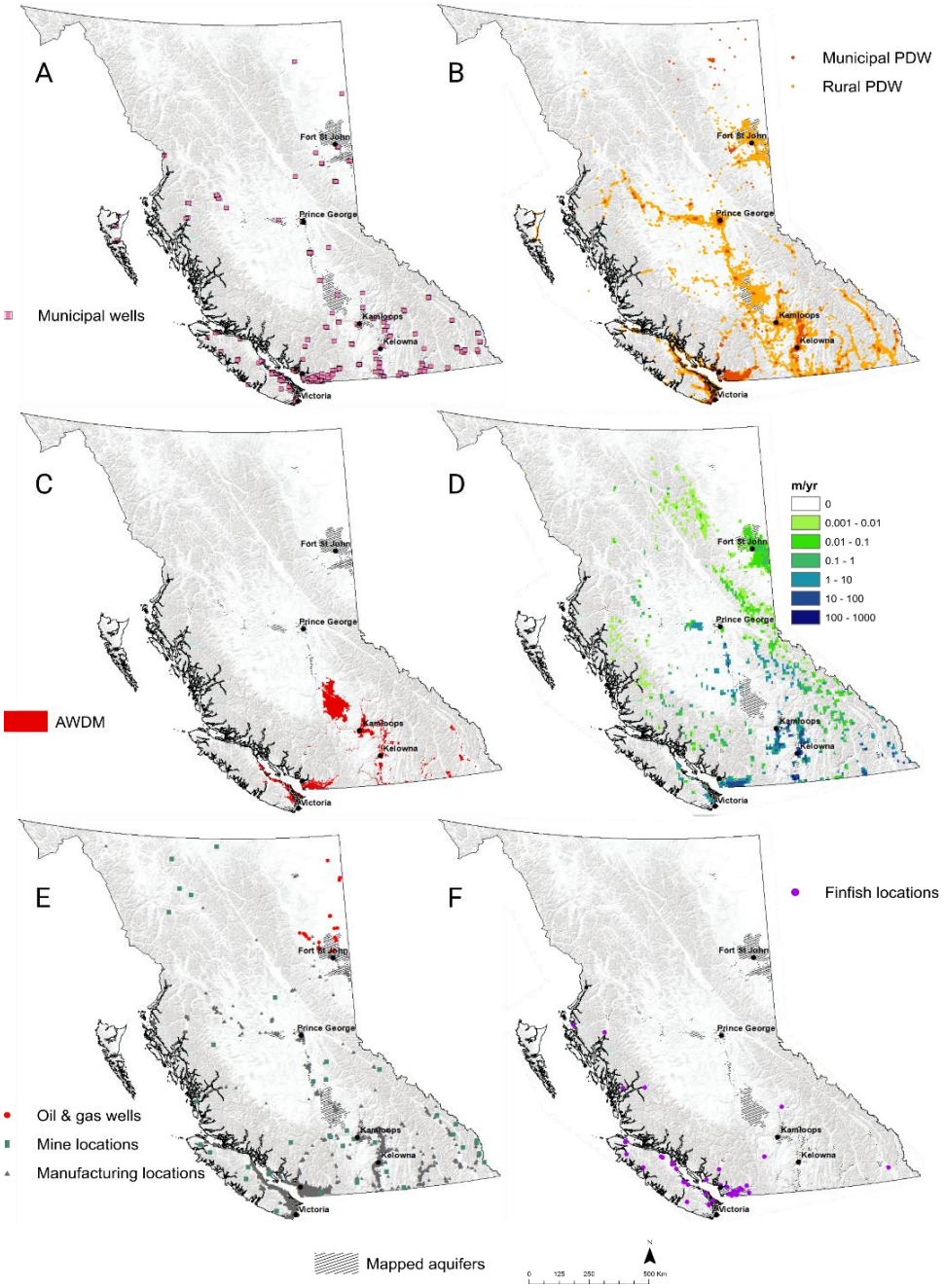

Figure 2.3. Distribution of spatial data available for each major sector. A) Derived municipal wells for the purpose of water distribution systems; B) private domestic wells (PDW) within municipalities (red) and in rural areas (orange); C) aquifers with reported groundwater abstraction volumes reported by the Agricultural Water Demand Model (AGWM) associated with irrigated agriculture (red); D) coverage of the Global Crop Water Model (GCWM) for total irrigated volume required in mm yr^{-1}; E) industrial diversion locations for oil and gas wells (red), manufacturing (grey) and mining locations (green); F) locations of finfish hatcheries (purple).

2. If the well only overlies one mapped aquifer, abstracted groundwater volume is attributed to this aquifer by default.
3. If the well overlies overlapping aquifers and no aquifer number is reported with well, reported lithology is used to correlate the well to the abstracted aquifer. For example, if a well was overlying two unconsolidated aquifers and one bedrock aquifer but the well reported an aquifer material of "Sand and Gravel", derived groundwater volumes were attributed equally to both unconsolidated aquifers.

When a volume is associated with a location, such as with a business location or rasterized data from a model output, the volume is equally attributed to each overlapping aquifer underlying the location. Realistically, most abstraction is focused in shallow aquifers, however the current state of the provincial database precludes improving this methodology. If volumes are assumed to be abstracted from mapped aquifers, our methodology recognizes that volume attribution to overlapping aquifers is more uncertain than non-overlapping aquifers (Figure 2.4).

3.2. MUNICIPAL WATER DISTRIBUTION SYSTEMS

The municipal water distribution system (MWDS) sector includes all users connected to a water distribution system operated by a municipality that supplies water to all major sectors within the proximity of the distribution network. MWDSs distribute freshwater from either surface water sources (such as reservoirs or streams), or from groundwater sources (abstracted from municipal wells). MWDSs are a key component in calculating groundwater abstraction as they often supply large volumes of groundwater to meet the municipal population demand. These demands are often met from a limited number of high yield wells concentrating large volumes of withdrawal to few aquifers, as opposed to distributing the sector's volumetric burden to many aquifers.

The following steps were used to determine annual volumes of groundwater abstracted for the MWDS sector:

1. determine population served water from a MWDS;

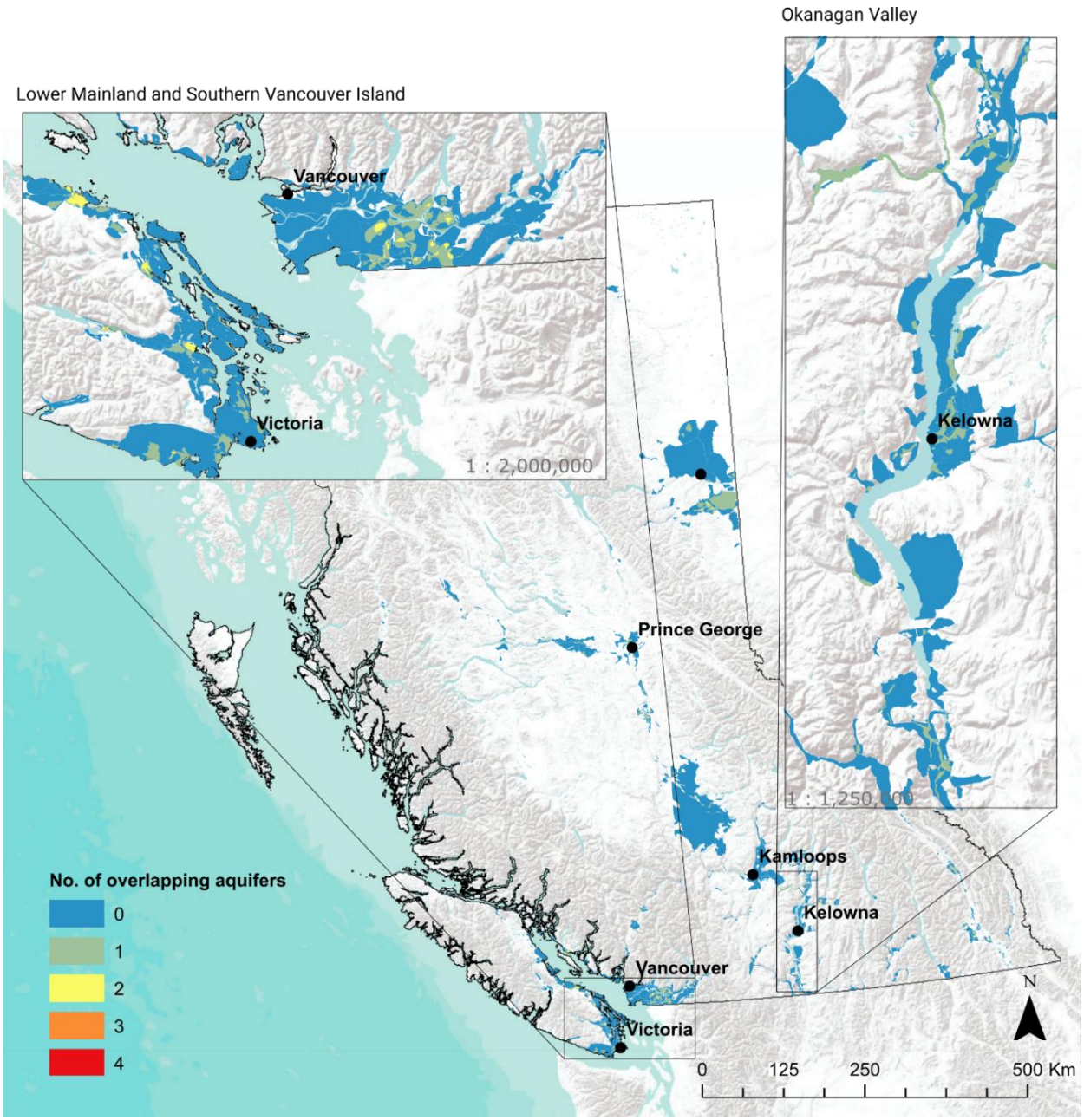

Figure 2.4. Status of provincially mapped aquifers (as of January 2018). Aquifer mapping has been prioritized in populated regions as map areas in the province are scarcely populated and consists of mountainous terrain. Non-overlapping mapped aquifers are illustrated in blue, with the two most populated regions enlarged.

2. derive total groundwater volume supplying MWDSs; and
3. determine the location of the groundwater withdrawal through attribution of municipal groundwater volumes to municipal wells.

The Municipal Water and Wastewater Survey (Environment Canada 2011) provides the most recent municipal scale sample data for 134 municipalities and 28 regional districts in BC. The survey reports on annual water use statistics based on data collected in 2009 and includes reported volumes total annual groundwater used per municipality and regional district. However, often this information was not reported, and therefore, other municipal, regional, or provincial scale data was used to infer total annual groundwater abstracted per municipality. As BC has a total of 162 municipalities, if a municipality was not included in the MWWS, data was used from the representative regional district.

Where annual groundwater volume was unreported, groundwater was either derived from; a) total annual volume and percent population using groundwater sourced MWDS; or b) total annual volume and surface water licences.

If total volume of groundwater sourced, V_{GW}, was not reported for a municipality, it was derived by:

$$V_{GW} = P_{GW} \cdot V_T \quad \text{(Eq 1)}$$

where:

V_{GW} is total volume of groundwater serviced through a MWDS ($m^3\ yr^{-1}$)
P_{GW} is percent of population serviced MWDS from groundwater (%)
V_T is total volume used by a MWDS ($m^3\ yr^{-1}$)

If V_T was unreported, it was derived using municipal population statistics and per capita provincial-scale statistics of annual water use of 180 $m^3\ yr^{-1}$ (Honey-Roses et al. 2016):

$$V_T = (P_{MWDS} \cdot p_{MUN}) \cdot V_{BC} \quad \text{(Eq 2)}$$

where:

V_T is total volume used by a MWDS (m^3 yr^{-1})
P_{MWDS} is percent population serviced MWDS (%)
p_{MUN} is municipal population (-)
V_{BC} is the per capita total volume of all water use (m^3 yr^{-1} pp^{-1})

If the percent of the population services MWDS was unreported, the municipality assumes P_{MWDS} is equal to 100%.

If P_{GW} was unreported, surface water licenses are used to constrain V_{GW}. The surface water license data is open-access and data was collected on existing municipal water licenses (as of July 18, 2017). The "Purpose of Use" variable was selected as "Waterworks: Local Provider" and the municipality was searched under the variable "Client Name". The "Quantity" variable indicates the maximum allowable annual stream diversion volume in m^3 yr^{-1}. Surface water licenses managed by the municipality were totalled for the annual volume of surface water (V_{SW}). Surface water licences were reported as allowable annual allocations. No data exists on the actual annual volume of water diverted from a stream, therefore, groundwater volumes derived with this method have higher uncertainty, and are possibly underestimated. V_{GW} abstracted for a municipality was taken as:

$$V_{GW} = V_T - V_{SW} \quad \text{(Eq 3)}$$

where:

V_{GW} is the annual volume of groundwater used by a MWDS (m^3 yr^{-1})
V_T is total volume used by a MWDS (m^3 yr^{-1})
V_{SW} is the volume of surface water license allocations (m^3 yr^{-1})

V_{GW} was then spatially distributed to wells based on a well query to identify municipal wells. The WELLS Database is a publicly accessible catalogue of all recorded water wells in the province managed by the Ministry of Environment and Climate Change of BC. The WELLS Database was queried based on the municipality name and the prefix (such as "City", "Village", "Municipality", or "District") within the "Surname" variable. Based on the "General Remarks" and "Well Use", wells were

Table 2.1. Sample data from the MWWS 2009 for the 10 most populated municipalities in BC.

		Method of water supply				Annual volume	
Municipality	Population	MWDS	PDW	Hauled water	Sourced ground-water	Surface water & groundwater	Groundwater
		(% of total population)				(m^3)	
Vancouver	610,389	100	-	-	-	118,070,806	-
Surrey	453,252	98	2	-	-	72,000,000	NA
Burnaby	223,063	NA	NA	NA	NA	NA	NA
Richmond	192,582	100	-	-	-	38,129,000	-
Abbotsford	134,988	82	18	-	7	20,904,000	1,463,280
Coquitlam	125,049	99	-	-	-	18,696,449	-
Kelowna	119,588	99	-	-	-	16,515,129	-
Saanich	112,332	NA	NA	NA	-	NA	NA
District of Langley	103,813	NA	NA	NA	NA	NA	NA
Delta	100,867	100	-	-	5	27,000,000	1,350,000

NA = data not reported

removed if “Dry”, “Test”, “Abandoned”, or “backfilled”. If the well query returned no results, a manual investigation was done to distribute the spatial location of groundwater use; Private Domestic Wells

Domestic users include all users self-supplying water for domestic household use (such as household water needs, lawn and garden watering). Private domestic wells are expected to abstract similar magnitude per capita of groundwater to MWDS, however, the spatial distribution on a regional or municipal scale buffers the abstracted volume over several aquifers.

The methodology for deriving the distribution of annual groundwater volume withdrawn was based on the following steps:

1. determine populations serviced by groundwater from private wells;
2. derive total groundwater volume; and
3. calculate volume per well based on well density in each municipality and regional district, respectively.

As the MWWS reports on water use statistics for municipalities and regional districts, which encompasse the rural populations living outside municipality boundaries. Populations using private wells, p_{PDW}, are divided into rural and urban regions based on their location. If the well was located within a municipal boundary, the derived groundwater volume was based on municipal statistics. Otherwise, the derived groundwater volume was based on the representative regional district data, which encompasses the remaining provincial area. Municipal and regional district boundary shapefiles are obtained from DataBC.

p_{PDW} for each municipality or regional district was derived using the percent population on wells (P_{PDW}) and the total population for a municipality or regional district (p_T):

$$p_{PDW} = p_T \cdot P_{PDW} \quad \text{(Eq 4)}$$

where:

- p_{PDW} is the population supplied residential water from a private domestic well (-)
- p_T is total population of a municipality or regional district region (not including municipal populations) (-)
- P_{PDW} is the percent of population supplied water via a private domestic well (%)

If P_{PDW} was unreported, municipal populations were assumed to be fully supported by the MWDS ($P_{PDW} = 0\%$). Conversely, rural populations were assumed to be supported by private domestic wells ($P_{PDW} = 100\%$).

Since the MWWS does not report on annual groundwater volumes for populations using wells, per capita annual residential water use, V_{BC}, was inferred from the provincial average, 130 m^3 $person^{-1}$ yr^{-1} (Honey-Roses et al. 2016). Based on V_{BC} and the p_{PDW}, the total annual groundwater volume for the private domestic sector (V_{PDW}) can be derived:

$$V_{PDW} = V_{BC} \cdot p_{PDW} \quad \text{(Eq 5)}$$

where:

V_{PDW}	is total annual groundwater volume for the private domestic sector ($m^3\ yr^{-1}$)
V_{BC}	is the per capita total volume of all water use (130 $m^3\ yr^{-1}\ pp^{-1}$)
p_{PDW}	is the population supplied residential water from a private domestic well (-)

V_{PDW} is equally spatially distributed to all "Private Domestic" wells within the representative municipality or regional district (Figure 2.3b).

3.3. INDUSTRIAL USE

The industrial sector represents self-supplied annual groundwater volumes for manufacturing, mining, and oil and gas production. Industrial use of water can be intensive and concentrated regionally. Industries are diverse, and so efforts were concentrated on estimating major industrial use within BC, namely, manufacturing, mining, and oil and gas.

Annual groundwater volumes and well extraction locations for oil and gas operations were reported by the BCOGC for 2013-2015 (BC Oil & Gas Commission 2013, 2014, 2015) and averaged to represent groundwater use for the oil and gas sector (Table S1). Deep wells (>250 m depth) were not included as they were less likely to be drawing from any mapped freshwater aquifers.

All the volumetric data for manufacturing and mining were reported from surveys at the provincial or national scale. The following general steps were taken to distribute total annual groundwater volume:

1. groundwater volumes were derived based on water intensity, production ratios, and provincial statistics;
1. determine manufacturing and mining locations; and
2. aquifer attribution inferred based on point location of each industry.

Statistics Canada reports total annual water volumes on a national scale for each manufacturing type based on a unique North American Industrial Classification System (NAICS) code.

The total annual groundwater volumes for BC were derived for manufacturing and mining industries from averages based on 2005-2011 Industrial Water Survey (Statistics Canada No Date). Mining water use does not include water extracted for mine dewatering, but rather focuses on the water used in ore production. Annual groundwater abstraction was reported per manufacturing type on a provincial-scale for all of Canada, and provincial annual groundwater volumes for total manufacturing industries in BC.

Some sub-sector manufacturing types are highlighted as being larger consumers of water, such as wood and paper manufacturing (Renzetti 1992). Several economic studies have been conducted on estimation techniques for industrial water demand (Mercer and Morgan 1974; Reynaud 2003; Worthington 2010); however, many require spatially distributed data unavailable for the province, such methods based on detailed economic demand and labour statistics. Therefore, a simpler analysis was conducted herein as a first order estimate.

For the sub-sectors of wood and paper manufacturing and mining (coal, metal, and non-metal sub-sectors), production volumes were used as a proxy to distribute national values to location points in BC based on a method by Vassolo and Döll (2005). The following equation was used to calculate total volume, V_T (m^3/yr), for each sub-sector based on total annual production, PV_i (tonne yr^{-1}), and water intensity, WI_i (m^3 $tonne^{-1}$) per sub-sector:

$$V_{BC} = PV_i \cdot WI_i \quad \text{(Eq 6)}$$

where:

V_{BC} is total annual volume required per sub-sector in BC (m^3 yr^{-1})

PV_i is the total annual production (tonne yr^{-1})

WI_i is the water intensity per sub-sector (m^3 $tonne^{-1}$)

WI_i values were calculated based on average production. Wood product manufacturing and paper manufacturing values are averaged over 2008 – 2012 (Table S2.1). The mining sub-sectors were averaged based on biannual reports over 2005 – 2013 (Table S2.2). This method assumes that national water intensity values can be applied to BC.

Where production volumes were not readily available, the water intensity was calculated per business location as opposed to per tonne of production. This water intensity per business was calculated based on the statistically significant correlation between the number of businesses in Canada compared to BC; therefore, inferred volumes of water used follow this trend (Figure S2.1). The number of industrial businesses in Canada (n_{CAN}) and BC (n_{BC}) were derived from EPOI, and the total annual water volumes (V_{CAN}) were reported by Statistics Canada to derive the total volume of annual water use per sub-sector for industries in BC, V_T:

$$V_{BC} = \frac{V_{CAN}}{n_{CAN}} \cdot n_{BC} \quad \text{(Eq 7)}$$

where:

V_{BC} is the total annual water use per sub-sector in BC ($m^3\,yr^{-1}$)
V_{CAN} is the total annual production ($m^3\,yr^{-1}$)
n_{CAN} is the number of businesses per sub-sector (-)

The proportion of V_{BC} sourced from groundwater was determined based on national surveys from Statistics Canada. The ratio per sub-sector of average annual self-supplied groundwater, f_{GW}, is determined per sub-sector and assumes all industrial businesses are represented by this ratio (Table 2.2). Total self supplied groundwater per sub-sector, V_{GW}, was derived by:

$$V_{GW} = f_{GW} \cdot V_{BC} \quad \text{(Eq 8)}$$

where:

V_{GW} is the total annual groundwater use per sub-sector in BC ($m^3\,yr^{-1}$)
f_{GW} is the self-supplied groundwater coefficient per sub-sector (-)
V_{BC} is the total annual water use per sub-sector in BC ($m^3\,yr^{-1}$)

Table 2.2. Groundwater coefficient applied to sub-sector volumes for manufacturing and mining industries.

Industrial Sub-Sector	Yearly range of bi-annual averages	Average self-supplied groundwater coefficient $f_{GW} = V_{GW} / V_T$
Manufacturing	2005-2013*	0.096
Mining	2005-2013**	0.354

**exclusive of 2009*

***exclusive of 2005, 2007, 2011*

Derived annual groundwater volumes for manufacturing and mining (Table S2.3 and S2.4), respectively, are equally allocated to locations based on the NAICS code (Figure 2.3e) and the spatial distribution of locations from EPOI (DMTI Spatial Inc. 2015) and operating mines as of 2015 compiled based on the British Columbia Geological Survey open file (Arnold 2016). The verification of location accuracy was out of scope for this project, therefore, location uncertainty is inherently associated with the dataset. Mining industry locations were obtained from "Selected exploration projects and operating mines in BC" by the British Columbia Geological Survey (accessed November 2016).

3.4. IRRIGATED AGRICULTURE

Agricultural water use includes all self-supplied groundwater for crop irrigation. Groundwater for irrigation obtained from all off-farm sources (tap water, treated wastewater, provincial sources, private sources, and other) was not included due to lack of readily available data. Volumes of groundwater sourced from municipal water, and treated wastewater for agricultural irrigation were reported in the MWDS sector.

For this sector, two agriculture water use models were used to derive annual groundwater volumes associated with irrigated agriculture. The first was a local-scale Agricultural Water Demand Model (AWDM) which was originally developed by the BC Ministry of Agriculture to predict water requirements for lands reserved for agriculture in the Okanagan, BC. The model provides current and future estimates of water demand by calculating and field verifying water use on a property

by property basis. Groundwater was assigned when no surface water licences exist on the property and when there were no obvious surface water sources. Crop irrigation system type, soil type and climate data were used to calculate water demand. Groundwater volumes are derived from crop irrigation for the following crop groups: alfalfa, apple, berry, cherry, domestic outdoor, forage, fruit, and golf. The model has been extended to include several regions in BC, however, many areas remain uncovered by the AWDM. The Global Crop Water Model (GCWM) was used to supplement the AWDM and was developed to simulate consumptive crop water use and crop yields in rain-fed and irrigated agriculture (Siebert and Döll 2008). This dataset was based on the global land use data set MIRCA2000 (Portmann et al. 2010) which provides monthly growing patterns for 26 crop classes under rain-fed and irrigated conditions for the period of 1998-2002. The model has a spatial resolution of roughly 10 x 10 km^2 (5 arc minute).

Firstly, the GCWM was used to determine the annual flux of water required per crop ($V_{irr,c}$). The data was in the form of a raster (cell i) which was summed to obtain the total volume of irrigation (V_{irr}) per cell:

$$V_{irr} = \sum V_{irr,\ c} \qquad \text{(Eq 9)}$$

where:

V_{irr} is the total annual flux of water required for all 26 crops (m yr^{-1})

$V_{irr,\ c}$ is the total annual flux of water required for a specific crop (m yr^{-1})

In order to determine the total annual groundwater volume from the V_{irr}, a groundwater coefficient, f_{GW}, was applied based on the method from Esnault et al. (2014). Percent irrigation water from self-supplied on-farm groundwater was reported in the Agricultural Water Survey (Statistics Canada No Date) and was used as the groundwater coefficient. The annual groundwater volume was derived based on the average area weighted value of V_{irr} and the aquifer area. To calculate the groundwater volume per aquifer:

$$V_{GW} = (\overline{V_{irr}} \cdot A_A) \cdot f_{GW} \qquad \text{(Eq 10)}$$

where:

V_{GW} is the volume of irrigated groundwater required per aquifer (m^3 yr^{-1})

$\overline{V_{irr}}$ is the weighted average annual flux of water required for all 26 crops (m yr^{-1})

A_A is the aquifer area (m^2)

f_{GW} is the percent irrigation water from self-supplied on-farm groundwater (%)

Attribution to aquifers was applied based on priority of data availability. On an aquifer by aquifer basis, the AWDM was prioritized over the GCWM dataset as it is a local scale dataset, however, it does not have complete coverage in BC. Therefore, where the AWDM has no reported groundwater volume, the GCWM derived V_{GW} was used (Figure 2.3c and d).

3.5. FINFISH AQUACULTURE

Finfish aquaculture use represents self-supplied groundwater volumes for the purpose of conservation and industrial finfish freshwater hatcheries. The methodology for deriving the annual groundwater withdrawal volume is based on the following steps:

1. locate hatcheries;
2. derive annual groundwater volume from the DFO (MacKinlay and Howard 2004); and
3. groundwater volume attributions to wells.

As the data is derived from several different sources (Figure 2.3f), duplicate values were removed based on availability of data and reliability of source. Freshwater Finfish Hatcheries (FFH) was the primary data source since it contains the largest number of locations and was available from DataBC, a reliable provincial database. Salmon Hatcheries (SH) dataset supplies information on type of hatchery; therefore, net cage locations were removed from the analysis as they are often used in the latter stages of salmon development and are kept in the ocean.

Table 2.3. Summary of data sources for finfish aquaculture in BC.

	Freshwater finfish hatcheries (FFH)	Salmon hatcheries (SH)	NAICS finfish aquaculture (NFA)	Salmonid Enhancement facilities (SAF)
Data Source	DataBC	DataBC	EPOI 2016	DFO
Number of locations	63	35	62	16
Water source reported	no	no	no	yes
Groundwater flow rate reported	no	no	no	yes

The EPOI reports on locations categorized as Aquaculture (NAICS code:112511 Finfish Farming and Fish Hatcheries). Since the culture type was unidentified, every location was assumed to be a freshwater facility. The Salmonid Enhancement Facilities (MacKinlay and Howard 2004) is a draft document prepared by the DFO Canada and highlights the location of all provincial hatcheries, information on water sources, and seasonal flow rates. If the SF, NFA, or the SAF hatchery locations were within 100 m of the FFH, they were assumed to be a duplicate.

Groundwater volumes are often used seasonally due to the reliable supply of water and constant cooler temperature (MacIsaac 2010). Annual groundwater volumes are unreported for all data sources; therefore, inferences are made based on available daily flow data provided by the DFO in the "Fish Health Plan for All Major Salmonid Enhancement Facilities" for many of the salmonid enhancement hatcheries (MacKinlay and Howard 2004). Reported groundwater daily flow rates were extrapolated over four months of seasonally active groundwater abstraction. Groundwater use was assumed if the hatchery was within 100m of a well categorized as "Industrial and Commercial" based on attributed from the WELLS Database. Where a facility was assumed to be using seasonal groundwater, an average value of abstraction was derived from the reported daily flows from the DFO, which was 8.93 x 10^6 m^3 yr^{-1} (10 ft^3 s^{-1} extrapolated over four months). Groundwater volumes were equally attributed to wells within 100m proximity of the facility and tagged as "Industrial & Commercial" wells (Figure 2.3f).

4. RESULTS

The combined annual groundwater abstraction from all major sectors was 562 Mm^3, of which 80% can be attributed to mapped aquifers and 20% of all abstractions were from unmapped aquifers. Of the mapped aquifers in BC, 1031 aquifers (n=1130) are being sourced for some quantity of groundwater. Self-supplied irrigated agriculture accounts for the highest proportion of annual groundwater withdrawal accounting for 37% of the total volume. Finfish aquaculture, industrial, municipal water distribution systems and private domestic wells account for 21%, 16%, 15%, and 11% respectively. Table 2.4 illustrates the volumetric comparison between the results from this study compared to the last reported estimation of groundwater abstraction volumes completed by Hess (1986). Total groundwater use has increased by 81% from 1981 to 2009, which is in trend with Statistics Canada population census of a 60% provincial population increase during this period.

Figure 2.6 illustrates the magnitude and spatial distribution of groundwater use per sector. Private domestic wells impact the largest number of mapped aquifers, abstracting from 79% of aquifers, however most annual areal abstraction fluxes are < 0.1 m per year. Conversely, municipal water distribution systems and finfish aquaculture impact a limited number of individual aquifers, however the magnitude of groundwater abstraction fluxes were ≥ 1 m per year for some aquifers (Table 2.4). Average annual groundwater abstraction fluxes (m) are 0.03, 0.02, 0.009, 0.005, and 0.003 for municipal water distribution systems, finfish agriculture, irrigated agriculture, private domestic wells, and industrial use respectively.

Most aquifers (n = 734) have abstraction from two or more major sectors. Aquifers dominated by one sector (defined as >50% of annual groundwater abstraction) are most prevalent for private domestic wells dominating 328 mapped aquifers, with the remaining sectors dominating ≤ 50 aquifers. This may be an artifact of aquifer mapping bias, where mapping was historically prioritized in regions of high groundwater well density (Berardinucci and Ronneseth 2002). However, it does highlight that the majority of aquifers are being abstracted by more than one sector, and therefore, estimates of irrigated agriculture alone would underestimate the annual groundwater flux.

Attribution of annual groundwater volumes to the aquifer were made via spatial relationships of point location or well location. Although, the well location at the land surface was relatively well known, the lack of aquifer data attributed to the locations provides uncertainty in accuracy of aquifer abstracted. For example, of the 91 municipalities identified as groundwater users, 60 municipalities overlie only one aquifer, 22 municipalities overlie two or more aquifers, and 9 municipalities do not overlie mapped aquifers. Where wells or locations do not overlie mapped aquifers, groundwater volumes were unattributed. With 22 municipalities overlying two or more aquifers, the volume attribution was divided equally among all underlying aquifers. Therefore, the groundwater volume is in the approximate location but the exact aquifer abstracted is uncertain. In the future, this problem will be minimized as licensable wells will be correlated to aquifers through the groundwater licencing process.

Unattributed volumes are concentrated in low population regions where aquifer mapping has not been prioritized. Finfish aquaculture has 32% of derived volume unattributed to aquifers, while industrial, private domestic wells, irrigated agriculture, and municipal water distribution systems have unattributed volumes of 31%, 26%, 10%, and 10% respectively. Finfish aquaculture has a large portion of derived groundwater volume unattributed due to high annual fluxes from few locations. In addition, finfish hatcheries, mining, oil and gas operations, rural private domestic wells, and some agriculture tend to be in non-populous regions resulting in their high unattributed groundwater volume percentage. In the case of municipal water distribution systems, five municipalities had reported groundwater use, however, no water supply wells were returned in the well query.

Aquifers in BC are currently classified based on development and vulnerability (Berardinucci and Ronneseth 2002). Development is ideally classified based on detailed water balance, however data is often not available, and classification is subjectively based on well density, known water use, aquifer productivity, and sources of recharge. Larger ratios of groundwater volume per aquifer area would be expected to classify as (I) *High* describing an aquifer with a high level of development; (II) *Moderate* for moderate groundwater use, and (III) *Low* for lower

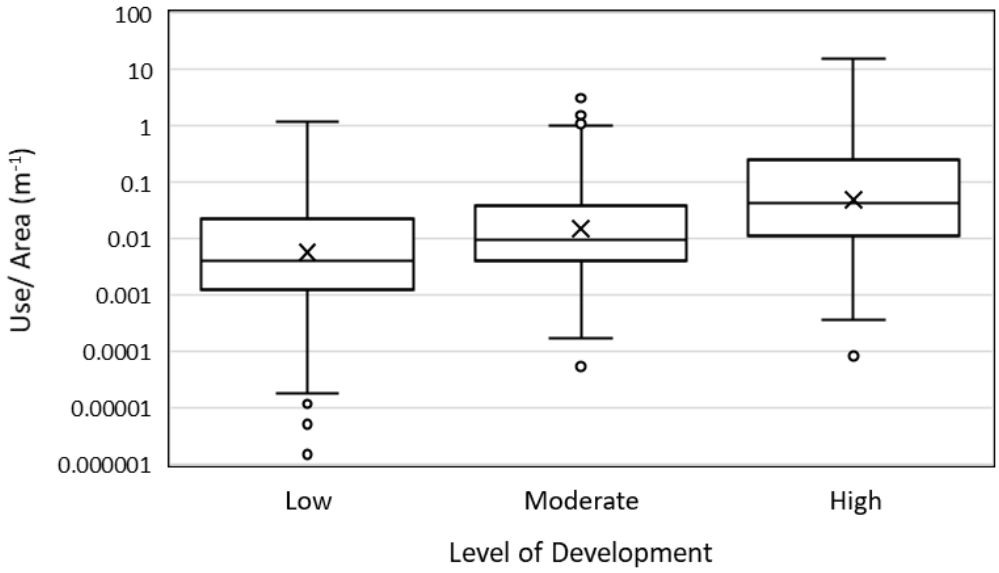

Figure 2.5. Resultant groundwater flux per aquifer compared to provincial classification.

development aquifers. When our results were compared to the provincial classification, we see high development aquifers plotting with larger ratios of groundwater use per unit (Figure 2.5). Although, our groundwater use estimates are also based on well data, we derived our estimates based on several different sources of data and sectoral distribution.

5. DISCUSSION

Multi-method approach to deriving groundwater use is critical to capture the regionally significant sectors of use. Many studies often only consider agricultural, industrial, and domestic groundwater use – which accounts for a substantial portion of groundwater use on a global-scale – however, may misrepresent groundwater abstractions in regions significantly impacted by other sectors on a local-scale (Howard and Gelo 2002; Wada et al. 2010; Gleeson et al. 2012; Richey et al. 2015). Figure 2.6 and Figure 2.7 highlights the variability in magnitude of sectoral groundwater use across the province and highlights the importance of spatially distributed sectoral estimates. In the coastal area of the province most groundwater use is attributed to finfish aquaculture, which is a regionally specific sector is importance. In addition, agriculture is only a significant user of groundwater in the southern and central regions.

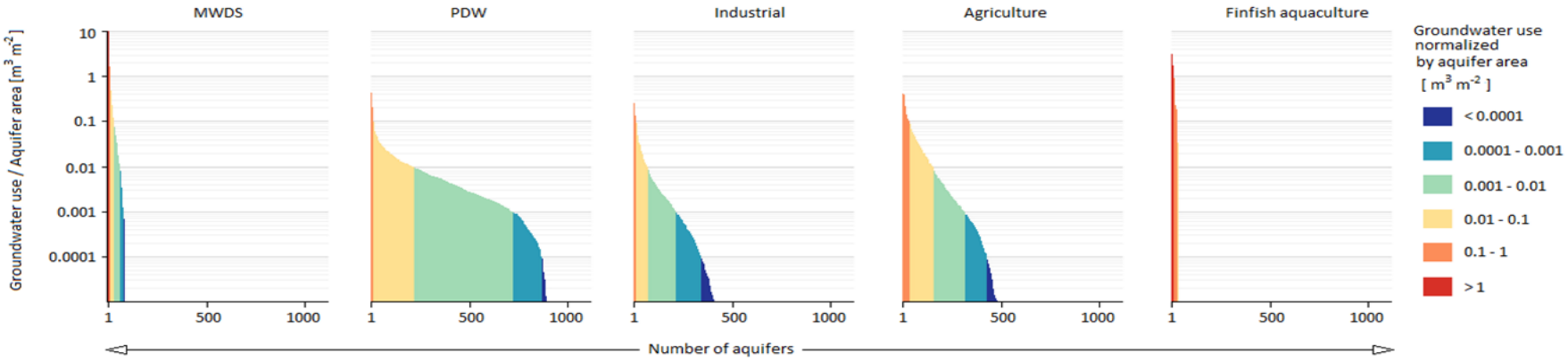

Figure 2.6. Groundwater use by sector normalized by aquifer area. plotted per major sector illustrating the magnitude of use from individual aquifers and the distribution of use across the number of aquifers.

Table 2.4. Resultant annual groundwater volume results compared to Hess (1986).

Sector (sub-sector)	Annual Groundwater Volume (Mm^3) This Study, 2017 Sector	This Study, 2017 Sub-Sector	Hess, 1986 Sector	Hess, 1986 Sub-Sector
Municipal Water Distribution Systems	83.7		60.5*	
Self-supplied:				
Domestic	61.8		21.4*	
Municipalities		16.6		
Regional Districts		45.2		
Industrial	89.3		44.1	
Manufacturing		80.5		27.3
Mining		8.3		16.9
Oil and gas		0.56		
Irrigated agriculture	211		59.1	
Finfish aquaculture	116		126	
Total	562		311	

** Hess (1986) reported groundwater volumes for municipalities and rural users, MWDS was equated to Hess's municipalities; and self-supplied domestic and commercial users were equated to Hess's rural users.*

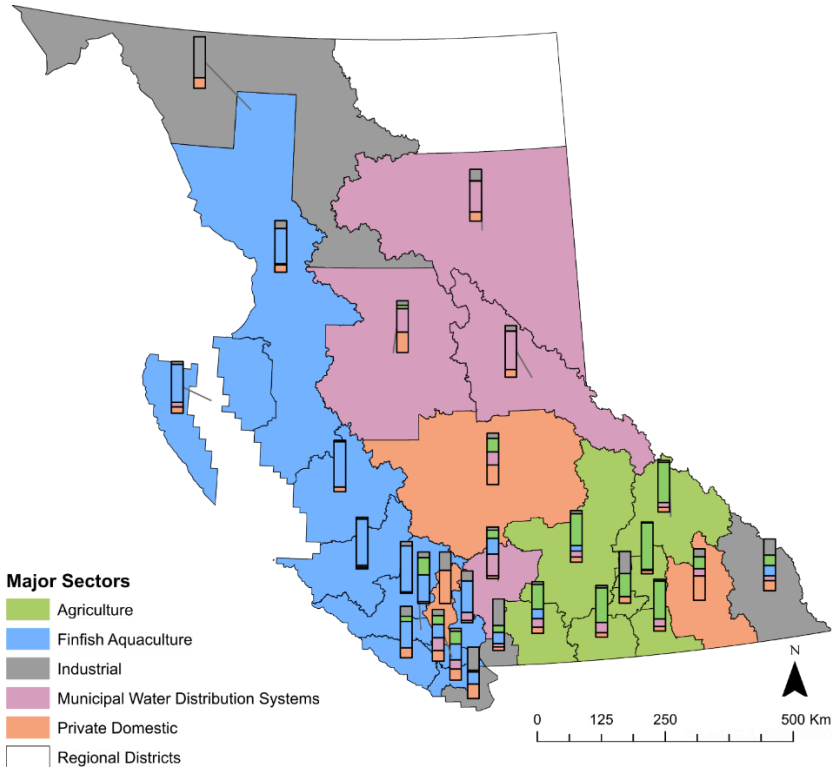

Figure 2.7. Derived dominant sectors per regional district. Stacked bar are representative of each regional district and represent the sectoral ratio of annual groundwater use.

By lumping municipal water distribution systems and private domestic use from wells into a single domestic sector can lead to poor management strategies as private domestic wells often have a low abstraction rates per aquifer compare to municipal water distributions which often lead to high abstraction rates.

As water withdrawal rates are often reported on national or provincial scale, methods of disaggregating often require secondary proxies (Alcamo et al. 1997; Vorosmarty et al. 2000; Wada et al. 2010). Methods for estimating water use often rely on per capita statistics (Alcamo et al. 1997; Vorosmarty et al. 2000; Richey et al. 2015), however due to the disproportional use of groundwater in the population, this assumption could lead to misrepresentative values of groundwater use. For example, Richey et al. (2015) estimates groundwater use from national groundwater withdrawal statistics for domestic and industrial water use using methods based on Vorosmarty et al. (2000). Vorosmarty et al. (2000) estimate total water use for

domestic and industrial groundwater use based on national per capita statistics, and spatial disaggregation of industrial use in proportion to urban populations. By disaggregating groundwater rates based on population, the inherent assumption is that groundwater use is proportional to population (essentially a per capita statistic). However, Figure 2.7 illustrates the percent difference in using the provincial per capita value (total sectoral groundwater use divided by the total population) and the regional district per capita (regional district sectoral groundwater use divided by regional district population). In addition, due to scarcity of data, global groundwater use data is often used in groundwater stress studies (Wada et al. 2010; Gleeson et al. 2012). Using downscaled values of groundwater use from global datasets can be misleading in regions where groundwater use is unregulated/newly regulated, as is the case in BC. Wada et al (2010) estimated groundwater abstraction based on country statistics of abstraction rates, however, this method reported zero groundwater consumption for BC, which our results show is misrepresentative of local scale values.

5.1. LIMITATIONS & METHOD UNCERTAINTY BY MAJOR SECTOR

The largest uncertainties in this study are associated with unavailable data or unreported values in provincial and national surveys. The following sections highlight the uncertainties and limitations by major sector. One of the primary challenges in this analysis was the lack of high resolution point-based volumetric data in order to spatially distribute the groundwater withdrawals. For the majority of derived groundwater volumes per sector, large uncertainty was introduced due to unreported values which required extensive interpolation from large scale volumes (reported on the provincial scale) to proxy point (such as business locations, or type of wells) to distribute the values to aquifer-scale. For this reason, this analysis should be considered a first order estimate of groundwater withdrawals in BC and we recommend this analysis be refined and updated once measured data is available.

5.1.1. MUNICIPAL WATER DISTRIBUTION SYSTEMS AND PRIVATE DOMESTIC WELLS

The MWDS and PDW groundwater volumes are derived from data in the MWWS (2009). Approximately one quarter (24%) of the BC population – 24% of municipalities and 43% of regional districts – did not report on type of serviced water. Based on the MWWS, total annual water use for MWDS was only reported for 39% of municipalities (n= 98) and 36% of regional districts (n = 18). The regional districts and municipalities with unreported total MWDS volumes were attributed a volume based on total water use per capita (180 m^3 yr^{-1}). Calculations for MWDS users relied on source water data and percent groundwater from the MWWS, as well as, surface water license data from municipal waterworks to derive annual groundwater withdrawals. Subsequently, 14% of municipalities (n = 23) were inferred as groundwater users due to lack of source water data supplying the MWDS.

Municipal and rural groundwater use have increased 66% and 111% respectively based on the findings of this study. However, based on population statistics, municipalities have seen a 78% increase and rural population have seen a 0.5% decline since 1981 (Statistics Canada 2011). The methodology for deriving municipal and rural groundwater volumes assumes a conservative approximation of groundwater use by defaulting unknown source of freshwater to groundwater use. Therefore, it is likely the rural volumes have been overestimated. Alternatively, municipal water distribution systems have seen a decline in water use compared to population increase. Surface water licences represent a maximum allowable diversion, where the actual surface water diversion is often less than the licensed volume. As groundwater volumes were taken as the difference between total water use and surface water allocations, groundwater volumes may have been underestimated where municipal water distribution systems did not divert their total annual allocation from surface water sources. Another possible reason for the decrease in municipal water use compared to population increase could be due to water use trends, such as per capita water use or a switch from groundwater to

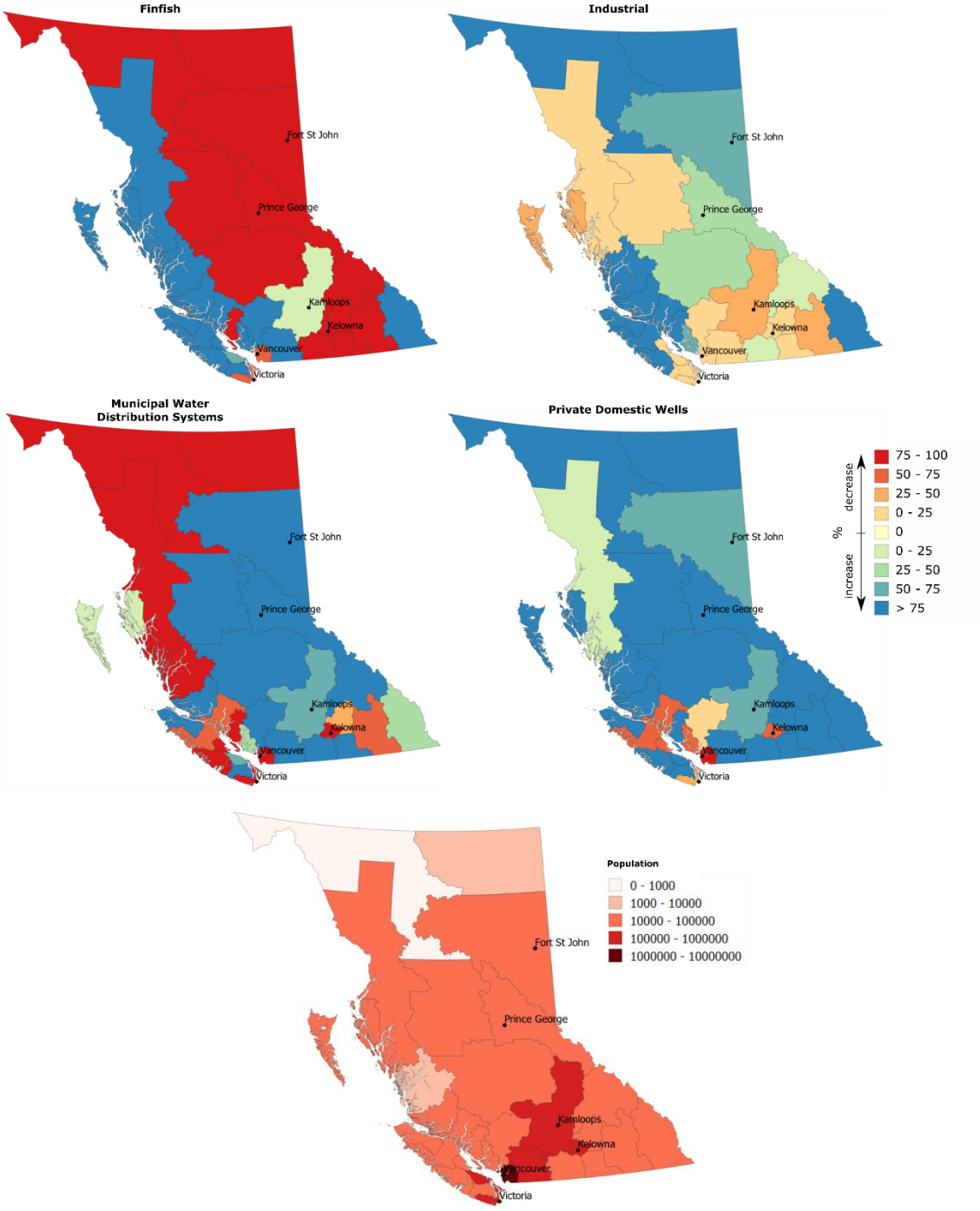

Figure 2.8. Percent change in per capita groundwater use compared to provincial values. (Top four panels) Percent difference in provincial per capita groundwater use per sector and regional district per capita groundwater use. (Bottom) Population per regional district.

surface water sources, however, due to lack of reported data, these are no more than speculations.

5.1.2. INDUSTRIAL

Groundwater abstraction data is most accurate for the oil and gas sector, as these are reported values attributed to wells. The manufacturing and mining groundwater abstraction data was only provided at a provincial-scale. Derived groundwater volumes for manufacturing industries had an average total annual water intake calculated at 715 Mm^3 yr^{-1}, which is comparable to the provincial average of 796 Mm^3 yr^{-1} reported by Statistics Canada in the Industrial Water Survey. Although derived total provincial abstracted groundwater volumes fell close to the expected value reported by the Industrial Water Survey, the largest uncertainty for manufacturing and mining industries is the spatial distribution of derived groundwater abstraction. Spatial variability is masked as it assumes 1) all locations supply a portion of their groundwater through self-supplied private wells, as no data exists as to which locations are connected to a MWDS, 2) all locations use some volume of groundwater based on the groundwater coefficient, and 3) all locations of the same sub-industry withdraw the same volume of groundwater as volumes are distributed using North American Industrial Classification System.

5.1.3. IRRIGATED AGRICULTURE

The main uncertainties in calculating groundwater volumes in the agricultural sector are in regions where the AWDM is unavailable as the GCWM uses a provincial scale groundwater coefficient to constrain groundwater volume. The AWDM reported agricultural use for 422 aquifers in BC, as opposed to the GCWM which reported for 653 aquifers, however the AWDM accounts for 99% of the attributed volume of groundwater use compared to the GCWM since the AWDM has focused on the areas of most intense irrigation. Since only total annual irrigation volume is included, the groundwater coefficient had to be inferred from provincial statistics. This assumes all farms are groundwater users, therefore, presenting a high uncertainty of groundwater volume location accuracy. As irrigation was determined

the major contributor of annual agricultural groundwater withdrawal, livestock was not included and will need to be added at a later date.

5.1.4. FINFISH AQUACULTURE

Based on the major sectoral annual groundwater volumes from this study, finfish aquaculture is the second largest user of groundwater, after agriculture, accounting for 116 Mm^3 of total annual groundwater use in BC. This value has large uncertainty since conservative inferences were made on groundwater flow rates, seasonal operation, and groundwater user locations. However, it is apparent that all aquifers being abstracted for the purpose of finfish aquaculture do have large withdrawal compared to aquifer area even at a conservative 4 months seasonal usage. These values should be verified with local studies to determine actual groundwater diversion to better constrain these volumes.

6. RECOMMENDATIONS & CONCLUSIONS

Groundwater is a critical source of freshwater supporting residential, commercial, industrial and agricultural sectors within BC. The Province has mapped and classified more than 1100 aquifers across BC, but the level of development for each aquifer has always been subjectively based on well density or the mapper's knowledge of groundwater use.

This chapter estimates groundwater use across BC for all the major groundwater use sectors and maps this groundwater use for each aquifer in the province for the first time. Data on major sectors of use was synthesized from provincial and national sources and spatially downscaled and interpolated to derive groundwater use volumes for currently mapped aquifers. Groundwater use was first classified based on means of distribution either through a municipal water distribution systems or self-supplied through private wells, and secondly, by major groundwater use sectors namely, domestic, industrial, irrigated agriculture, and finfish aquaculture. The methodologies used in deriving the spatially distributed groundwater use volumes are different for each sector based on the data availability and scale of reporting. Results suggest that BC uses a total of ~562 million cubic metres of groundwater

annually. The largest annual groundwater use by major sectors is agriculture (38%), finfish aquaculture (21%), industrial (16%), municipal water distribution systems (15%), and domestic private well users (11%). This study is a preliminary assessment, as the majority of the groundwater volumes were unreported per sector, and therefore, different methodologies are used to interpolate available data.

Sectoral groundwater use is critical for local regions and aquifer-scale groundwater stress studies which are significantly impacted by changes in the groundwater use nominator. Based on the results from this study, we have identified the importance of regionally important sectors, such as finfish aquaculture in the coastal regions.

The methods herein presented can be useful for regional scale estimates of groundwater use in data scarce regions and could be modified for application in other regions. In particular, one of the major limitations is the lack of pumping data, however, the location of wells can be used to spatially distribute groundwater volumes instead of population of area based assumptions. In addition, estimating municipal water distribution systems is a critical component of total groundwater use, which account for a large majority compared to self-supplied users.

A few detailed recommendations derived from the results as well as challenges encountered during this analysis include:

- Identify local sectors which may be critically impacting the abstraction of groundwater within the study area.
- Compare annual groundwater volumes to results from local or regional studies which could help determine the accuracy of estimates in different regions.
- Create and provide public access to data on regional groundwater sources and volumes of use. The largest uncertainty in this groundwater use analysis was due to a lack of available data.
- Water meters should be encouraged for all well users to improve estimates of water use.

CHAPTER 3:
Multi-scale, multi-method recharge estimation for diverse mountainous environments: quantifying recharge for unconfined aquifers in British Columbia

1. INTRODUCTION

Recharge is a critical value in aquifer stress studies, and regional assessment techniques are vital in the sustainable management of groundwater resources. Quantifying aquifer-scale estimates of recharge in diverse hydrologic environments is particularly difficult due to the limited number of techniques which can be applied over a large spatial area (Flint et al. 2002; Scanlon et al. 2002). Mountainous regions have a number of recharge mechanisms dependent on geology, landscape, and climatic spatial variability (Winter 2001; Wilson and Guan 2004; Scanlon et al. 2006). Watershed within or in proximity to mountainous terrain exhibit spatial variability in relief, with steep slopes and deeply incised valleys as well as extreme climatic temporal and spatial variability, and complex interactions with surface water. Groundwater recharge, for the purpose of this study, is defined as the flux of water reaching the water table (Lerner et al. 1990). More specifically, aquifer recharge is the influx of water across an aquifer boundary, either from vertical percolation or lateral movement of groundwater to the aquifer. While aquifer recharge is a critical component in regional management of groundwater resources, it is difficult to accurately estimate, mainly due to limitations in methodology and data availability.

Groundwater recharge in mountainous areas has been a topic of study for several decades, spanning regional flow characterization (Bakker et al. 1999; De Vries and Simmers 2002; Allen et al. 2010b), influence of mountain and valley bottom streams

(Covino and McGlynn 2007; Ajami et al. 2011) and mountain block and mountain front recharge (Manning and Solomon 2004, 2005; Wilson and Guan 2004). However, recharge in mountainous terrain is often examined on a local scale, which takes considerable time and is often unrealistic for regional scale aquifer assessments. Very little literature describes regional recharge estimation techniques to deal with diverse hydrologic environments, particularly in mountainous terrain.

For the purpose of this study, long-term annual recharge was estimated from an aquifer-centric position, where by, an average annual recharge value will be representative of the entire aquifer area. Based on previous local recharge studies in BC (Allen et al. 2004b; Toews 2007; Liggett 2008), direct diffuse and indirect recharge, from the stream or from mountain block/front processes, are the primary aquifer-scale recharge mechanisms. Figure 3.1 illustrates the relationships between process, observation, or model scales of this study (Blöschl and Sivapalan 1995). *Process scale* is based on the characteristic extent, period, or integral scale of the process. Figure 3.1 highlights the natural extent of the spatial and temporal scales of the major recharge processes important to the aquifer scale. *Observation scale* is based on the constraints of measurement techniques and logistics. The observation scale corresponds to the data used in the analysis which is representative of a specific scale which is illustrated in Figure 3.1 as the representative scales of the resultant WTF, HELP, and PCR-GLOBWB data sets. The *model* scale is the resultant scale of the modelled space and time, namely the final results at the aquifer scale.

The three major recharge processes were identified from previous studies which were interpreted to occur significantly at the aquifer-scale in mountainous terrain: 1) direct diffuse; 2) indirect recharge from streams and 3) indirect recharge from the mountain front/block. Figure 3.1 illustrates the spatial scale and temporal scales of recharge processes relative to aquifer recharge. Spatial scales are representative of possible scales at which the processes occur at the surface, assuming Darcian flux scales. Temporal scales are the timing of process from infiltration into groundwater to the aquifer boundary. Direct recharge occurs at all scales, and therefore extends from 1 m^2 to >10000 km^2 on a temporal scale of hours to years as water vertically

percolates through the unsaturated zone. Indirect recharge processes are more complex, composed of horizontal and vertical fluxes. Where recharge to an aquifer occurs from a perennial stream, the spatial flux will be dependent on the perennial drainage density of the area, and position of the stream relative to the aquifer. The temporal scale will be relative to the distance travelled horizontally and the saturated hydraulic conductivity. Recharge from ephemeral streams are a type of focused recharge from the surface, similar to direct recharge over a smaller area. Mountain recharge processes of mountain block recharge and mountain front recharge occur mainly as horizontal flux and vertical fluxes, respectively, to the aquifer boundary. The spatial scales of these processes are larger, occurring over the mountainous area. Temporal scale of mountain block recharge can possible be on the order of > 100 years in some low permeability bedrock deposits.

The objective is to use multi-scale methods to examine the recharge mechanisms and provide more reliable recharge estimate in complex mountainous terrain. Scanlon et al. (2002) emphasize the importance of using multi-method approach when quantifying recharge due to uncertainties inherent with each approach. We propose, that in addition to a multi-method approach, method and data input scales should be chosen to represent the resultant spatial scale, in order to decrease uncertainty in recharge estimation. Three methods were used to quantify long-term annual aquifer recharge on various spatial scales using readily available data. We consider 404 unconfined aquifers across BC. Local-scale recharge was estimated using the water table fluctuation (WTF) method outlined by Cuthbert (2014). The groundwater hydrograph from the well was assumed to be representative of the fluxes within the aquifer. Unique recharge estimates were quantified per well for a limited number of aquifers. Aquifer-scale recharge was quantified based on generalized aquifer parameters of soil and aquifer material, regional climate, and water table depth. Recharge was modelled using the Hydrologic Evaluation of Landfill Performance (HELP) model (Schroeder et al. 1994) which is a quasi-2D water balance model which was previously used extensively in British Columbia for recharge and groundwater system studies (Allen et al. 2004; Scibek and Allen 2006;

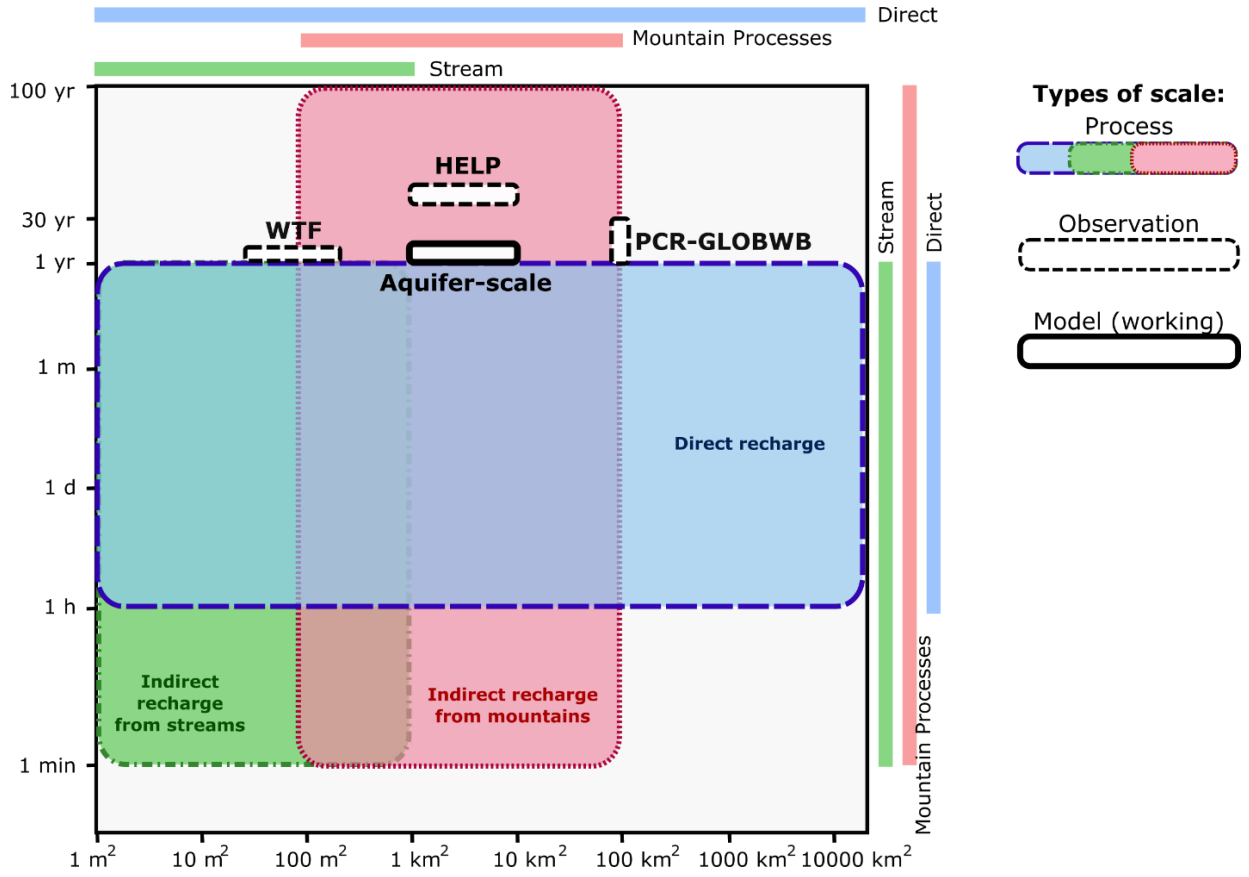

Figure 3.1 Comparing process scale and model scale. Process scales of direct recharge (blue) and indirect recharge from streams (green) and mountains (pink) compared to model scales from the water table fluctuation (WTF) method, HELP model (a 1D water balance model), and PCR-GLOBWB (a global hydrology model).

Toews 2007; Allen 2010; Liggett and Allen 2010). Regional scale aquifer recharge was attributed the areal average recharge flux modelled by PCR-GLOBWB (Van Beek and Bierkens 2009) which is a global hydrologic model with a resolution of 10 km².

2. STUDY AREA

The spatial variability and magnitude of recharge to aquifers is influenced primarily by climate which is strongly associated with physiographic areas. The annual flux of groundwater recharge is the balance between precipitation, runoff, and evapotranspiration (ET) fluxes. BC is one of the most hydroclimatically complex regions in North America due to varying relief and proximity to Pacific Ocean (Pike

et al. 2010). Lowlands and intermontane areas can be found in the interior of the province, although the region is predominantly composed of mountainous terrain. The topography ranges from sea-level on the western Pacific coast to mountain peaks greater than 2000 m above sea level. The physiological features have been subdivided into units which are topographically alike (Holland 1976) as summarized in Table 3.1 and spatially distributed in Figure 3.2. The physiographic features of BC have a direct influence on the spatial and temporal distribution of regional climate patterns that vary with elevation, distance from the coast, exposure to prevailing winds, and seasons (Moore et al. 2010).

The range of climatic regimes are captured by the 14 biogeoclimatic zones, named for the dominant tree species within each zone (Church and Ryder 2010). The climates vary from humid on the coast, semi-arid in the interior, and artic conditions in the high alpine and northern regions. Annual precipitation varies from greater than 4000 mm yr^{-1} in the coastal regions to less than 200 mm yr^{-1} in a series of rain belts and rain shadows.

Table 3.1. Physiographic landforms of British Columbia.

Feature	Relative relief	Description
Plain	Flat	Level or nearly level land
Depression	Flat - Low	Basin-like; below sea level
Basin	Flat - Low	Drainage area; flanked by higher elevations
Lowlands	Low	Undulating or hilly; flanked by higher elevations
Plateau	Low - Moderate	Wide valleys, upland surfaces
Trench	Low - High	Large flat valley; flanked by mountain ranges
Foothills	Moderate – High	Transitional mountain/hill ranges
Highlands	Moderate – High	Transitional mountains; partially dissected
Mountains	High	Mountainous; dissected terrain

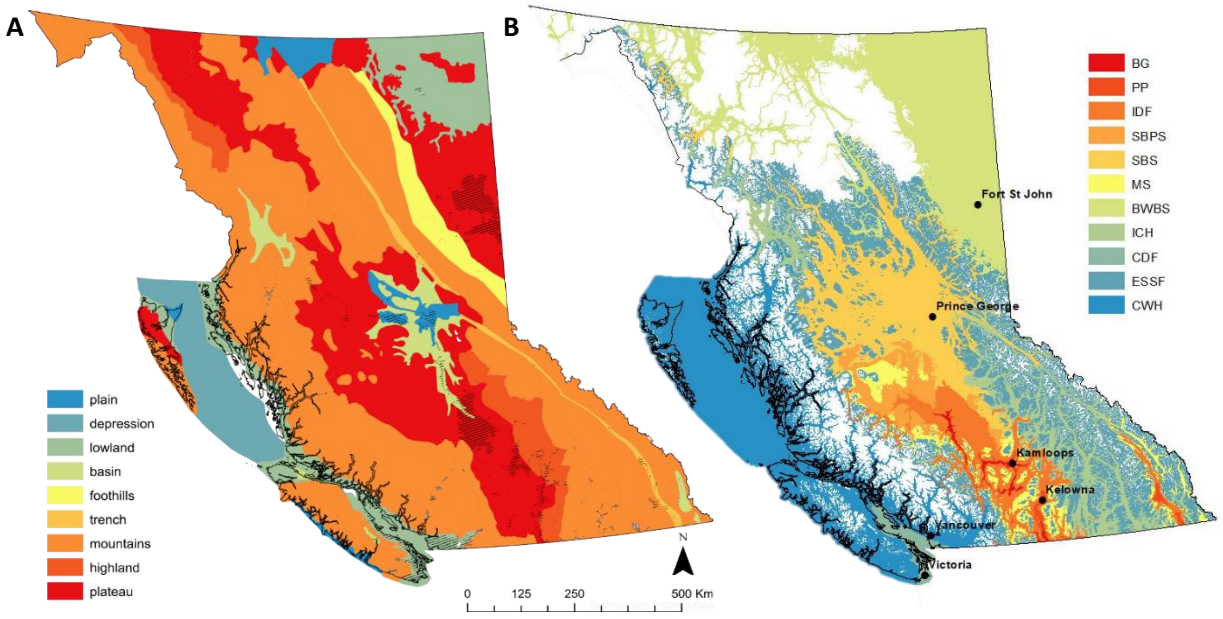

Figure 3.2. Physiographic and climatic setting of BC. (A) Major landforms of the region. Physiographic zones were classified by major topographic features. Mapped aquifers overly the map in hashed areas. B) Biogeoclimatic zones of BC. The spectrum of colors represents the regions of relatively lower precipitation to highest precipitation. BG: Bunchgrass; PP: Ponderosa Pine; IDF: Interior Douglas-fir; SBPS: Sub-Boreal Pine-Spruce; SBS: Sub-Boreal Spruce; MS: Montane Spruce; BWBS: Boreal White and Black Spruce; ICH: Interior Cedar-Hemlock; CDF: Coastal Douglas-fir; ESSF: Engelmann Spruce-Subalpine Fir; CWH: Coastal Western Hemlock.

Coastal areas are dominated by a Mediterranean winter-wet, summer-dry pattern, whereas in the lee of the Coast Mountains throughout most of the Interior, precipitation exhibits weaker or little seasonality. Climatic moisture regimes, which reflect the balance between precipitation and the evaporative demand, are also variable. Warm and drier environments, such as the Interior, have a greater moisture deficit compared to coastal wet environments, such as the Coastal Mountains. At greater elevations, climate plays an additional complex role, with an increase in rainfall, precipitation falling as snow, and decreased moisture deficits compared to lower reliefs (Pike et al. 2010).

Streamflow regimes vary spatially and temporally based on the characteristic system defined as rain-dominated, snow-dominated, or hybrid (Eaton and Moore 2010; Allen et al. 2010b). Rain dominated systems are found primarily in the coastal

lowland areas and at lower elevations on the western Coast Mountains. These regions are strongly influenced by precipitation intensity with relatively little smoothing or lagging evident in stream hydrographs. The year to year variation in seasonal distribution of rainfall is significant due to the intensity of weather systems and is unlikely to resemble the long-term average pattern. The interior plateau and mountain areas at higher elevations are dominated by snow-dominated regimes. These systems integrate precipitation inputs over the winter and spring within the snowpack then release the stored water during spring-summer melt. As a result, the monthly discharge pattern for a given year is generally similar to long term monthly averages. In coastal and near-coastal regions, the hydrological regime is more complex, and described as a hybrid regime. These regimes are most heavily dependent on air temperature which determines the relative strength of rain and snowmelt on the system. Direct groundwater recharge in these systems can be seasonally variable dependent on the timing of ground thaw conditions and precipitation.

In general, aquifers can be divided into two systems which describe the aquifer-stream dynamics: direct recharge-driven or stream-driven (Allen et al. 2010b). Direct recharge-driven systems involve the aquifer receiving most of the influx of water from precipitation events, such as direct diffuse recharge and mountain block recharge. Direct recharge-driven systems predominantly discharge to streams during low flows. The stream-driven system defines aquifers where flow to the stream is bi-direction, with the aquifer receiving recharge from the stream seasonally.

The geological characteristics of aquifers are another important determinant in the magnitude and timing of the hydrological response in the aquifer (Hantush 1967; Allen et al. 2010b). In equivalent climatic and physiographic settings, more permeable aquifers with relatively high storage capacity (eg. sand and gravel aquifers) will be able to respond more rapidly to infiltration events compared to lower permeable aquifers of limited storage capacity (ie. bedrock aquifers).

Table 3.2. Classification of unconfined aquifers in BC.

Aquifer Type	Setting	Material	Range; Average (km^2)
Type 1	*Along streams*		
1a	High order streams; low gradient	Mostly sand and gravel Some silt and clay	<1 – 140; 27
1b	Moderate order streams; low to moderate gradient	Mostly sand and gravel	<1 – 120; 15
1c	Low order streams along valleys limited in lateral extent	Mostly sand and gravel Some silt and clay	<1 – 23; 7
Type 2	*Deltaic*		
	Deltas at mouth of rivers or streams	Sand and gravel	<1 – 19; 4
Type 3	*Alluvial / colluvial*		
	Alluvial fans or colluvial origin	Sand and gravel	<1 – 54; 5
Type 4	*Glacial / pre-glacial fluvial*		
4a	Glaciofluvial outwash or ice contact	Sand and gravel	<1 – 90; 8

Aquifer mapping has been limited to developed regions which are mainly in the southern and central region of the province (Berardinucci and Ronneseth 2002). Glacial and tectonic history greatly influence the surficial and bedrock geology of the region (Winkler et al. 2010). Most unconfined unconsolidated aquifers were formed during the period of glacial melting and retreat and therefore aquifers are mainly composed of sand and gravel deposition under fluvial or glaciofluvial environments (Wei et al. 2014).

Within the mapped region, aquifers generally fall into six categories which describe unconsolidated sand and gravel aquifers, and bedrock aquifers (Wei et al. 2007, 2014). Aquifer type 1-4a are generally shallow and unconfined which are mainly composed of sand and gravel material, Table 3.2 has a short description of each sub-type. As most aquifers are of glacial or fluvial depositional origin, unconfined aquifers are described as sand and gravel material, however, small discontinuous silt or clay layers may exist within the aquifer, in particular along streams of lower

energy (Wei et al. 2014). Unconsolidated aquifers are often limited in size by mountainous terrain, where aquifers are generally confined to valleys or floodplains. Average aquifer size ranges by different classification type from 4-27 km^2.

The bedrock geology of the Cordillera is complex and regionally varying due to the regions geologic, tectonic, and volcanic history (Wei et al. 2014). Despite the complexity of the bedrock material, bedrock permeability exists primarily due to the development of fractures and faults from mechanical weathering processes and/or unloading causing relatively high fracture density (Welch and Allen 2014) and the permeability is often anisotropic as the fractures and faults have specific orientations (Wei et al. 2007). Unlike unconsolidated aquifers, bedrock aquifers are not classified based on confinement, but rather by rock type. Level of vulnerability is commonly used to describe and aquifer's susceptibility to surface contamination, and therefore, is often used to categorize bedrock unconfined and confined aquifers (Berardinucci and Ronneseth 2002). Unconfined bedrock aquifers are mainly composed of fractured sedimentary rock (Type 5a) or fractured igneous intrusive, metamorphic, or volcanic rock (Type 6b).

3. DATA AND METHODS

3.1. LOCAL-SCALE

3.1.1. THEORETICAL BACKGROUND

Water table fluctuation observations through the analysis of groundwater hydrographs reflect the balance between groundwater recharge rate, q_c, and the net groundwater drainage rate, D, experienced by unconfined aquifers at the observation well location. Water level fluctuations are in response to spatially averaged recharge (Healy and Cook 2002). Derived recharge rates are representative of the local area surrounding the observation well, and often estimates within the same aquifer can yield spatially varying recharge results due to local heterogeneities (Crosbie et al. 2005; Cuthbert and Tindimugaya 2010).

The water table fluctuation method (WTF method) of recharge estimation was first proposed by Meinzer and Stearns (1927) and has been widely used because it is relatively simple to apply (Healy and Cook 2002; Scanlon et al. 2002). The method has historically been applied to derive recharge on an event basis, however, recent methodological advances have inferred modified versions to derive the long-term annual steady state recharge. In particular, Crosbie et al. (2005) developed a modified WTF methodology for the rising limb of the hydrograph, whereas, Cuthbert (2010) analyzed the falling limb of the hydrograph, equating the linear phase of the groundwater head recession rate to the quasi steady-state annual groundwater discharge flux. The method is based on the premise that under steady-state conditions, when $q_c < D$, a groundwater head decline will occur. If q_c is zero, the groundwater hydrograph will first exhibit a head recession with linear head recession rate, followed by the transitional and exponential phases of the head recession rate. The groundwater head recession rate may vary in space and time dependant on antecedent conditions, aquifer properties, and boundary conditions (Cuthbert 2014). This method is applicable for diverse recharge environments, and the limitations will be further discussed in subsequent sections.

The theoretical background described below is for an ideal homogeneous, horizontal aquifer bounded at one end (x = L) by a river, assumed to be a constant head boundary and at the other (x = 0) by a no flow boundary representing a flow divide (Figure 3.3). When $q_c = 0$, the net groundwater drainage rate, D, is equal to the groundwater flux recession. Cuthbert (2014) shows that for an ideal aquifer, D is equal to the prior steady state recharge ($D/q_c \approx 1$) and remains very close to this value for significant lengths of time for moderate to low diffusivity aquifers. Under these conditions, D is equal to the representative linear phase of groundwater head recession, $\partial h/\partial t$, multiplied by specific yield, S_Y:

$$q_c \approx D = S_y \frac{\partial h}{\partial t} \qquad \text{(Eq 11)}$$

where

q_c is the recharge rate (m)

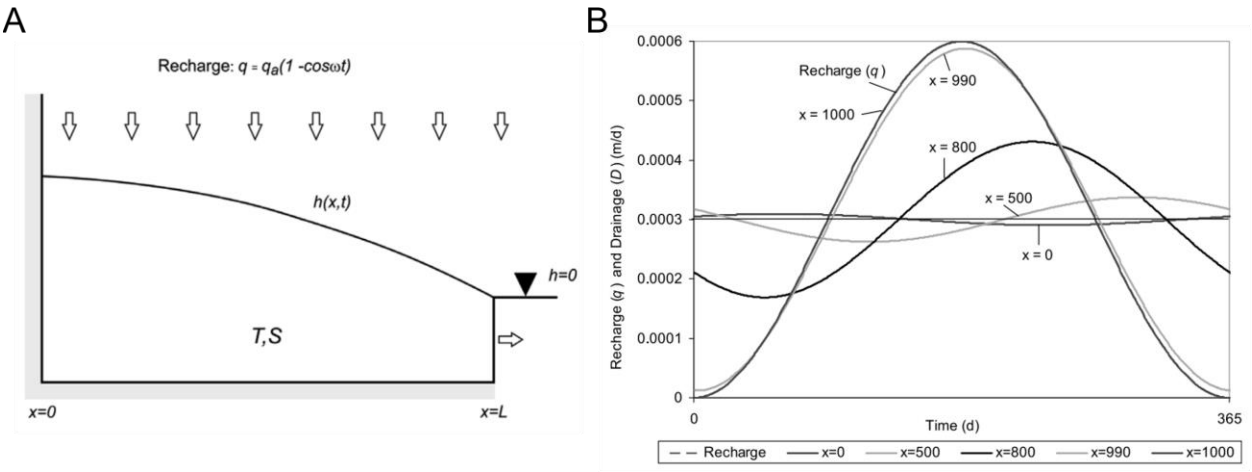

Figure 3.3. Ideal aquifer setting and variation in groundwater head recession on annual time scale. (A) Ideal aquifer receiving sinusoidal recharge. The drainage divide is x =0 and the constant head boundary is x =L). (B) Plot of recharge and drainage rate against time for various values of x (with T = 10 m^2/d, S_y = 0.02, L = 1000m, q_a = 0.0003 m/d). Modified from Cuthbert (2010).

D is the net groundwater drainage rate (m)

S_Y is specific yield (-)

∂h is the change in hydraulic head (m)

∂t is the change in time (day^{-1})

During the linear phase of $\partial h/\partial t$, the groundwater head decline initially decays at a constant rate, during which time, D is infinitesimally smaller than the q_c. D will be within 0.5% of q_c for the length of time determined by t_{lin}:

$$t_{lin} < \frac{d^2 S}{16T} \qquad \text{(Eq 12)}$$

where

t_{lin} is the linear phase starting from t_0

d is the distance from the observation well to the drainage outlet (m)

T is transmissivity (m^2 day^{-1})

Often recessions will not often begin under steady-state conditions, but rather quasi-steady state, where the recharge signal, q_c varies sinusoidally around an average

value q_a (Figure 3.3). The temporal variation of the net groundwater drainage rate, D, has a small amplitude, A, of oscillation of D (or q_a when $t < t_{lin}$). The magnitude of the oscillation increases with proximity to the drainage outlet. The relative variation in D can be calculated for a particular periodic signal, set of aquifer properties and location relative to a drainage divide using the following equation:

$$A = \left| q_a \left(\frac{cosh\, \lambda x}{cosh\, \lambda L} \right) \right| \quad \text{(Eq 13)}$$

where

$$\lambda^2 = \frac{i\omega S}{T} \quad \text{(Eq 14)}$$

- A is amplitude of oscillation representing the temporal variation of q_a (m)
- q_a is the net groundwater drainage rate (m)
- T is transmissivity ($m^2\ day^{-1}$)
- x is distance of the well to the drainage divide (m)
- L is distance from drainage divide to the stream (m)
- ω is the angular frequency of the sinusoidal temporal variation of D (day^{-1})

In reality, deviations from the ideal aquifer scenario are common, and the effects on the straight line recession are discussed in the next section. Cuthbert (2010) also notes that the above approximation holds true in even small nonidealized cases such as the nonlinearized cases, for nonsinusoidal recharge, for aquifers with moderately sloping bases, and certain cases of spatially variable recharge. The recession behavior exhibited by non-ideal aquifer varies spatially and temporally based on aquifer properties, geometry, and location of the monitoring point relative to catchment boundaries. Several reasons for deviation from nonlinear recessions are common, and summarized below based on (Cuthbert 2014).

Smoothing Effect. Observation wells that exhibit smooth fluctuations in groundwater levels were indicative of rare periods of no recharge. This smoothing effect on the hydrograph is common in temperate to humid regions due to the wet climates (Cuthbert 2014). This response is to be expected as water continues to reach the

water table for days after the last precipitation, and periods of no recharge were difficult to determine. When the rate of recession becomes constant with an increasing period since precipitation, recharge was assumed to equate to 0 and the linear recession was observed.

Proximity to drainage boundary. Proximity to the drainage boundary decreases the linear phase of the recession by dampening the hydrograph response. As a result, for monitoring locations too close to the drainage boundary, recession rates would be expected to decrease with time.

Transmissivity varies significantly with h. Aquifer properties are assumed to be constant in time and space, however when transmissivity or storativity vary significantly with h in reality, aquifers will show significant head dependent variations in recession rates. To test for T variance in aquifers, the ratio of variance in h to minimum saturated thickness should be sufficiently small. Saturated minimum thickness data was equated to the well depth, and the average linear recession rate represents the variation in h. In addition, as significant uncertainty was inherent in the aquifer attributes, hydrographs were also observed for changes in linear recession with depth.

Dynamics of spatially varying recharge/discharge. The effect of dynamic or spatially varying groundwater abstraction may significantly affect the recession, where in periods of active pumping, recessions will be faster due to the increased discharge within the aquifer. Due to the scarcity of pumping data, hydrographs were interpreted to be significantly influenced by pumping if they presented with erratic fluctuations out of phase with precipitation, or behaviors of pumping recovery. Subjective manual evaluation of the hydrographs was made to identify influences of pumping.

Nonequilibrium flow at a range of scales. Where groundwater recharge is not evenly distributed in time and space, the redistribution of water within both the unsaturated and saturated zones may complicate the form of groundwater recession. The recessions resulting from these preferential flow events occur

without hydraulic equilibrium between the pathways and the matrix. Initial groundwater declines are typically steep decaying at a decreasing rate as the mound recedes and spread out across the catchment. At later times following the recharge events, the groundwater recession resumes the natural background behavior. These processes occur at a range of spatial scales, capturing focused flow from depression, or mountain front processes.

Shallow water tables. Shallow water tables can affect the groundwater recession in two major ways. Firstly, as the available storage increases with depth to the water table, the rate of recession may be steeper at early times until the water table is sufficiently lower than the ground surface. Second, evaporation is likely to drive the upward flux which leads to nonlinearity in the observed recession, with faster rates expected at earlier times.

Transience in specific yield. The effect of transience in specific yield is observed in the hydrograph as an early time recession than at later times due to the increase in hydraulic conductivity with lowering moisture content in the zone above the capillary fringe. However, this effect can be hard to separate from the smoothed effect of recharge pulses during passage through the unsaturated zone and would have a similar response to the variation in specific yield with depth to water table.

3.1.2. DATA AND METHODS

Firstly, the groundwater head decline, $\partial h/\partial t$, estimation was automated using RStudio. Daily water table depth and precipitation data were used to automate groundwater head changes during periods proceeding precipitation. The first three days preceding the last day of precipitation were neglected for two major reasons: l) in some larger catchments, the water table was still rising due to delayed water reaching the water table; 2) the recession was often anomalously steep following a precipitation. Recession rates was estimated as the slope of the $\partial h/\partial t$ for each period. Periods where the slope was positive were neglected as groundwater heads rising during the period of no precipitation are indicative of water reaching the water table. In addition, dry periods with a slope of $R^2 \leq 0.97$ were neglected, as the period was

likely influenced by external effects which can impact the straight line recession. Further discussion on these effects are discussed in subsequent sections. Secondly, as drainage outlets can dominate the recessional behavior of the groundwater hydrographs when wells are within close proximity (Cuthbert 2014), distance to the nearest stream within the representative local watershed was estimated in an ESRI Spatial Analysis (ArcGIS Desktop). Aquifer properties were used to calculated approximate t_{lin} and A/D in order to compare observed and calculated values of t_{lin} and A/D. Thirdly, hydrographs were manually investigated, and the mean of $\partial h/\partial t$ was taken for interpreted periods of straight line recession.

Groundwater hydrograph data was collected from the BC Provincial Groundwater Observation Well Network (Ministry of Environment and Climate Change). The network consists of 172 observation wells, of which 63 observation wells measure daily frequency of water table depth for unconfined aquifers. The wells range in record length from less than a year to 52 years (average 20 years) spanning periods from 1962 - 2013.

Precipitation data with daily records was downloaded from Pacific Climate Impacts Consortium (University of Victoria) for Environment Canada climate stations. As the observation well record does not always overlap perfectly with climate station observations, climate stations within 25 km of the observation well are used to inform daily precipitation. Priority was given to the closest climate stations, with subsequent stations filling in any missing data.

Aquifer properties are summarized in Table 3.3. Unconfined unconsolidated aquifers were determined based on reported aquifer sub-type, which was used to distinguish unconfined unconsolidated aquifers from confined unconsolidated aquifers. Unconfined bedrock aquifers are not distinguished from confined bedrock aquifers, in the aquifer sub-type classification. High vulnerability classification was used to determine unconfinement for bedrock aquifers (Wei et al. 2014). Vulnerability level is a provincial metric to determine the risk level of an aquifer to surface contamination.

Table 3.3. Aquifer sub-type attributes of hydraulic conductivity, aquifer thickness, and specific yield.

BC Classification of aquifer sub-type*	Number of aquifers	Aquifer material (Gleeson et al. 2011)	K_{sat} m day^{-1}	b (m)	S_Y (-)
1a; 1b; 2; 3; 4a	49	coarse grained unconsolidated	10.9	4 - 577	0.2
5a	11	coarse grained siliciclastic sedimentary	0.264	10 - 98	0.05

K_{sat} was derived based on aquifer sub-type material and reported values from Gleeson et al. (2011). Aquifer thickness, b, was unreported, therefore, the observation well was assumed to fully penetrate the aquifer, and b was equated to the depth of the well from the surface. Transmissivity was estimated based on K_{sat} and b.

3.1.3. ESTIMATING METHOD PARAMETERS

Distance to the catchment divide, x, and drainage outlet, d, were estimated for each observation well to determine the total length, L, and to subsequently estimate t_{lin} and A/D. Mapped groundwater divides were unavailable, hence, surface watersheds are used to determine approximate boundary conditions. Surface watersheds were obtained from the Freshwater Atlas, a provincial standardized dataset for mapping BC's hydrologic features and derived from 1:20,000 scale topographic maps (Carver and Gray 2009). The distance to the drainage divide, x, and constant head boundary, d, were taken as a linear measurement from the well to the closest watershed boundary or stream, respectively, based on the likely the direction of groundwater flow.

The linear phase length, t_{lin}, and the variation in recession rate, A/D, were estimated using the above aquifer properties and a range of S_Y values. In general, specific yield values are normally dependent primarily on aquifer material and should be fairly consistent based on aquifer sub-type classification. Specific yield values derived from local pumping tests have a large range of derived S_Y values ranging from 0.00023 to 0.68 with a mean value of 0.088 for unconsolidated aquifers with no apparent pattern based on precipitation zone (Carmichael et al. 2008a, b;

Carmichael 2013, 2014). One possible explanation for the diversity in S_Y values for the unconfined aquifers may be the heterogeneous material of some of the aquifers. In general, they are described as sand and gravel, however small interbedded clay layers and other fine sediments common to glaciofluvial environments may be affecting the measured S_Y. Due to the regional nature of this study, further local scale measurements would be required to quantify representative S_Y values. Therefore, t_{lin} and A/D were derived based on typical values of S_Y = 0.2 and S_Y = 0.05, for unconsolidated and bedrock aquifers respectively (Johnson 1967).

3.2. AQUIFER-SCALE

The HELP (Hydrologic Evaluation of Landfill Performance – (Schroeder et al. 1994) software used in this study is implemented in Unsat Suite Plus 2.2 (Waterloo Hydrogeologic Inc. 2004). HELP is a quasi one-dimensional (1D) water balance software that simulates vertical infiltration through multiple soil layers and internally calculates evapotranspiration and overland flow. Required inputs include profile geometry, surface settings, and climate, soil and aquifer material properties. The profile was a simple horizontal two layer design, 1 m soil layer and underlying aquifer layer, representative of the unsaturated zone, and the "bottom" of the model was used to represent the water table (Figure 3.7). Aquifer recharge, the parameter of interest, is the vertical flux of water that passes through the profile, exiting at the "bottom" as recharge to the aquifer.

Localized recharge modelling using HELP in the Grand Forks aquifer (Scibek and Allen 2004) and the Abbotsford-Sumas aquifer (Scibek and Allen 2006b) suggested the parameters with the greatest impacts on recharge include soil parameters, precipitation data, hydraulic conductivity of the aquifer and the thickness of unsaturated zone (Scibek and Allen 2006c). Parameters with moderate effect include soil thickness, and soil and vadose zone porosity. Low sensitivity parameters with no noticeable change or very small (<5% change) include the vegetation type, wilting point, field capacity and the initial moisture content of the profile. Taking these results into consideration, data was collected and analyzed so that aquifers could be categorized into characteristic climate, soil, aquifer types, and modeled in HELP.

3.2.1. DATA

Detailed methods can be found in Chapter 3: Appendix, which describes case, surface water, and weather generator settings in more detailed.

CLIMATE DATA

Each of the aquifers across the province was sorted into a singular biogeoclimatic zones (Figure 3.4b). Biogeoclimatic zones define the different ecosystems, climate and flora that exist in the different zones across BC. Representative climate station and biogeoclimatic zone climate data was obtained from personal communication with Will MacKenzie of the Ministry of Forest, Lands, Natural Resource Operations, and Rural Development (Table S3.1).

Table 3.4 contains the input variables for growing season start and end date, quarterly relative humidity, precipitation, temperature, and wind speed were generalized for each biogeoclimatic zone based on climate normals from 1960-1990.

PROFILE ATTRIBUTES

In HELP, a vertical profile is created to represent the soil and aquifer materials. In this study, each vertical profile had two layers: a soil layer and underlying aquifer layer (Figure 3.4a and d). The base of the vertical profile represents the average water table depth.

Soil materials were categorized using the British Columbia soils maps (Ministry of Agriculture and Ministry of Environment and Climate Change) and the Soil Landscapes of Canada (SLC) version 3.2. The BC soils map data are at higher resolution, but data quality and availability are extremely heterogeneous. In contrast, the SLC data is at coarser resolution but is consistently mapped and has reasonable values of saturated hydraulic conductivity (K_{sat}) data for the soils overlying most aquifers in BC For this reason, we pair the SLC data (Figure 3.4a) with soil types from HELP using the expected K_{sat} as mapped. In order to transfer these values into HELP, the K_{sat} values were matched with existing HELP materials and given a soil type (Table S3.2).

Aquifer parameters (primarily K_{sat}) were derived from Gleeson et al. (2011) since the MENV data for aquifers only includes transmissivity and it is difficult to translate transmissivity into hydraulic conductivity when aquifer thickness is variable and often not readily available. Calculating aquifer thickness for every aquifer across the province was beyond the scope of this project. Gleeson et al. (2011) compiled permeability values for different hydrolithologies from calibrated regional-scale groundwater models. Hydrolithologies from Gleeson et al (2011) are paired directly with aquifer types (1 - 6) to derive expected hydraulic conductivity values for aquifer sub-types (Wei et al. 2014) (Figure 3.4d). The recent MENV connectivity policy suggests transmissivities for aquifer types 1, 2, 3 and 4 are within an order of magnitude and are consistent with the proposed hydraulic conductivities, drawn from Gleeson et al (2011). We therefore model four aquifer types (A1 – 4) with characteristic K_{sat} values (Table S3.3). There is one single aquifer code for all unconsolidated aquifers (A1) and three aquifer codes for bedrock aquifers (sedimentary – A2; carbonate – A3; and crystalline/volcanic – A4).

The vertical profile thickness is the distance from the top of the soil profile to the base of the profile. For recharge modelling studies, the profile represents the vadose zone with the water table forming the lower bounds. The average annual water table depth is used to define the thickness (Allen et al. 2004) (Figure 3.4d). Water passing through the base of the profile represents recharge. Whereas, in reality, the water table moves up and down seasonally, in HELP, the thickness remains fixed for the duration of the simulation. Soil morphology and precipitation have been shown to have significant effect on shallow water table depths (Calzolari and Ungaro 2012; Ghose et al. 2018). Therefore, water table depth is averaged per unique derived HELP code combination of soil and aquifer type (Table S3.4).

For this study, the mean water table depth for each aquifer across BC was derived from Fan et al. (2013). Mapping the mean depth for all the aquifers across the province based on well data was beyond the scope of this project.

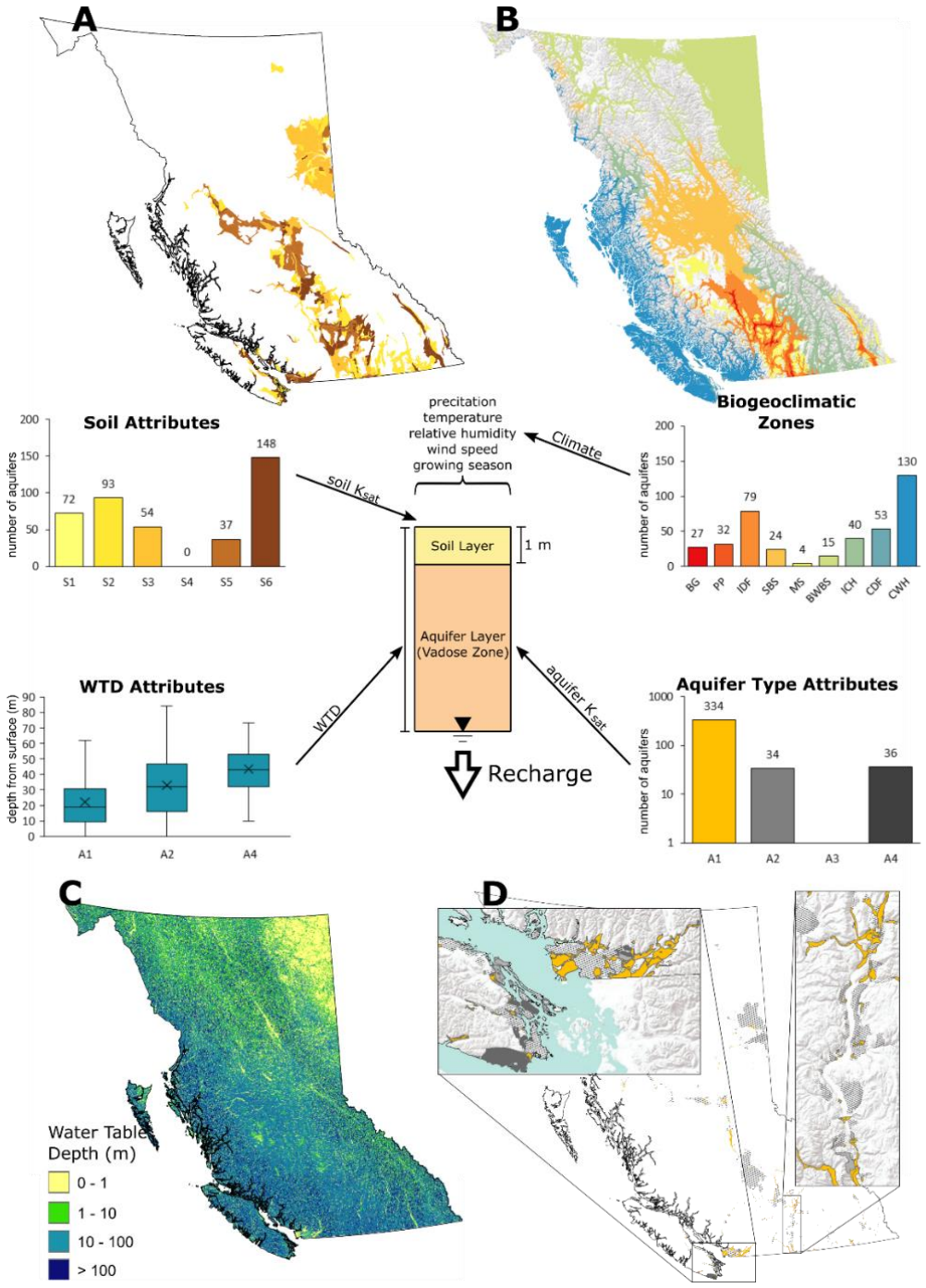

Figure 3.4. Overview of attributes used to generalize mapped aquifers. A. Soil attributes; B. Biogeoclimatic Zones; C. Water table depth – here water table depth distribution was categorized by aquifer type; however in this study, combinations of BGCZ, Soil and Aquifer type were used to derive an average water table depth value; C. Aquifer type.

Table 3.4. Input variables per biogeoclimatic zone for WGEN in HELP.

	units	BWBS	CDF	CWH	ICH	IDF	MS	PP	SBS
Growing season									
start	day	161	97	129	150	148	167	126	161
end	day	248	308	287	261	261	250	278	251
Relative Humidity									
Q1 - Jan, Feb, Mar	%	61	81	78	69	66	64	72	63
Q2 - April, May, Jun	%	59	71	69	61	58	60	60	57
Q3 - July, Aug, Sept	%	63	68	68	59	55	59	58	58
Q4 - Oct, Nov, Dec	%	68	75	76	69	64	65	66	67
Precipitation									
January	mm	68.8	160.4	290.8	99.8	59.6	93.0	44.2	74.2
February	mm	47.4	122.9	229.7	69.4	39.1	62.3	27.0	49.3
March	mm	44.7	98.9	195.5	56.7	29.8	52.7	17.5	42.2
April	mm	34.3	56.3	148.5	47.7	30.1	41.4	21.9	33.4
May	mm	55.5	44.7	101.8	54.8	37.3	45.3	26.1	44.5
June	mm	77.4	33.6	80.9	62.4	39.9	48.8	24.3	57.9
July	mm	87.9	25.1	66.1	62.9	36.7	44.5	26.0	58.9
August	mm	74.9	33.9	84.7	63.3	39.6	47.1	30.8	57.8
September	mm	74.3	53.8	147.1	64.3	36.2	47.5	27.7	58.8
October	mm	80.9	107.8	298.4	81.7	41.1	71.9	25.4	69.4
November	mm	67.6	167.5	322.7	93.3	56.4	95.3	36.5	69.4
December	mm	68.6	183.3	311.1	109.7	66.3	98.2	50.0	76.1
Temperature									
January	C°	-14.1	2.8	-1.6	-8.0	-7.0	-8.2	-4.7	-10.5
February	C°	-10.6	4.3	0.4	-4.5	-3.5	-5.4	-1.1	-6.6
March	C°	-6.1	5.8	2.4	-0.8	0.5	-2.6	3.1	-2.5
April	C°	1.0	8.3	5.3	3.9	5.0	1.6	7.6	2.7
May	C°	6.6	11.6	8.8	8.5	9.5	6.1	12.1	7.5
June	C°	11.0	14.6	12.0	12.4	13.4	9.9	16.2	11.4
July	C°	13.2	16.9	14.4	15.0	16.1	12.5	18.9	13.8
August	C°	12.2	17.0	14.6	14.7	15.8	12.4	18.5	13.2
September	C°	7.6	14.1	11.6	10.1	11.2	8.4	13.7	8.8
October	C°	2.1	9.6	6.9	4.2	5.4	3.0	7.6	3.6
November	C°	-7.7	5.4	1.8	-2.5	-1.6	-3.9	0.8	-4.2
December	C°	-12.4	3.1	-1.2	-7.2	-6.5	-8.1	-4.0	-9.4
Average Wind Speed	km hr^{-1}	7.0	10.0	12.0	5.2	10.0	12.0	5.4	10.0

3.3. REGIONAL-SCALE

Annual recharge was output from the macroscale hydrological model PCR-GLOBWB (Van Beek and Bierkens 2009). PCR-GLOBWB simulates for each grid cell (0.5° x 0.5° grid globally and approximate grid size of 10 km^2 for BC) and each time step (daily) the water storage in two vertically stacked soil layers (Store 1 and 2 in Figure 3.5) with maximum depths of 0.3 and 1.2m respectively, and for an underlying groundwater reservoir layer (Store 3). Changes in water storage are attributed to vertical water exchanges between the layers (infiltration, percolation, and capillary rise) and between the top layer and the atmosphere (rainfall, evapotranspiration, and snowmelt). The model also calculated interception (canopy) and snow storage. Meteorological forcing was applied to the model with a daily resolution and is constant over the grid cell.

Sub-grid variability is taken into account through short and tall vegetation (extracts water from top layer and both layers respectively), open water (lakes, reservoirs, floodplains, and wetlands), and soil types (Figure 3.5). Specific runoff from a cell to the river ($Q_{Channel}$) consists of surface runoff (based on Store 1), interflow (runoff form the second soil reservoir), and baseflow (groundwater discharge). In order to model surface water runoff, interflow, and baseflow, an estimate of drainage density of perennial streams within each grid cell is required. Surface runoff and interflow are parameterized based on grid-scale variability of soil saturation based on the values within the digital soil map of the world (Food et al. 2003). Interflow is not explicitly modelled, however average slope length and drainage distance are used to capture drainage between high and low conductivity soils common in mountainous area soils. Recharge flux is output as the flux from the second soil layer (Store 2) to the groundwater layer (Store 3).

The model is run based on global datasets outlined in Van Beek and Bierkens (2009) and was not run at a higher resolution for BC as high resolution data coverage was not available for many of the input parameters required by the model.

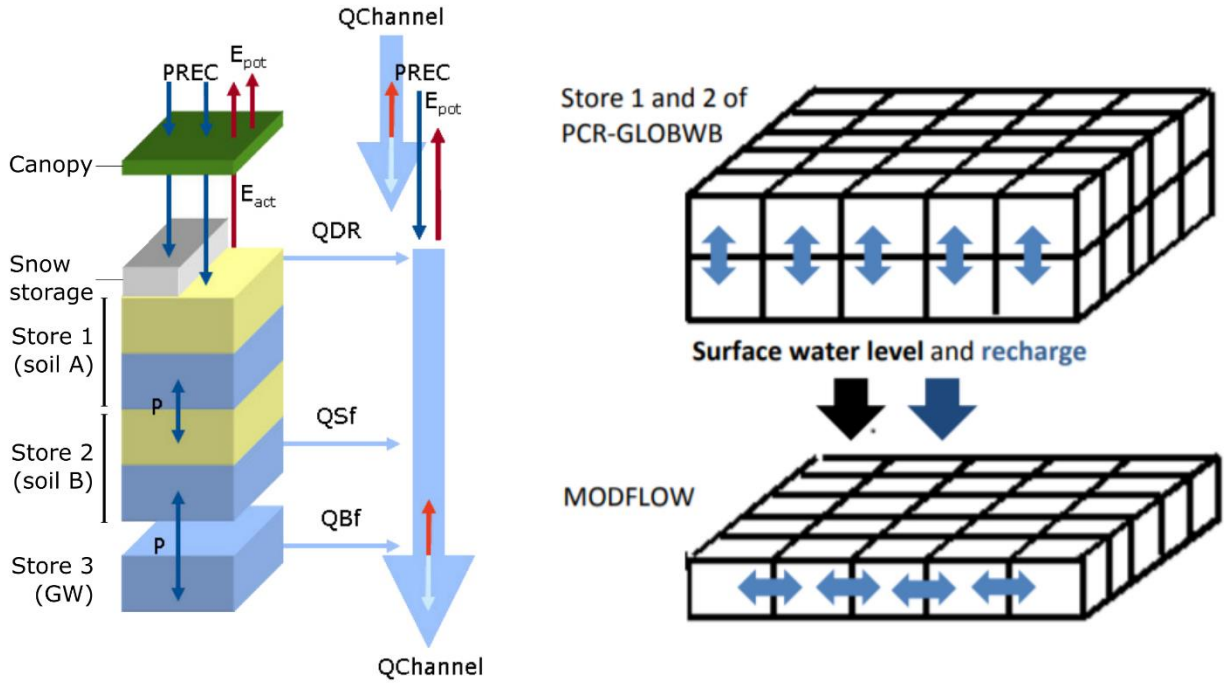

Figure 3.5. Conceptual model of PCR-GLOBWB. Store 1 and 2 represent unsaturated soil compartments, whereas, store 3 represents the saturated zone as a coupled MODFLOW groundwater model. The total local gains (Q_{DR}, Q_{Sf}, Q_{Bf}) are routed along the local drainage direction to yield channel discharge ($Q_{Channel}$). Precipitation (PREC); potential evapotranspiration (E_{pot}); actual evapotranspiration (E_{act}); snowpack (Snow storage); direct runoff (Q_{DR}); interflow (Q_{Sf}); baseflow (Q_{bf}); percolation (P). (right) The modelling strategy used to couple PCR-GLOBWB and MODFLOW. (Van Beek and Bierkens 2009; De Graaf et al. 2015)

4. RESULTS

4.1. LOCAL-SCALE

Of the 63 provincial observation wells, 10 wells were interpreted to have straight-line recessions assumed to be representative of long-term annual recharge. Many of the hydrographs were significantly affected by dominant signals from effects of shallow water tables, proximity to drainage boundaries or pumping. The average

Table 3.5. Results from water table fluctuation method.

BGCZ	Aquifer number	Observation well number	t_{lin} (days)		Recharge (mm)	A/D_{calc} (%)
			observed	calculated		
BG	74	296	-	22	1339	18%
BG	259	75	5	26	1892	9.2%
PP	297	154	30	9	374	22%
SBS	659	386	-	19	848	21%
CDF	41	360	13	17	2017	17%
CDF	447	128	15	2	664	50%
CDF	709	197	14	143	2794	0.30%
CDF	709	316	60	352	1964	0.0%
CWH	15	2	60	30	1728	7.7%
CWH	15	272	25	125	1094	0.50%
CWH	15	299	60	1	1359	75%
CWH	35	354	60	0	784	100%
CWH	159	329	60	0	2285	92%

recession rate was 8120 mm yr^{-1} (σ = 478 mm) and 9220 mm yr^{-1} (σ = 831 mm) for five unconsolidated and five bedrock aquifers respectively. Estimated average aquifer recharge was 791 mm yr^{-1} (σ = 549 mm), however, specific yield values were based on textbook values for unconsolidated materials (S_Y = 0.2) and bedrock (S_Y = 0.05) and therefore, were significantly uncertain for most observation locations.

4.1.1. EFFECTS TO THE OBSERVATION OF A NATURAL RECESSION

Table S3.5 summarizes the major effect on the observation of straight line recession for each hydrograph. Of the 63 observation wells analyzed, 53 observation wells had groundwater hydrographs where observable straight line recessions were dominated by effects from non-ideal aquifers.

18 observation wells had very smooth hydrograph records where episodic fluctuations from precipitation were dampened (ex. observation well 2 - Figure 3.6). In BC, pronounced wet and dry seasons amplified the temporal effect of a recession and it tends to occur seasonally based on dry months. The smoothing effect is

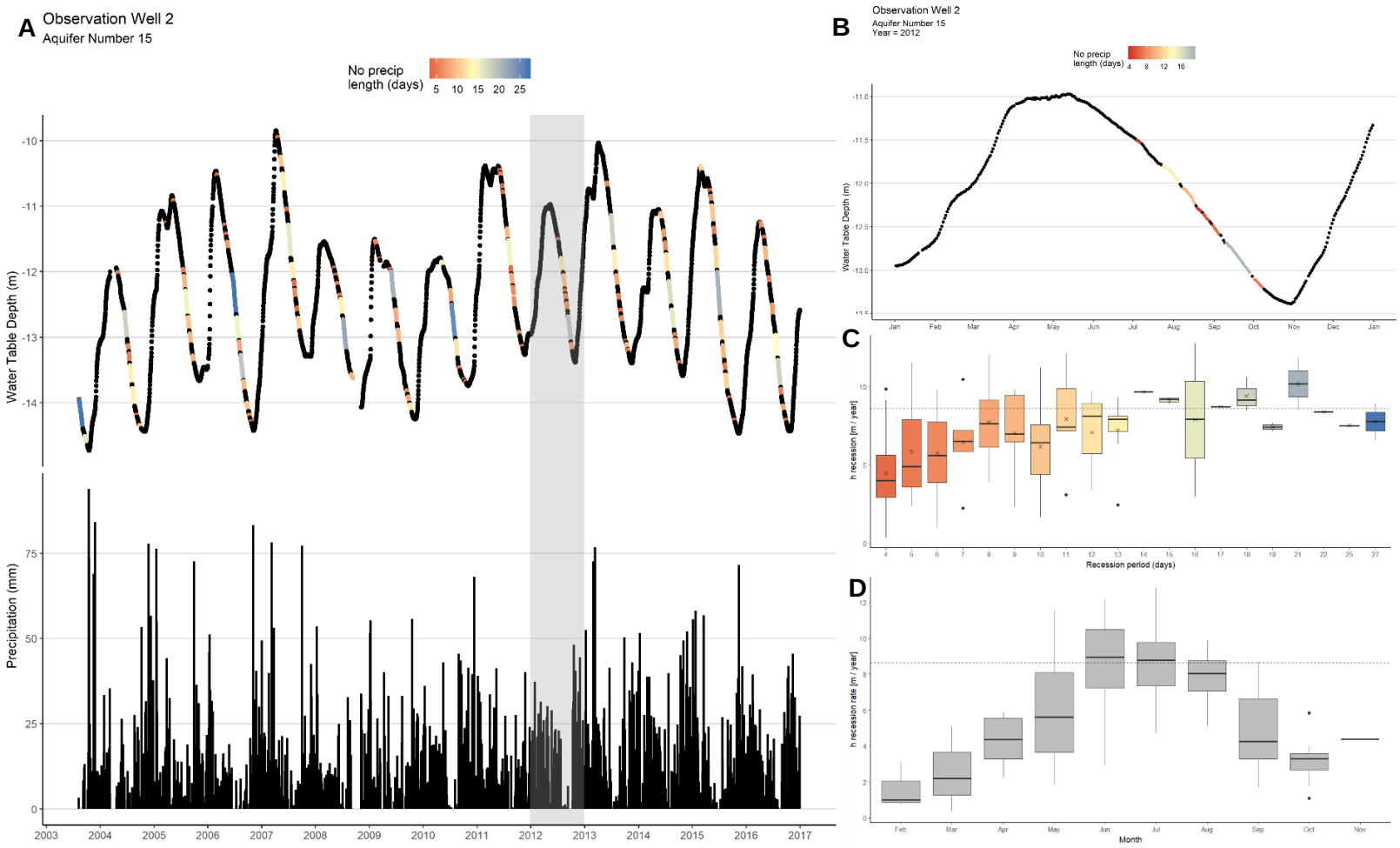

Figure 3.6. Example of a smoothed annual groundwater hydrograph record. A: Total length of record, with precipitation (mm) and water table depth (m). Colors illustrate relative length of periods of no precipitation. B: A Smoothed annual record where event based fluctuations are dampened. C: Results of groundwater head recessions by length of period with no precipitation. D: Results of groundwater head recessions per month. Dashed lines in C and D illustrate the average groundwater head recession exclusive of periods < 14 days.

thought to be primarily due to thick unsaturated zones or coverings of superficial deposits which affect the vertical percolation of water through the unsaturated zone. Observed recession rates in smoothed hydrographs often enter exponential behavior as the dry season progresses, which explains the decrease in observed head decline.

24 observation well location were significantly influenced by the proximity to a drainage boundary, shortening the linear phase (<1 day). t_{lin} is sensitive to d, and most wells (n = 14) had similarly calculated and observed values of t_{lin} < 1 day. The wells where calculated tlin is greater than observed t_{lin} are indicative of either aquifers where d is smaller than calculated, or aquifer attributes (S_Y, b, K_{sat}) are misrepresented by the average values used.

Variance in h with T is assessed by calculating the average annual Δh normalized by T. Where values of $\frac{var(h)}{b}$ are large (ex. > 50%) indicates that the natural recession is governed in part by the position of the water table within the profile. Variance of h with T could also be attributed to strongly sloping aquifers. 3 observation wells with a minimum saturated thickness of less than 10 m had >55% variance in h to saturated thickness (in comparison to the average of 2%), therefore, the method was deemed not applicable.

10 wells were significantly affected by pumping based on subjective analysis of the groundwater hydrograph. Significant effects from pumping manifest on groundwater hydrograph as rapid fluctuations or illustrates patterns of a well in recovery from seasonal pumping (see Chapter 3: Appendix - 4. WTF Method – Resultant graphs). In addition, the groundwater head recession per month illustrates no pattern and fluctuates randomly due to significant effects from the pumping. Summer agriculture in BC often requires groundwater abstraction which has a seasonal effect on observation well hydrographs. If recession rates showed little variance for non-pumping months, the aquifer was assumed to be in quasi-steady state conditions, and the recession in non-pumping months was assumed to be representative.

Shallow water tables are a common attribute for many of the aquifers in BC. Only 1 observation well was thought to be significantly affected by faster recession at early times where the linear phase was likely too short to observe the groundwater head recession rate after the effect.

4.1.2. LINEAR PHASE AND PERCENT AMPLITUDE OF VARIATION

Due to the uncertainty in the calculated linear phase, observed straight line recession lengths were used in addition to the calculated linear phase. The calculated values were corrected to the resultant straight-line recession observed in the hydrograph. The relationship between the calculated and observed linear phases was used to inform the uncertainty in aquifer properties. Based on equations 2 and 3, the linear phase and percent amplitude of variation are sensitive to the estimated distance to the stream, d, specific yield, and transmissivity.

Estimated distance to the nearest constant head boundary is uncertain, as distinguishing between ephemeral and perennial streams was difficult. In particular, mountainous climates are conducive to variable streamflow supported by seasonal snowmelt or intense rainfall events at higher elevations. Perennial streams are difficult to differentiate as many streams remain ungauged in the province. The nearest stream was assumed to be of a constant head annually, independent or the classified stream order. To illustrate the uncertainty in estimated distance to constant head boundary, Figure S3.3 shows that the nearest distance to a lake or main river can be 100 m to 10 km further than the estimated distance to the nearest stream. This increase in d would significantly increase the linear phase length by several orders of magnitude. Similarly, the increase in d, would increase the total length from the drainage divide to the constant head boundary, L, and would decrease the amplitude of variation by several orders magnitude. However, 38% of aquifers were classified as subtype 1 or 2, which is an aquifer classified as along a stream or at the mouth of a river or stream.

4.2. AQUIFER-SCALE

Recharge results were obtained for 52 unique combinations of biogeoclimatic zone, soil K_{sat}, aquifer K_{sat}, and water table depth and then attributed to the 404 unconfined aquifers with the appropriate combination of variables. The mean R_{HELP} for all the aquifers was 329 mm yr^{-1} with a median of 145 mm yr^{-1}, with the mean results per biogeoclimatic zone in Table 3.6. The spatial distribution of HELP results of recharge normalized by annual precipitation is illustrated in Figure S3.4.

A histogram of the frequency soil types overlying aquifers across BC shows that soil types S2, S3, S5 and S6 are most common, while soil type S4 is absent (Figure S3.5a). Soil types for each aquifer are explicitly linked to the soil hydraulic conductivity for each aquifer given that the soils derive from weathering of local materials. The distribution of unconfined aquifer types shows that type A1 (unconsolidated sand and gravel) is most common, A2 (sedimentary bedrock) and A4 (crystalline and volcanic bedrock) being moderately common, and A3 (carbonate bedrock) is uncommon (Figure S3.5b).

Table 3.6. Summary of annual steady-state recharge results averaged per biogeoclimatic zone derived from the HELP method.

Biogeoclimatic Zones	BGCZ (Abbrv.)	Average R_{HELP} (mm yr^{-1})	Average R_{HELP} / Precipitation (%)	(σ)
Bunchgrass	BG	40	12%	3%
Ponderosa Pine	PP	66	19%	2%
Interior Douglas-fir	IDF	81	16%	2%
Sub-Boreal Spruce	SBS	134	19%	3%
Montane Spruce	MS	95	13%	4%
Boreal White and Black Spruce	BWBS	199	25%	4%
Interior Cedar—Hemlock	ICH	222	26%	0%
Coastal Douglas-fir	CDF	713	66%	4%
Coastal Western Hemlock	CWH	952	42%	3%

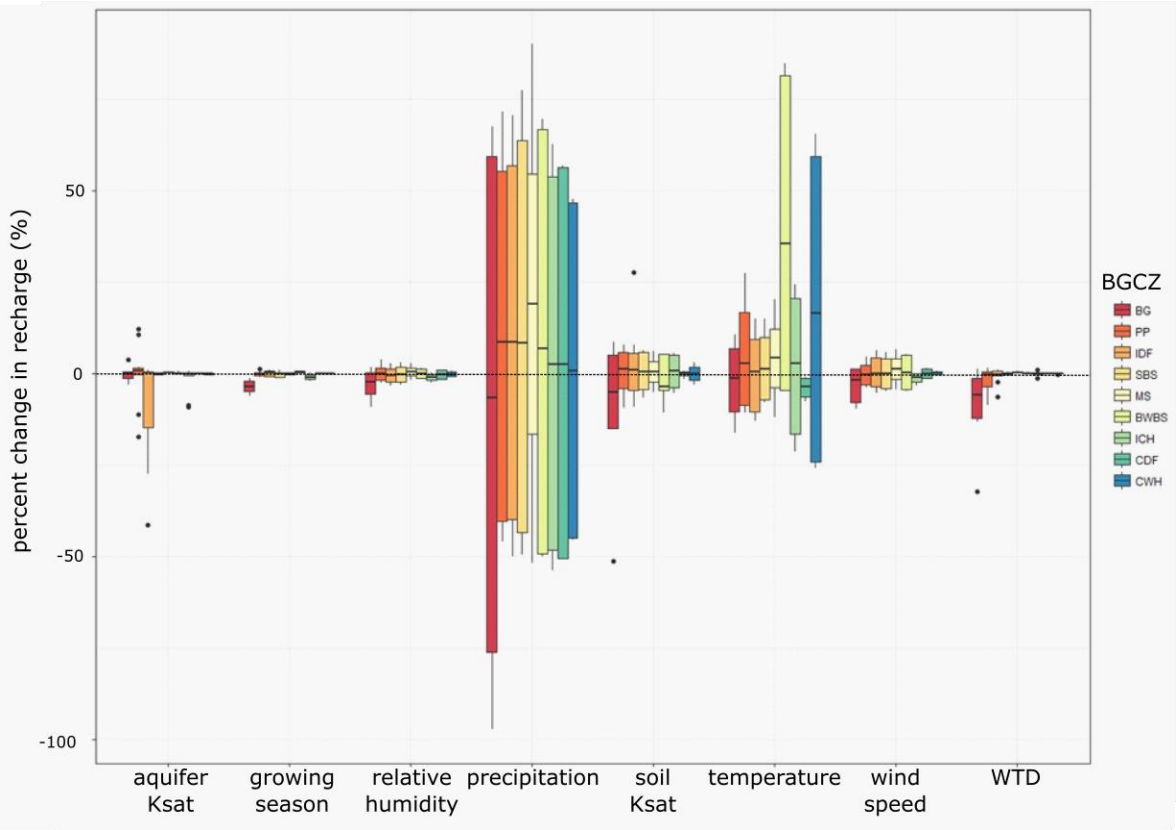

Figure 3.7 Parameter sensitivity to percent change in recharge per biogeoclimatic zone. The percent change in derived recharge values after each parameter is deviated by one standard deviation. AQ: Aquifer permeability; GWS: Growing season length; HUM: quarterly relative humidity; PRC: Precipitation; SOIL: Soil permeability; TMP: Temperature; WND: Wind speed; WTD: Water table depth. Biogeoclimatic zones are ordered from relatively low precipitation (red) to zones of high precipitation (blue). BG: Bunchgrass; PP: Ponderosa Pine; IDF: Interior Douglas-fir; SBPS: Sub-Boreal Pine-Spruce; SBS: Sub-Boreal Spruce; MS: Montane Spruce; BWBS: Boreal White and Black Spruce; ICH: Interior Cedar-Hemlock; CDF: Coastal Douglas-fir; ESSF: Engelmann Spruce-Subalpine Fir; CWH: Coastal Western Hemlock.

A one-at-time sensitivity analysis was conducted by varying aquifer K_{sat}, soil K_{sat}, aquifer depth, growing season length, relative quarterly humidity, wind, temperature and precipitation by their respective standard deviations. Results are illustrated in Figure 3.7 where precipitation has the strongest influence on derived recharge values for all biogeoclimatic zones. Soil K_{sat} and wind speed have a moderate effect (<10%) on R_{HELP}.

Changes in temperature yield a significant increase (60-80%) in R_{HELP} for the biogeoclimatic zones of BWBS and CWH; with a minor increase (~20%) in recharge for MS and ICH. This is due to the effect of frozen soil on runoff and infiltration rates (Schroeder et al. 1994). In these zones, a small increase in temperature significantly decreases the number of days under frozen soil conditions and the subsequent annual runoff flux. The model domain created in HELP has no surface slope, however, runoff can be generated when the soil is frozen, the temperature is above 0°C; and snowmelt occurs. Snowmelt occurs when the daily modelled temperature is above 0°C, and water is stored at the surface in snowpack. The soil remains frozen until the average of the previous 30 days is above 0°C. There is a moderate correlation between modelled runoff and reported mean annual snowfall per biogeoclimatic zone (Figure S3.6). In addition to runoff generated by soil conditions, the magnitude of runoff is determined based on the infiltration capacity of the soils. As expected, modelled runoff is larger (between 2 – 50 mm annually) in soils of lower permeability. This is due to the HELP model routines which determine snowmelt and infiltration. If there is snow on the surface, snowmelt occurs when the daily air temperature is above 0 °C, however if the soil is frozen, meltwater is unable to infiltrate into the soil and meltwater is lost to runoff.

4.3. REGIONAL -SCALE

Recharge results were obtained for 392 aquifers with a mean R_{PCR} of 393 mm yr^{-1} with a median of 229 mm yr^{-1}. The coverage of PCR-GLOBWB was variable in alpine areas due to data scarcity and coastal areas primarily classified as ocean (Figure S3.7). As a result, grid-cell values of zero near coastal regions and high alpine were removed from the analysis. Additionally, where $R_{PCR} < 0$, indicating zones where discharge flux was greater than the recharge flux, grid-cell recharge was manually adjusted to 0.

Table 3.7. Summary of average recharge per aquifer based on PCR-GLOBWB.

Biogeoclimatic Zones	BGCZ (Abbrv.)	Average R_{PCR} (mm yr^{-1})	Average R_{PCR} / Precipitation (%)	(σ)
Bunchgrass	BG	39	12%	3%
Ponderosa Pine	PP	86	24%	8%
Interior Douglas-fir	IDF	156	31%	11%
Sub-Boreal Spruce	SBS	195	28%	8%
Montane Spruce	MS	255	34%	7%
Boreal White and Black Spruce	BWBS	132	17%	11%
Interior Cedar—Hemlock	ICH	483	56%	15%
Coastal Douglas-fir	CDF	1012	93%	31%
Coastal Western Hemlock	CWH	822	36%	27%

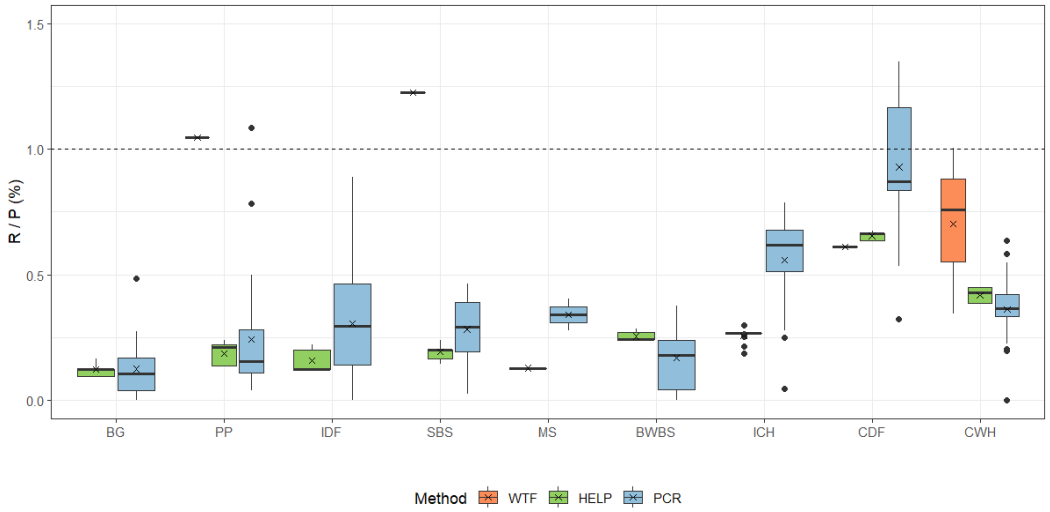

Figure 3.8. Annual recharge in mm yr^{-1} classified per biogeoclimatic zone. The mean value of recharge for each method is represented by an "x". WTF (min) represents the average recharge per aquifer based on unconsolidated (Sy = 0.02) and bedrock (Sy = 0.005) specific yield. WTF (max) represents the average recharge per aquifer based on maximum values of specific yield for unconsolidated (Sy = 0.2) and bedrock (Sy = 0.05) aquifers. BG: Bunchgrass; PP: Ponderosa Pine; IDF: Interior Douglas-fir; SBPS: Sub-Boreal Pine-Spruce; SBS: Sub-Boreal Spruce; MS: Mountane Spruce; BWBS: Boreal White and Black Spruce; ICH: Interior Cedar-Hemlock; CDF: Coastal Douglas-fir; ESSF: Engelmann Spruce-Subalpine Fir; CWH: Coastal Western Hemlock.

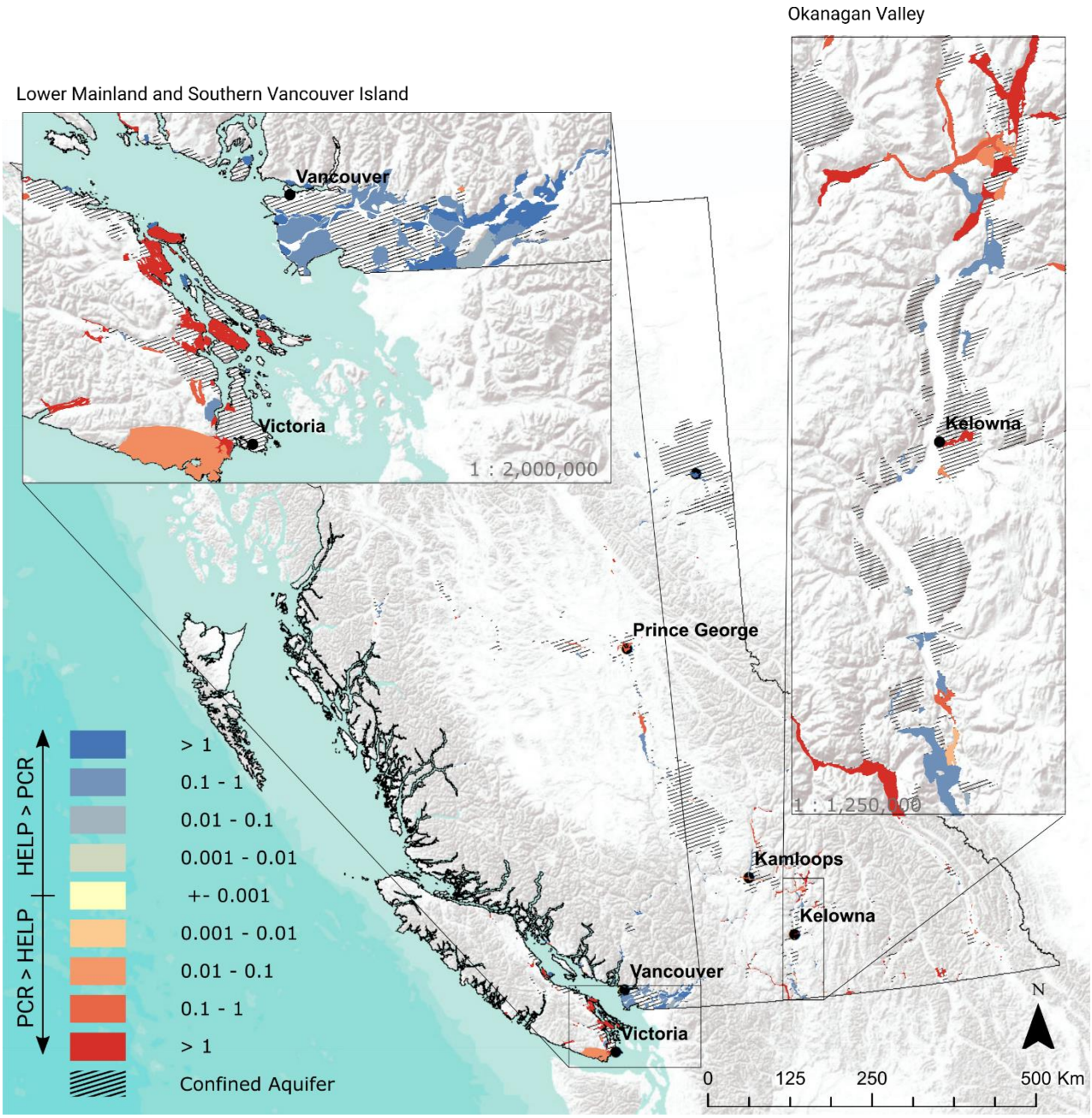

Figure 3.9 Modelled different of annual recharge (m yr^{-1}) of R_{HELP} and R_{PCR} for unconfined aquifers in BC.

Colors indicate the flux difference between modeled recharge results. Hashed aquifers represent confined aquifers.

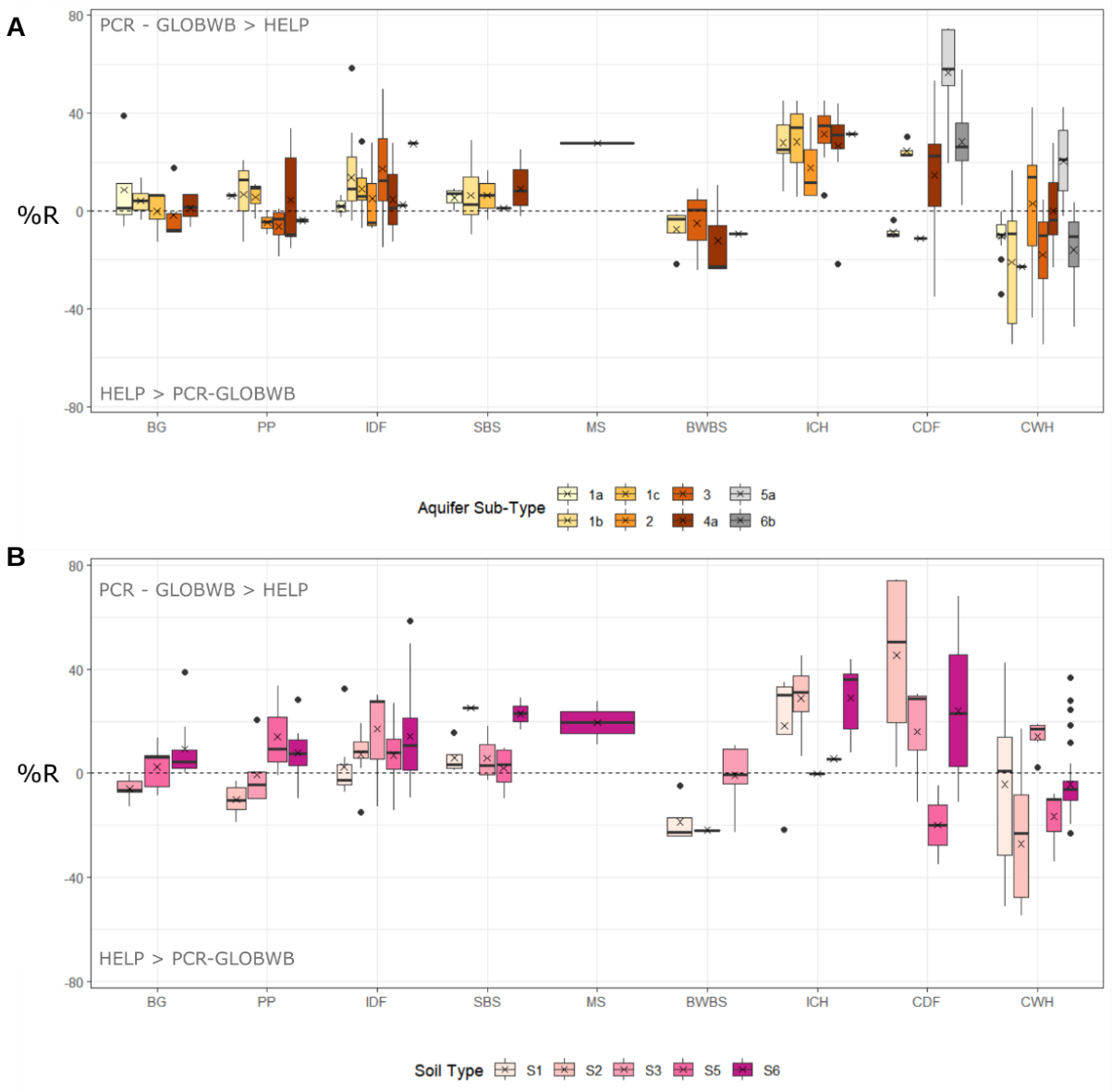

Figure 3.10 Resultant difference in estimated values of annual recharge normalized by average BGCZ annual precipitation from HELP and PCR-GLOBWB. (A) Distribution of aquifer sub-type. (B) distribution of aquifer soil types.

4.4. COMPARING RECHARGE WITH DIFFERENT METHODS

Figure 3.8 highlights the magnitude and variability of recharge normalized by precipitation estimated for all methods classified by biogeoclimatic zones. Derived recharge is normalized within each zone by the average annual precipitation per biogeoclimatic zone based on climate normal from 1961-1990. The HELP and PCR-GLOBWB results have an increasing trend of derived percent recharge with zones

of increasing precipitation. The spatial distribution of R_{HELP} compared to R_{PCR} is illustrated in Figure 3.9. The difference in percent recharge values derived from HELP and PCR-GLOBWB modelling is classified by biogeoclimatic zone and aquifer and soil types, respectively, illustrated in Figure 3.10. There are no significant trends by aquifer type, however there is a small trend in the arid biogeoclimatic zones (BG and PP) where higher soil permeabilities (S1 and S2) result in $R_{HELP} > R_{PCR}$, and lower permeabilities (S5 and S6) result in $R_{PCR} > R_{HELP}$.

5. DISCUSSION: RECHARGE METHODS ACROSS SCALES IN DIVERSE MOUNTAIN ENVIRONMENTS

Quantifying recharge on a regional scale is essential for groundwater management and the use of model methods is the only technique available in data scarce areas (Ireson et al. 2006; Van Camp et al. 2013), a common issues shared in many studies for quantifying the impact of future climate change on recharge rates (Scanlon et al. 2006; Holman et al. 2009; Allen et al. 2010a). The main uncertainties in our study were 1) limitations associated with input data within the framework of each model/method scale (observation scale) relative to aquifer-scale; 2) uncertainty associated with model processes in diverse hydrologic environments.

5.1. LIMITATIONS IN OBSERVATION-SCALE INPUT DATA

The differences in estimated average annual recharge for biogeoclimatic zones from the three methods highlight the discrepancies of data input and spatial representation of the observation scale (results from methods/models) relative to the process scales. The following section discusses the limitations of scales of input data for aquifer properties, precipitation, and ET employed by each model/method in quantifying aquifer-scale recharge.

5.1.1. AQUIFER PROPERTIES

All the method used in this analysis are based on aquifer permeability values from Gleeson et al. (2011) directly or indirectly. The WTF method and HELP model both apply the geometric mean permeability of each hydrolithology to associated aquifer material based on sub-type classification for estimating aquifer attributes associated

with straight line recessions and recharge, respectively. Whereas, the PCR-GLOBWB model calculates the geometric mean permeability over the grid cell based on the sub-grid heterogeneity of polygons of high resolution global lithology map (GLiM) from Hartmann and Moosdorf (2012) and the representative geometric mean permeability estimates from Gleeson et al. (2011).

Assuming average aquifer-scale recharge is dependent on average aquifer permeability (Lerner et al. 1990; Winter 2001), the uncertainty in permeability can be quantified based on the uncertainty in reported ranges of permeability represented by each method. Variability defined within an aquifer type can influence permeability ranges by orders of magnitude (Carmichael et al. 2008b; Carmichael 2013, 2014), therefore, as the variability of permeability increases within an aquifer derived aquifer-scale recharge uncertainty increases.

LOCAL-SCALE

Based on the analysis of the hydrographs in the WTF method, observed versus calculated linear phases were often under or overestimated. Due to the lack of local aquifer data, average aquifer permeability, which was based on values relative to aquifer material classifications, was used to estimate transmissivity, allocate average values of specific yield, and subsequently the length of the linear recession and amplitude of variation. Differences in observed and calculated linear phase length can be attributed to either aquifer attributes (S_Y and T) or based on proximity to drainage outlet. In addition, based on some of the observed values of S_Y from Carmichael et al. (2008a, 2008b, 2013, 2014), mapped unconfined aquifers may be confined based on the representative S_Y values. Therefore, where the calculated t_{lin} over or underestimated the observed linear phase reflects the heterogeneity within the aquifer relative to the average values.

Uncertainties and limitations in derived annual recharge values from the WTF method were due to the lack of detailed data relative to the monitoring location within the aquifer. Even though some observation wells, namely 296 (aquifer 74), 360 (aquifer 41), and 386 (aquifer 659), had similar estimated and observed values of

linear phase length based on regional data, high uncertainty remains in values of distance to stream, specific yield and transmissivity as several unique combinations of values could allude to the same linear phase length. Due to the sensitivity of estimated recharge to specific yield, without a locally representative value, estimated recharge values are highly uncertain. Therefore, the use of average aquifer values is not recommended for representative values of the local scale aquifer properties as the hydrograph is too sensitive to local heterogeneities.

Quantifying the uncertainty of estimated recharge relative to average aquifer-scale recharge was difficult to constrain as the method was sensitive to local aquifer material heterogeneities. Aquifer material heterogeneity can range on orders of magnitude, however, with an increase of spatial area, the representative areal average flux masks local heterogeneities and dampens the range of uncertainty. As the WTF method estimates recharge for a local area smaller than the aquifer-area, several monitoring locations within the aquifer would be required to estimate an average aquifer-scale value and decrease the uncertainty.

AQUIFER-SCALE

The applied method of HELP used aquifer-scale geometric mean values of soil and aquifer hydraulic conductivity. By using the geometric mean of soil data and aquifer-scale permeability, local heterogeneities of flow processes within the aquifer are masked, and aquifer-scale direct recharge is estimated. Assuming soils and aquifers were correctly classified by soil type and aquifer sub-type, soil permeabilities and aquifer permeabilities from Gleeson et al. (2011) should be representative of the actual average aquifer permeability. Uncertainty relative to heterogeneities in aquifer material can therefore be quantified based on the range of average values.

REGIONAL-SCALE

For PCR-GLOBWB, permeability was geometrically averaged over an approximately 100 km^2. Therefore, the uncertainty of aquifer permeability is relative to the range of heterogeneity in mapped permeability within the grid-cell

and the fraction of area representative of actual aquifer permeability. Therefore, as the range of heterogeneity within the cell was masked by the average value, uncertainty increases with a decrease in aquifer area relative to the grid-cell area.

5.1.2. PRECIPITATION

The physiographic features of mountainous terrain and relief attribute to many local heterogeneities observed in climate and vegetation. Climate and vegetation parameters are important factors in the magnitude and direction of the vertical flux of water. Precipitation and potential ET in mountainous terrain are often elevation dependent, therefore, as a result, capturing the representative average aquifer-scale climate can be especially difficult.

Climates have a large spatial coverage, however, in mountainous terrain, elevation can significantly impact important local scale climates (Moore et al. 2010). Based on our results, we see that precipitation is a critically sensitive parameter to direct recharge. Therefore, care should be taken when using areal scale average precipitation values for aquifer scale recharge estimates.

HELP and PCR-GLOBWB both use spatially averaged climate data. HELP utilizes zonal averages based on similar vegetation groups and climates. Whereas, PCR-GLOBWB precipitation is based on a global dataset, and precipitation is modeled at 0.5 degree resolution (approximately 10 km^2). As a result, PCR-GLOBWB represents an aerial average within proximity of the aquifer. However, as precipitation magnitude can be variable at different elevations, aquifer representation is dependent on elevation. As most aquifers are located in valleys, modeled precipitation would be less representative of aquifer precipitation. In contrast, HELP uses biogeoclimatic zones to inform precipitation volumes. As biogeoclimatic zones are elevation dependent, precipitation averages are likely more representative of annual aquifer precipitation.

5.1.3. EVAPORATION AND TRANSPIRATION

Using average values of ET to represent aquifer-scale conditions will be more uncertain for ET values averaged over heterogeneous elevations and vegetation types. ET is similarly modeled in HELP and PCR-GLOBWB based on areal and regional values. Actual ET is difficult to measure; however, ET fluctuates with vegetation type and decrease with increase in elevation.

The dynamics of ET are much more complex at a local scale, especially in mountainous terrain, and although climate data may be representative of aquifer-scale climate, limitations exist in the methods of modeling.

HELP values of ET are based on biogeoclimatic zone climate data, namely, evaporative zone depth, maximum leaf area index, wind speed, growing season and quarterly humidity. As aquifers were modeled according to representative climate region, these values are relatively representative of aquifer climate conditions. The resultant inverse correlation between precipitation zone and modeled ET in HELP compared to the increasing potential ET reported for each biogeoclimatic zones highlights some possible uncertainty in HELP modeled ET. Analysis into ET conditions were considered out of scope of this study, but future analysis should be made ti further explore the disparity in trending modeled and potential ET. One possible explanation in the difference in modeled and potential ET, is in the value of input leaf area index which is equivalent to a “good strand of grass”. This was the highest possible value available in the model, however in reality, aquifers are likely overlain with more heterogeneous vegetation types with variable ET values. Therefore, although the input values of climate data to HELP may be representative of the aquifer-scale climate, the internal computation is limited by the vegetation effect on ET, which affects the recharge estimation.

In PCR-GLOBWB, actual ET is partitioned into soil evaporation and plant transpiration. Soil evaporation is modeled under bare soil conditions and influenced by melt water stored in snow cover, saturated hydraulic conductivity and unsaturated hydraulic conductivity. However, evaporation is modeled based on

average climate conditions which are possibly not well representative of aquifer-scale climate. Similarly, although, plant transpiration is based on sub-grid variability (represented as a fraction of land surface) of four vegetation types, transpiration is similarly based on areal averaged values which may not be representative of aquifer-scale values.

5.2. SCALE DEPENDANT RELATIONSHIPS ON RECHARGE PROCESSES

Direct recharge is the most commonly modeled recharge flux, and many methods exists at various temporal and spatial scales (Scanlon et al. 2002). In order to represent recharge effectively in a groundwater model, considerations in processes controlling the rate of recharge and the objective of the modelling study should be considered (Sanford 2002). The results from this study illustrate that down-scaling and up-scaling observed recharge values relative to the aquifer-scale is especially problematic in diverse hydrologic environments. As has been shown in previous literature, recharge is significantly influenced by geology, vegetation, climate, and physiography (Winter 2001; Sanford 2002), and therefore, for direct recharge to be considered independent of scale, all factors must also show independence with an increase or decrease of scale relative to the method and the model scale.

The methods and models used in this study are constrained to estimating vertical recharge processes which can be misleading for aquifers sensitive to significant horizontal indirect recharge processes common in mountainous terrain. Mountain block and front or indirect recharge from streams have been shown to have significant contributions to annual aquifer recharge in the area (Smerdon et al. 2009).

LOCAL-SCALE

The WTF method is potentially the most comprehensive of the methods used in this study as water level fluctuations occur due to changes in aquifer storage (Healy and Cook 2002; Cuthbert 2010). The WTF method has the ability to estimate vertical fluxes of recharge accurately (diffuse and focused), however, uncertainty in estimated “net recharge” increases where substantial recharge occurs from

horizontal fluxes at the aquifer boundaries (ex. stream-driven or mountain block recharge). In addition, as the well is a point scale estimate (typically representative of the area in proximity to the well), focused horizontal flow will result in a higher groundwater head recession rate – indicative of a higher long-term annual recharge rate (Cuthbert and Tindimugaya 2010; Cuthbert et al. 2016). However, the signal from the focused indirect recharge dampens with an increased distance away from the well. As preferential recharge is a heterogeneous flux within the aquifer area, well scale observations would be expected to estimate a larger range of possible annual recharge fluxes relative to the well's location within the aquifer area. Therefore, for aquifers where recharge processes are thought to be more complex (direct & indirect processes) as is typical in mountainous terrain (Wilson and Guan 2004), several observation wells would be required to make aquifer-scale recharge estimates.

In addition, due to the sensitivity of the groundwater hydrograph to local scale effects, such a pumping, observing representative linear recessions was difficult to constrain without more well scale data (S_Y and T).

AQUIFER-SCALE

HELP models the average diffuse vertical recharge to the water table based on average aquifer data. As the modelled processes are constrained to vertical direct recharge, the major limitation of this method of estimating "net recharge" is relative to the significance of direct diffuse recharge for each aquifer. Aquifers which receive significant recharge flux from any indirect process initiated from outside the aquifer area will not be considered in the estimated recharge.

In addition, HELP is limited by the storage-routing unsaturated flow process (Allen et al. 2010a). Critical assumptions in the routines employed by the model introduce inherent uncertainty in the modelled processes. HELP makes the following critical assumptions: (1) vertical upward flux of water only occurs in the evaporative zone (set to 20cm); and (2) all water that percolates past the evaporative zone depth will eventually recharge the water table. Based on these assumptions and the nature of

the spatial distribution of aquifers, aquifers significantly influenced by additional recharge from indirect recharge processes or extra losses based on runoff/interflow processes or high ET from greater than 20 cm depth would be expected to under- or overestimate recharge fluxes. Without more local spatially distributed aquifer-scale recharge studies in various biogeoclimatic zones, quantifying the limitations of the HELP model's ability to accurately represent the fluxes affecting direct diffuse recharge remain unknown.

REGIONAL-SCALE

PCR-GLOBWB represents the areal average direct diffuse recharge, and as a result, includes focused and horizontal indirect recharge processes which occur within the grid cell. However, due to the structure of grid-cell models, quantifying the proportional influence of individual recharge processes is near impossible as the boundaries of the grid cell do not necessarily delineate the aquifer basin boundaries. As a result, the uncertainty associated with the representative nature of the grid cell is relative to similarity with the aquifer properties. Therefore, although PCR-GLOBWB is a more comprehensive model compared to HELP, due to the large areal scale of the grid cells, the uncertainty in estimated direct diffuse recharge is relative to the similarity in aquifer properties to grid-cell properties.

6. CONCLUSION

Quantifying recharge for spatially distributed aquifers in diverse hydrologic environments is challenging due to the complexities and heterogeneities in aquifer recharge processes, particularly in mountainous terrain. Aquifer-scale recharge estimates are critical in water management studies and data scarcity is the main motivation for the need to explore limitations and uncertainty in recharge estimation methods at a regional scale. Using three methods to quantify aquifer-scale recharge using methods at various spatial scales, this study has highlighted major limitations associated with methods which estimate recharge when the observation scale is relatively larger or smaller resolution compared to process scale.

Recharge estimates in diverse hydrologic environments, such as mountainous BC, are significantly limited by the (1) heterogeneity of recharge processes; (2) the model/method's ability to estimate horizontal and vertical fluxes into and out of the aquifer; and (3) the scale of the observed results relative to the aquifer-scale.

Particular care should be taken when using recharge estimates from methods or models which have input data or model processes at a scale smaller or larger than the working scale. Local scale methods, such as the WTF method, can accurately measure recharge for a representative distance from the monitoring well, however, without more detailed data at the local scale, recharge estimates are highly uncertain due to (1) effects within proximity to the well which may influence the linear recession, such as pumping or low permeability surficial deposits; (2) the representative nature of the recharge estimate relative to the aquifer; and (3) the difficulties associated with accurate estimating of specific yield. In addition, the WTF method is commonly used to quantify aquifer recharge in the province (Hodge 1977, 1995; Liskop and Allen 2005), however, care should be taken in the temporal scale of the time-steps relative to the estimated length of the linear phase of the groundwater head recession based on aquifer-properties. Due to the increased observation scale relative to the modeled area and the inability to quantify specific recharge fluxes, the uncertainty associated with recharge estimates from PCR-GLOBWB increases in regions where heterogeneity in geology, topography, and climate are high within the grid-cell.

CHAPTER 4:
Quantifying a crucial yet missing flux: groundwater's contribution to environmental flows in aquifer stress analysis

1. INTRODUCTION

Groundwater is a critical resource supporting human well-being (Konikow and Kendy 2005; Aldaya 2017), freshwater ecosystems (Constantz 1998; Barlow and Leake 2012; Noorduijn et al. 2018), and economic activities (Siebert and Döll 2010; Wada et al. 2012; Dalin et al. 2017). If groundwater abstraction exceeds groundwater recharge for prolonged periods, the declining storage of aquifer groundwater leads to persistent groundwater depletion (Wada et al. 2010; Famiglietti 2014a). Quantifying groundwater stress promotes the sustainable management of groundwater resources and groundwater supported ecosystems (Barlow and Leake 2012; Gleeson et al. 2012; Gleeson and Richter 2017). Water stress studies provide a framework to understand the dynamics for evaluating changes in groundwater resources by comparing water availability to human water use (van Beek L. P. H. et al. 2011; Wada et al. 2011; Richey et al. 2015; Mehran et al. 2017) and can promote sustainable practices in stressed regions through management and policy changes (Tringali et al. 2017; Bhanja et al. 2017).

Groundwater quantity stress is often approached as a comparison between use and availability where availability is often represented as the mean annual groundwater recharge (van Beek L. P. H. et al. 2011; Wada et al. 2011; Richey et al. 2015). Gleeson et al. (2012) proposed the novel approach of considering groundwater's contribution to environmental flows within the framework of defining availability. Scientific literature supports environmental flow regimes as essential to sustain freshwater and estuarine ecosystems and the human livelihood and well-being that depend on

the ecosystems' (Zektser et al. 2005; Acreman et al. 2014; Harwood et al. 2014; Gleeson and Richter 2017). However, few methods have been proposed in the literature to quantify groundwater's contribution to environmental flows (Gleeson and Richter 2017).

The objective of this project is primarily to determine aquifer-scale estimates of stress using the groundwater footprint (GF), which is often expressed as a unitless measure of GF normalized by aquifer area (GF/A). The GF is a ratio of use to availability, where availability is the difference between aquifer recharge and the aquifer's contribution to environmental flows. When the GF/A > 1, the aquifer is considered stressed, whereas, when the GF/A < 1, the aquifer is less stressed.

Two methods are used to quantify groundwater's contribution to environmental flows. The first method is a groundwater-centric approach from the application of the groundwater presumptive standard defined by Gleeson and Richter (2018), which suggests that high levels of ecological protection are maintained if 90% of baseflow is preserved. The second surface-water centric approach is a novel method which quantifies groundwater's contribution to environmental flows from streamflow using region-specific streamflow sensitivity metrics and local environmental flow policies. The groundwater presumptive standard approach is advantageous because it is a peer-reviewed method and aligned with groundwater stress management as it is derived explicitly from groundwater baseflow. However, limitations exist in using modelled baseflow values as observation data on measured aquifer-scale baseflow fluxes in the field is inherently difficult. Using a surface-water centric approach is an indirect method of quantifying groundwater's contribution to environmental flows, however, streamflow data is often more abundant than groundwater data, and making comparisons between modeled streamflow and gauged streams can help constrain method uncertainty.

Local studies are preferred as they capture a more holistic conceptual model and allow for the local management of well-scale allocations. However, due to the data scarcity at the local resolution and the large spatial distribution of the study area,

modeled values of baseflow and streamflow from the global hydrologic surface water and groundwater coupled model PCR-GLOBWB is used (Van Beek and Bierkens 2009). The first approach uses annual baseflow outputs from the groundwater layer of the model, whereas, the second surface water-centric approach uses streamflow outputs. In an effort to mitigate some uncertainty in the aquifer scale estimates of GF/A, the GF is calculated using four sets of data in order to determine higher or lower certainty in stress, based on the number of calculation which return GF/A > 1.

2. BACKGROUND

2.1. GROUNDWATER FOOTPRINT

It is commonly accepted that water stress can be defined by a ratio of water use to availability (Alcamo et al. 1997). Groundwater availability can be defined as the renewable water resource, whereas, use is the volume of water extracted form an aquifer.

$$Stress = \frac{Use}{Availability} \quad \text{(Eq 15)}$$

In an effort to quantify aquifer stress, the groundwater footprint provides an indication of area required to support known groundwater withdrawals and maintain environmental flow needs (Gleeson et al. 2012). The GF is defined as:

$$GF = \frac{C}{R - E} * A \quad \text{(Eq 16)}$$

where

GF is the area required to support known annual groundwater withdrawal and maintain environmental flows [m^2]

A is aquifer area [m^2]

C is area-averaged annual consumption of groundwater [$m^3\,yr^{-1}$]

R is annual recharge rate [$m^3\,yr^{-1}$]

E is the annual groundwater contribution to environmental streamflow [m^3 yr^{-1}]

Groundwater consumption (C) is the "use" numerator and is defined as the volume of groundwater removed from an aquifer. Groundwater availability is represented as the difference between recharge (R), which represent the natural influx of groundwater into the aquifer, and groundwater's contribution to environmental flows (E), which is a proportion of natural discharge to streams in order to maintain high standards of hydrologic and ecological protection.

2.2. GROUNDWATER'S CONTRIBUTION TO ENVIRONMENTAL FLOWS

Streamflow is considered the "master variable" due to the strong influence streamflow has on many critical physiochemical characteristics of rivers, including water temperature, geomorphology, and in-channel and off-channel habitat diversity (Poff et al. 1997). Previous EFN studies have historically been focused on hydrologic alterations as a result to surface water alterations such as dams, impoundments, and stream dependent water diversions (Poff and Zimmerman 2010) even though, it has long been understood that groundwater extraction reduces streamflow via the interception of groundwater that otherwise would have been discharged to the stream (Konikow and Kendy 2005; Barlow and Leake 2012; Famiglietti 2014a).

Streams are typically the primary discharge outlet of groundwater systems, and groundwater discharge is often the primary component of streamflow (Barlow and Leake 2012). Baseflow is generally described as the portion of streamflow derived from groundwater or other delayed sources, such as from lakes, reservoirs, snowpack, or glaciers, however, for the purpose of this study, baseflow derived from groundwater is the focus (herein referred to as *baseflow*). The magnitude of the baseflow flux is driven by hydraulic gradient between the aquifer and the stream, as well as, the hydraulic conductivity of the geologic material between the groundwater/surface water interface.

Interception of natural discharge from the aquifer to the stream occurs over various timescales relative to the distance between the pumping well and the stream (Barlow and Leake 2012). As pumping occurs, groundwater levels around the well decline into a cone of depression which establishes a new hydraulic gradient forcing water into the well. Initially, all the water abstracted from the well comes from aquifer storage, however over prolonged pumping, the cone of depression widens until all the water abstracted is derived from streamflow which highlights the various timescales over which pumping may be observed (Figure 4.1). When abstraction occurs in close proximity to a stream (ex. 10 m – 100 m), the impacts of pumping on the stream hydrograph may be limited temporally to day, months, or seasons relative to the time during which pumping is occurring, and limited spatially to the area around the well (Figure 4.2a). At greater distances from the stream (ex. 100 m – 10 km), seasonally variable pumping can be attenuated, such that streamflow depletion occurs throughout the year (Figure 4.2b). When pumping occurs a significant distance from the stream (ex. >10 km), the impact of pumping is delayed and may not be observable for decades (Figure 4.2c).

2.2.1. STREAMFLOW REGIMES IN BC

Streamflow regimes vary spatially and temporally based on the characteristic system defined as rain-dominated, snow-dominated, or hybrid (Eaton and Moore 2010; Allen et al. 2010b). Low flow zones in BC were regionalized by Coulson and Obedkoff (1998) by plotting drainage area by low flows (m^3/s), where a series of asymptotic curves separate the different low flow zones. Zones of homogeneous hydrologic characteristics were based on data in the region and used to extrapolate characteristics to ungauged drainage basins.

Due to the diverse hydrologic climate and topography, BC can be characterized by rain dominated, snow dominated, and mixed (rain and snow) regimes (Allen et al. 2010b; Eaton and Moore 2010). Rain dominated systems are found primarily in the coastal lowland areas and at lower elevations on the western Coast Mountains. These regions are strongly influenced by precipitation intensity with relatively little smoothing or lagging evident in stream hydrographs. The year to year variation in

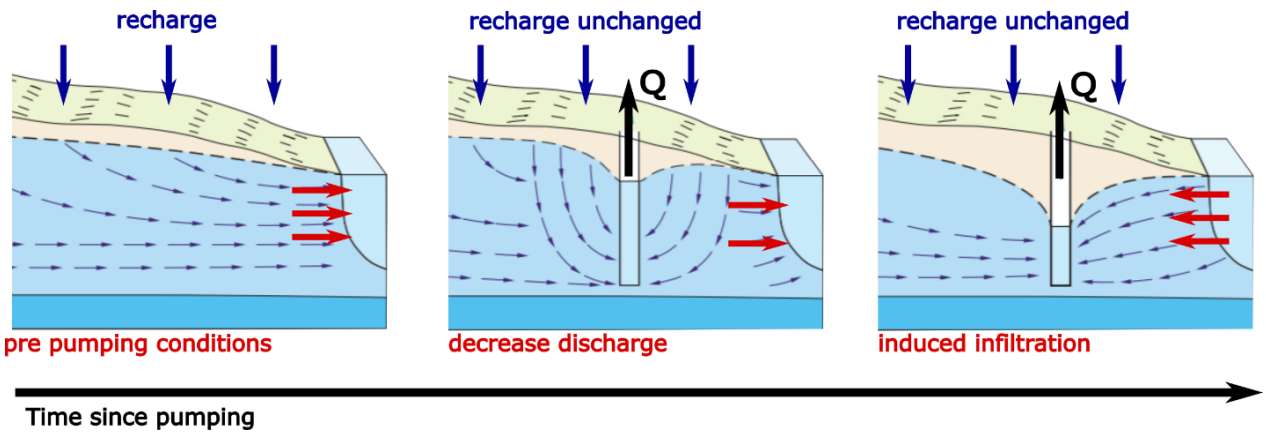

Figure 4.1 Streamflow depletion from groundwater pumping. During pre-pumping conditions, the aquifer discharge is equal to aquifer recharge. When pumping begins, the cone of depression forms in a radius around the well, where declines in water table direct groundwater to the well. Under continued pumping, the cone of depression widens, inducing infiltration from the stream, diverting the natural aquifer discharge from the stream to the abstracted volume (modified from Barlow and Leake 2012 and Gleeson and Richter 2017).

seasonal distribution of rainfall is significant due to the intensity of weather systems and is unlikely to resemble the long-term average pattern. The highest monthly flows are typically in early-winter (November - December), and lowest monthly flows occur in late-summer (July - August) when precipitation-generating weather systems are at a minimum. The interior plateau and mountain areas at higher elevations are dominated by snow-dominated regimes. These systems integrate precipitation inputs over the winter and spring within the snowpack then release the stored water during spring-summer melt. As a result, high flows in late-spring/summer (May-July) occur from increasing temperatures and meltwater. Low flows are generally experienced in the winter, however they may also occur during the late summer and fall as a result of low precipitation inputs and the exhaustion of the snowpack water supply. The monthly discharge pattern for a given year is generally similar to long term monthly averages. In coastal and near-coastal regions, the hydrological regime is more complex, and described as a hybrid regime. These regimes are most heavily dependent on air temperature which determines the relative strength of rain and snowmelt on the system. Direct groundwater recharge in these systems can be seasonally variable dependent on the timing of ground thaw conditions and precipitation.

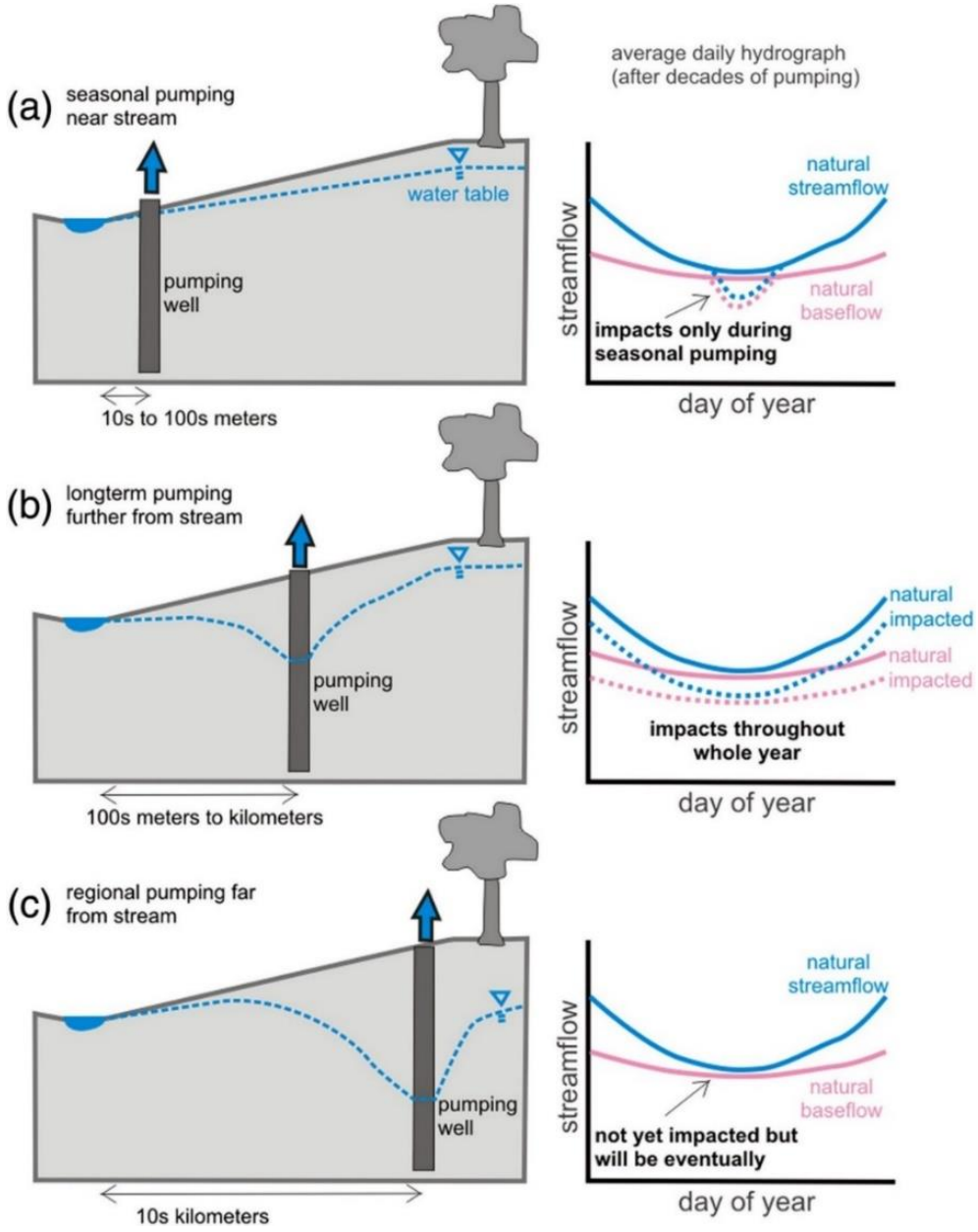

Figure 4.2. The impacts on streamflow are highly variable through time and space. Daily hydrographs at the end of decades of pumping to the right show natural streamflow and baseflow conditions and the resultant impacted streamflow and baseflow as dashed lines. (a) Seasonal pumping near a stream can potentially only impact part of the daily hydrograph. (b) Long-term pumping further from the stream could impact through the whole year. (c) Regional pumping far from the stream could potentially not significantly impact the stream for decades after the start of pumping. (Figure from Gleeson and Richter, 2017).

3. METHODS AND DATA

3.1. GROUNDWATER FOOTPRINT

3.1.1. THEORETICAL BACKGROUND

Four calculations of GF were made based on data from W, R_{HELP}, R_{PCR}, E_{PS}, and E_{LF} all reported in $m^3\ yr^{-1}$ for an aquifer area:

$$GF_1 = \frac{W}{R_{HELP} - E_{PS}} * A \quad \text{(Eq 17)}$$

$$GF_2 = \frac{W}{R_{PCR} - E_{PS}} * A \quad \text{(Eq 18)}$$

$$GF_3 = \frac{W}{R_{HELP} - E_{LF}} * A \quad \text{(Eq 19)}$$

$$GF_4 = \frac{W}{R_{PCR} - E_{LF}} * A \quad \text{(Eq 20)}$$

where

$GF_{1\text{-}4}$ is the groundwater footprint [m^2]
W is annual volume of groundwater use [$m^3\ yr^{-1}$]
R_{HELP} is annual volume of recharge modelled by HELP [$m^3\ yr^{-1}$]
R_{PCR} is annual volume of recharge modelled by PCR-GLOBWB [$m^3\ yr^{-1}$]

E_{PS} is annual volume of groundwater's contribution to environmental flows derived based on the groundwater presumptive standard [$m^3\ yr^{-1}$]

E_{LF} is annual volume of groundwater's contribution to environmental flows derived based on the low flows method [$m^3\ yr^{-1}$]

Each combination of input parameters has inherent uncertainties, so aquifers were categorized using a simple and transparent stress index that also clarifies the uncertainty of results. If all calculations of the GF/A indicate GF/A > 1 where the method is applicable, the aquifer is considered *stressed (high certainty)*. If GF/A > 1 based on at least one set of data, the aquifer is considered *stressed (less certainty)*. If all

calculations indicate GF/A < 1, the aquifer is considered *less stressed*. The GF calculation is based on regional data and the data is limited by uncertainties, and therefore, an aquifer with a GF/A = 2 is not considered more stressed than a GF/A = 10.

3.1.2. WITHDRAWAL DATA

Groundwater consumption (C) is commonly defined as the volume of groundwater removed from an aquifer; however, due to the lack of data on groundwater use in BC, withdrawal (W) is used as a proxy for C in the equation to represent the availability in the GF calculation. W was derived based on readily available data and statistics on sectoral use and represents a conservative approximation of groundwater use until additional data can be used to supplement or replace current derived sectoral groundwater volumes. An important differentiation between C and W in this study, is that C represents the volume of water after return flows to an aquifer are accounted for from groundwater extracted volumes. For example, groundwater extracted for the purpose of irrigated agriculture is often in excess of the required amount and volumes of freshwater not consumed by the crops are returned to the aquifer. As data was unavailable to make consistent and scientifically sound approximation of C, W is used as a conservatively large approximation and accounts for the volume of groundwater removed from an aquifer via wells. Groundwater withdrawal is estimated for the domestic, municipal, commercial, industrial, agricultural, and finfish aquaculture sectors.

3.1.3. RECHARGE DATA

Recharge (R) represent the natural influx of groundwater into the aquifer. One of the main challenges with this component is that aquifers in BC represent a large spatial distribution and diverse climate. Although many local studies exist in populated areas of BC (Zebarth et al. 1998; Allen et al. 2004; Scibek and Allen 2006a; Denny et al. 2007), in order to analyze the magnitude of aquifers in the province and make a comparative analysis, two approaches are used to identify recharge. A hydrologic modelling software HELP - Hydrologic Evaluation of Landfill Performance (Schroeder et al. 1994) is used to determine aquifer scale estimates of

natural recharge (R_{HELP}). A new 'generalized' methodology is derived in this study which assigns aquifers into biogeoclimatic zones, maps soil and aquifer types, and then simulates R with the HELP model as was done in the localized modelling studies. HELP is a one-dimensional, water balance software that simulates vertical infiltration through multiple soil and aquifer layers within the vadose zone, and internally calculates evapotranspiration and runoff that may contribute to overland flow. The second approach uses spatially downscaled estimates of R_{PCR} derived from PCR-GLOBWB. As HELP and PCR-GLOBWB only simulate the vertical percolation from precipitation, confined aquifers are excluded from the recharge analysis.

3.2. GROUNDWATER PRESUMPTIVE STANDARD

3.2.1. E_{PS} THEORETICAL BACKGROUND

The groundwater presumptive standard is based on the Sustainability Boundary Approach of Richter (2010) which involves restricting hydrologic alterations to within a percentage-based range of natural or historical flow variability (Figure 4.3). The groundwater presumptive standard is a standard for managing groundwater pumping appropriate for maintaining environmental flows by explicitly including the potential impacts of groundwater pumping over long temporal scales. The groundwater presumptive standard suggests that high levels of ecological protection will be provided if groundwater pumping decreases monthly natural baseflow by less than 10% through time (Gleeson and Richter 2017).

$$E_{PS} = 0.9 \cdot Q_{bf} \quad \text{(Eq 21)}$$

where

E_{PS} is groundwater's contribution to environmental flows based on the groundwater presumptive standard [m yr^{-1}]

Q_{bf} is baseflow, the flux from the aquifer to the stream [m yr^{-1}]

Baseflow is commonly defined as "the portion of [stream] flow that comes from groundwater or other delayed sources" (Hall 1968; Tallaksen 1995) and can originate

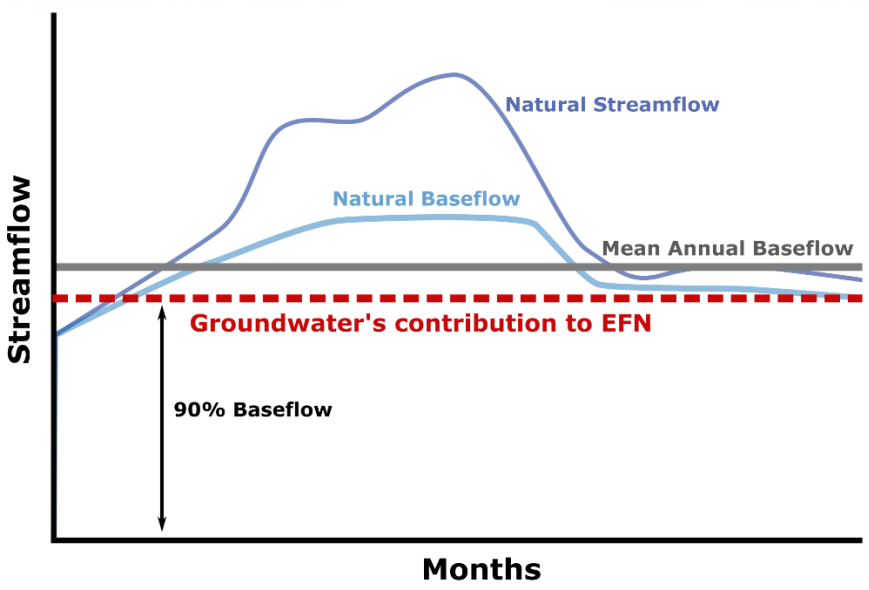

Figure 4.3 Theoretical application of E_{PS}. Groundwater's contribution to environmental flows (EFN) is based on 90% the average annual baseflow.

from groundwater, lakes, reservoirs, snowpack, or glaciers. For the purpose of this study, baseflow is defined as groundwater-derived baseflow since the focus of this study is on aquifer stress. The groundwater presumptive standard of 10% should be considered nested within and part of current environmental flow frameworks for streamflow rather than additional 10%. This presumptive standard is intended to provide estimation of E where detailed scientific assessment of environmental flow cannot be undertaken.

3.2.2. BASEFLOW DATA

Spatially distributed estimates of baseflow were derived from a high-resolution global-scale groundwater model (De Graaf et al. 2015). The linear groundwater store of PCR-GLOBWB (Van Beek and Bierkens 2009) is represented as a MODFLOW layer simulating groundwater flows and groundwater heads in a single-layer unconfined aquifer at a spatial scale of approximately 100 km^2 for British Columbia. Aquifer properties are prescribed and the MODFLOW layer was forced by long-term averages of surface water levels and groundwater recharge (running period 1960 – 2000) outputs from PCR-GLOBWB. Aquifer properties in the model were

based on the high resolution global lithology map (Hartmann and Moosdorf 2012) and global permeability estimates of Gleeson et al. (2014). Large lakes and the ocean are represented as a Dirichlet boundary condition, where the ocean groundwater head was set to 0 m, and water levels of the lakes were set at elevation levels provided by the HydroSHEDS (Lehner et al. 2008) digital elevation map. The steady-state groundwater recharge output from PCR-GLOBWB was multiplied by the cell area for input into the recharge package of the MODFLOW calculation. Groundwater body and surface water body interactions are incorporated in the groundwater model through MODFLOW river (Q_{RIV}) and drain (Q_{DRN}) packages to represent large rivers (width > 10 m) and small rivers (width < 10 m), respectively. Baseflow, Q_{bf}, is taken as the sum of two model outputs:

$$Q_{bf} = Q_{drn} + Q_{riv} \quad \text{(Eq 22)}$$

where

Q_{bf} is the flux of flow from aquifer into the stream [$m^3\ yr^{-1}$]

Q_{riv} is the flow from the aquifer to large (width > 10 m) [$m^3\ yr^{-1}$]

Q_{drn} is the flow from the aquifer to small rivers (width < 10 m) [$m^3\ yr^{-1}$]

Flow from the groundwater system to large rivers, Q_{riv}, occurs when the modelled groundwater head is above the calculated river bottom using the RIV package. Groundwater flow to small rivers was modelled using the DRN package, where water can leave the groundwater system through the drain when heads rise above the drainage level, which is the surface elevation specified in PCR-GLOBWB. Where Q_{RIV} or Q_{DRN} had positive values, indicating a positive flux from the stream to the aquifer, these values were set to zero, and E_{PS} is consequently equal to 0. As Q_{bf} is reported as $m^3\ d^{-1}$, volumes were converted to annual fluxes ($m\ yr^{-1}$) and area averaged for the spatial coverage of a mapped aquifer. de Graaf (2015) used an additional component of total groundwater discharge is included to represent local sags, springs, and minor streams higher up in mountainous areas. This additional drainage flux is not included in our calculation of baseflow, as our goal is to quantify aquifer baseflow. As most aquifers in our study region are located in valley bottoms,

the additional component is assumed to capture drainage occurring outside the boundary of the aquifer.

3.3. LOW FLOW ZONE APPROACH

3.3.1. E_{LF} THEORETICAL BACKGROUND

During low flow conditions, groundwater is often the sole source of river water, and is a critical flux particularly in montane environments which sustains downstream water supplies and provide other ecosystem services (Frisbee et al, 2010; Batlle-Anguilar et al, 2014). Low-flows are often identified using streamflow hydrographs or flow duration curves and the Q90 or Q80 rule, where flows lower than the 90th or 80th percentile respectively, equate to low flow conditions (Coulson and Obedkoff 1998; Pastor et al. 2014). This second approach, uses a surface water centric position to identify groundwater fluxes from streamflow hydrographs and explicitly considers surface water environmental flow metrics. The environmental flow metrics in this methodology are based on the environmental flow policy for British Columbia (Province of British Columbia 2016b), but similar methodologies are used globally (Pastor et al. 2014).

Based on monthly streamflow sensitivity classification and estimated annual contributions of groundwater to streamflow, quantifying groundwater's contribution to environmental flows based on this method can be described as:

$$E_{LF} = k_{EFN} \cdot Q_{GW} \quad \text{(Eq 23)}$$

where

E_{LF} is groundwater's contribution to environmental flows [m^3 yr^{-1}]
k_{EFN} is the coefficient representing the proportion of annual streamflow reserved for EFN [-]
Q_{GW} is mean annual groundwater supported streamflow [m^3 yr^{-1}]

In order to derive the mean annual groundwater supported streamflow, mean monthly streamflow data is classified into low, moderate, and high sensitivity months. The classification of mean monthly streamflow (MMF) as high sensitivity

months are assumed to represent low flow conditions supported primarily by groundwater. Quantifying the mean annual groundwater supported streamflow is derived using the extrapolation of the representative month based on the sensitivity classification. Groundwater discharge to streams increases during high flow conditions, and therefore, using the annual extrapolation of the minimum MMF would yield an underestimation of annual groundwater supported streamflow. The maximum MMF during low flow conditions was used as a representative month to provide a conservative estimate of groundwater's contribution to streamflow. For major streams which never enter low flow conditions, the representative month is the lowest MMF within the intermediate or high flow conditions. As modelled streamflow is represented by a grid cell area, streamflow is composed of two main parameters, $Q_{LF,\ upstream}$, the upstream sourced flow, and Q_{LF}, the flow sourced from within the local grid cell area. The local additions equate to the sum of discharges into the stream from the local cell area, such as baseflow, runoff, interflow. The ratio of local additions to streamflow, f_{local}, are derived as follows:

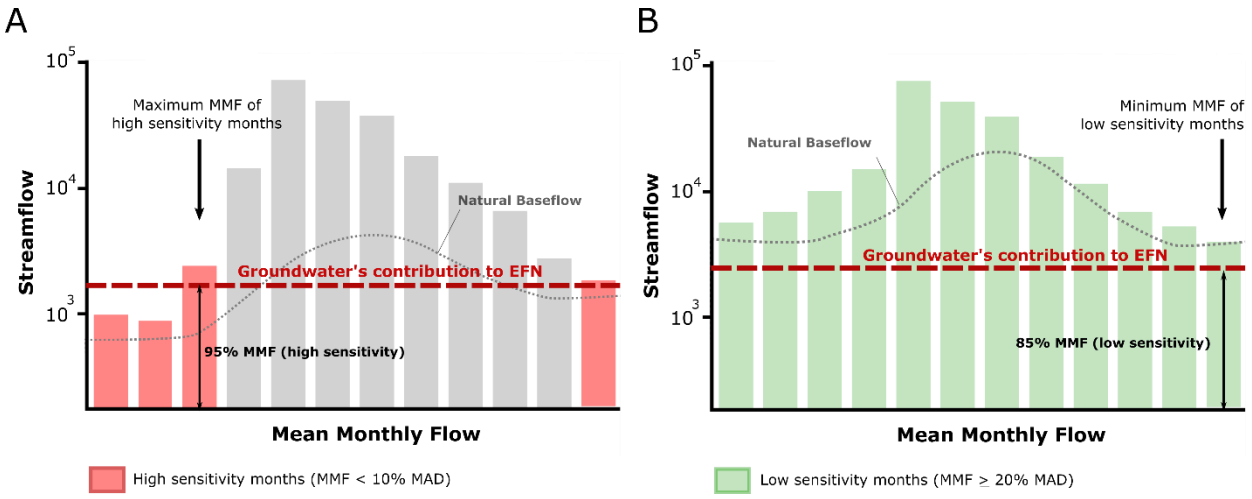

Figure 4.4 Example of streamflow hydrograph illustrating E_{LF} method. MMF is classified into high, moderate or low sensitivity based on the MMF relative to MAD. (A) For high sensitivity streams, the highest MMF within the high sensitivity months is used to estimate groundwater's annual contribution of environmental flow needs (EFN). (B) For moderate and low sensitivity streams, k_{EFN} is 90% or 85% of the minimum MMF, respectively.

$$f_{local} = \left(1 - \frac{Q_{LF,\ upstream}}{Q_{LF}}\right) \quad \text{(Eq 24)}$$

where

f_{local} is the ratio of locally derived streamflow (from grid cell area) to total streamflow [-]

$Q_{LF,\ upstream}$ is the upstream flow of the representative MMF [$m^3\ yr^{-1}$]

Q_{LF} is the representative MMF [$m^3\ yr^{-1}$]

Q_{GW} represents groundwater's annual contribution to streamflow normalized by grid cell area, and Q_{LF} is the mean monthly flow for the representative month:

$$Q_{GW} = \frac{12 \cdot f_{local} \cdot Q_{LF}}{A_{cell}} \quad \text{(Eq 25)}$$

where

Q_{GW} is mean annual groundwater supported streamflow [$m^3\ yr^{-1}$]

f_{local} is the ratio of locally derived streamflow (from grid cell area) to total streamflow [-]

Q_{LF} is the representative MMF [$m^3\ yr^{-1}$]

A_{cell} is area of the grid cell (~100 km^2) [m^2]

3.3.2. STREAMFLOW SENSITIVITY

Figure 4.4 demonstrates an example of a flow hydrograph is first classified into low flow, intermediate, and high flow months based on mean monthly flow statistics. To derive Q_{GW}, the mean annual groundwater supported streamflow, mean monthly streamflow data is classified into low, moderate, and high sensitivity months based

Table 4.1 Classification of flow sensitivities based on BC's EFN policy using mean monthly flows and mean annual discharge values.

Hydrologic season	BC stream classification	Determination method	k_{EFN}
Low flow	High sensitivity	< 10 % MAD	95%
Intermediate flow	Moderate sensitivity	10 -20 MAD	90%
High flow	Low sensitivity	≥ 20% MAD	80%

on the BC EFN policy assuming all streams are fish bearing. The classification of high sensitivity streams (Table 4.1) are assumed to represent low flow conditions and supported primarily by groundwater.

3.3.3. STREAMFLOW DATA

Streamflow is output from the macroscale hydrological model PCR-GLOBWB (Van Beek and Bierkens 2009). PCR-GLOBWB simulates for each grid cell (0.5° x 0.5° grid globally and approximate grid size of 10 km^2 for British Columbia) and each time step (daily) the water storage in two vertically stacked soil layers with maximum depths of 0.3 and 1.2m respectively, and for an underlying groundwater reservoir layer (Store 3). Changes in water storage are attributed to vertical water exchanges between the layers (infiltration, percolation, and capillary rise) and between the top layer and the atmosphere (rainfall, evapotranspiration, and snowmelt). The model also calculated interception (Canopy) and snow storage (T). Meteorological forcing was applied to the model with a daily resolution and is constant over the grid cell.

Sub-grid variability is taken into account through short and tall vegetation (extracts water from top layer and both layers respectively), open water (lakes, reservoirs, floodplains, and wetlands), soil types. Specific runoff from a cell to the river ($Q_{Channel}$) consists of surface runoff (based on Store 1), interflow (runoff form the second soil reservoir), and baseflow (groundwater discharge). In order to model surface water runoff, interflow, and baseflow, an estimate of drainage density of perennial streams within each grid cell is required. Surface runoff and interflow are parameterized based on variability within grid soil saturation based on the values within the digital soil map of the world (FAO 2003). Interflow is not explicitly modelled, however average slope length and drainage distance are used to capture drainage between high and low conductivity soils common in mountainous area soils.

Surface water constitutes a separate land cover class which differs from the land surface proper as described above. The main processes are the direct input to or withdrawals from the open water due to precipitation, potential evaporation and water consumption, and the resulting lake storage ad river discharge. Total runoff

from the land surface proper, based on the resultant volumes from the above mentioned processes of direct runoff, interflow and baseflow, are fed without delay to the river network prior to routing. For full details of the model see Van Beek and Bierkens (2009).

3.4. MODEL PERFORMANCE OF MEAN MONTHLY STREAMFLOW AND LOW FLOW PERIODS

The seasonal cycle can be characterized by three different performance metrics which provide insight into the model's ability to capture aspects of the mean annual cycle (Gudmundsson et al. 2012). Mean monthly flow (MMF) data from 1960-2010 was gathered for 81 gauged streams across the province managed by Environment Canada. Drainage basins ranges from 6 - 217,000 km^2 and eight low flow zones characterized by a combination of pluvial and nival dominated regimes.

The model's ability to capture mean monthly streamflow is quantified using the relative bias:

$$\Delta\mu_{monthly} = \frac{\mu_m - \mu_o}{\mu_o} \qquad \text{(Eq 26)}$$

where

$\Delta\,\mu_{monthly}$ is the relative bias per month [-]
μ_m is the modeled mean monthly flow [m^3 yr^{-1}]
μ_o is the observed mean monthly flow [m^3 yr^{-1}]

Zero is the optimal value of is $\Delta\,\mu_{monthly}$, where negative values indicate underestimation and positive values indicate overestimation.

The MSE is commonly used to quantify total model error, however the MSE does not distinguish between different error components. Gudmundsson et al. (2012) uses the components of the MSE, following Gupta et al. (2009), to quantify the relative contribution of each component to the total error to be assessed. As low flow periods are more important than the annual performance, MSE and the decomposition into

relative error from bias, amplitude, and correlation was based on the three months during low flow periods. Low flow periods were based on the low flow zones.

$$MSE = \frac{1}{N}\sum_{i=1}^{N}(\mu_m - \mu_o)^2 \quad \text{(Eq 27)}$$

$$MSE = A + B + C \quad \text{(Eq 28)}$$

where

MSE is the mean squared error [$m^3\ yr^{-1}$]
μ_m is the modeled mean monthly flow [$m^3\ yr^{-1}$]
μ_o is the observed mean monthly flow [$m^3\ yr^{-1}$]
A is bias [-]
B is amplitude [-]
C is correlation [-]

with

$$A = (\mu_m - \mu_o)^2 \quad \text{(Eq 29)}$$

$$B = (\sigma_m - \sigma_o)^2 \quad \text{(Eq 30)}$$

$$C = 2\sigma_m\sigma_o(1 - r) \quad \text{(Eq 31)}$$

where

σ_m is the standard deviation of modeled mean monthly flow [$m^3\ yr^{-1}$]
σ_o is the standard deviation of observed mean monthly flow [$m^3\ yr^{-1}$]
r is Pearson's correlation coefficient [-]

The model's ability to capture the mean low flow is quantifies using the relative bias (A). The error in variance is captured by amplitude (B), which is the spread from the lowest to the highest monthly value and indicates the difference in seasonal cycle magnitude. The error in correlation (C) is the model's ability to capture the timing of the seasonal cycle.

4. RESULTS

4.1. QUANTIFYING MODEL PERFORMANCE OF STREAMFLOW

Figure 4.6 shows the $\Delta\mu_{monthly}$ for the various low flow zones and range of drainage basin areas of the observed gauged streams. Modeled MMF values were moderately underestimated compared to observed MMF in drainage areas >10,000 km^2. In contrast, the error in MMF magnitude for small drainage areas (<100 km^2) had a large distribution of values, whereby the model significantly overestimated observed values. Drainage areas between 100 - 10000 km^2 had a similar response to error in MMF, whereby more than half of the comparison between modeled and observed MMF were underestimated, whereby the other half was overestimated.

Based on the results of bias ($\Delta\mu_{monthly}$) for drainage areas and the uneven distribution of drainage basin size within each Low Flow Zone, Low Flow Zone analysis of error was performed for drainage basin areas of 100 – 10,000 km^2. In general, there is no observed relationship with rainfed and melt-fed streamflow, however the model had greater performance in modeled MMF in the zones of Vancouver Island, Coast Mountains, Southeast Mountains.

The total model error was assessed using mean squared error (MSE) for only the low flow periods classified by each zone. Error for smaller drainage areas (<100 km^2) were on average over two orders of magnitude lower than large drainage areas (>10,000 km^2). This significant difference between the MSE results from different drainage basins is a product of the difference in mean low flow (averaged over 3 months) which in absolute terms, will increase with drainage basin size due to the relative increase of streamflow with drainage basin size, as opposed to the relative difference in mean flow (illustrated in Figure 4.6a).

The bottom panels of show the decomposition of the MSE into relative components on error in bias (mean), amplitude (variance), and timing (correlation). The sum of the axis values of each data point equal one. Points in the center are an equal contribution of the three error components. In general, the relative error in mean values dominates total error of the modeled values, where almost 100% of the

modeled error for drainage areas >1,000 km^2 are due to Vancouver Island and Georgia Basin attribute most of the MSE to error in mean, however have slightly higher errors in correlation and variance respectively compared to the other Low Flow Zones dominated by errors in mean.

4.2. GROUNDWATER'S CONTRIBUTION TO ENVIRONMENTAL FLOWS

Derived values of E_{PS} have relatively regionally consistent result of groundwater's contribution to environmental flows compared to E_{LF} estimates. Similarly, E_{LF} resulted in a larger distribution of values.

The resultant E_{PS} is based on a fraction of the sum of the RIV and DRN outputs from PCRGLOBWB. The RIV outputs to modeled streamflow have variable coverage over the province, which is to be expected, as many rivers in BC have stream width of less than 10 m. RIV cells were corrected to zero if there was a positive flux from the stream to groundwater (SF 4.1a). DRN is the modeled flux representative of smaller rivers, which makes up the majority of modeled baseflow in BC (SF 4.1b). Modeled small rivers can only have a positive flux from groundwater to streamflow. Based on the general trend of E_{PS} results, environmental flows have a larger contribution of streamflow from groundwater along the coast and in mountainous areas, with no discharge for many areas in the interior of the province. E_{LF} values were similarly higher in mountainous areas, however, along major rivers, groundwater's contribution to streamflow is anomalously high.

Figure 4.9 highlights the distribution of modeled low flow month representative of the annual low flow flux for E_{LF}. In general, the timing of modeled low flow periods were in agreement with observed monthly low flows based on streamflow hydrographs from observation wells used in the model performance (Section 4.1 – SF 4.2). k_{EFN} was based on the minimum MMF stream sensitivity, illustrated in Figure 4.8a. In general, most high sensitivity streams were located in mountainous areas, with low sensitivity in the interior and coastal areas. The difference between the minimum MMF and the MMF of the maximum high sensitivity month is shown in Figure 4.8b. When the raster distribution of resultant fluxes from E_{PS} and E_{LF} were

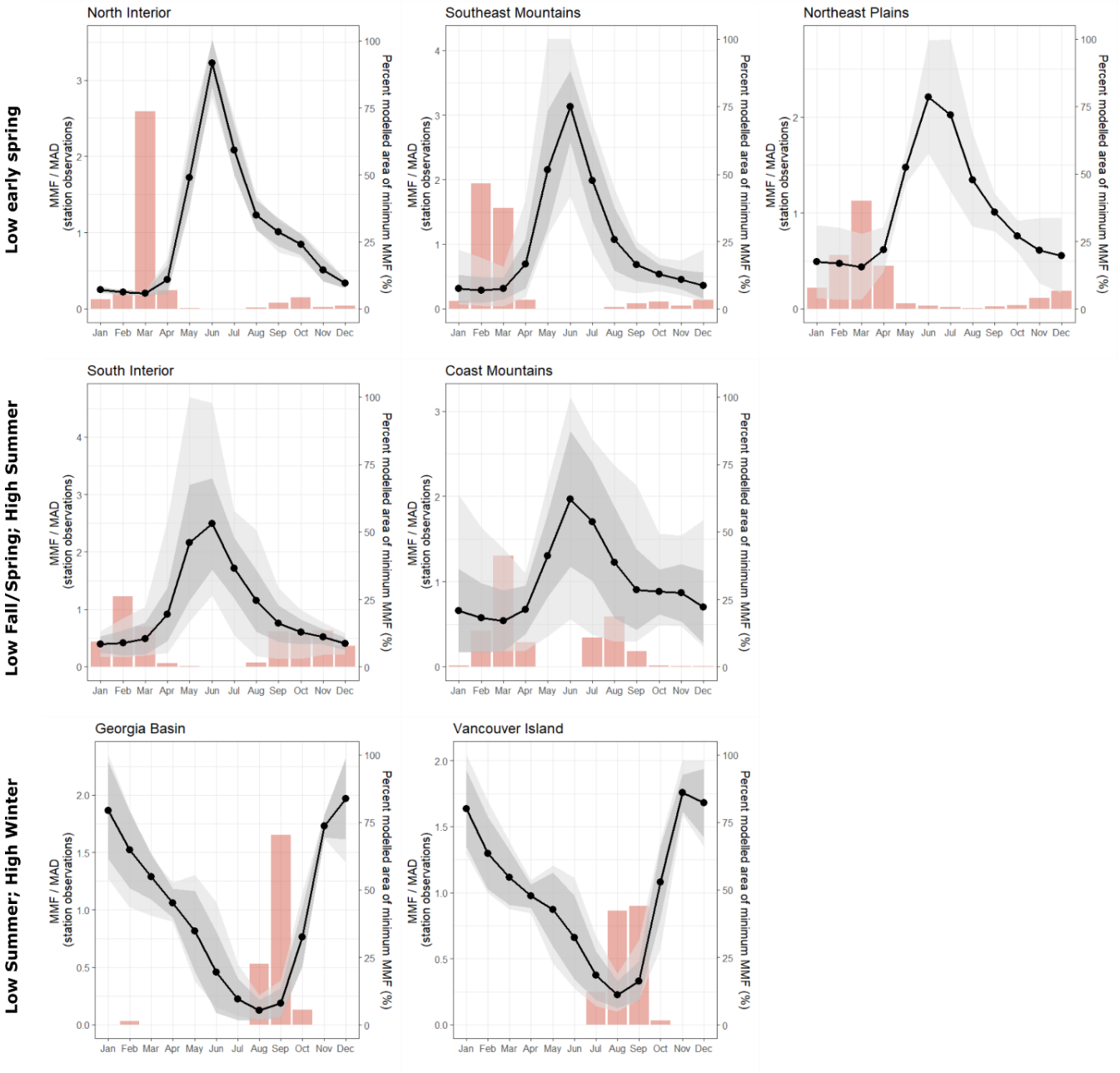

Figure 4.5. Gauged stream hydrographs for observation stations used in sensitivity analysis classified by low flow zone. Black line is the average streamflow, dark grey shaded area represents the standard deviation and light grey shading indicated the minimum and maximum mean monthly flow. Right hand axis represents the pink bar graphs highlighting the low flow seasonality in each low flow zone. The pink bars are the percent of area of each low flow zone with the minimum mean monthly streamflow.

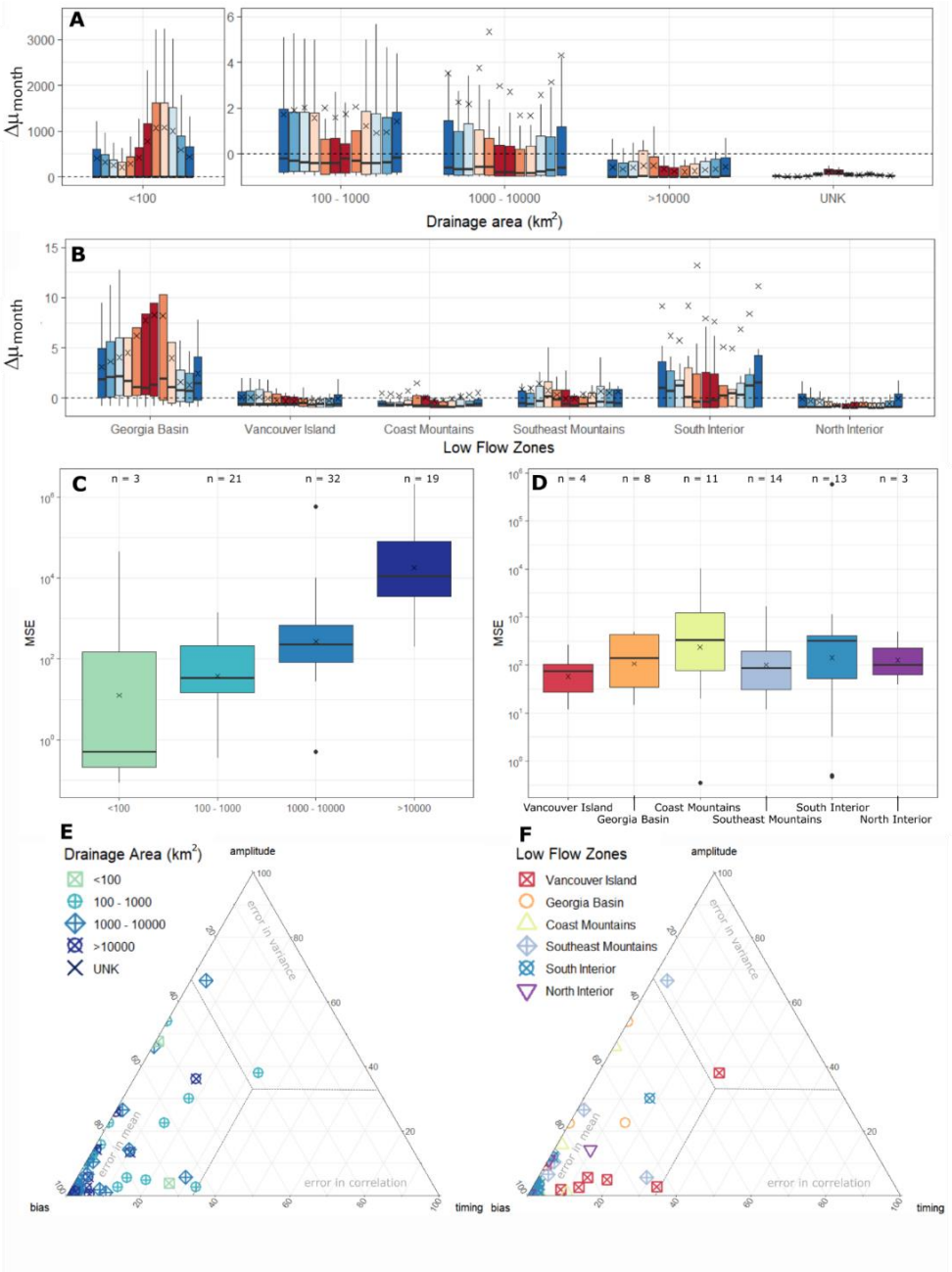

Figure 4.6. Sensitivity analysis results comparing modeled MMF from PCR-GLOBWB and gauged streams. The error in mean by month from January to December by drainage area size (A) and low flow zone (B). The mean squared error (MSE) assessing the total modeled error during the 3 monthe period of low flows for drainage basin area (C) and low flow zone (D). The ternary diagrams diagnose the relative error in the components of bias, amplitude of variation and correlation of the MSE by drainage basin area (E) and low flow zone (F).

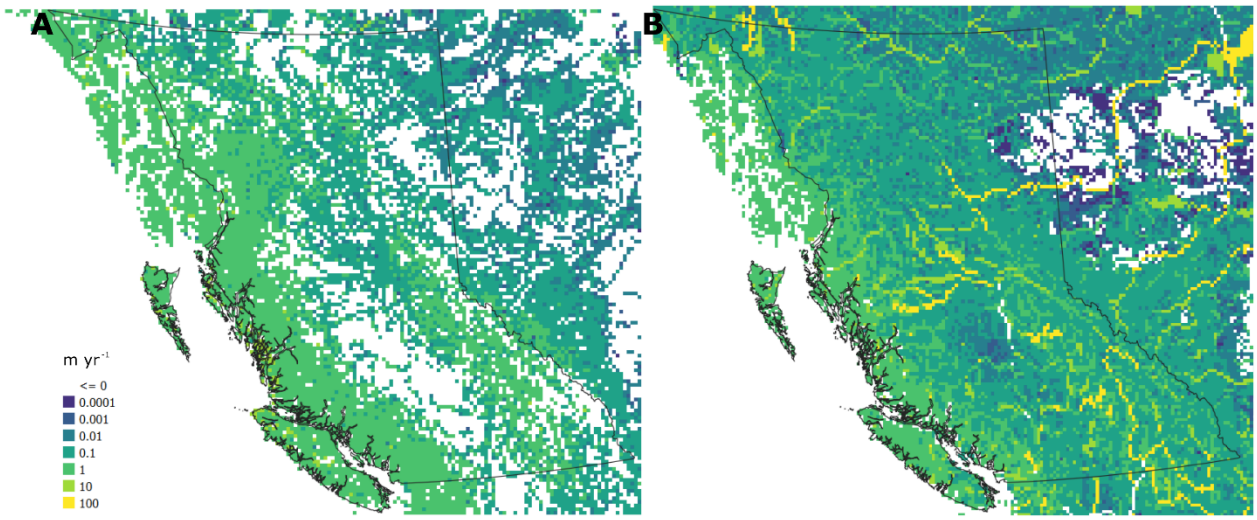

Figure 4.7 Derived raster results for E_{PS} (A) and E_{LF} (B).

compared, E_{PS} was consistently greater than E_{LF} in mountainous terrain (Figure 4.9). E_{LF} tend to be larger than E_{PS} values in the interior and along major rivers. Both methods resulted in variable distribution of E_{PS} and E_{LF} across the province ranging from 0 – 3.7 m yr^{-1} and 431 m yr^{-1}, respectively (Figure 4.7). E_{PS} was derived for 367 unconfined aquifers with flux values ranging from 0 to 1.07 m yr^{-1} with an average value of 0.234 m yr^{-1}.Similarly, E_{LF} was estimated for 373 aquifers with a resultant range from 0 to 36.1 m yr^{-1} with an average value of 7.704 m yr^{-1}. Derived E_{PS} and E_{LF} had limited model coverage in coastal areas, and as a result, E was not estimated for many island aquifers.

Figure 4.10 illustrates the distribution and magnitude of E_{PS} and E_{LF} by biogeoclimatic zone. Recharge values were taken from PCR-GLOBWB, R_{PCR}, and represents the vertical percolation of water to the groundwater layer. There was no significant trend between the ratio of E_{PS} to R_{PCR} relative to precipitation zones or low flow zones, and values averaged 72%, with some anomalously high ratios where R_{PCR} is very low. Ratios of E_{LF} relative to R_{PCR} were typically greater than 1, indicating the required discharge to support environmental flows from the aquifer is greater than recharge. 32 aquifers had ratios of E_{LF} relative to R_{PCR} > 100, which indicates, E_{LF} was likely overestimated for many of these aquifers. The remaining aquifers had an average E_{LF} seven times greater than R_{PCR}. There is no visible trend when

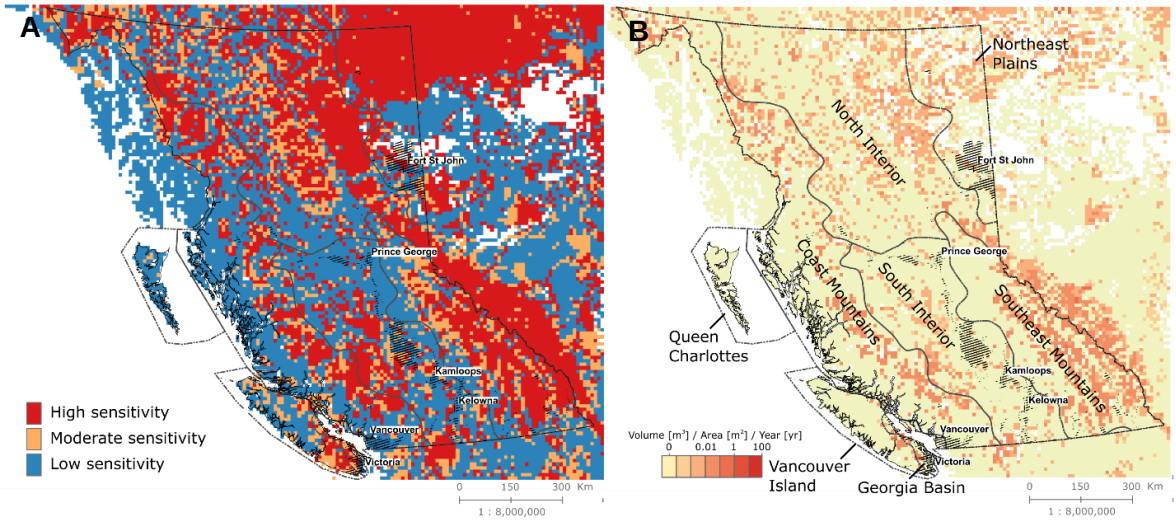

Figure 4.8. Distribution of k_{EFN} and high sensitivity flow range. (A) k_{EFN}, sensitivity distribution based on minimum MMF. (B) Difference in minimum and maximum MMF for months classified as "high sensitivity".

classified by biogeoclimatic zones, however, a moderately significant decreasing trend and an increase in variability with Low Flow Zones, particularly between pluvial (Vancouver Island and Georgia Basin) and nival regimes, with the exception of the North Interior zone. When E_{PS} and E_{LF} values are compared, E_{PS} estimates are greater than E_{LF} in the rainfall dominated low flow zones, and, variability of E_{LF} estimates were larger in snowmelt dominated regimes in comparison to rainfall dominated regimes (Figure 4.10).

4.3. GROUNDWATER FOOTPRINT

Aquifers were classified as *stressed (high certainty)* where all applicable aquifer stress results were GF/A > 1, *stressed (low certainty)* where at least one of the aquifer stress results were GF/A > 1, *less stressed* where all applicable aquifer stress results were GF/A < 1, and *method not applicable* where (1) aquifers were confined, (2) missing parameter due to data coverage, or (3) where E > R resulting in a negative availability (Figure 4.13). Of the unconfined aquifers (n = 404) in the province, 43 aquifers (11%) are

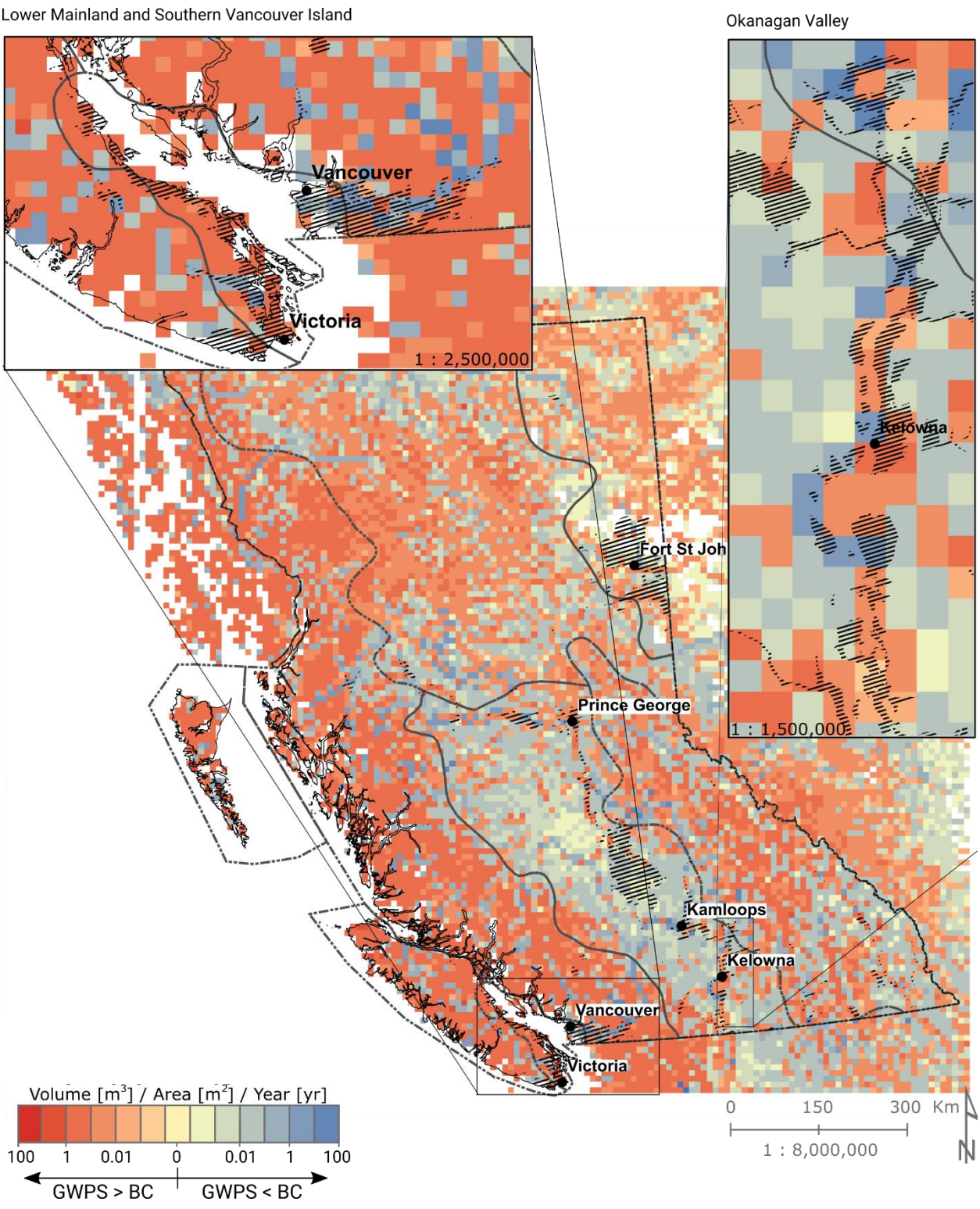

Figure 4.9 Comparison of E_{PS} (GWPS) and E_{LF} (using low flow months based on BC EFN policy).

Figure 4.10. Results from derived aquifer-scale estimates of E_{PS} and E_{LF} by biogeoclimatic and low flow zones. Groundwater's contribution to environmental flows as a percent of recharge from PCR-GLOBWB classified by biogeoclimatic zone (A) and low flow zone (B). (C) Absolute flux values of E.

stressed with high certainty, 32 aquifers (8%) are stressed with low certainty, 296 aquifers (70%) are less stressed, and 29 aquifers (11%) were not included due to missing parameters or issues where modelled recharge was less than environmental flows.

Aquifers located in more arid environments tend to be more stressed compared to aquifers in higher precipitation zones. This relationship is closely linked to the trends in availability, which tend to increase in zones of more precipitation, accommodating more withdrawal, as average withdrawal has no significant trend with zones of precipitation. Availability, which relies on recharge and groundwater's contribution to environmental flows, has a significant increasing trend in zones of higher precipitation. The increasing rate of availability flux is a result of the

increased rate of recharge flux compared to the rate of increasing flux for groundwater's contribution to environmental flows. Pluvial regimes tend to have increased availability flux compared to nival regimes. Although aquifer recharge and groundwater's contribution to environmental flows is greater in nival regimes, we see that recharge has a stronger trend than E, attributing to the decreasing trend in availability from pluvial to nival regimes. Although availability is influenced by pluvial and nival regimes, no significant trend exists with groundwater stress, indicating abstraction has greater control on aquifer stress in these regimes.

Groundwater use data is determined based on estimated annual sectoral abstractions. Based on the dominant sector contributing to the majority (>50%) of groundwater abstractions, average groundwater stress was the result of abstractions for finfish aquaculture, municipal water distribution systems, and agriculture. However, when we compare groundwater stress to dominant sector per biogeoclimatic zone, drier zones (such as BG, PP, and IDF) can attribute most of their stress to abstractions for the purpose of agriculture or municipal water distribution systems, in contrast to wetter climates which have variable sectors attributing to aquifer stress.

5. DISCUSSION

5.1. QUANTIFYING THE GROUNDWATER CONTRIBUTION TO ENVIRONMENTAL FLOWS

Aquifer-scale method of estimating E are critical for aquifer-scale management, allocation licences, and mitigation of stream supported ecosystem deterioration. Herein, the two methods of estimating E are discussed along with model and method limitations. Advantages and disadvantages exists for both methods. Namely, E_{PS} is advantageous as it is more aligned with groundwater stress management and represents a peer-reviewed approach to evaluating E. However, validating baseflow estimates in the field is inherently difficult (Tallaksen 1995; Smakhtin 2001), therefore, uncertainty exists in using modelled baseflow values. In contrast, the E_{LF}

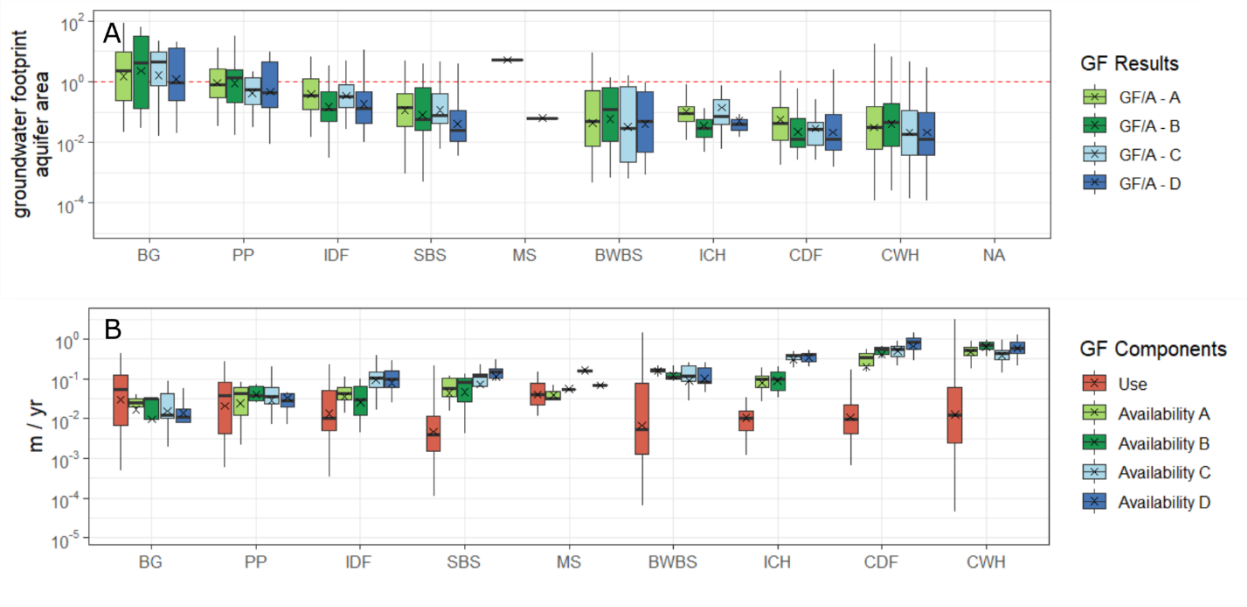

Figure 4.11. Groundwater footprint results per biogeoclimatic zone (BGCZ). (A) Results of the groundwater footprint by BGCZ. (B) The components of groundwater use and availability within the groundwater footprint.

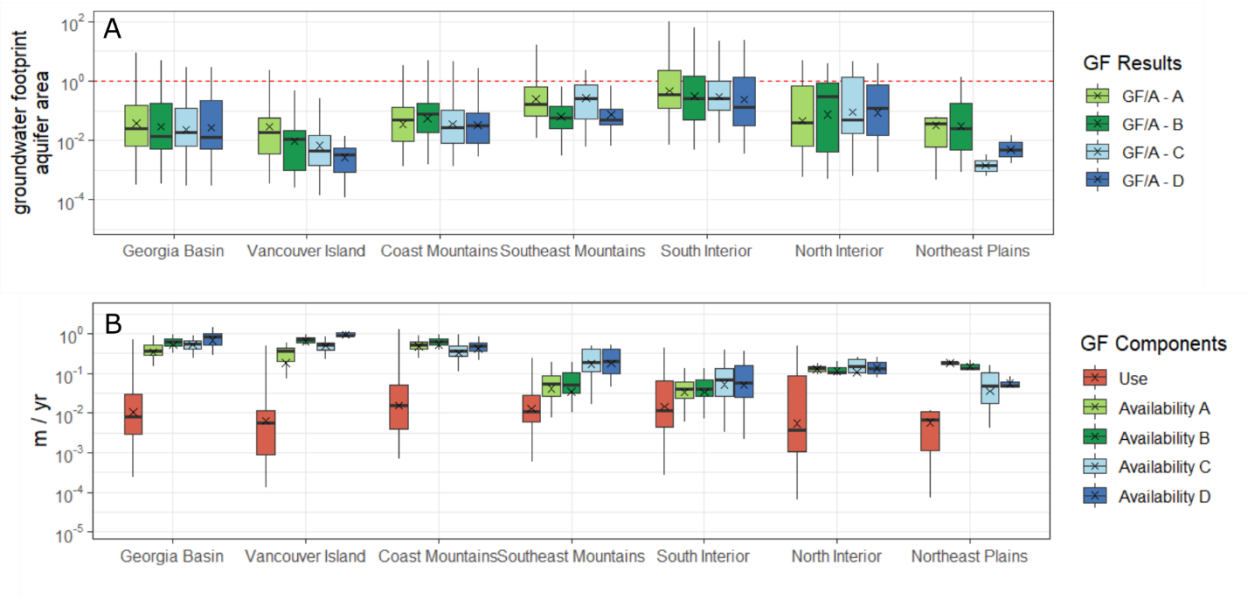

Figure 4.12 Groundwater footprint results per low flow zone (LFZ). (A) Results of the groundwater footprint by LFZ. (B) The components of groundwater use and availability within the groundwater footprint.

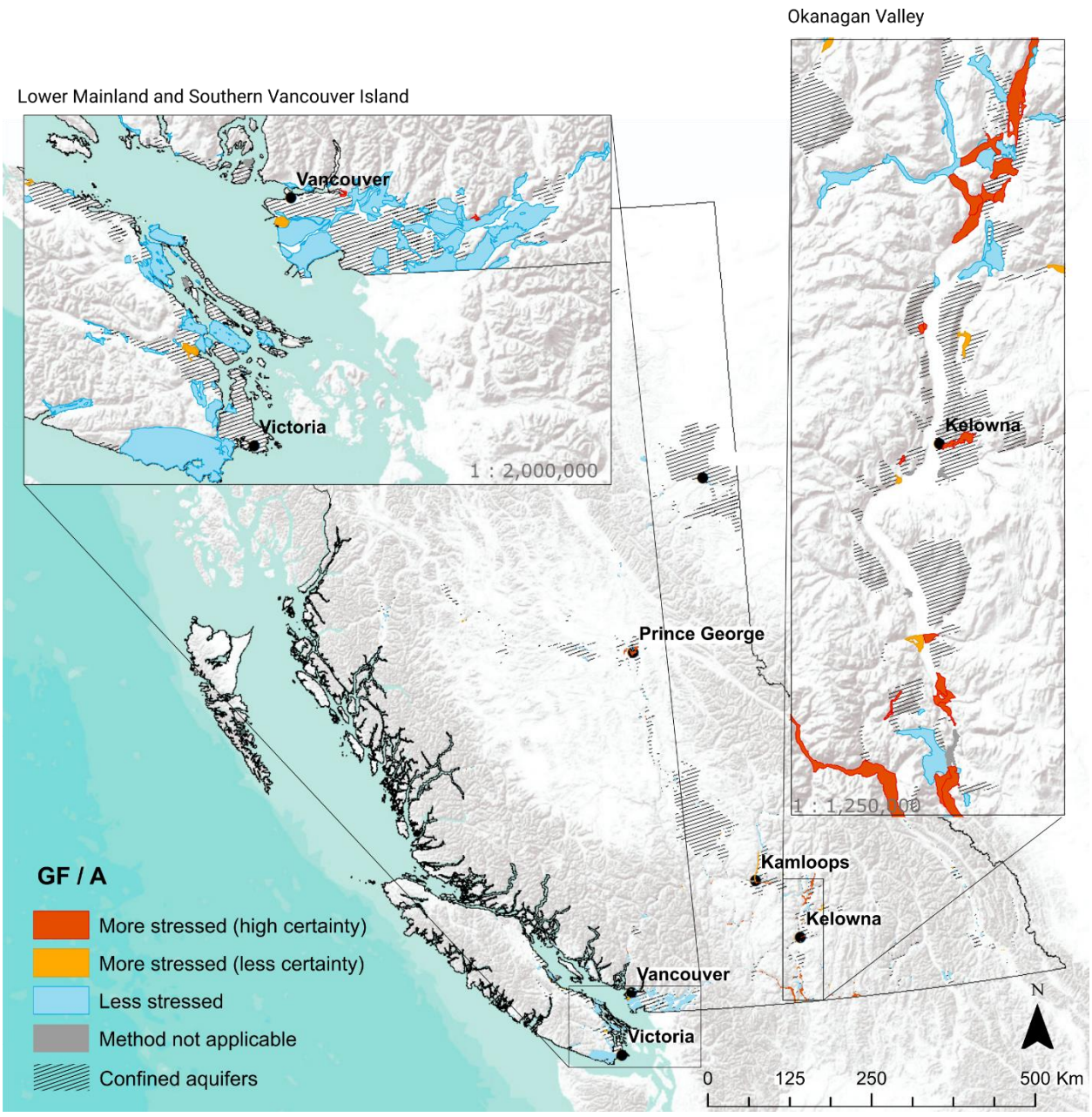

Figure 4.13 Map of aquifer stress for unconfined aquifers in BC. Aquifers were classified as 'stressed (high certainty)' where all applicable aquifer stress results were GF/A > 1, 'stressed (low certainty)' where at least one of the aquifer stress results were GF/A > 1, 'less stressed' where all applicable aquifer stress results were GF/A < 1, and 'method not applicable' where aquifers were confined or where E > R resulting in a negative availability.

method quantifies E using streamflow data, however, the surface water centric approach does not consider groundwater fluxes explicitly. Advantages include being able to apply a regionally specific value to represent k_{EFN} based on stream sensitivity and streamflow data is often more abundant and measurable compared to baseflow data.

5.1.1. MODEL LIMITATIONS

Numerical models can be useful in providing first order estimates of E, which can act as a placeholder until more detailed local studies can be initiated. Unfortunately, the discrepancy between model area and aquifer area introduces uncertainty and limitations in the application of the model in hydrologically complex environments.

The output of data at a 6' resolution which is larger than most unconfined aquifers in this regional study. As PCR-GLOBWB represents a water balance, each cell is representative of the average processes occurring within the cell, and as a result, sub-grid heterogeneity is often masked. E_{PS} is based on estimating the magnitude of aquifer baseflow which, in the field, would be the average flux based on the heterogeneous fluxes across the aquifer. Groundwater discharge to the stream is dependent on aquifer-stream hydrologic connectivity and head difference between the aquifer and the stream. Although these processes are expressed in the model, the sub-grid heterogeneity, and the representative nature of the cell to the aquifer, is highly uncertain. In addition, modeled baseflow in PCR-GLOBWB was taken as the sum of RIV and DRN outputs from the model which are representative of large and small streams respectively. Only large streams, captured by the RIV package (Figure S4.1), consider fluxes from the stream to the aquifer, however the coverage of "large" streams by the model is variable across the province, and without further investigation through local studies, the true dynamics of the stream-aquifer relationships are uncertain. Similarly, the anomalously high values of E_{LF} are indicative of model processes being misrepresentative of aquifer scale processes. In addition, the streamflow sensitivity analysis highlights the increased error in bias of modeled values relative to drainage basin area. As a result, E estimates for aquifers

in smaller drainage basins (<100 km^2) or large drainage basins (>10,000 km^2) are expected to be more uncertain.

5.1.2. METHOD LIMITATIONS

The groundwater presumptive standard is a peer reviewed volumetric allocation approach that is easily implemented, readily understood, and provides a stable and reliable basis of maximum allowable abstraction on an annual basis. By quantifying groundwater specific fluxes, E_{PS} estimates reflect a percent of aquifer recharge, and aquifer abstraction can be limited through management and licencing of water use. The approach is limited by data availability, and therefore, E estimates are often dependent on modeled values of baseflow, which can be difficult to quantify in diverse hydrologic environments, such as mountainous terrain. In addition, the arbitrary fixed value of 90%, which is based on the conservative protection of groundwater's contribution to environmental flows over variable temporal and spatial scale of pumping, doesn't account for regionally specific environmental flow policies, nor does it account for variable stream sensitivity to groundwater fluxes. However, from a groundwater-centric approach, it does provide a conservative metric for protecting the long-term effects of pumping on groundwater's contribution to streamflow.

The low flow surface-water-centric approach to quantifying groundwater's contribution to streamflow, is similarly a volumetric allocation method, however with an emphasis on protecting low flow periods. Low flow periods are often supported by groundwater processes (Poff et al. 1997; Smakhtin 2001; Barlow and Leake 2012), however, in diverse hydrologic environments, this assumption is often untrue. For example, at high elevations, influences of meltwater on the hydrograph can decrease the ratio of groundwater to surface water supported low flows. The flexible ratio of k_{EFN} to streamflow sensitivity protects streams which have more variable flow conditions, such as in headwater areas. This approach is less conservative for low sensitivity streams, as allocations increase in these areas, which does not explicitly protect against the long term affects of groundwater abstraction, but rather sets a limit on maximum abstraction mitigating low flow deterioration.

Both methods estimated annual aquifer-scale quantification of groundwater availability. Applied on monthly time scales, the low flows approach would quantify groundwater relative to streamflow sensitivity, as opposed to a fixed ratio of groundwater availability based on aquifer discharge. Further research would be required to fully understand the implications of applying these methods at smaller temporal resolutions.

5.2. QUANTIFYING GROUNDWATER STRESS USING ENVIRONMENTAL FLOWS

Results from this analysis highlight the importance of considering environmental flows in aquifer availability. Methods which quantify aquifer availability solely on recharge would be over allocating groundwater resources possibly leading to detrimental effects on local ecosystems, but by depleting groundwater's contribution to environmental flows, could significantly influence downstream ecosystems. Based on the results, arid environments tend to have increased groundwater footprints. The simplicity of the groundwater footprint ratio of use

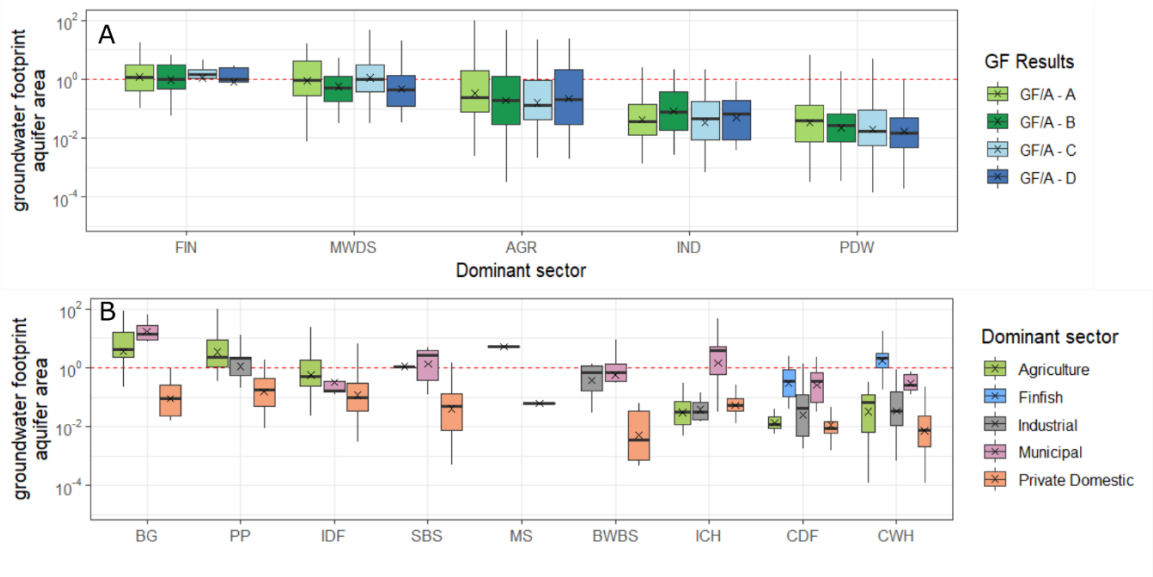

Figure 4.14. Groundwater use by sector and the relationship to groundwater footprint. (A) GF/A classified per sector. (B) GF/A classified per sector spatially distributed per biogeoclimatic zone.

over availability identifies aquifers which are prone to aquifer stress, either by high abstraction rates, or through low availability. Low availability is often relative to climatic factors, whereas, high groundwater abstraction is relative to magnitude of demand from economic sectors. For example, Figure 4.11 illustrates typically similar rates of abstraction across biogeoclimatic zones, however, aquifer stress is decreased in biogeoclimatic zones of increased precipitation zone due to higher rates of available groundwater (R – E).

Groundwater stress at the provincial scale is mainly attributed to finfish aquaculture, municipal water distribution systems, and agriculture. However, the spatial distribution of sectoral groundwater use across the province (Figure 4.14), illustrates aquifer stress is not the result of one sector, but rather aquifer stress is a regionally varying issue based on the dominant sector within each biogeoclimatic zone. For example, the aquifer stress in the Interior is attributed mainly to high agricultural and municipal water distribution system use, as opposed to the coastal areas, where finfish aquaculture is the main driver of aquifer stress.

For the sustainable management of groundwater resources, conjunctive management of groundwater and supporting systems, can help identify regions of high availability. Similarly, by understanding the sectoral quantification of groundwater resources, practices can be enforced and encouraged in regions which can sustainably support the demand of water.

6. CONCLUSION

The objective of this study was to determine aquifer-scale estimates of stress using the groundwater footprint (GF) and quantify aquifer availability as the difference between recharge and groundwater's contribution to environmental flows.

Two methods are used to quantify groundwater's contribution to environmental flows. The first method is a groundwater-centric approach from the application of the groundwater presumptive standard defined by Gleeson and Richter (2018), which suggests that high levels of ecological protection are maintained if 90% of baseflow is preserved. The second surface-water centric approach is a novel method

which quantifies groundwater's contribution to environmental flows from streamflow using region-specific streamflow sensitivity metrics and local environmental flow policies. The groundwater presumptive standard approach is advantageous because it is a peer-reviewed method and aligned with groundwater stress management as it is derived explicitly from groundwater baseflow. Using a surface-water centric approach is an indirect method of quantifying groundwater's contribution to environmental flows, however, streamflow data is often more abundant than groundwater data, and making comparisons between modeled streamflow and gauged streams can help constrain method uncertainty. Both methods used PCR-GLOBWB due to data scarcity across most of the province, which is often typical in mountainous terrain. In general, in the Interior of the province, the low flow zone approach estimated higher values of environmental flows however, in mountainous terrain and coastal areas, the groundwater presumptive standard had higher values of groundwater's contribution to environmental flows. Due to the resolution of the model, E estimates for aquifers in smaller drainage basins (<100 km^2) or large drainage basins (>10,000 km^2) are expected to be more uncertain.

Aquifer stress has been seen to decrease in zones of high precipitation, which can be attributed to higher volumes of aquifer availability as groundwater use is more or less constant within each biogeoclimatic zone. Finfish aquaculture and municipal water distribution systems are the dominant sectors inducing aquifer stress on the provincial scale. However, as groundwater use is spatially distributed, patterns of sectoral groundwater use emerge within biogeoclimatic zone which can help in understanding how groundwater resources are used in the province, as well as, develop local management strategies based on sectoral groundwater use.

Estimates from this study were completed as a first order quantification of aquifer stress. Local scale studies are critical for more detailed fluxes, as methods used in this analysis have high uncertainties due to the scale of the methods used. Diverse hydrologic environments are especially difficult to aquifer accurate estimates using data at a higher resolution, heterogeneity captured by areal averages at a larger

resolution may not be representative of aquifer-scale processes. These first order estimates provide the first groundwork to understanding how groundwater use varies across the province and which sectors may be attributed to stress regionally.

CHAPTER 5:
Conclusions

Quantifying groundwater stress promotes the sustainable management of groundwater resources and groundwater supported ecosystems (Barlow and Leake 2012; Gleeson et al. 2012; Gleeson and Richter 2017). Water stress studies provide a framework to understand the dynamics for evaluating changes in groundwater resources by comparing water availability to human water use (van Beek L. P. H. et al. 2011; Wada et al. 2011; Richey et al. 2015; Mehran et al. 2017) and can promote sustainable practices in stressed regions through management and policy changes (Tringali et al. 2017; Bhanja et al. 2017).

The main objective of this thesis was to address current provincial knowledge gaps through aquifer-scale estimates of annual volumes for groundwater withdrawal, recharge, and groundwater's contribution to environmental flows as a means to provide screening level estimates of aquifer-scale stress quantified using the groundwater footprint. A major part of this thesis included a synthesis of varying scales of data. Where possible, local-scale data was used; however, in many cases, due to lack of spatially distributed data, national or global-scale data was used. Chapters 2-4 each highlight the limitations and uncertainties of the results so these are not repeated herein.

The first chapter of this thesis illustrates the importance of sectoral groundwater use estimates in aquifer-scale analysis. Results suggest that BC uses a total of ~562 million cubic metres of groundwater annually. The largest annual groundwater use by major sectors is agriculture (38%), finfish aquaculture (21%), industrial (16%), municipal water distribution systems (15%), and domestic private well users (11%).

The second chapter of this thesis explores three multi-scale methods of estimating aquifer-scale recharge in diverse hydrologic environments. Local-scale recharge

was estimated using the water table fluctuation (WTF) method outlined by Cuthbert (2014). Aquifer-scale recharge was quantified based on generalized aquifer parameters of soil and aquifer material, regional climate, and water table depth. Regional scale aquifer recharge was attributed the areal average recharge flux modelled by the global hydrologic model, PCR-GLOBWB. Results show that generally recharge predictably varies with precipitation and that the average recharge is 791 mm for the local-scale method, 462 mm (32% of precipitation) for the aquifer-scale and 393 mm (33%) for the global hydrologic model.

The third chapter of this thesis estimates groundwater's contribution to environmental flows across the province for this first time using two separate approaches and synthesises data from the previous chapters to quantify aquifer stress using the groundwater footprint. The first approach uses the groundwater presumptive standard, which is a general standard for managing groundwater pumping. The second method introduces a novel approach for estimating the contribution of groundwater to environmental flows using the existing environmental flow needs framework and an understanding of low flow zone hydrology. In general, both methods show larger contributions from groundwater to environmental flows in the Lower Mainland and southern Vancouver Island compared to the Interior. For each aquifer, the groundwater footprint (expressed as the unitless ratio of groundwater footprint to aquifer area) is calculated four times; using results from each of the two methods used to estimate recharge and each of the two methods used to estimate the groundwater contribution to environmental flows. Of the unconfined aquifers (n = 404) in the province, 43 aquifers (11%) are stressed with high certainty, 32 aquifers (8%) are stressed with low certainty, 296 aquifers (70%) are less stressed, and 29 aquifers (11%) were not included due to missing parameters or issues where modelled recharge was less than environmental flows.

In conclusion, this thesis has contributed valuable knowledge on groundwater resources in BC, and additionally, provides methods which can be further applied in data scarce hydrologically complex landscapes.

FUTURE DIRECTIONS

This thesis is a first order estimate of aquifer stress spatially distributed across the province. As such, this thesis provides a useful starting place for a number useful and potentially interesting future research directions.

Firstly, large uncertainties exist due to model and method resolution compared to aquifer scale. Due to data scarcity and variability in hydrologic conditions across the province, many estimates in this analysis are based on larger resolution data compared to aquifer scale estimates. For example, groundwater use, although spatially distributed by sector, is still limited due to large uncertainties inherent in the methodology. As a result, next steps include comparing results from this study to local estimates of groundwater use and recharge. Based on the comparison, we will better understand the limitations and uncertainty associated with regional studies in quantifying aquifer scale fluxes.

Secondly, in mountainous terrain, aquifer-scale flux processes are more complex, due to the heterogeneous geology, topography and climate. As a result, further analyses should be complete at the aquifer scale using methods which consider horizontal fluxes to and from the aquifer, such as stream-aquifer connectivity, and aquifer-mountain block connectivity. In addition, with a comparison of local scale studies which consider major fluxes into and out of the aquifer, we can better understand the limitations of using the methodologies above in diverse hydrologic environments. Due to the scope of the analyses, constraining uncertainty and limitations of the methods is crucial to be able to apply these methods in other areas. Comparing PCR-GLOBWB input parameters of permeability to aquifer permeability values would help constrain PCR-GLOBWB ability to model aquifer-scale processes. In addition, further investigation into how the model performs in rain-dominated and snow-dominated regimes would be crucial to properly constrain the limitations in our estimates of recharge and groundwater's contribution to environmental flows.

Thirdly, future work can be done based on climate change projections for forecasting future aquifer stress scenarios in order to mitigate negative effects on BC's groundwater resources. Although large uncertainties exist in future climate predictions, there is considerable evidence that there will be substantial impacts on environmental and human interests (Allen et al. 2004a; Merritt et al. 2006; Neilsen et al. 2006; Scibek and Allen 2006b).

And finally, this research has focused mainly of unconfined aquifers as most development is concentrated in upper aquifers due to lower costs of well drilling and easier access to shallow water tables. In the future, for a holistic perspective on the current state of aquifers, aquifer stress analysis should be expanded to included confined aquifers.

References

Acreman M, Arthington AH, Colloff MJ, et al (2014) Environmental flows for natural, hybrid, and novel riverine ecosystems in a changing world. Front Ecol Environ 12:466–473

Aeschbach-Hertig W, Gleeson T (2012) Regional strategies for the accelerating global problem of groundwater depletion. Nat Geosci 5:853

Ajami H, Troch PA, Maddock T, et al (2011) Quantifying mountain block recharge by means of catchment-scale storage-discharge relationships. Water Resour Res 47:

Alcamo J, Döll P, Kaspar F, Siebert S (1997) Global change and global scenarios of water use and availability: an application of WaterGAP1.0

Aldaya MM (2017) Eating ourselves dry: Environmental science. Nature 543:633–634. doi: 10.1038/543633a

Allen DM, Cannon AJ, Toews MW, Scibek J (2010a) Variability in simulated recharge using different GCMs. Water Resour Res 46:

Allen DM, Mackie DC, Wei M (2004a) Groundwater and climate change: a sensitivity analysis for the Grand Forks aquifer, southern British Columbia, Canada. Hydrogeol J 12:270–290

Allen DM, Scibek J, Wei M, Whitfield P (2004b) Climate Change and Groundwater: A Modelling Approach for Identifying Impacts and Resource Sustainability in the Central Interior of British Columbia. Climate Change Action Fund, Natural Resources Canada, Ottawa, Ontario

Allen DM, Whitfield PH, Werner A (2010b) Groundwater level responses in temperate mountainous terrain: regime classification, and linkages to climate and streamflow. Hydrol Process 24:3392–3412. doi: 10.1002/hyp.7757

Alley WM, Clark BR, Ely DM, Faunt CC (2018) Groundwater Development Stress: Global-Scale Indices Compared to Regional Modeling. Groundwater 56:266–275

Arbués F, Garcıa-Valiñas MÁ, Martınez-Espiñeira R (2003) Estimation of residential water demand: a state-of-the-art review. J Socio-Econ 32:81–102

Arnold H (2016) Selected exploration projects and operating mines in British Columbia, 2015

Bakker M, Anderson EI, Olsthoorn TN, Strack OD (1999) Regional groundwater modeling of the Yucca Mountain site using analytic elements. J Hydrol 226:167–178

Barlow PM, Leake SA (2012) Streamflow depletion by wells–Understanding and managing the effects of groundwater pumping on streamflow. US Geological Survey

BC Oil & Gas Commission (2013) 2013 Annual Report on Water Use for Oil and Gas Activity

BC Oil & Gas Commission (2014) 2014 Annual Report on Water Use for Oil and Gas Activity

BC Oil & Gas Commission (2015) 2015 Annual Report on Water Management for Oil and Gas Activity

Berardinucci J, Ronneseth K (2002) Guide to using the BC aquifer classification maps for the protection and management of groundwater. Ministry of Water, Land and Air Protection, Victoria, B.C.

Bhanja SN, Mukherjee A, Rodell M, et al (2017) Groundwater rejuvenation in parts of India influenced by water-policy change implementation. Sci Rep 7:. doi: 10.1038/s41598-017-07058-2

Blöschl G, Sivapalan M (1995) Scale issues in hydrological modelling: a review. Hydrol Process 9:251–290

Bredehoeft JD, Young RA (1983) Conjunctive use of groundwater and surface water for irrigated agriculture: Risk aversion. Water Resour Res 19:1111–1121

Calzolari C, Ungaro F (2012) Predicting shallow water table depth at regional scale from rainfall and soil data. J Hydrol 414–415:374–387. doi: 10.1016/j.jhydrol.2011.11.008

Carmichael V (2013) Compendium of Re-evaluated Pumping Tests in the Regional District of Nanaimo, BC. 941

Carmichael V (2014) Compendium of Re-evaluated Pumping Tests in the Cowichan Valley Regional District, Vancouver Island, British Columbia. 1178

Carmichael V, Allen DM, Gellein C, Kenny S (2008a) Compendium of aquifer hydraulic properties from re-evaluated pumping tests in the Okanagan Basin, British Columbia. Ministry of Environment, Water Stewardship Division, Victoria, B.C.

Carmichael V, Kenny S, Allen DM, Gellein C (2008b) Compendium of aquifer hydraulic properties from re-evaluated pumping tests in the North Okanagan, British Columbia. Ministry of Environment, Science and Information Branch, Victoria, B.C.

Carver M, Gray M (2009) Assessment Watersheds for Regional Level Applications (Freshwater Atlas)

Castaño S, Sanz D, Gómez-Alday JJ (2010) Methodology for quantifying groundwater abstractions for agriculture via remote sensing and GIS. Water Resour Manag 24:795–814

Changming L, Jingjie Y, Kendy E (2001) Groundwater exploitation and its impact on the environment in the North China Plain. Water Int 26:265–272

Church M, Ryder JM (2010) Physiography of British Columbia. In: Compendium of forest hydrology and geomorphology in British Columbia. Ministry of Forests and Range, British Columbia

Constantz J (1998) Interaction between stream temperature, streamflow, and groundwater exchanges in alpine streams. Water Resour Res 34:1609–1615. doi: 10.1029/98WR00998

Coulson CH, Obedkoff W (1998) British Columbia streamflow inventory. Water Inventory Section, Resources Inventory Branch

Covino TP, McGlynn BL (2007) Stream gains and losses across a mountain-to-valley transition: Impacts on watershed hydrology and stream water chemistry. Water Resour Res 43:

Crosbie RS, Binning P, Kalma JD (2005) A time series approach to inferring groundwater recharge using the water table fluctuation method. Water Resour Res 41:

Cuthbert MO (2014) Straight thinking about groundwater recession. Water Resour Res 50:2407–2424

Cuthbert MO (2010) An improved time series approach for estimating groundwater recharge from groundwater level fluctuations. Water Resour Res 46:

Cuthbert MO, Acworth RI, Andersen MS, et al (2016) Understanding and quantifying focused, indirect groundwater recharge from ephemeral streams using water table fluctuations. Water Resour Res

Cuthbert MO, Tindimugaya C (2010) The importance of preferential flow in controlling groundwater recharge in tropical Africa and implications for modelling the impact of climate change on groundwater resources. J Water Clim Change 1:234–245

Dalin C, Wada Y, Kastner T, Puma MJ (2017) Groundwater depletion embedded in international food trade. Nature 543:700

De Graaf IEM, Sutanudjaja EH, Van Beek LPH, Bierkens MFP (2015) A high-resolution global-scale groundwater model. Hydrol Earth Syst Sci 19:823–837

De Vries JJ, Simmers I (2002) Groundwater recharge: an overview of processes and challenges. Hydrogeol J 10:5–17

Denny SC, Allen DM, Journeay JM (2007) DRASTIC-Fm: a modified vulnerability mapping method for structurally controlled aquifers in the southern Gulf Islands, British Columbia, Canada. Hydrogeol J 15:483

DMTI Spatial Inc. (2015) CanMap Content Suite, v2015.3

Eaton B, Moore RD (2010) Regional Hydrology. In: Compendium of forest hydrology and geomorphology in British Columbia. Ministry of Forests and Range, British Columbia

Environment Canada (2011) 2011 Municipal Water Use Report: Municipal Water Use 2009 Statistics

Esnault L, Gleeson T, Wada Y, et al (2014) Linking groundwater use and stress to specific crops using the groundwater footprint in the Central Valley and High Plains aquifer systems, US. Water Resour Res 50:4953–4973

Famiglietti JS (2014a) The global groundwater crisis. In: Nat. Clim. Change. https://www.nature.com/articles/nclimate2425. Accessed 1 May 2018

Famiglietti JS (2014b) The global groundwater crisis. Nat Clim Change 4:945

Fan Y, Li H, Miguez-Macho G (2013) Global patterns of groundwater table depth. Science 339:940–943

Flint AL, Flint LE, Kwicklis EM, et al (2002) Estimating recharge at Yucca Mountain, Nevada, USA: comparison of methods. Hydrogeol J 10:180–204

Food, Land AO of the UN, Division WD (2003) Digital soil map of the world and derived soil properties. FAO, Land and Water Development Division

Ghose D, Das U, Roy P (2018) Modeling response of runoff and evapotranspiration for predicting water table depth in arid region using dynamic recurrent neural network. Groundw Sustain Dev 6:263–269. doi: 10.1016/j.gsd.2018.01.007

Gleeson T, Richter B (2017) How much groundwater can we pump and protect environmental flows through time? Presumptive standards for conjunctive management of aquifers and rivers. River Res Appl 34:83–92

Gleeson T, Smith L, Moosdorf N, et al (2011) Mapping permeability over the surface of the Earth. Geophys Res Lett 38:

Gleeson T, Wada Y (2013) Assessing regional groundwater stress for nations using multiple data sources with the groundwater footprint. Environ Res Lett 8:044010

Gleeson T, Wada Y, Bierkens MFP, van Beek LPH (2012) Water balance of global aquifers revealed by groundwater footprint. Nature 488:197–200. doi: 10.1038/nature11295

Gudmundsson L, Wagener T, Tallaksen LM, Engeland K (2012) Evaluation of nine large-scale hydrological models with respect to the seasonal runoff climatology in Europe. Water Resour Res 48:. doi: 10.1029/2011WR010911

Gupta HV, Kling H, Yilmaz KK, Martinez GF (2009) Decomposition of the mean squared error and NSE performance criteria: Implications for improving hydrological modelling. J Hydrol 377:80–91. doi: 10.1016/j.jhydrol.2009.08.003

Hantush MS (1967) Growth and decay of groundwater-mounds in response to uniform percolation. Water Resour Res

Hartmann J, Moosdorf N (2012) The new global lithological map database GLiM: A representation of rock properties at the Earth surface. Geochem Geophys Geosystems 13:

Harwood A, Girard I, Johnson S, et al (2014) Environmental Flow Needs, Approaches, Successes and Challenges-Summary Report. Consult Rep Prep Can Counc Minist Environ Ecofish Res Ltd

Healy RW, Cook PG (2002) Using groundwater levels to estimate recharge. Hydrogeol J 10:91–109

Hess PJ (1986) Ground-water use in Canada, 1981. In: IWD technical bulletin. Environment Canada

Hodge WS (1977) A preliminary geohydrological study of Saltspring Island. Groundw Sect Hydrol Branch Water Manag Div Minist Environ Land Parks

Hodge WS (1995) Groundwater conditions on Saltspring Island. Groundw Sect Hydrol Branch Water Manag Div Minist Environ Land Parks

Holland SS (1976) Bulletin 48: Landforms of British Columbia, A Physiographic Outline

Holman IP, Tascone D, Hess TM (2009) A comparison of stochastic and deterministic downscaling methods for modelling potential groundwater recharge under climate change in East Anglia, UK: implications for groundwater resource management. Hydrogeol J 17:1629–1641. doi: 10.1007/s10040-009-0457-8

Honey-Roses J, Gill D, Pareja C (2016) BC Municipal Water Survey 2016. Sch Community Reg Plan Univ Br Columbia

Howard KWF, Gelo KK (2002) Intensive groundwater use in urban areas: the case of megacities. Intensive Use Groundw Chall Oppor 484

Ireson A, Makropoulos C, Maksimovic C (2006) Water resources modelling under data scarcity: coupling MIKE BASIN and ASM groundwater model. Water Resour Manag 20:567–590

Johnson AI (1967) Specific yield: compilation of specific yields for various materials.

Konikow LF, Kendy E (2005) Groundwater depletion: A global problem. Hydrogeol J Heidelb 13:317–320. doi: http://dx.doi.org/10.1007/s10040-004-0411-8

Kreye R, Ronneseth K, Wei M (2001) An Aquifer Classification System for Groundwater Management in British Columbia. Ministry of Environment, Water, Air and Climate Change Branch

Kundzewicz ZW, Doell P (2009) Will groundwater ease freshwater stress under climate change? Hydrol Sci J 54:665–675

Lapworth DJ, MacDonald AM, Tijani MN, et al (2013) Residence times of shallow groundwater in West Africa: implications for hydrogeology and resilience to future changes in climate. Hydrogeol J 21:673–686

Lerner DN, Issar AS, Simmers I (1990) Groundwater recharge: a guide to understanding and estimating natural recharge. Heise Hannover,, Germany

Liggett JE (2008) Comparison of approaches for aquifer vulnerability mapping and recharge modelling at regional and local scales, Okanagan Basin, British Columbia. PhD Thesis, Dept. of Earth Sciences-Simon Fraser University

Liskop T, Allen DM (2005) Observation well testing and recharge characterization of the Okanagan Basin, BC. BC Minist Water Land Air Prot

Llamas MR (1998) Groundwater overexploitation. In: Proceeding of the UNESCO Congress on “Water in the 21st Century: a looming crisis

MacIsaac EA (2010) Salmonids and the Hydrologic and Geomorphic Features of Their Spawning Streams in British Columbia. In: Compendium of forest hydrology and geomorphology in British Columbia. Ministry of Forests and Range, British Columbia

MacKinlay D, Howard K (2004) Fish Health Management Plan for All Major Salmonid Enhancement Facilities

Manga M (1999) On the timescales characterizing groundwater discharge at springs. J Hydrol 219:56–69

Manning AH, Solomon DK (2004) Constraining mountain-block recharge to the eastern Salt Lake Valley, Utah with dissolved noble gas and tritium data. Groundw Recharge Desert Environ Southwest U S Water Sci Appl Ser 9:139–158

Manning AH, Solomon DK (2005) An integrated environmental tracer approach to characterizing groundwater circulation in a mountain block. Water Resour Res 41:

Mehran A, AghaKouchak A, Nakhjiri N, et al (2017) Compounding impacts of human-induced water stress and climate change on water availability. Sci Rep 7:6282

Meinzer OE, Stearns ND (1927) A study of groundwater in the Pomperaug Basin, Connecticut. US Geol Surv Water-Supply Pap 2309:

Mercer LJ, Morgan WD (1974) Estimation of commercial, industrial and governmental water use for local areas. Wiley Online Library

Merritt WS, Alila Y, Barton M, et al (2006) Hydrologic response to scenarios of climate change in sub watersheds of the Okanagan basin, British Columbia. J Hydrol 326:79–108

Ministry of Agriculture, Ministry of Environment and Climate Change BC Soil Survey

Ministry of Environment and Climate Change Provincial Groundwater Observation Well Network - Groundwater Levels data

Moore RD, Spittlehouse DL, Whitfield PH, Stahl K (2010) Weather and Climate. In: Compendium of forest hydrology and geomorphology in British Columbia. Ministry of Forests and Range, British Columbia

Neilsen D, Smith CAS, Frank G, et al (2006) Potential impacts of climate change on water availability for crops in the Okanagan Basin, British Columbia. Can J Soil Sci 86:921–936

Noorduijn SL, Cook PG, Simmons CT, Richardson SB (2018) Protecting groundwater levels and ecosystems with simple management approaches. Hydrogeol J 1–13

Pacific Climate Impacts Consortium, University of Victoria BC Station Data

Pastor AV, Ludwig F, Biemans H, Hoff H (2014) Accounting for environmental flow requirements in global water assessments. Hydrol Earth Syst Sci 18:5041–5059. doi: 10.5194/hess-18-5041-2014

Pavelic P, Patankar U, Acharya S, et al (2012) Role of groundwater in buffering irrigation production against climate variability at the basin scale in South-West India. Agric Water Manag 103:78–87

Pike RG, Redding TE, Moore RD, et al (2010) Compendium of forest hydrology and geomorphology in British Columbia. Land Manag Handb-Minist For Range Br Columbia

Poff NL, Allan JD, Bain MB, et al (1997) The Natural Flow Regime. BioScience 47:769–784. doi: 10.2307/1313099

Portmann FT, Siebert S, Döll P (2010) MIRCA2000—Global monthly irrigated and rainfed crop areas around the year 2000: A new high-resolution data set for agricultural and hydrological modeling. Glob Biogeochem Cycles 24:

Province of British Columbia (2016a) Water Sustainability Act

Province of British Columbia (1909) Water Act

Province of British Columbia (2016b) Environmental Flow Needs Policy

Renzetti S (1992) Estimating the structure of industrial water demands: the case of Canadian manufacturing. Land Econ 396–404

Reynaud A (2003) An econometric estimation of industrial water demand in France. Environ Resour Econ 25:213–232

Richey AS, Thomas BF, Lo M-H, et al (2015) Quantifying renewable groundwater stress with GRACE. Water Resour Res 51:5217–5238

Rutherford S (2004) Groundwater use in Canada. West Coast Environmental Law

Rutulis M (1989) Groundwater drought sensitivity of southern Manitoba. Can Water Resour J 14:18–33

Sanford W (2002) Recharge and groundwater models: an overview. Hydrogeol J 10:110–120. doi: 10.1007/s10040-001-0173-5

Scanlon BR, Faunt CC, Longuevergne L, et al (2012) Groundwater depletion and sustainability of irrigation in the US High Plains and Central Valley. Proc Natl Acad Sci 109:9320–9325

Scanlon BR, Healy RW, Cook PG (2002) Choosing appropriate techniques for quantifying groundwater recharge. Hydrogeol J 10:18–39

Scanlon BR, Keese KE, Flint AL, et al (2006) Global synthesis of groundwater recharge in semiarid and arid regions. Hydrol Process Int J 20:3335–3370

Schroeder PR, Dozier TS, Zappi PA, et al (1994) The hydrologic evaluation of landfill performance (HELP) model: engineering documentation for version 3

Scibek J, Allen DM (2006a) Comparing modelled responses of two high-permeability, unconfined aquifers to predicted climate change. Glob Planet Change 50:50–62

Scibek J, Allen DM (2006b) Modeled impacts of predicted climate change on recharge and groundwater levels. Water Resour Res 42:

Siebert S, Burke J, Faures J-M, et al (2010) Groundwater use for irrigation–a global inventory. Hydrol Earth Syst Sci 14:1863–1880

Siebert S, Döll P (2008) The Global Crop Water Model (GCWM): Documentation and first results for irrigated crops

Siebert S, Döll P (2010) Quantifying blue and green virtual water contents in global crop production as well as potential production losses without irrigation. J Hydrol 384:198–217

Smakhtin VU (2001) Low flow hydrology: a review. J Hydrol 240:147–186

Smerdon BD, Allen DM, Grasby SE, Berg MA (2009) An approach for predicting groundwater recharge in mountainous watersheds. J Hydrol 365:156–172

Soil Landscapes of Canada Working Group (2010) Soil Landscapes of Canada version 3.2

Srinivasan V, Thompson S, Madhyastha K, et al (2015) Why is the Arkavathy River drying? A multiple-hypothesis approach in a data-scarce region. Hydrol Earth Syst Sci 19:1905–1917

Statistics Canada (No Date) Industrial Water Survey 2013. http://www23.statcan.gc.ca/imdb/p2SV.pl?Function=getSurvey&SDDS=5120. Accessed 7 Oct 2016a

Statistics Canada (No Date) Agricultural Water Survey 2014. http://www23.statcan.gc.ca/imdb/p2SV.pl?Function=getSurvey&SDDS=5145. Accessed 7 Oct 2016b

Statistics Canada (2011) Canada's rural population since 1851

Tallaksen LM (1995) A review of baseflow recession analysis. J Hydrol 165:349–370

Toews MW (2007) Modelling climate change impacts on groundwater recharge in a semi-arid region, southern Okanagan, British Columbia. Dept. of Earth Sciences-Simon Fraser University

Tringali C, Re V, Siciliano G, et al (2017) Insights and participatory actions driven by a socio-hydrogeological approach for groundwater management: the Grombalia

Basin case study (Tunisia). Hydrogeol J 25:1241–1255. doi: 10.1007/s10040-017-1542-z

Tsur Y (1990) The stabilization role of groundwater when surface water supplies are uncertain: the implications for groundwater development. Water Resour Res 26:811–818

van Beek L. P. H., Wada Yoshihide, Bierkens Marc F. P. (2011) Global monthly water stress: 1. Water balance and water availability. Water Resour Res 47:. doi: 10.1029/2010WR009791

Van Beek LPH, Bierkens MF (2009) The global hydrological model PCR-GLOBWB: conceptualization, parameterization and verification. Utrecht Univ Utrecht Neth

Van Camp M, Mjemah IC, Al Farrah N, Walraevens K (2013) Modeling approaches and strategies for data-scarce aquifers: example of the Dar es Salaam aquifer in Tanzania. Hydrogeol J 21:341–356. doi: 10.1007/s10040-012-0908-5

Vassolo S, Döll P (2005) Global-scale gridded estimates of thermoelectric power and manufacturing water use. Water Resour Res 41:

Vorosmarty CJ, Green P, Salisbury J, Lammers RB (2000) Global water resources: Vulnerability from climate change and population growth. Sci Wash 289:284–8

Wada Y, Beek Lph, Bierkens MF (2012) Nonsustainable groundwater sustaining irrigation: A global assessment. Water Resour Res 48:

Wada Y, van Beek LP, van Kempen CM, et al (2010) Global depletion of groundwater resources. Geophys Res Lett 37:

Wada Y, van Beek LPH, Bierkens MFP (2011) Modelling global water stress of the recent past: on the relative importance of trends in water demand and climate variability. Hydrol Earth Syst Sci 15:3785–3808. doi: 10.5194/hess-15-3785-2011

Wada Y, Wisser D, Bierkens MFP (2014) Global modeling of withdrawal, allocation and consumptive use of surface water and groundwater resources. Earth Syst Dyn Discuss 5:15–40

Wei M, Ronneseth K, Allen D, et al (2007) Types and general characteristics of aquifers in the Canadian Cordillera Hydrogeologic Region. In: Proceedings 8th Annual Canadian Geotechnical Society-International Association of Hydrogeologists Joint Conference, OttawaGeo2007: The Diamond Jubilee Conference, Ottawa

Wei M, Ronneseth K, Allen DM, et al (2014) Cordilleran Hydrogeological Region. Canada's Groundwater Resources

Welch LA, Allen DM (2014) Hydraulic conductivity characteristics in mountains and implications for conceptualizing bedrock groundwater flow. Hydrogeol J

Wilson JL, Guan H (2004) Mountain-block hydrology and mountain-front recharge. Groundw Recharge Desert Environ Southwest U S 9:

Winkler RD, Moore RD, Spittlehouse DL, et al (2010) Hydrologic Processes and Watershed Response. In: Compendium of forest hydrology and geomorphology in British Columbia. Ministry of Forests and Range, British Columbia

Winter TC (2001) The concept of hydrologic landscapes. JAWRA J Am Water Resour Assoc 37:335–349

Worthington AC (2010) Commercial and industrial water demand estimation: Theoretical and methodological guidelines for applied economics research. Estud Econ Apl 28:237–258

Zebarth BJ, Hii B, Liebscher H, et al (1998) Agricultural land use practices and nitrate contamination in the Abbotsford Aquifer, British Columbia, Canada. Agric Ecosyst Environ 69:99–112

Zektser S, Loáiciga HA, Wolf JT (2005) Environmental impacts of groundwater overdraft: selected case studies in the southwestern United States. Environ Geol 47:396–404

APPENDIX A:
Chapter 2

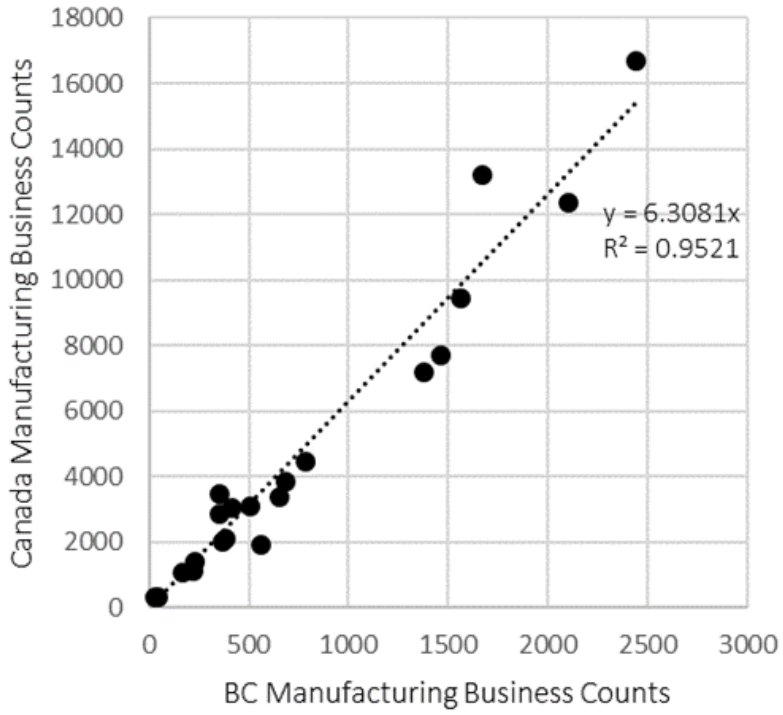

Figure S2.1 Relationship between manufacturing business counts in Canada and BC. Each point represents a different subsector of manufacturing.

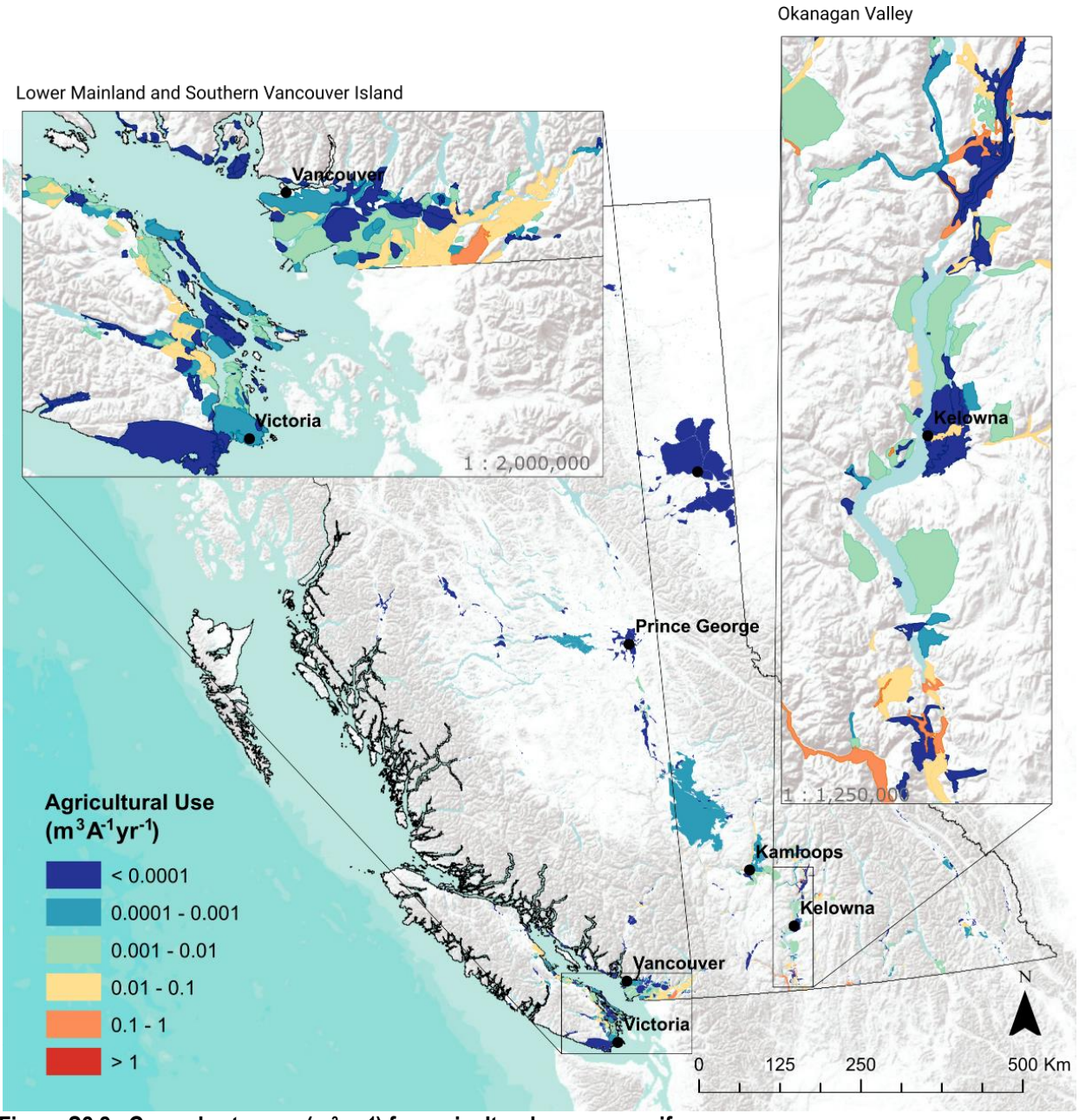

Figure S2.2a Groundwater use (m^3 yr^{-1}) for agricultural use per aquifer.

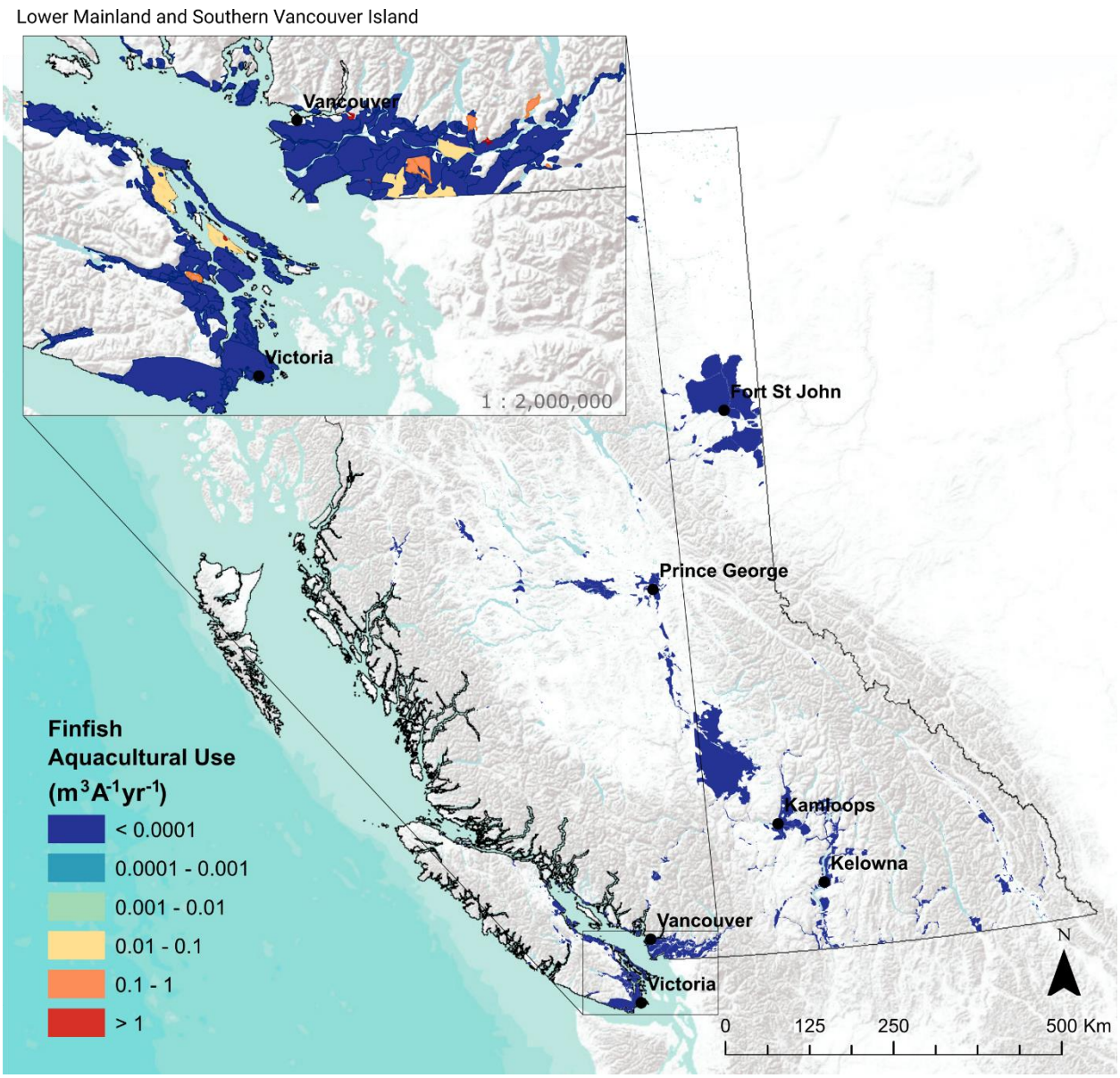

Figure S2.2b Groundwater use (m^3 yr^{-1}) for finfish aquaculture use per aquifer.

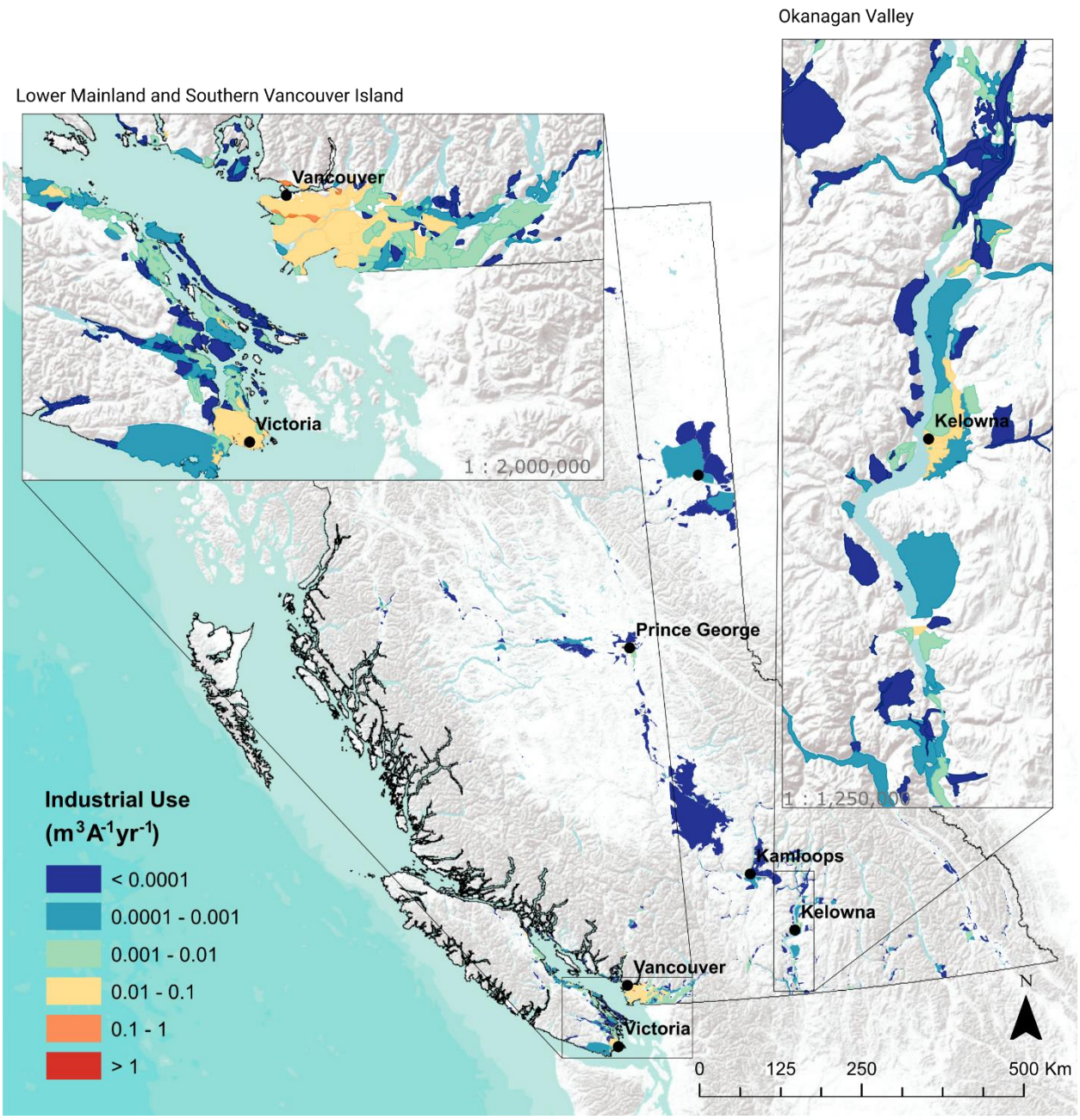

Figure S2.2c Groundwater use (m^3 yr^{-1}) for industrial use per aquifer.

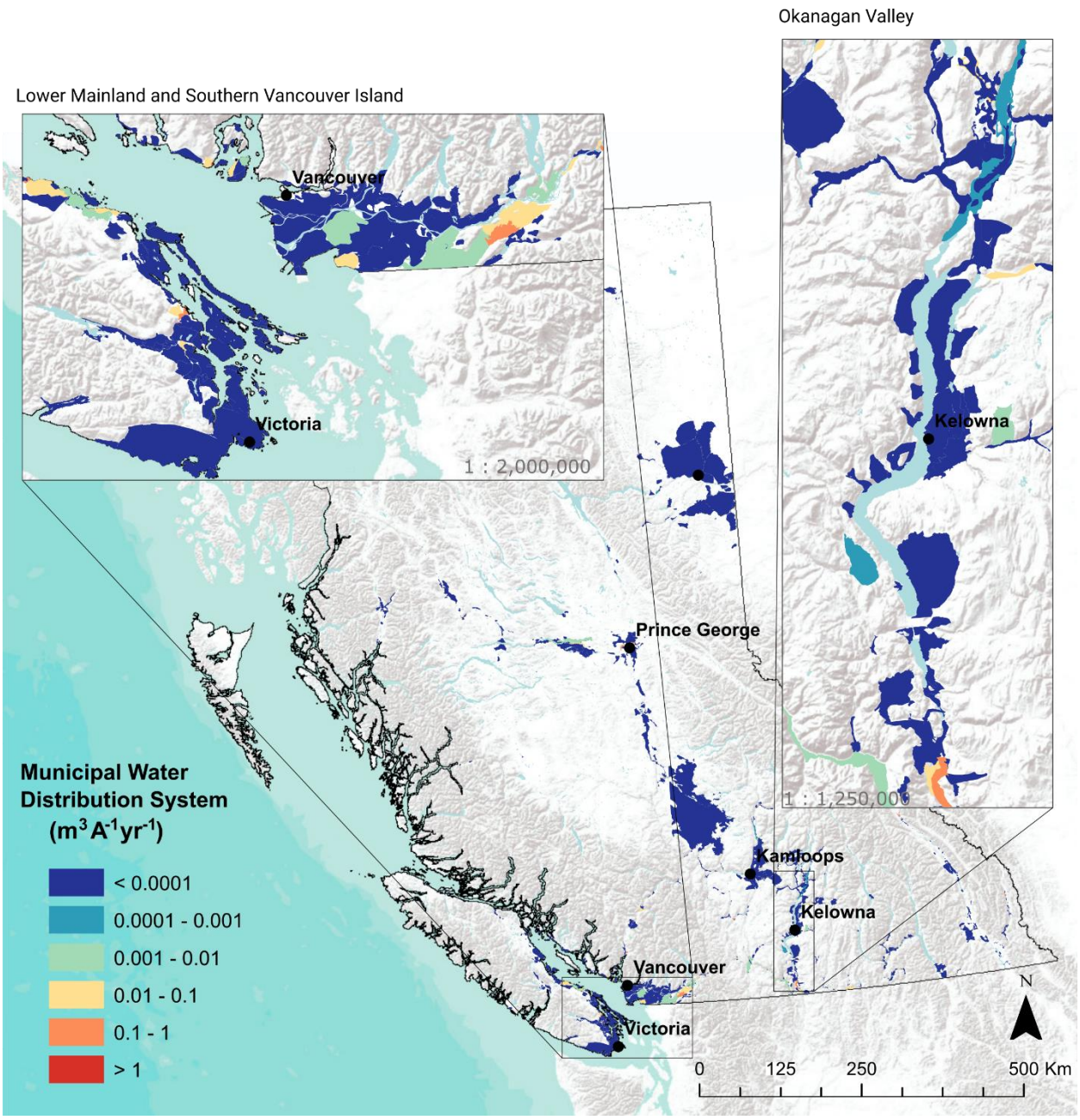

Figure S2.2d Groundwater use (m^3 yr^{-1}) for municipal water distribution use per aquifer.

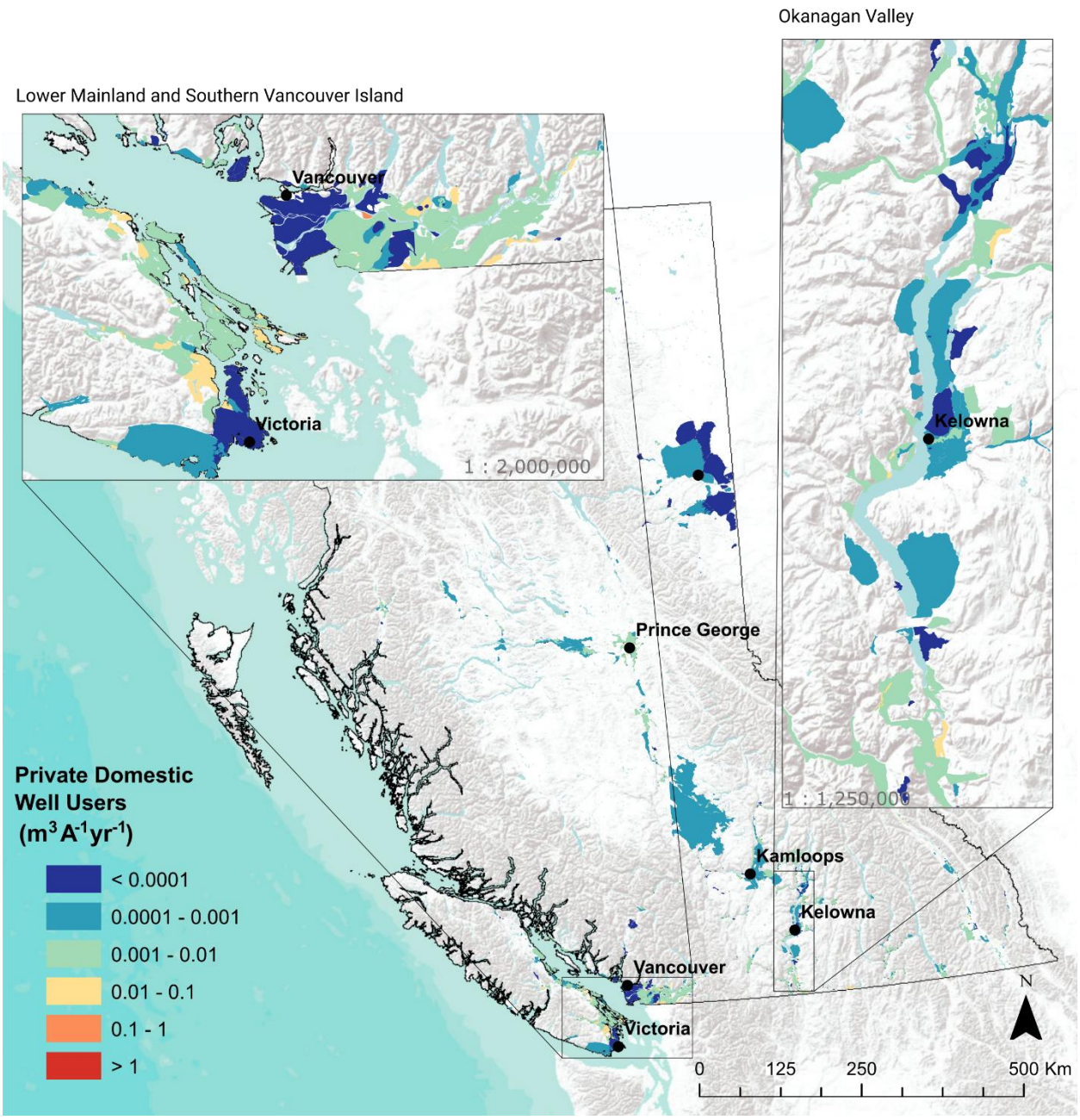

Figure S2.2e Groundwater use (m^3 yr^{-1}) for private domestic wells per aquifer.

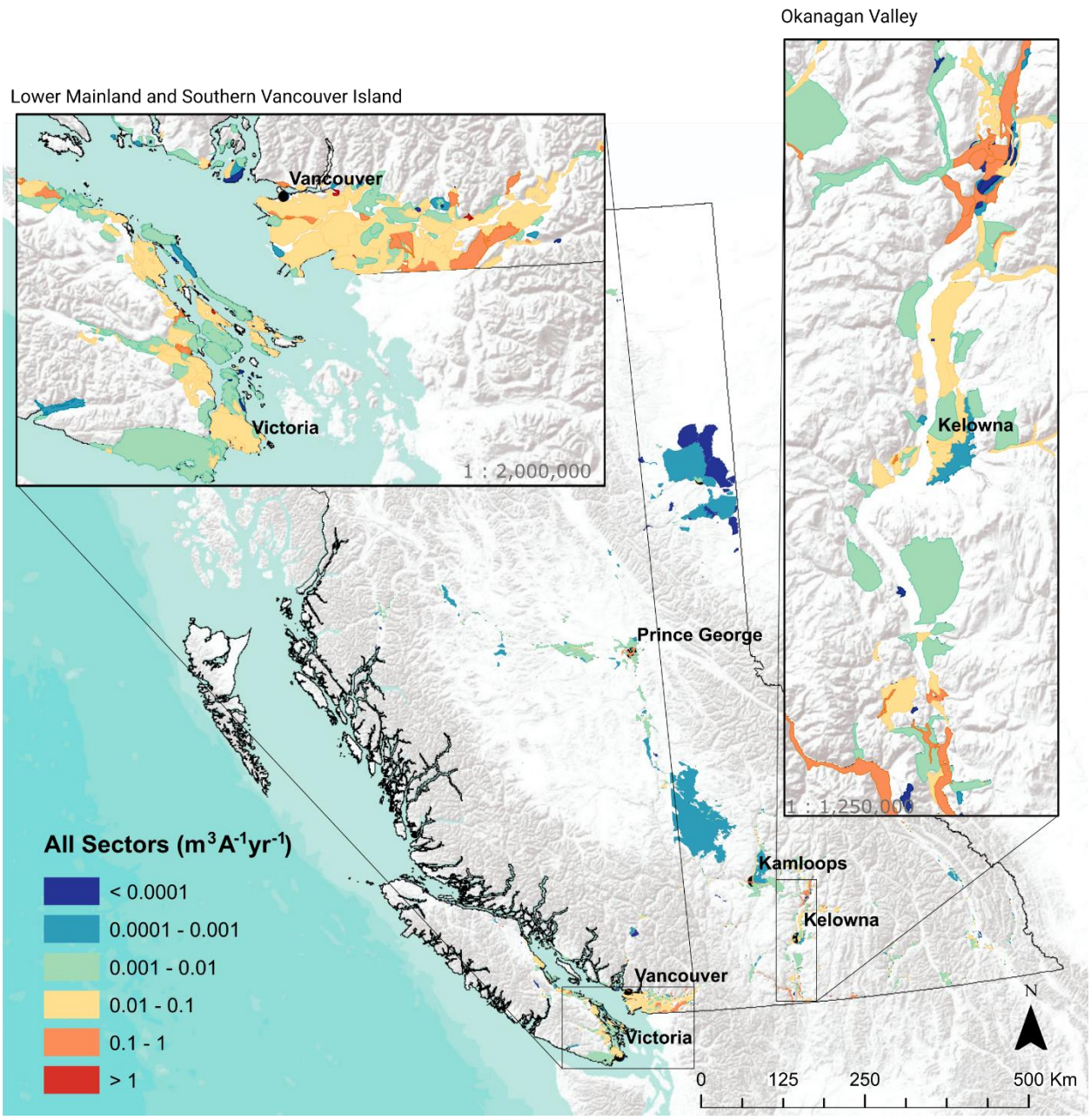

Figure S2.2f Groundwater use (m^3 yr^{-1}) for all major sectors per aquifer.

Table S2.1 Calculation of average water intensity for Canadian manufacturing industries and sub-industries. Data based on annual production and water intake biannual data collected through 2008-2012 (Source: Statistics Canada).

Manufacturing Industry	**Average production in Canada**	**Average total water used**	**Average water intensity**
(sub-industry)	(tonnes)	(m^3)	(m^3 $tonne^{-1}$)
Paper Manufacturing	30,314,400	1,837,640,000	61
Newsprint	5,428,400		
Printing and writing paper	4,864,600		
Wood pulp	20,021,400		
	(m^3)	(m^3)	(m^3 m^{-3})
Wood product manufacturing	70,896,939	58,000,000	0.73
Hardwood lumber	1,590,540		
Softwood lumber	61,073,820		
Structural panels	8,232,579		

Table S2.2 Calculation of average water intensity for Canadian mining industries. Data based on annual production and water intake biannual data collected through 2005-2013 (Source: Statistics Canada).

Sub-Industry	**Average production in Canada**	**Average total water withdrawn**	**Average water intensity**
	(tonnes)	(m^3)	(m^3 $tonne^{-1}$)
Metallic	36,005,954	324,120,000	9.1
Industrial Mineral	336,652,753	69,600,000	0.21
Coal*	66,655,000	33,450,000	0.49

**Total water intake was not reported for 2005, therefore the average total water intake was averaged over 2007-2013*

Table S2.3 Annual groundwater volume withdrawn for wood and paper manufacturing in BC.

Manufacturing Industry (sub-industry)	Average production in B.C. 2008 - 2012 (biannual) (tonne^{-1})	Average water intensity (Canadian production) (m^3 tonne^{-1})	Total Water (m^3)	Ground-water factor (%)	Total ground-water (m^3)
Paper	6,038,000	61	65,000,000	9.2	34,000,000
Pulp and paper shipments	6,038,000				
	(m^3)	(m^3 m^{-3})	(m^3)	(%)	(m^3)
Wood Product	89,071,871	0.73	370,000,000	9.2	6,000,000
Timber scaled	61,974,891				
Lumber	27,096,980				
Total					40,000,000

Table S2.4 Annual groundwater volume withdrawn for mining in BC.

Manufacturing Industry	Average production in B.C. 2008 - 2012 (biannual) (tonne^{-1})	Average water intensity (Canadian production) (m^3 tonne^{-1})	Total Water (m^3)	Groundwater Factor (%)	Total Groundwater (m^3)
Metallic	335,794	9.1	3,100,000	0.35	1,100,000
Industrial Mineral	35,161,200	0.21	7,500,000	0.35	2,700,000
Coal	26,210,400	0.49	13,000,000	0.35	4,600,000
Total Mining					8,400,000

Table S2.5 Surface water and groundwater use statistics per municipality.

Municipality	Pop.	Surface water allocation	% Population		Num. wells		Groundwater ($Mm^3\ yr^{-1}$)		Regional WDS	
	(x 1000)	(Mm^3/yr)	MWDS	PDW	MWDS	PDW	MWDS	PDW	Multi-WDS	% GW
100 Mile House	1.9	0.05	100	-	1	-	0.29	-	-	-
Abbotsford	135.0	0.98	82	18	26	3070	1.46	3.16	-	-
Alert Bay	0.5	0.35	100	-	-	-	-	-	-	-
Anmore	2.1	0.15	100	-	-	-	-	-	GVWD	-
Armstrong	4.8	0.18	100	-	2	-	0.05	-	-	-
Ashcroft	1.7	0.41	100	-	-	-	-	-	-	-
Barriere	1.8	6.65	100	-	1	-	0.08	-	-	-
Belcarra	0.7	-	-	100	-	152	-	0.09	GVWD	-
Bowen Island	3.4	0.00	100	-	12	-	0.62	-	-	-
Burnaby	223.1	-	100	-	-	-	-	-	GVWD	-
Burns Lake	2.1	9.96	100	-	-	-	-	-	-	-
Cache Creek	1.1	1.00	100	-	-	-	-	-	-	-
Campbell River	31.2	6.79	99	1	-	131	-	0.04	-	-
Canal Flats	0.8	3.84	85	15	-	62	-	0.01	-	-
Castlegar	7.9	26.33	100	-	-	-	-	-	-	-
Central Saanich	16.1	-	100	-	-	-	-	-	CRD	-
Chase	2.5	0.16	100	-	2	-	0.28	-	-	-
Chetwynd	2.7	3.32	98	1.8	-	82	-	0.01	-	-
Chilliwack	76.6	10.80	92	8	10	1039	10.66	0.80	-	-
Clearwater	2.4	2.20	100	-	1	-	0.11	-	-	-
Clinton	0.6	0.83	85	15	-	26	-	0.01	-	-
Coldstream	10.4	-	86	14	1	111	0.77	0.19	RDNO	-
Colwood	16.1	-	100	-	-	-	-	-	CRD	-
Comox	13.6	-	100	-	-	-	-	-	CVWD	-
Coquitlam	125.0	7.96	99	1	-	69	-	0.16	GVWD	-
Courtenay	23.9	-	100	-	-	-	-	-	CVWD	-
Cranbrook	19.5	0.02	100	0.5	-	238	-	0.01	-	-
Creston	5.3	5.32	100	-	1	-	0.08	-	-	-
Cumberland	3.2	0.57	99	1	-	15	-	0.00	-	-
Dawson	11.2	121.04	100	-	-	-	-	-	-	-
Delta	100.9	-	100	-	1	-	1.35	-	GVWD	-

Duncan	5.0	36.11	100	-	-	-	-	-	-	-
Elkford	2.5	2.39	100	-	8	-	1.43	-	-	-
Enderby	2.9	0.23	100	-	1	-	0.22	-	-	-
Esquimalt	17.1	-	100	-	-	-	-	-	CRD	-
Fernie	4.4	5.64	100	-	-	-	-	-	-	-
Fort St James	1.5	-	100	-	-	-	-	-	-	-
Fort St John	18.6	31.97	100	-	7	-	3.25	-	-	-
Fraser Lake	1.1	5.42	100	-	-	-	-	-	-	-
Fruitvale	2.0	-	98	2	1	8	0.11	0.01	-	-
Gibsons	4.5	5.22	100	-	6	-	0.75	-	-	-
Gold River	1.4	-	100	-	5	-	0.24	-	-	-
Golden	3.8	-	99	1	8	53	1.26	0.00	-	-
Grand Forks	4.2	26.22	97	3	14	69	1.97	0.02	-	-
Granisle	0.3	0.96	100	-	-	-	-	-	-	-
Greenwood	0.7	3.98	100	-	-	-	-	-	-	-
Harrison Hot Springs	1.5	0.81	65	35	-	40	-	0.07	-	-
Hazelton	0.3	0.10	100	-	-	-	-	-	-	-
Highlands	2.1	-	100	-	-	-	-	-	-	-
Hope	6.1	0.29	95	4	8	210	0.76	0.03	-	-
Houston	3.0	0.00	70	25	7	135	0.38	0.10	-	-
Hudson Hope	1.0	-	70	20	3	75	0.01	0.03	-	-
Invermere	3.3	4.65	95	5	-	80	-	0.02	-	-
Kamloops	87.2	1.00	100	-	4	-	0.35	-	-	-
Kaslo	1.1	1.24	100	-	-	-	-	-	-	-
Kelowna	119.6	112.66	99	1	-	981	-	0.16	-	-
Kent	5.7	-	25	75	6	336	0.22	0.55	-	-
Keremeos	1.4	-	100	-	1	-	0.25	-	-	-
Kimberley	6.7	89.96	100	-	-	-	-	-	-	-
Kitimat	8.9	5.86	100	0.1	-	50	-	0.00	-	-
Ladysmith	7.9	1.34	100	-	-	-	-	-	-	-
Lake Country	11.5	6.90	100	-	-	-	-	-	-	-
Lake Cowichan	3.1	12.48	100	-	-	-	-	-	-	-
Langford	27.4	-	100	-	-	-	-	-	CRD	-
Langley - City	25.4	-	100	-	-	-	-	-	GVWD	-
Langley - District	103.8	-	100	-	-	-	-	-	GVWD	-
Lantzville	3.7	-	100	-	6	-	0.66	-	RDN	100
Lillooet	2.3	26.75	70	20	-	155	-	0.06	-	-
Lions Bay	1.4	4.98	100	-	-	-	-	-	-	-

Logan Lake	2.1	-	100	-	-	-	-	-	-	-
Lumby	1.7	0.86	100	-	-	-	-	-	-	-
Lytton	0.2	1.66	100	-	-	-	-	-	-	-
Mackenzie	3.7	0.37	100	-	2	-	0.74	-	-	-
Maple Ridge	75.4	-	80	20	-	1192	-	1.96	GVWD	-
Masset	0.9	-	100	-	2	-	0.16	-	-	-
McBride	0.6	1.16	100	-	-	-	-	-	-	-
Merritt	7.4	38.41	100	-	13	-	3.08	-	-	-
Metchosin	4.9	-	100	-	-	-	-	-	CRD	-
Midway	0.7	1.04	100	-	-	-	-	-	-	-
Mission	37.2	9.64	80	20	-	1395	-	0.97	-	-
Montrose	1.0	-	100	-	21	-	0.19	-	-	-
Nakusp	1.6	4.31	95	5	1	25	0.12	0.01	-	-
Nanaimo	83.2	3.22	73	26.3	-	404	-	2.84	RDN	-
Nelson	10.2	80.64	100	-	-	-	-	-	-	-
New Denver	0.5	4.49	100	-	-	-	-	-	-	-
New Hazelton	0.6	0.10	100	-	-	-	-	-	-	-
New Westminster	64.9	-	100	-	-	-	-	-	GVWD	-
North Cowichan	29.0	0.40	80	20	19	1623	3.77	0.75	-	-
North Saanich	11.0	-	100	-	-	-	-	-	CRD	-
North Vancouver - City	48.0	0.07	100	-	-	-	-	-	GVWD	-
North Vancouver*	85.3	4.21	100	0.1	-	35	-	0.01	GVWD	-
NRRM	5.8	-	-	95	-	201	-	0.71	-	-
Oak Bay	18.0	-	100	-	-	-	-	-	CRD	-
Oliver	5.0	0.18	100	0.5	15	130	3.91	0.00	-	-
Osoyoos	5.0	0.24	100	-	14	-	0.66	-	-	-
Parksville	12.0	0.07	100	-	25	-	2.16	-	RDN	100
Peachland	5.3	6.26	95	5	-	35	-	0.03	-	-
Pemberton	2.5	0.00	100	-	5	-	0.44	-	-	-
Penticton	33.3	4.74	99	1	-	128	-	0.04	-	-
Pitt Meadows	17.9	-	100	-	-	-	-	-	GVWD	-
Port Alberni	17.7	65.78	100	-	-	-	-	-	-	-
Port Alice	0.8	-	100	-	1	-	0.15	-	-	-
Port Clements	0.4	-	100	-	2	-	0.07	-	-	-
Port Coquitlam	56.3	-	100	-	-	-	-	-	GVWD	-
Port Edward	0.6	11.62	100	-	-	-	-	-	-	-
Port Hardy	4.1	17.53	100	-	-	-	-	-	-	-
Port McNeill	2.6	-	100	-	4	-	0.46	-	-	-

Port Moody	32.8	-	100	-	-	-	-	-	GVWD	-
Pouce Coupe	0.7	0.12	100	-	-	-	-	-	-	-
Powell River	13.1	21.06	3	6	-	6	-	0.10	-	-
Prince George	73.1	47.46	85	15	25	1026	17.78	1.43	-	-
Prince Rupert	12.7	96.94	100	-	-	-	-	-	-	-
Princeton	2.6	0.17	100	-	17	-	0.29	-	-	-
Qualicum Beach	8.8	-	100	-	17	-	1.58	-	RDN	100
Queen Charlotte	1.0	0.19	85	15	3	80	0.13	0.02	-	-
Quesnel	9.8	133.20	98	2	-	283	-	0.03	-	-
Radium Hot Springs	0.9	1.25	100	-	-	-	-	-	-	-
Revelstoke	7.1	4.53	100	-	-	-	-	-	-	-
Richmond	192.6	-	100	-	-	-	-	-	GVWD	-
Rossland	3.5	28.71	99	1	-	13	-	0.00	-	-
Saanich	112.3	2.33	100	-	-	-	-	-	CRD	-
Salmo	1.1	2.50	99	1	2	13	0.30	0.00	-	-
Salmon Arm	17.3	2.50	100	-	3	-	0.62	-	-	-
Sayward	0.3	4.98	86	14.3	-	2	-	0.01	-	-
Sechelt	8.9	-	100	-	-	-	-	-	-	-
Sicamous	2.7	0.00	100	-	1	-	0.48	-	-	-
Sidney	11.4	-	100	-	-	-	-	-	CRD	-
Silverton	0.2	0.84	40	59.9	-	1	-	0.02	-	-
Slocan	0.3	0.00	100	-	-	-	-	-	-	-
Smithers	5.4	6.97	90	10	10	55	0.87	0.07	-	-
Sooke	11.0	-	100	-	-	-	-	-	CRD	-
Spallumcheen	5.1	0.01	100	-	-	-	-	-	RDNO	-
Sparwood	3.8	0.63	84	16	-	92	-	0.08	-	-
Squamish	16.6	8.46	100	0.25	4	139	3.61	0.01	-	-
Stewart	0.5	-	100	-	5	-	0.09	-	-	-
Summerland	11.5	3.12	100	-	4	-	0.10	-	-	-
Surrey	453.3	-	98	2	-	2837	-	1.18	GVWD	-
Tahsis	0.3	0.50	86	14.3	-	-	-	0.01	-	-
Taylor	1.4	42.98	100	-	-	-	-	-	-	-
Telkwa	1.3	13.70	100	-	-	-	-	-	-	-
Terrace	11.5	14.51	95	5	-	33	-	0.07	-	-
Tofino	1.9	2.21	100	-	-	-	-	-	-	-
Trail	7.6	20.74	100	-	-	-	-	-	-	-
Tumbler Ridge	2.7	0.02	100	-	7	-	0.46	-	-	-
Ucluelet	1.6	1.95	100	-	-	-	-	-	-	-

Valemont	1.0	-	99	1	-	6	-	0.00	-	-
Vancouver	610.4	-	100	-	-	-	-	-	GVWD	-
Vanderhoof	4.4	1.18	80	20	1	297	0.95	0.11	-	-
Vernon	38.7	17.01	97	3	-	451	-	0.15	RDNO	-
Victoria	81.8	-	100	-	-	-	-	-	CRD	-
View Royal	9.4	-	100	-	-	-	-	-	CRD	-
Warfield	1.8	1.63	100	-	-	-	-	-	-	-
Wells	0.2	0.00	100	-	1	-	0.04	-	-	-
West Kelowna	26.6	1.36	90	10	-	301	-	0.35	-	-
West Vancouver	42.6	1.66	98	2	-	13	-	0.11	GVWD	-
Whistler	10.2	7.08	100	-	-	-	-	-	-	-
White Rock	19.1	-	100	-	8	-	3.44	-	-	-
Williams Lake	11.1	0.88	99	1	3	329	4.02	0.01	-	-
Zeballos	0.1	1.25	86	14.3	-	3	-	0.00	-	-

**District*

GVWD: Greater Vancouver Water District
CRD: Capital Regional District
CVWD: Comox Valley Water District
RDN: Regional District of Nanimo
RDNO: Regional District of North Okanagan

APPENDIX B:
Chapter 3

S3.1 DETAILED HELP METHODS

S3.1.1 CASE SETTINGS

Case settings describe parameters that are used to set the major functions of the model and characteristics of the one dimensional (1D) simulation. For recharge modelling, runoff and initial moisture settings are the key variables.

Runoff is calculated through the Curve Number (CN), which describes the runoff vs. infiltration behavior of water on the profile surface. HELP takes into account the surface slope, soil texture, and vegetation class to determine the value of CN. In this study, the default option to automatically calculate the CN was selected (it can also be user specified). The surface slope was set to zero for all profiles to minimize the amount of surface runoff generated because this water cannot be routed. When HELP predicts frozen conditions to exist, the value of CN is increased, resulting in a higher calculated runoff. This value was used for the Grand Forks, Abbotsford-Sumas and province wide investigation, which maximizes the amount of recharge calculated.

The initial moisture content for the model was model-generated (it can also be user specified). HELP calculates this value by estimating the initial moisture settings for each storage layer, and running a simulation for one year.

S3.1.2 SURFACE WATER SETTINGS

The surface water settings are user specified; including the runoff area and vegetation class that control how the water on the surface of the profile behaves.

Runoff area defines the percent of area on the surface of the profile for which runoff is possible. Given that the Grand Forks and Abbotsford-Sumas studies both used 100%, this value was also used for the provincial wide study.

The vegetation class defines the class of vegetation on the surface which controls the amount of evapotranspiration. Vegetation class represents the leaf area index (LAI). The options in HELP are limited because the software was developed for modelling infiltration of water in a landfill. We consistently used a 'Good Stand of Grass', the highest value of 5, across British Columbia which leads to lower recharge than the other vegetation classes (such as bare soil). Values higher than 5 are common for treed areas (e.g. 18 for conifers); therefore, recharge values may be overestimated in treed areas of BC

S3.1.3 WEATHER GENERATOR SETTINGS

A Weather Generator (WGEN) is available for use with HELP in Unsat Suite Plus. WGEN generates a stochastic daily weather series of specified length for input to the model. Within WGEN, the station of preference can be selected and the climate statistical parameters accepted or edited, or a new station can be created. The statistical parameters within the WGEN climate station database include total precipitation for each month, mean daily temperature for each month, and a variety of other climate parameters that are used to generate the stochastic weather series. WGEN also requires evaporative zone depth, maximum leaf area index, growing season start and end date, average wind speed, and relative humidity for calculation of evapotranspiration.

Maximum leaf area index defines the density of trees and vegetation in the area. As described above, the value used consistently across the province was 4, to be consistent with the Grand Forks model.

Evaporative depth describes the maximum depth at which water can be lost from recharge to satisfy evapotranspiration demand. The depth is a function of soil properties and vegetation. Within HELP, the possible values include 20 cm, 51 cm and 91 cm. The minimum value allows for maximum evapotranspiration,

minimizing recharge, which was conservatively and consistently used across the province.

Growing season was determined by first frost free day and last frost free day, which is a common climatological meteorological definition (Brown 1976; Menzel et al. 2003). Average annual wind speed was obtained from Environment Canada's climate normals website for a representative station from each biogeoclimatic zone.

S3.1.3 SOIL & AQUIFER PROPERTIES

Drainage layer orientation is a selection between two drainage method profiles in HELP. Any given layer of a profile may be selected as either vertical or horizontal. Horizontal orientation is used in landfill or drainage design as it allows for input of a specified lateral flow into or out of the layer. The layers created in HELP for the province wide report were created as vertical drainage layers given that vertical drainage (i.e. recharge) was the parameter of interest in this study.

Slope defines the angle at which the surface of the soil and aquifer align. For simplicity, the slope used for all of these profiles is zero across the province, which maximizes the recharge calculated.

The soil layer thickness defines the depth of soil modelled from the profile surface down to the start of the aquifer material. For consistency across the province, soil thickness was assumed to be 1m, which is consistent with previous modelling for both Abbotsford-Sumas and Grand Forks models.

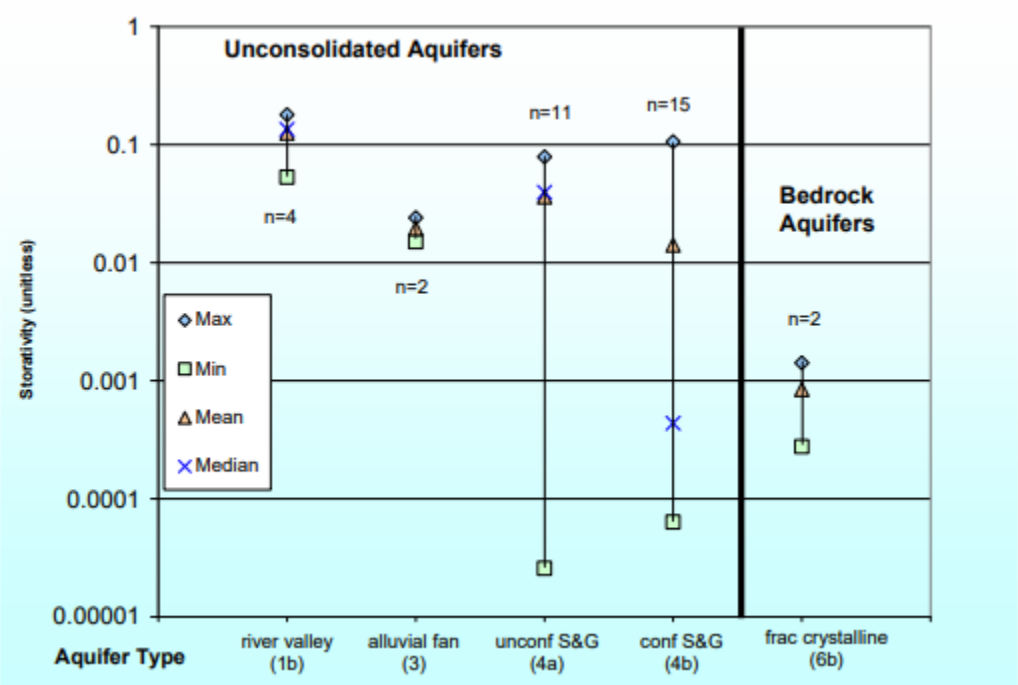

Figure S3.1 Storativity values by aquifer type for aquifers in the Okanagan Basin Region (Carmichael et al. 2008b).

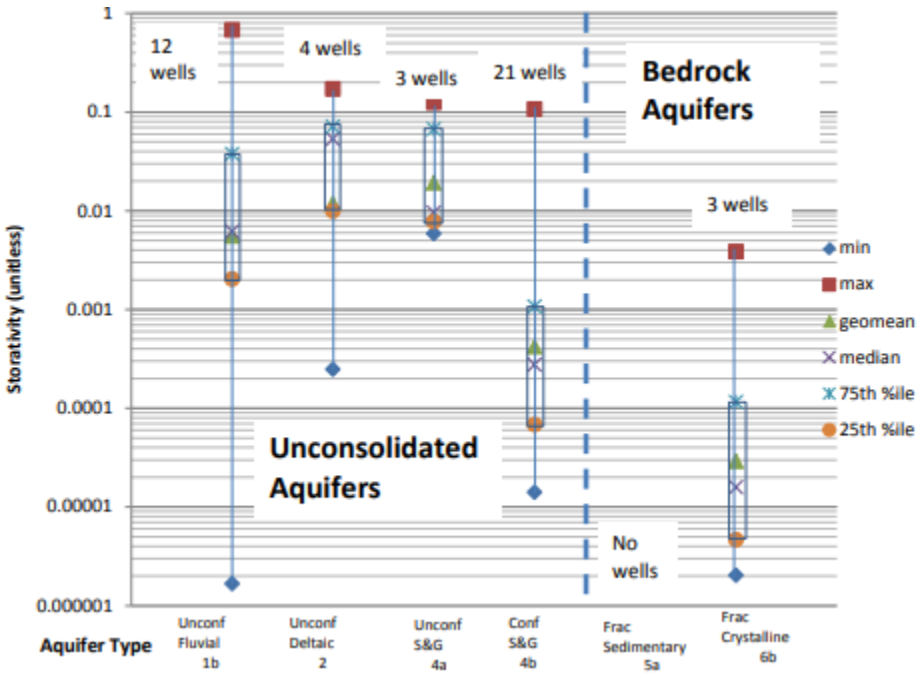

Figure S3.2 Storativity values by aquifer type for aquifers in the Cowichan valley Region (Carmichael 2014).

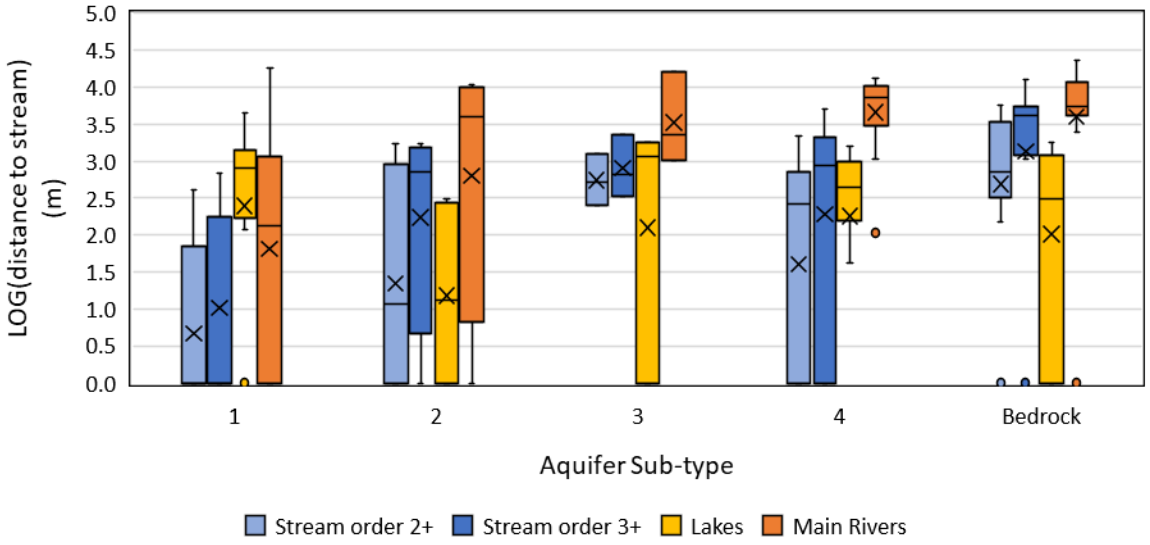

Figure S3.3 The difference in distance to nearest stream versus the distance to specified stream orders.

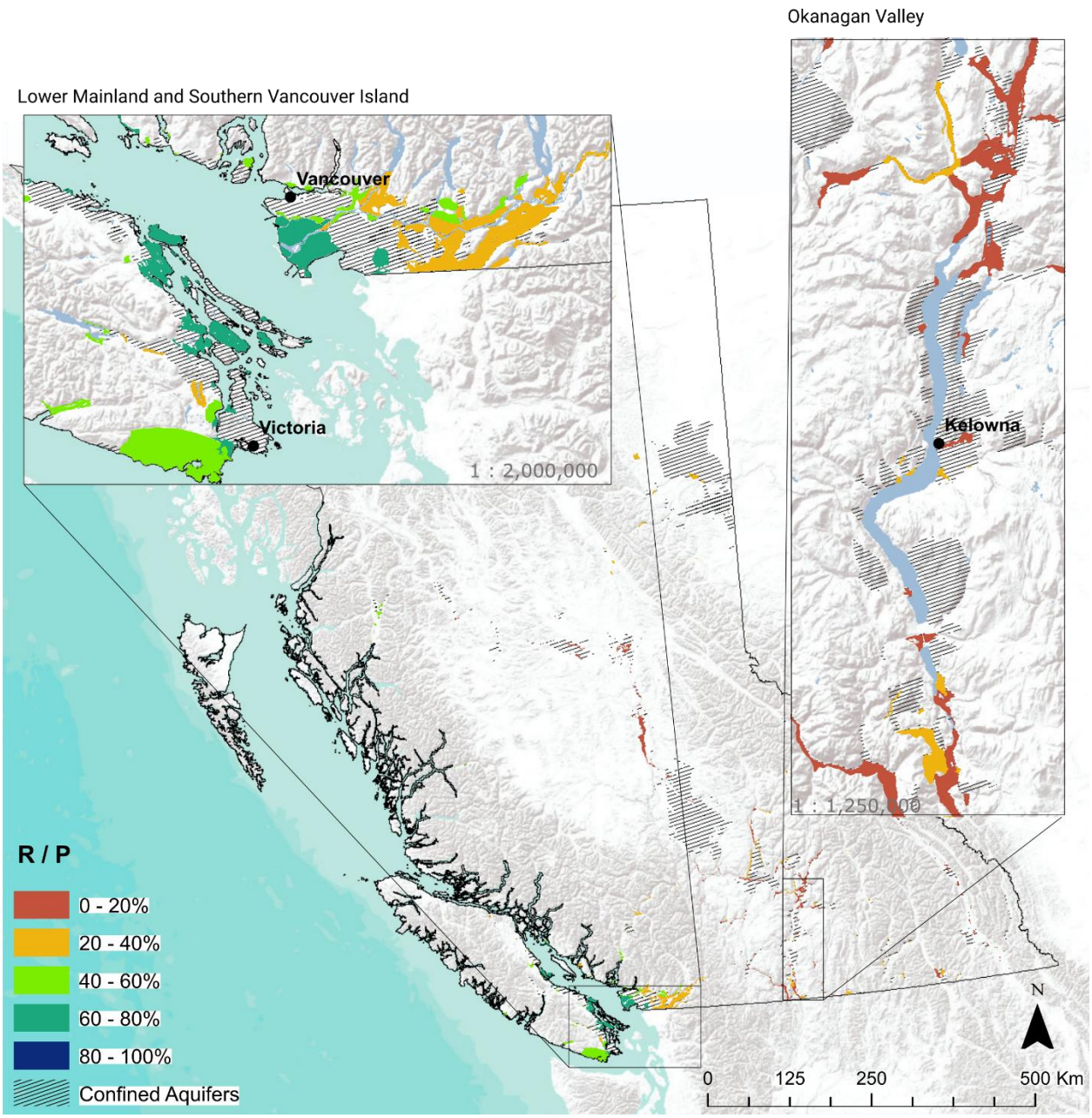

Figure S3.4 HELP modelled recharge (R_{HELP}) as a percent of precipitation distributed to mapped aquifers in BC (Recharge / Precipitation).

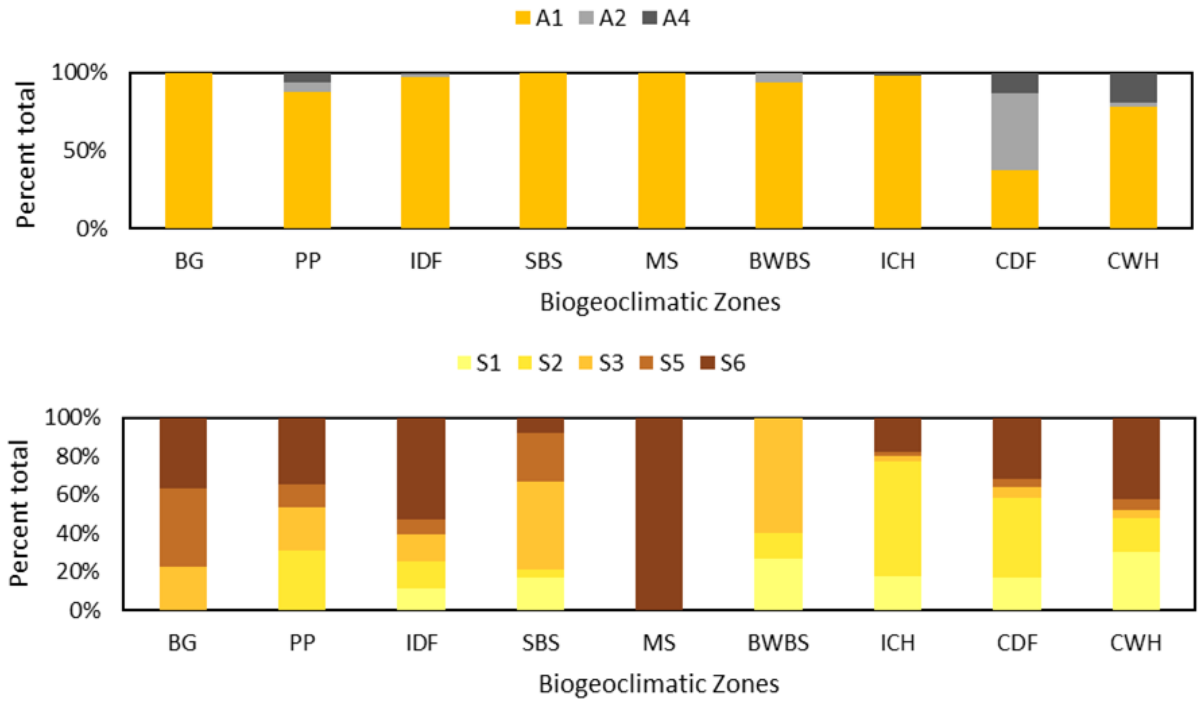

Figure S3.5 Distribution of type of aquifer and soil type per BGCZ.

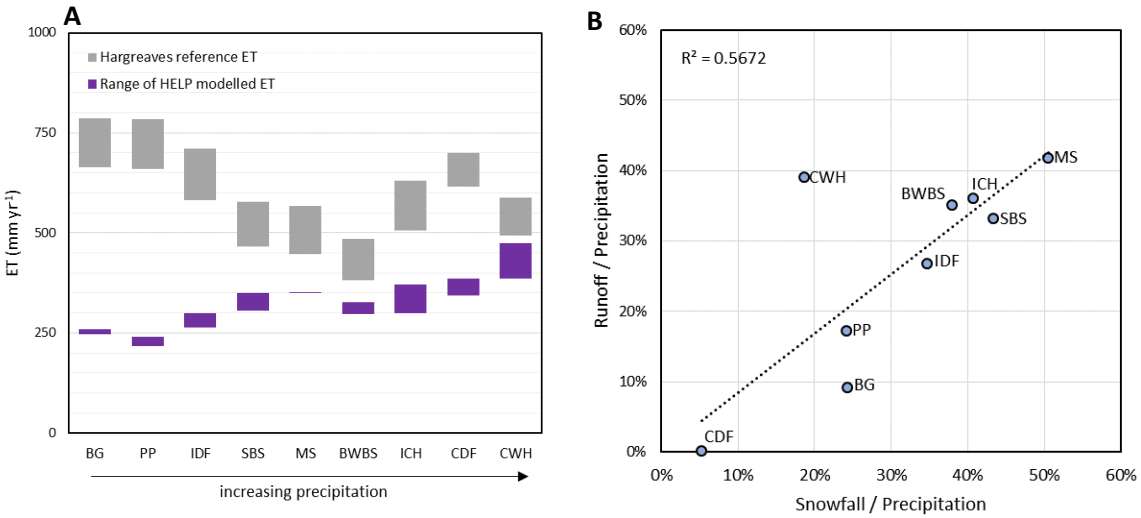

Figure S3.6 HELP modeled values of evapotranspiration (A) and runoff/precipitation (B) compared to observations. (A) Modelled range of actual evapotranspiration in HELP compared to reference potential evapotranspiration per biogeoclimatic zone (B) Percent modelled runoff/precipitation compared to biogeoclimatic zone climate normals (1961-1990) of percent annual snowfall to precipitation. Modelled runoff is generated when HELP soil profile conditions are frozen.

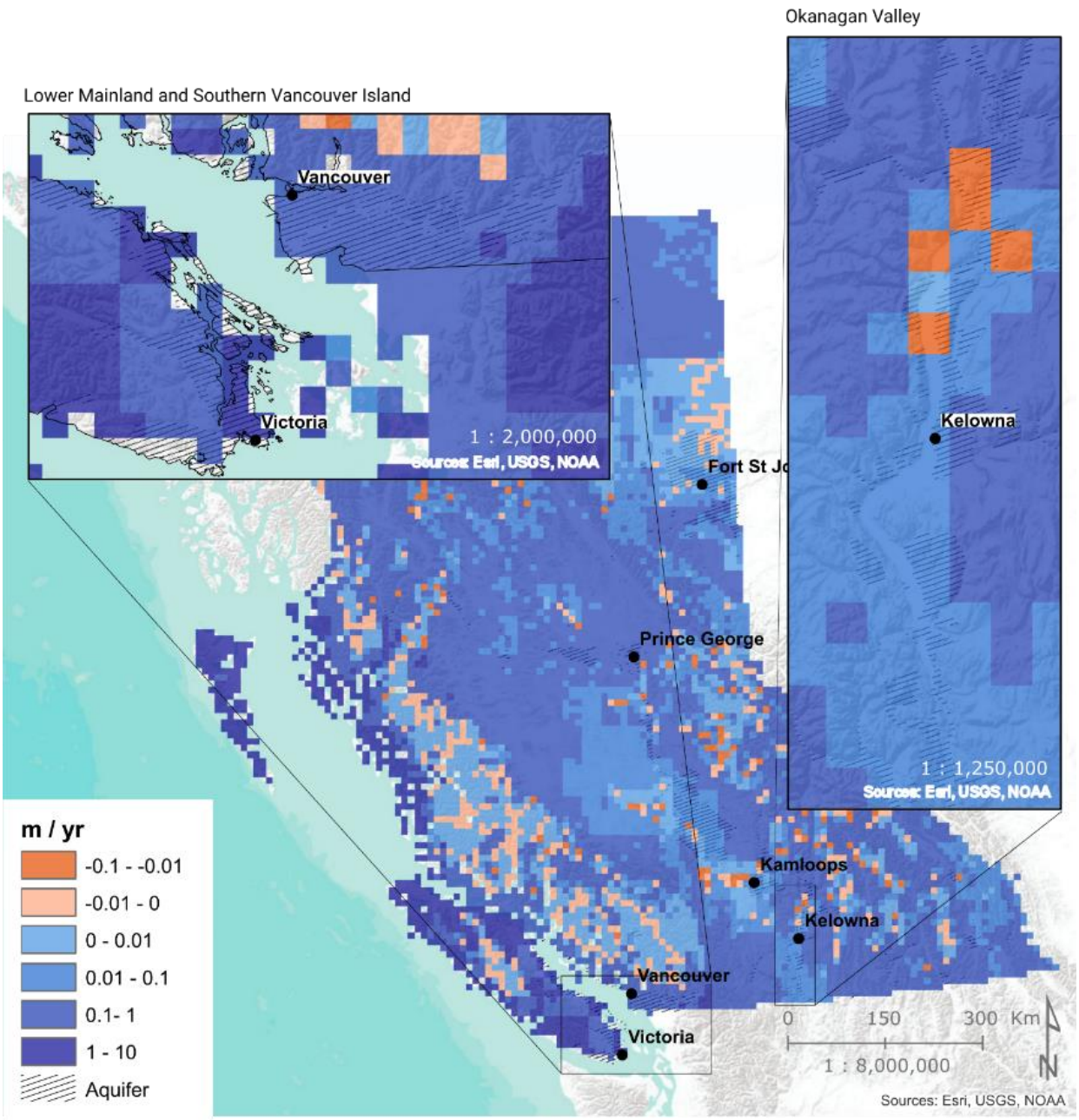

Figure S3.7 Model coverage of PCR-GLOBWB recharge across BC. Red and orange cells were corrected to zero

Table S3.1 Representative station reported per BGCZ. HELP has an internal database of separate climate stations which represent the representative location.

BGCZ	Representative Station*	Closest HELP climate station	Latitude
BG	Kamloops	Kamloops	50.70
BWBS	Fort Nelson A	Smithers	58.84
CDF	Victoria Int'l A	Victoria	48.63
CWH	Haney UBC	Vancouver	49.23
ICH	Revelstoke	Cranbrook	49.21
IDF	150 Mile House	Williams Lake	52.11
MS	Peachland	Peachland	49.87
PP	Kelowna	Penticton	49.86
SBS	Prince George A	Prince George	53.91

**B.C. Ministry of Forests, Lands, Natural Resource Operation and Rural Development*

Table S3.2 Defining HELP soils based on SLC 3.2 (Soil Landscapes of Canada Working Group 2010).

HELP Soil Class	SLC 3.2	HELP default input values	
	K_{sat} cm hr^{-1}	HELP Soil Type	K_{sat} cm hr^{-1}
S1	33.0 30.0	Coarse Sand	33.0
S2	21.0 17.4	Sand	21.0
S3	10.0	Fine Sand	10.0
S4	5.20	Loamy Sand	5.20
S5	3.00	Sandy Loam	3.00
S6	1.00 0.300 0.200	Silty Loam	0.684

**When SLC returns a K_{sat} of 0, soil class is assumed to be S1.*

Table S3 3 Defining aquifer types for HELP analysis

HELP Soil Class	B.C. aquifer classification	(Gleeson et al. 2011)	HELP default input values	
	Sub-type*	Aquifer material	HELP Soil Type	K_{sat} cm hr^{-1}
A1	1a; 1b; 2; 3; 4a	coarse grained unconsolidated	coarse sand	45.3
A2	5a; 6a	coarse grained siliciclastic sedimentary	silty loam	1.1
A3	5b	carbonate	loamy sand	5.7
A4	6b	crystalline; volcanic	silty loam	0.029

**when sub-type of aquifer is "UNK", aquifer material is used to determine HELP aquifer type. If aquifer material is sand or gravel, aquifer type is "A1", if bedrock material, aquifer type is "A2".*

Table S3.4 Average water table depths used for the HELP modelling based on unique combinations of biogeoclimatic zones, soil and aquifer type. Blank cells indicate no aquifers with these combinations. μ = mean, σ = standard deveiation.

Soil & Aquifer	Water table depth (m)																	
	BG		PP		IDF		SBS		MS		BWBS		ICH		CDF		CWH	
	μ	σ	μ	σ	μ	σ	μ	σ	μ	σ	μ	σ	μ	σ	μ	σ	μ	σ
S1_A1					27.7	23.3	17.8	4.9			8.5	1.6	12.3	12.6	24.1	0.1	26.6	26.3
S1_A2					84.4	0.0									15.7	15.2	20.2	26.2
S1_A4																	45.0	20.0
S2_A1			38.2	32.1	31.2	13.2	8.1	0.0			11.6	2.2	33.4	15.9	14.3	0.0	22.8	17.4
S2_A2			59.6	1.0											37.8	14.7		
S2_A4			52.8	0.0									31.2	0.0	44.4	6.9	45.2	14.4
S3_A1	33.8	19.4	26.4	13.4	44.4	23.9	12.5	8.0			21.6	15.8	22.9	0.0	19.3	17.3	19.5	15.3
S3_A2											14.4	0.0					47.6	0.0
S3_A4					37.0	0.0												
S5_A1	29.5	14.1	24.6	8.4	26.0	11.8	17.2	6.9					5.3	0.0	24.9	21.6	7.9	8.8
S6_A1	33.9	16.8	18.8	10.5	20.2	13.4	10.3	11.9	9.2	6.6			22.0	19.0	9.1	9.4	13.4	12.7
S6_A2															25.9	9.3	22.9	0.0
S6_A4															28.8	10.8	43.2	24.7

Table S3.5 Results from the WTF method for observation wells.

ow	aq num	BGCZ	K_{sat} (m/d)	SW* (m)	DD* (m)	b (m)	WTD	t_{lin} (days)	h/t (m/yr)	Effects**							R (mm)	A/D (%)
										1	2	3	4	5	6	7		
2	15	CWH	10.872	700	282	34	mod	60	8.64	T							1728	7.7%
272	15	CWH	0.264	1980	479	37	shallow	25	5.47								1094	0.45%
299	15	CWH	10.872	127	102	43	shallow	60	6.79								1359	75%
354	35	CWH	10.872	2	288	10	mod	60	3.92	T							784	100%
360	41	CDF	0.00696	465	176	30	shallow	13	10.08								2017	17%
296	74	BG	10.872	570	31	32	shallow	22	6.69								1339	18%
329	159	CWH	0.00696	41	150	86	shallow	60	11.43								2285	92%
75	259	BG	10.872	794	335	34	shallow	5	9.46	T							1892	9.2%
154	297	PP	0.00696	350	523	81	shallow	30	1.87	T							374	22%
128	447	CDF	10.872	109	1185	10	shallow	15	3.32								664	50%
386	659	SBS	0.00696	402	36	22	shallow	19	4.24								848	21%
197	709	CDF	10.872	1003	852	30	mod	14	13.97								2794	0.30%
316	709	CDF	10.872	581	135	20	shallow	60	9.82								1964	0.011%
406	8	CWH	10.872	451	227	102	shallow	12			T						-	-
8	15	CWH	10.872	215	20	87	mod	30		T		T					-	-
301	15	CWH	10.872	326	217	110	mod	0		T			T				-	-
414	35	CWH	10.872	116	288	44	deep	0			T		T				-	-
415	35	CWH	10.872	116	288	117	deep	0			T		T				-	-
275	41	CDF	0.00696	1616	48	91	shallow	299		T			T				-	-
353	41	CDF	10.872	428	223	36	shallow	15		T	T				T		-	-
349	68	CWH	10.872	370	134	37	shallow	428			T						-	-
378	92	SBS	10.872	12	1939	49	deep	0		T	T						-	-
185	97	IDF	10.872	382	220	43	shallow	17			T						-	-
260	115	SBS	0.00696	1775	259	93	deep	0			T		T				-	-
346	134	BG	10.872	23	26	42	NA	NA	-	-	-	-	-	-	-	-	-	-
423	134	BG	10.872	63	27	82	NA	NA	-	-	-	-	-	-	-	-	-	-
217	158	PP	10.872	823	166	75	shallow	86		T	T						-	-
312	161	CDF	0.00696	27	38	17	shallow	0			T						-	-
337	162	CDF	10.872	1357	27	10	mod	60		T		T					-	-
390	162	CDF	10.872	438	26	14	deep	0			T		T				-	-

432	162	CDF	10.872	170	49	38	mod	9			T						-	-
355	172	CDF	0.00696	388	24	27	shallow	0			T						-	-
318	186	CDF	10.872	8	70	43	shallow	30					T		T		-	-
204	187	CDF	0.00696	74	280	37	shallow								T		-	-
96	193	BG	10.872	30	740	20	shallow	0		T	T			T			-	-
101	193	BG	0.00696	14	145	23	shallow	0		T	T			T			-	-
365	229	IDF	10.872	574	489	577	shallow	14			T						-	-
332	254	BG	10.872	620	353	32	mod	0	-	-	-	-	-	-	-	-	-	-
407	255	BG	10.872	420	117	28	mod	15				T					-	-
405	256	BG	10.872	925	215	319	mod	30		T				T			-	-
203	259	BG	0.00696	324	213	11	deep	5					T				-	-
403	261	PP	10.872	301	130	40	deep	10					T				-	-
302	307	ICH	10.872	292	79	84	NA	NA	-	-	-	-	-	-	-	-	-	-
172	345	IDF	10.872	33	37	10	mod	0			T			T			-	-
180	353	IDF	10.872	1032	13	57	mod	0			T		T				-	-
364	370	SBS	10.872	473	29	41	deep	3					T				-	-
352	390	CWH	10.87\2	46	63	30	shallow	0			T		T				-	-
371	415	CWH	10.872	137	57	479	shallow	10			T						-	-
288	438	CDF	10.872	740	49	37	mod	86			T						-	-
306	482	IDF	10.872	149	60	36	NA	NA	-	-	-	-	-	-	-	-	-	-
74	507	ICH	10.872	117	520	12	deep	0			T						-	-
362	521	IDF	10.872	298	366	10	shallow	9				T					-	-
363	540	PP	10.872	390	13	28	mod	13		T				T			-	-
286	635	BWBS	10.872	22	126	76	NA	NA	-	-	-	-	-	-	-	-	-	-
389	664	CDF	10.872	250	191	45	shallow	4			T						-	-
196	709	CDF	0.264	2775	228	18	shallow	30							T		-	-
385	709	CDF	10.872	965	467	16	mod	265					T				-	-
283	711	CDF	10.872	412	300	19	shallow	21			T						-	-
373	722	CDF	10.872	298	119	10	shallow	30				T					-	-
268	740	CDF	0.00696	1033	167	10	shallow	303			T						-	-
401	808	PP	10.872	1480	196	24	shallow	0		T	T						-	-
375	825	ICH	1.368	150	111	58	mod	0		T	T						-	-
408	834	CDF	10.872	216	1	26	deep	15					T				-	-

** Distance to the nearest constant head boundary (SW); Distance to the nearest drainage divide (DD)*

*** 1: Smooth groundwater hydrograph; 2: Too close to drainage boundary; 3: T varies with h; 4: Close proximity to pumping; 5: Non-equilibrium recharge; 6: Shallow water table; 7: Transience in S_Y*

Table S3.6 Results from sensitivity analysis for HELP aquifer codes per biogeoclimatic zone.

BGCZ	AQ		GWS		HUM		PRC		SOIL		TMP		WND		WTD	
	-σ	+σ	-σ	+σ	-σ	+σ	-σ	+σ	-σ	+σ	-σ	+σ	-σ	+σ	-σ	+σ
BG	1	-1	-3	-4	-6	1	-82	61	-27	6	-12	8	1	-8	-1	-18
PP	-2	2	-	-	-2	2	-40	59	-5	6	-9	19	3	-3	1	-4
IDF	-17	1	1	-1	-2	2	-42	60	-5	9	-10	11	4	-4	1	-2
SBS	-	-	-	-1	-2	2	-45	67	-5	6	-7	11	4	-4	-	-
MS	1	-	-	-	-2	3	-52	90	-5	6	-12	20	7	-4	-	1
BWBS	-	-	-	-	-1	1	-49	67	-4	1	-4	81	5	-4	-	-
ICH	-3	-	-	-1	-2	-	-49	56	-4	5	-17	22	-	-2	-	-
CDF	-	-	-	-	-2	1	-51	56	-1	1	-7	-1	1	-1	-	-
CWH	-	-	-	-	-1	1	-45	47	-2	2	-24	60	1	-	-	-

S3.2 WATER TABLE FLUCTUATION METHOD - R SCRIPTS

S3.2.1 JOINING CLIMATE STATIONS TO OBSERVATION WELLS

The following script joins climate stations within 25km radius of the nearest observation wells.

```
setwd("E:/ThesisStuff/MoE_aquifer_stress/3.Working_Folder/Working/3.
Recharge/WTF")

OW_CS_data <- read.csv("2.Processing/OW_CS_overlap.csv")

OW_CS_data$ow.s.date <-
as.POSIXct(strptime(as.character(OW_CS_data$ow.s.date),'%Y-%m-%d'))
OW_CS_data$ow.e.date <-
as.POSIXct(strptime(as.character(OW_CS_data$ow.e.date),'%Y-%m-%d'))
OW_CS_data$cs.s.date <-
as.POSIXct(strptime(as.character(OW_CS_data$cs.s.date),'%Y-%m-%d'))
OW_CS_data$cs.e.date <-
as.POSIXct(strptime(as.character(OW_CS_data$cs.e.date),'%Y-%m-%d'))

OW_CS_data$overlap1 <- ifelse((OW_CS_data$ow.s.date >
OW_CS_data$cs.s.date) &
                                (OW_CS_data$ow.s.date >
OW_CS_data$cs.e.date) &
                                (OW_CS_data$ow.e.date >
OW_CS_data$cs.s.date) &
                                (OW_CS_data$ow.e.date >
OW_CS_data$cs.e.date),
                              "OUT","IN")
OW_CS_data$overlap2 <- ifelse((OW_CS_data$ow.s.date <
OW_CS_data$cs.s.date) &
                                (OW_CS_data$ow.s.date <
OW_CS_data$cs.e.date) &
                                (OW_CS_data$ow.e.date <
OW_CS_data$cs.s.date) &
                                (OW_CS_data$ow.e.date <
OW_CS_data$cs.e.date),
                              "OUT","IN")

OW_CS_data$overlap.final <- ifelse(OW_CS_data$overlap1 == "IN" &
OW_CS_data$overlap2 == "IN", "IN", "OUT")

dat <- subset(OW_CS_data, OW_CS_data$overlap.final == "IN")
dat.10km <- subset(dat, dat$distance.m <= 25000)
dat.10km$ow.len <- (dat.10km$ow.e.date - dat.10km$ow.s.date)
dat.10km$cs.len <- (dat.10km$cs.e.date - dat.10km$cs.s.date)/86400

dat.10km$cs.s_ow.s <- (dat.10km$cs.s.date - dat.10km$ow.s.date)
dat.10km$overlap.d <- ifelse(dat.10km$cs.s_ow.s > 0,
```

```
                                (dat.10km$cs.len -
dat.10km$cs.s_ow.s)/86400,
                                dat.10km$cs.len)

write.csv(dat.10km, file = paste("3.Results/OW_CS_join.csv",sep =""))
```

S3.2.2 CALCULATING AND PLOTTING HEAD RECESSIONS DURING DRY PERIODS

The following script joins observation well data to daily precipitations data and calculated periods of no precipitation, and subsequently calculates groundwater head recessions.

```
library(gridExtra)
library(ggplot2)
library(grid)
library(data.table)
library(readxl)
library(ggpmisc)
library(plyr)

#open list of wells
setwd("E:/ThesisStuff/MoE_aquifer_stress/3.Working_Folder/Working/3.
Recharge/WTF")
OW_data <- read.csv("1.Data/OW_data.csv")
OW_CS_data <- read.csv("1.Data/OW_CS_join.csv")
OW.WTFresults <- data.frame(Obs_well = OW_data$Obs_Num,
                            Result = NA,
                            Slope = NA,
                            std.slope = NA,
                            change.h = NA)
ow.num.list <- unique(OW_CS_data$ow.num)

#functions
OW_Climate_join <- function(data, cs_data, i) {
  OW.file <- read.csv(paste("1.Data/OW_stations/OW",data[i,1],
                            "-data.csv",sep=""))
  OW.file$nTime <- substr(OW.file$Time,12,16)
  OW.file$Date <-
as.POSIXct(strptime(as.character(substr(OW.file$Time,1,10)),
                                      '%Y-%m-%d'))

  #keep only 12:00 values; gets rid of hourly data
  OW.sub1 <- subset(OW.file, OW.file$nTime == "12:00")
  OW.sub1$timediff <-
c(0,difftime(OW.sub1$Date[2:(length(OW.sub1$Date))] ,
OW.sub1$Date[1:length(OW.sub1$Date)-1], units="days"))

  #all data at daily timestep
  OW.sub2 <- subset(OW.sub1, OW.sub1$timediff == "1")
  dt.OW <- data.table(Date =
as.character((substr(OW.sub2$Date,1,11))),
                      WTD = OW.sub2$Value)

  cs_ow_data <- subset(cs_data, cs_data$ow.num == data[i,1])

  OW_CS <- data.table()
```

```
  dt.CS <- data.table()

  for (cs in 1:nrow(cs_ow_data)) {
    try(CS.file <-
read.csv(paste("1.Data/Climate_data/EC/",cs_ow_data$cs.num[cs],".ascii
", sep =""), header = TRUE, skip = 1))
    try(dt.CS <- data.table(Date =
as.character(substr(CS.file$time,2,11)),
                            CS.precip =
CS.file$ONE_DAY_PRECIPITATION,
                            CS.id = cs_ow_data$cs.num[cs]))
    try(dt.merge <- merge(dt.OW, dt.CS))
    try(OW_CS <- rbind(OW_CS, dt.merge, fill=TRUE))
  }
  try(OW_CS <- OW_CS[!duplicated(OW_CS$Date), ])
  try(OW_CS <- subset(OW_CS, OW_CS$CS.precip != "None"))
  try(OW_CS$Date <- as.POSIXct(OW_CS$Date))
  try(OW_CS$WTD <- OW_CS$WTD * -1)
  try(OW_CS$Year <- year(OW_CS$Date))
  return(OW_CS)
}
count_dry_periods <- function(data) {
  data.0precip <- subset(data, data$CS.precip == 0)
  data.0precip$timediff <-
c(0,difftime(data.0precip$Date[2:(length(data.0precip$Date))] ,
data.0precip$Date[1:length(data.0precip$Date)-1], units="days"))

  # find number of days without precip
  period = 1
  data.0precip$period <- 0
  for (k in 2:nrow(data.0precip)) {
    if(data.0precip$timediff[k] == 1) {
      data.0precip$period[k] <- period
      data.0precip$period[k-1] <- period
    } else {
      period = period + 1
    }
  }

  data.0precip.periods <- subset(data.0precip, data.0precip$period !=
0)

  count.dry = 1
  data.0precip.periods$drycount <- 1
  data.0precip.periods$slope <- NA

  for (j in 2:nrow(data.0precip.periods)) {
    if (data.0precip.periods$period[j] ==
data.0precip.periods$period[j-1]) {
      count.dry = count.dry + 1
      data.0precip.periods$drycount[j] <- count.dry
```

```
    } else {
      count.dry = 1
      data.0precip.periods$drycount[j] <- count.dry
    }
  }

  final <-
data.0precip.periods[,list(s.Date=min(Date),e.Date=max(Date), dry.len
= max(drycount)),by=period]
  return(final)
}
plot_dry_periods <- function(data, OW.CS.data) {
  year.count <- count(OW.CS.data, 'Year')
  year.count <- subset(year.count , year.count$freq > 30)

  OW.CS.data$fills <- NA

  year.list <- unique(year.count$Year)

  all.WTD.data <- data.table()
  all.precip.data <- data.table()

  for (n in 1:length(year.list)) {
    year.ow <- subset(OW.CS.data, OW.CS.data$Year == year.list[n])
    year.slopes <- subset(data, data$year == year.list[n])
    year.ow$fills <- NA

    for (c in 1:nrow(year.slopes)) {
      year.ow$fills[year.ow$Date >= year.slopes$s.Date[c] &
year.ow$Date <=year.slopes$e.Date[c]] <- year.slopes$dry.len[c]
    }
    WTD.data <- year.ow
    WTD.data$panel <- "a"
    precip.data <- year.ow
    precip.data$panel <- "b"
    plot.data <- rbind(precip.data, WTD.data)
    plot.data$panel <- factor(plot.data$panel, levels = c("a", "b"))

    precip.WTF.facet <- ggplot(data = plot.data) +
      facet_grid(panel~., scale = "free") +
      geom_point(data = WTD.data, aes(x = Date, y = WTD, color =
fills)) +
      scale_fill_gradient2(low = "#d73027",
                           mid = "#ffffbf",
                           high = "#4575b4",
                           midpoint = 14,
                           na.value = "#000000",
                           aesthetics = "colour",
                           name = "No precip \nlength (days)") +
      geom_segment(data = precip.data,
                   aes(x=Date, xend=Date, y=0, yend=CS.precip),
```

```
                    size=1) +
      scale_y_continuous(name = "Precipitation (mm)
Water Table Depth (m)") +
      theme_classic() +
      ggtitle(paste("Observation Well",ow.num),
              subtitle = paste("Aquifer Number", aq.num,
                               "\nYear =", year.list[n])) +
      theme(legend.position = "top",
            panel.grid.major.y = element_line(colour="#d9d9d9",
size=0.5),
            axis.title.x = element_blank(),
            strip.text = element_blank()) +
      scale_x_datetime(date_breaks = "1 month",
                       date_labels = "%b")

    all.WTD.data <- rbind(all.WTD.data, WTD.data)
    all.precip.data <- rbind(all.precip.data, precip.data)

    ggsave(paste("3.Results/WTF - modified/OW_hrecessions_yearly/OW",
ow.num ,"_",year.list[n],".png", sep=""),
           plot = precip.WTF.facet,
           height = 10,
           width = 10
           )
  }
  precip.WTF.facet.all <- plot_all(all.WTD.data, all.precip.data)

  ggsave(paste("3.Results/WTF - modified/OW_hrecessions_total/OW",
ow.num ,".png", sep=""),
         plot = precip.WTF.facet.all,
         height = 10,
         width = 10
  )
  return(length(year.list))
}
plot_yearly <- function(all.WTF.data, data, year) {
  WTD.data <- data
  WTD.data$panel <- "a"
  precip.data <- data
  precip.data$panel <- "b"
  plot.data <- rbind(precip.data, WTD.data)
  plot.data$panel <- factor(plot.data$panel, levels = c("a", "b"))

  precip.WTD.facet <- ggplot(data = plot.data) +
    facet_grid(panel~., scale = "free") +
    geom_point(data = WTD.data, aes(x = Date, y = WTD, color = fills))
+
    scale_fill_gradient2(low = "#d73027",
                         mid = "#ffffbf",
                         high = "#4575b4",
                         midpoint = 14,
```

```
                        na.value = "#000000",
                        aesthetics = "colour",
                        name = "No precip \nlength (days)") +
    geom_segment(data = precip.data,
                 aes(x=Date, xend=Date, y=0, yend=CS.precip),
                 size=1) +
    scale_y_continuous(name = "Precipitation (mm)
Water Table Depth (m)") +
    theme_classic() +
    ggtitle(paste("Observation Well",ow.num),
            subtitle = paste("Aquifer Number", aq.num,
                             "\nYear =", year)) +
    scale_x_datetime(date_breaks = "1 month",
                     date_labels = "%b") +
    theme(legend.position = "top",
          panel.grid.major.y = element_line(colour="#d9d9d9",
size=0.5),
          panel.grid.major.x = element_line(colour="#d9d9d9",
size=0.5),
          axis.title.x = element_blank(),
          strip.text = element_blank())


  all.WTD.data <- rbind(all.WTD.data, WTD.data)
  all.precip.data <- rbind(all.precip.data, precip.data)
  return(precip.WTD.facet)
}
plot_all <- function(WTD, precip) {
  WTD.data <- WTD
  WTD.data$panel <- "a"
  precip.data <- precip
  precip.data$panel <- "b"
  plot.data <- rbind(precip.data, WTD.data)
  plot.data$panel <- factor(plot.data$panel, levels = c("a", "b"))

  precip.WTD.facet <- ggplot(data = plot.data) +
    facet_grid(panel~., scale = "free") +
    geom_point(data = WTD.data, aes(x = Date, y = WTD, color = fills))
+
    scale_fill_gradient2(low = "#d73027",
                         mid = "#ffffbf",
                         high = "#4575b4",
                         midpoint = 14,
                         na.value = "#000000",
                         aesthetics = "colour",
                         name = "No precip \nlength (days)") +
    geom_segment(data = precip.data,
                 aes(x=Date, xend=Date, y=0, yend=CS.precip),
                 size=1) +
    scale_y_continuous(name = "Precipitation (mm)
Water Table Depth (m)") +
```

```
    theme_classic() +
    ggtitle(paste("Observation Well",ow.num),
            subtitle = paste("Aquifer Number", aq.num)) +
    scale_x_datetime(date_breaks = "1 year",
                     date_labels = "%Y") +
    theme(legend.position = "top",
          panel.grid.major.y = element_line(colour="#d9d9d9",
size=0.5),
          axis.title.x = element_blank(),
          strip.text = element_blank())

  return(precip.WTD.facet)
}
calc_slope <- function(data, OW.CS.data, ow.num) {
  my.formula <- y*3.154e+7 ~ x
  data$slope0.m <- NA
  data$rsq0 <- NA
  data$slope3.m <- NA
  data$rsq3 <- NA
  data$slope5.m <- NA
  data$rsq5 <- NA

  for (n in 1:nrow(data)) {
    period.data <- subset(OW.CS.data, OW.CS.data$Date >=
data$s.Date[n] & OW.CS.data$Date <= data$e.Date[n])

    #calculate slope for each interval of P = 0 (Starting only 4 days
after precipitation ends)
    if (nrow(period.data) > 3) {

      #calc slope and convert from m/s to m/yr (* seconds in a year)
      mod.0 = lm(WTD ~ Date, data = period.data)
      data$slope0.m[n] <- coef(mod.0)[2]*31557600
      data$rsq0[n] <- summary.lm(mod.0)$r.squared

      mod.3 = lm(WTD ~ Date, data = period.data[3:nrow(period.data)])
      data$slope3.m[n] <- coef(mod.3)[2]*31557600
      data$rsq3[n] <- summary.lm(mod.3)$r.squared

      mod.5 = lm(WTD ~ Date, data = period.data[5:nrow(period.data)])
      data$slope5.m[n] <- coef(mod.5)[2]*31557600
      data$rsq5[n] <- summary.lm(mod.5)$r.squared
    }
  }
  write.csv(data, file =
paste("3.Results/R_intervals/OW",ow.num,"_results.csv",sep =""))
  data <- subset(data, data$rsq3 > 0.97 & data$slope3.m < 0)
  return(data)
}
plot_slope <- function(data, ow.num, aq.num, avg.slope, num.yrs) {
```

```
  plot1 <- ggplot(data, aes(x = factor(dry.len), y = (slope3.m*-1),
fill = dry.len)) +
    geom_boxplot() +
    scale_fill_gradient2(low = "#d73027",
                         mid = "#ffffbf",
                         high = "#4575b4",
                         midpoint = 14,
                         na.value = "#000000",
                         aesthetics = "fill",
                         name = "No precip \nlength (days)") +
    scale_y_continuous(name = "h recession [m / year]",
                       breaks = seq(0,500,5)) +
    geom_hline(yintercept=avg.slope, linetype="dashed") +
    scale_x_discrete(name = "Recession period (days)") +
    ggtitle(paste("Observation Well ",
                  ow.num," - Aquifer ",
                  aq.num, " (", num.yrs," year record)", sep = ""),
            subtitle = paste("Specific yield : ", aq.Sy, " (",
aq.Sy.min,")",
                             "            t.lin < ", signif(t.lin,3),
                             " (", signif(t.lin.min,3), ")", " days",
                             "            t.crit < ",
signif(t.crit,3),
                             " (", signif(t.crit.min,3), ")", " days",
                             "            Amplitude = ",
signif(aq.A*100,3)," %",
                             " (", signif(aq.A.min*100,3), " %", ")",
                             "\nAverage h recession: ",
signif(avg.slope,3), " m",
                             sep ="")) +
    theme_classic() +
    theme(legend.position = "none",
          plot.title = element_text(size = 11),
          plot.subtitle = element_text(size = 9)) +
    stat_summary(geom = "point",
                 shape = 4,
                 aes(y = (slope3.m*-1)),
                 fun.y = mean)
  data$month <- factor(data$month, levels = c("Jan", "Feb", "Mar",
"Apr","May","Jun", "Jul", "Aug", "Sep", "Oct", "Nov", "Dec"))
  plot2 <- ggplot(data, aes(x = month, y = (slope3.m*-1))) +
    geom_boxplot(fill = "#bdbdbd") +
    scale_y_continuous(name = "h recession rate [m / year]",
                       breaks = seq(0,500,2)) +
    geom_hline(yintercept=avg.slope, linetype="dashed") +
    xlab("Month") +
    theme_classic()
  plot3 <- grid.arrange(plot1, plot2)

  ggsave(paste("3.Results/WTF -
modified/OW_result_graphs/OW",ow.num,"_results.png", sep=""),
```

```
         plot = plot3,
         width = 10,
         height = 10,
         dpi = 120)
}
change_h <- function(data) {
  year.list <- unique(data$Year)
  sum.h = 0
  len.yr = 0
  for (n in 1:length(year.list)) {
    change.h = 0
    subdata <- subset(data, data$Year == year.list[n])

    start.h <- ifelse(subdata$Date[1] == paste(year.list[n],"-01-01",
sep=""),subdata$WTD[1],NA)
    end.h <- ifelse(subdata$Date[nrow(subdata)] ==
paste(year.list[n],"-12-31", sep=""),subdata$WTD[nrow(subdata)],NA)
    change.h <- ifelse(is.na(start.h) && is.na(end.h), NA, (start.h -
end.h))
    sum.h <- ifelse(is.na(change.h), sum.h, change.h + sum.h)
    len.yr <- ifelse(is.na(change.h), len.yr, len.yr + 1)
  }
  return(sum.h / len.yr)
}


#run code
for (i in 1:nrow(OW_data)) {
  ow.num <- OW_data$Obs_Num[i]
  #Aquifer properties
  aq.T <- OW_data$T[i]
  aq.Sy <- OW_data$Sy[i]
  aq.Sy.min <- OW_data$Sy.min[i]
  aq.d <- OW_data$d[i]
  aq.L <- OW_data$L[i]
  aq.num <- OW_data$Aq_Num[i]
  aq.A <- OW_data$A[i]
  aq.A.min <- OW_data$A.min[i]
  t.lin <- ((aq.d^2)*aq.Sy)/(16*aq.T)
  t.lin.min <- ((aq.d^2)*aq.Sy.min)/(16*aq.T)
  t.crit <- (0.15*(aq.L^2)*aq.Sy)/aq.T
  t.crit.min <- (0.15*(aq.L^2)*aq.Sy.min)/aq.T

  #match OW with climate precip data from 5 closest stations
  OW_CS <- OW_Climate_join(OW_data, OW_CS_data, i)

  #test if OW_CS overlaps (in some cases precip data range does not
overlap OW range)
  if(nrow(OW_CS) != 0) {
    OW_CS$CS.precip <- as.character(OW_CS$CS.precip)
    OW_CS$CS.precip <- as.numeric(OW_CS$CS.precip)
```

```
    #add month of observation
    OW_CS$Month <- months(OW_CS$Date, abbreviate = TRUE)

    #count dry periods with start and end dates
    final <- count_dry_periods(OW_CS)

    final$year <- year(final$s.Date)
    final$month <- months(final$s.Date, abbreviate = TRUE)
    final <- subset(final,final$dry.len>3)

    #plot yearly hydrographs with dry periods > 3 days

    final <- calc_slope(final, OW_CS, ow.num)
    write.csv(final, file = paste("3.Results/WTF -
modified/csv_results/ow_",ow.num,".csv",sep =""))

    num.yrs <- plot_dry_periods(final, OW_CS)

    avg.slope <- ifelse((max(final$dry.len)-7) > 14,
           (mean(subset(final, final$dry.len >= max(final$dry.len)-
7)$slope3.m*-1)),
           (mean(subset(final, final$dry.len >= 14)$slope3.m)*-1))
    std.slope <- ifelse((max(final$dry.len)-7) > 14,
                        (sd(subset(final, final$dry.len >=
max(final$dry.len)-7)$slope3.m*-1)),
                        (sd(subset(final, final$dry.len >=
14)$slope3.m)*-1))

    plot_slope(final, ow.num, aq.num, avg.slope, num.yrs)

    avg.change.h <- change_h(OW_CS)

    OW.WTFresults$Result[i] <- "h/t calc"
    OW.WTFresults$Obs_well[i] <- ow.num
    OW.WTFresults$Slope[i] <- avg.slope
    OW.WTFresults$std.slope[i] <- std.slope
    OW.WTFresults$change.h[i] <- avg.change.h
    print(paste("Done OW ", ow.num, ".", sep=""))
  } else {
    print(paste("Obs well",ow.num,"- No overlap with climate data"))
    OW.WTFresults$Result[i] <- "No overlap with climate data"
  }
}

#save results
write.csv(OW.WTFresults, file = paste("3.Results/WTF -
modified/WTF_Results.csv",sep =""))
```

S3.3 WTF RESULTANT GRAPHS

Pages 174 to 232 illustrate the results from the WTF method. Water table levels are plotted above daily precipitation from the nearest climate stations (radius of 20 km). Water levels are color coded where groundwater head fluctuations are receding and classified by length of consecutive no precipitation period. Boxplots are of resultant modeled average groundwater head recession (m yr^{-1}) classified by length of consecutive no precipitation period (above), and classified by month (below).

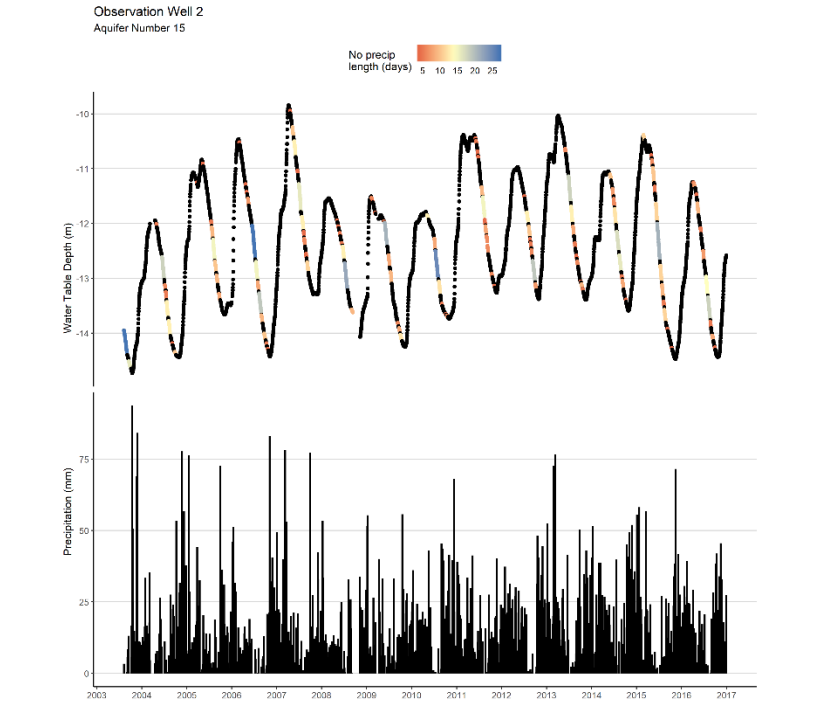
Observation Well 2
Aquifer Number 15
No precip length (days)
5 10 15 20 25
Water Table Depth (m)
-10
-11
-12
-13
-14
Precipitation (mm)
75
50
25
0
2003 2004 2005 2006 2007 2008 2009 2010 2011 2012 2013 2014 2015 2016 2017

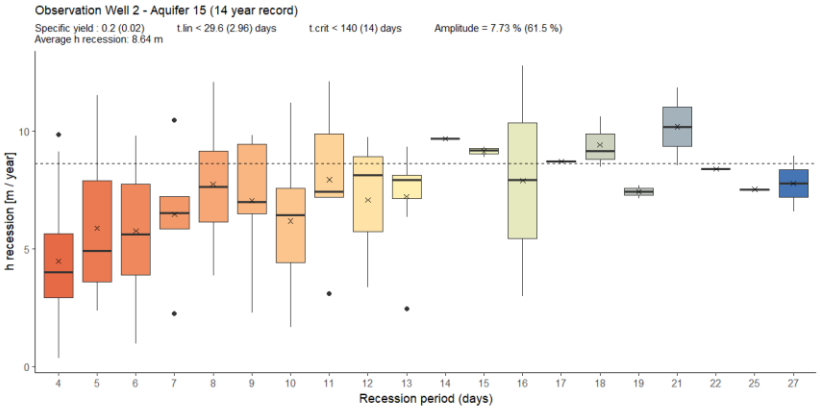
Observation Well 2 - Aquifer 15 (14 year record)
Specific yield : 0.2 (0.02)
t.lin < 29.6 (2.96) days
t.crit < 140 (14) days
Amplitude = 7.73 % (61.5 %)
Average h recession: 8.64 m
h recession [m / year]
10
5
0
4 5 6 7 8 9 10 11 12 13 14 15 16 17 18 19 21 22 25 27
Recession period (days)

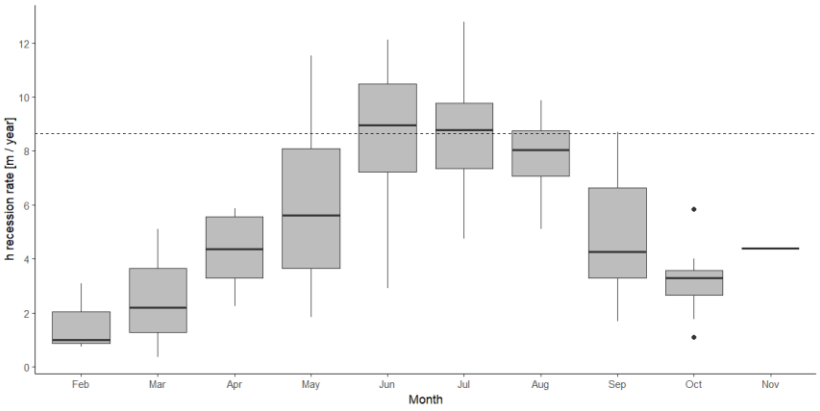
h recession rate [m / year]
12
10
8
6
4
2
0
Feb Mar Apr May Jun Jul Aug Sep Oct Nov
Month

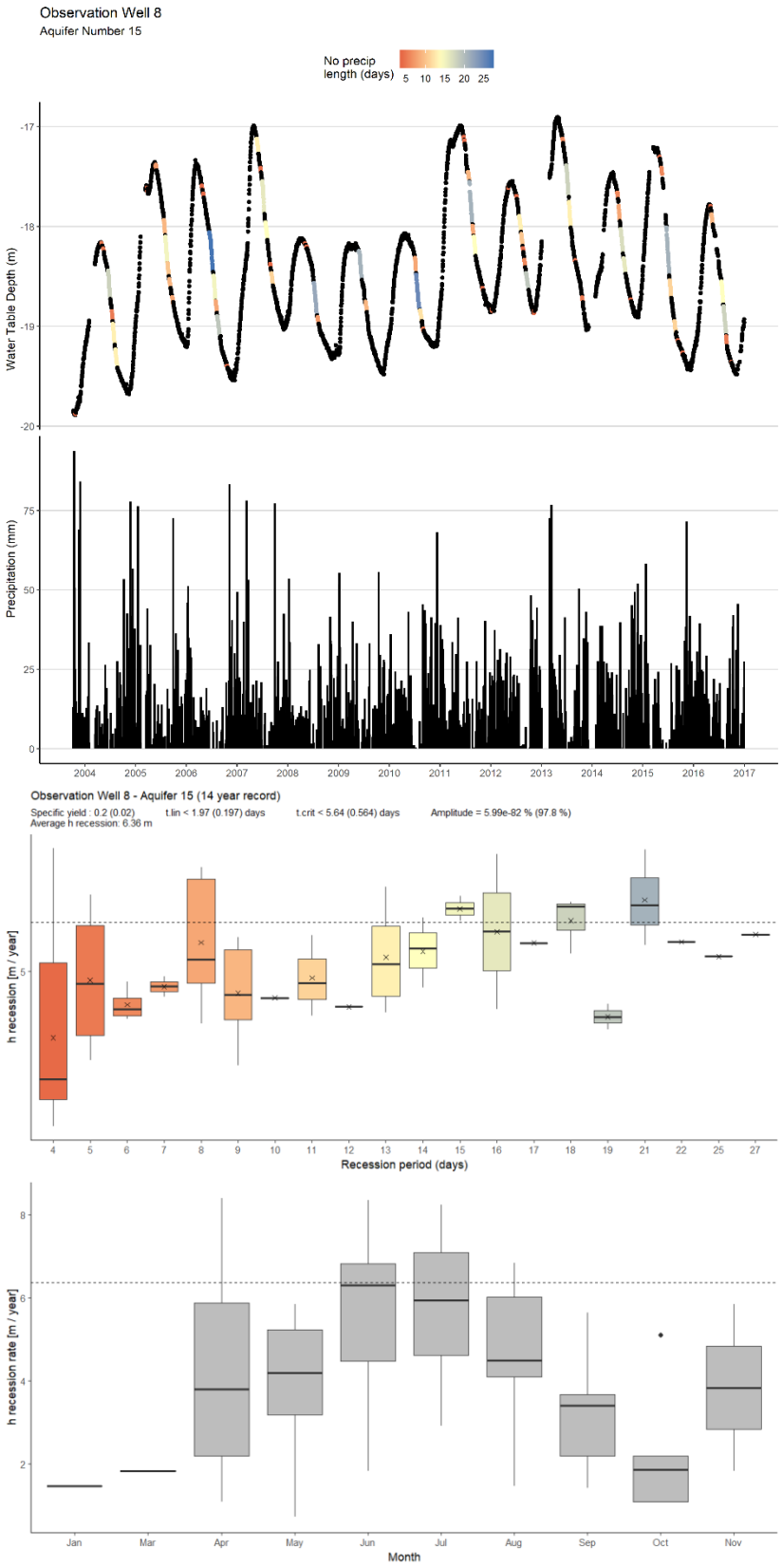
Observation Well 8
Aquifer Number 15
No precip length (days)
5 10 15 20 25
Water Table Depth (m)
-17
-18
-19
-20
Precipitation (mm)
75
50
25
0
2004 2005 2006 2007 2008 2009 2010 2011 2012 2013 2014 2015 2016 2017
Observation Well 8 - Aquifer 15 (14 year record)
Specific yield : 0.2 (0.02)
t.lin < 1.97 (0.197) days
t.crit < 5.64 (0.564) days
Amplitude = 5.99e-82 % (97.8 %)
Average h recession: 6.36 m
h recession [m / year]
5
4 5 6 7 8 9 10 11 12 13 14 15 16 17 18 19 21 22 25 27
Recession period (days)
h recession rate [m / year]
8
6
4
2
Jan Mar Apr May Jun Jul Aug Sep Oct Nov
Month

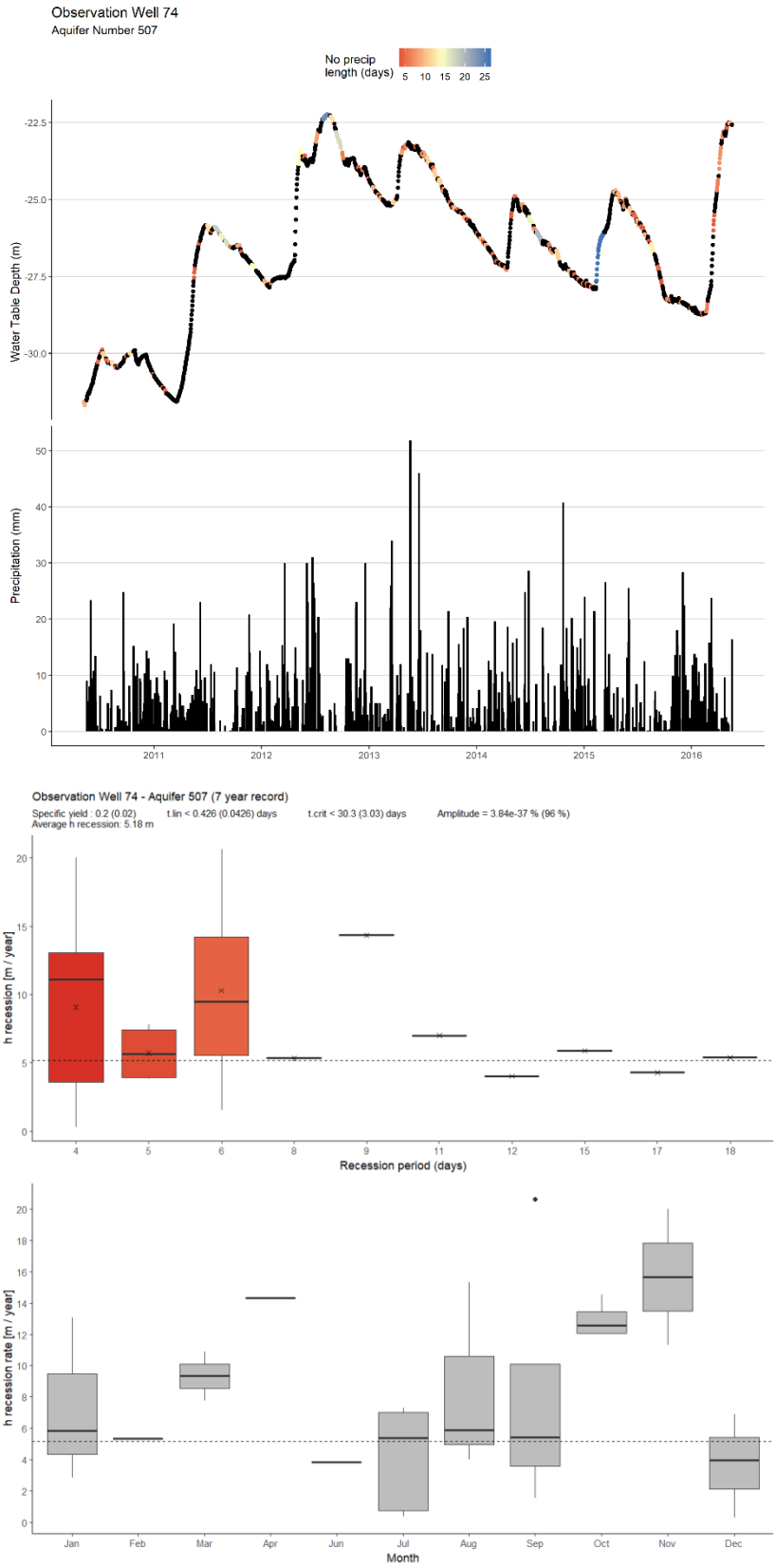
Observation Well 74
Aquifer Number 507
No precip length (days)
5 10 15 20 25
Water Table Depth (m)
-22.5
-25.0
-27.5
-30.0
Precipitation (mm)
50
40
30
20
10
0
2011
2012
2013
2014
2015
2016
Observation Well 74 - Aquifer 507 (7 year record)
Specific yield : 0.2 (0.02)
t.lin < 0.426 (0.0426) days
t.crit < 30.3 (3.03) days
Amplitude = 3.84e-37 % (96 %)
Average h recession: 5.18 m
h recession [m / year]
20
15
10
5
0
4
5
6
8
9
11
12
15
17
18
Recession period (days)
h recession rate [m / year]
20
18
16
14
12
10
8
6
4
2
0
Jan
Feb
Mar
Apr
Jun
Jul
Aug
Sep
Oct
Nov
Dec
Month

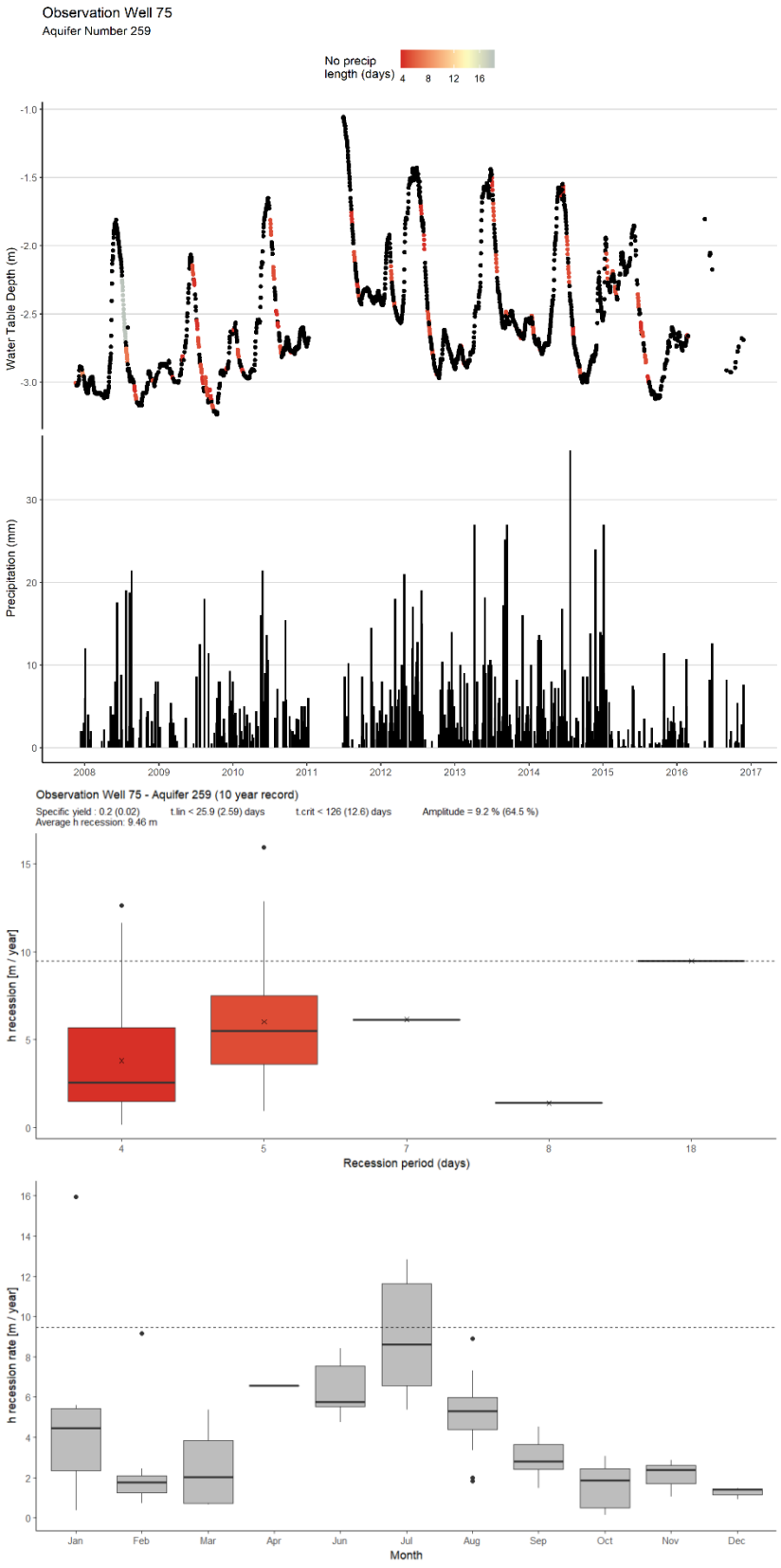
Observation Well 75
Aquifer Number 259
No precip length (days)
4
8
12
16
Water Table Depth (m)
-1.0
-1.5
-2.0
-2.5
-3.0
Precipitation (mm)
30
20
10
0
2008
2009
2010
2011
2012
2013
2014
2015
2016
2017
Observation Well 75 - Aquifer 259 (10 year record)
Specific yield : 0.2 (0.02)
t.lin < 25.9 (2.59) days
t.crit < 126 (12.6) days
Amplitude = 9.2 % (64.5 %)
Average h recession: 9.46 m
h recession [m / year]
15
10
5
0
4
5
7
8
18
Recession period (days)
h recession rate [m / year]
16
14
12
10
8
6
4
2
0
Jan
Feb
Mar
Apr
Jun
Jul
Aug
Sep
Oct
Nov
Dec
Month

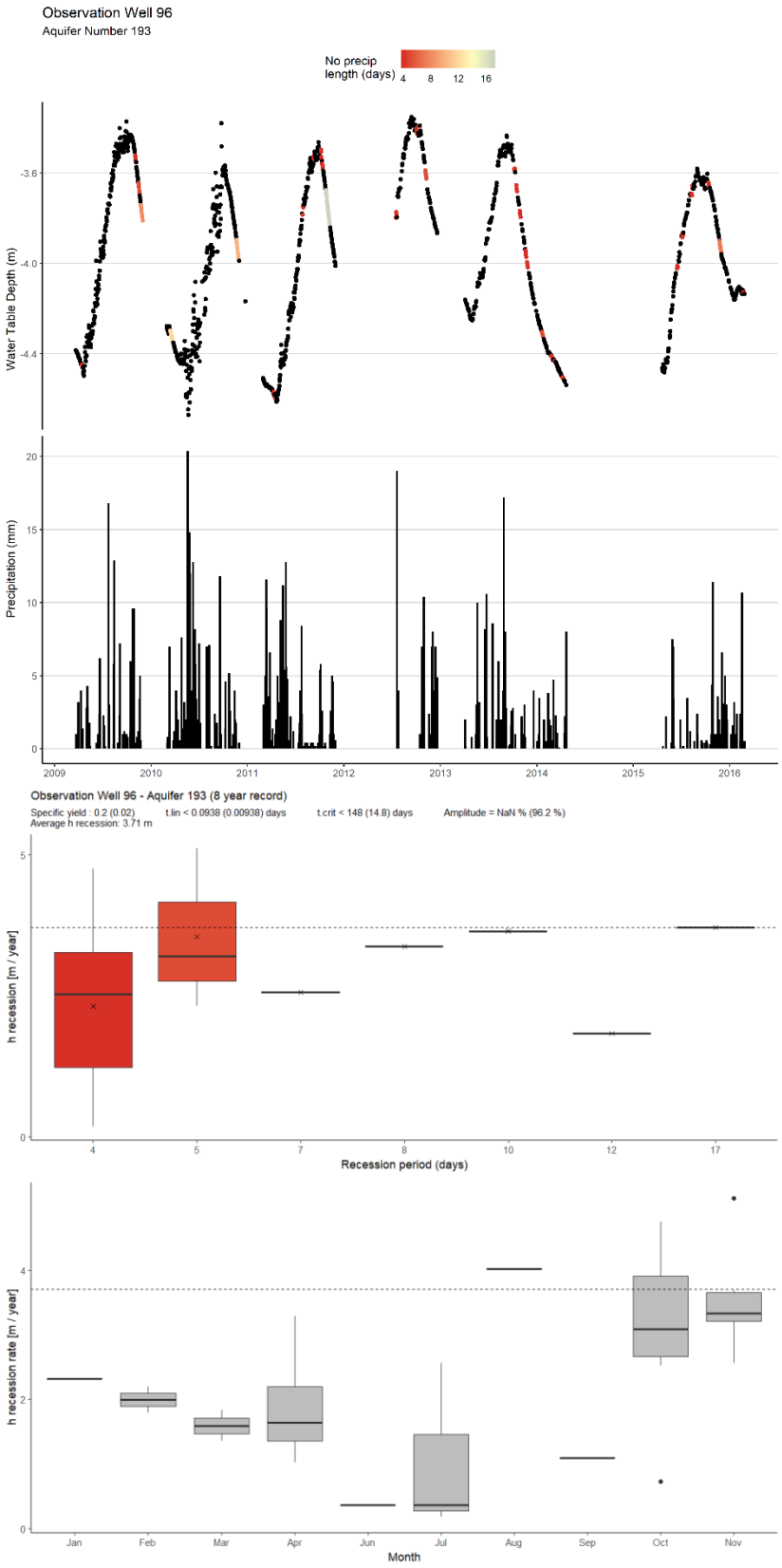
Observation Well 96
Aquifer Number 193
No precip length (days)
4
8
12
16
Water Table Depth (m)
-3.6
-4.0
-4.4
Precipitation (mm)
20
15
10
5
0
2009
2010
2011
2012
2013
2014
2015
2016
Observation Well 96 - Aquifer 193 (8 year record)
Specific yield : 0.2 (0.02)
t.lin < 0.0938 (0.00938) days
t.crit < 148 (14.8) days
Amplitude = NaN % (96.2 %)
Average h recession: 3.71 m
h recession [m / year]
5
0
4
5
7
8
10
12
17
Recession period (days)
h recession rate [m / year]
4
2
0
Jan
Feb
Mar
Apr
Jun
Jul
Aug
Sep
Oct
Nov
Month

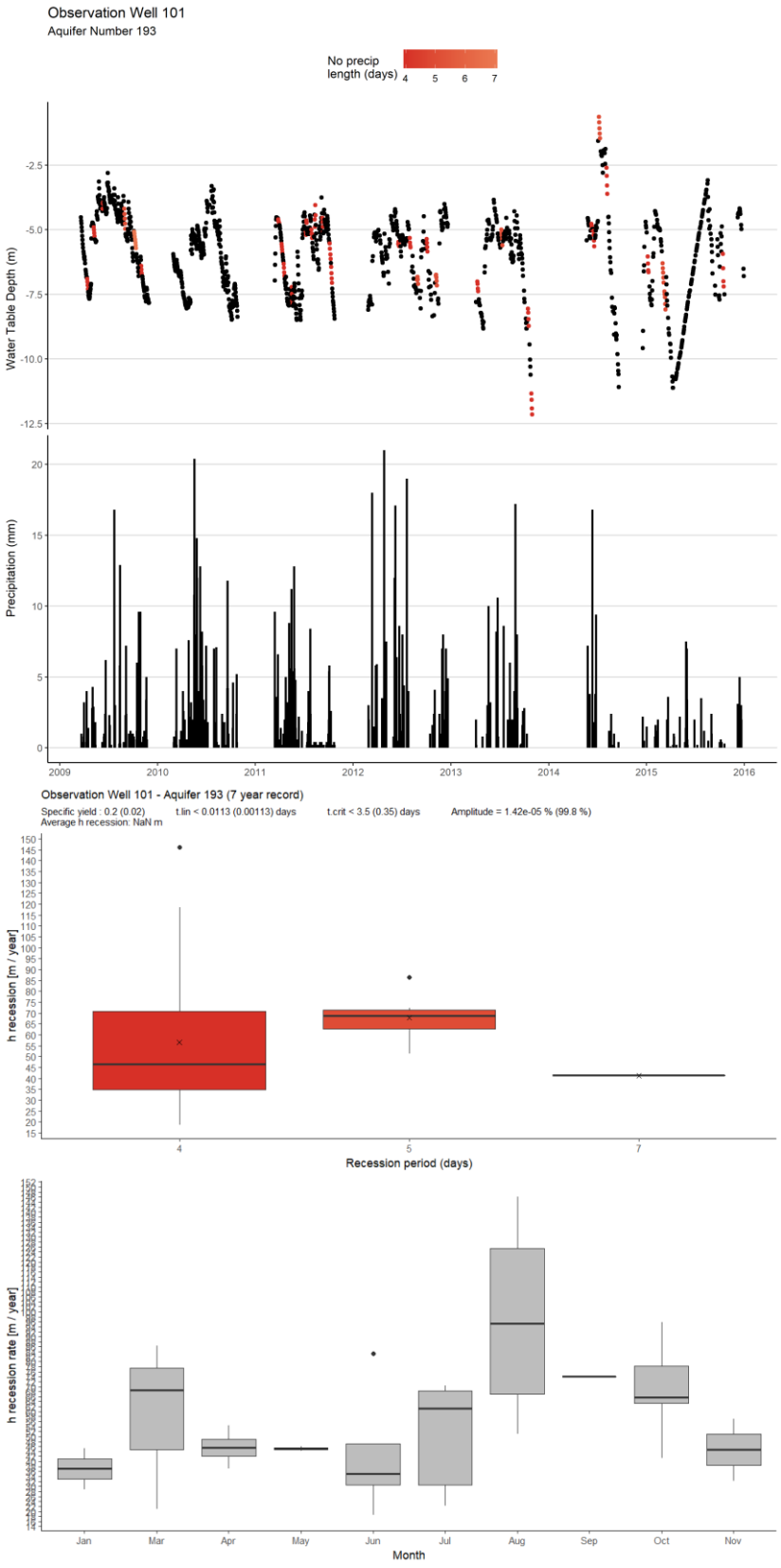
Observation Well 101
Aquifer Number 193
No precip length (days)
4
5
6
7
Water Table Depth (m)
-2.5
-5.0
-7.5
-10.0
-12.5
Precipitation (mm)
20
15
10
5
0
2009
2010
2011
2012
2013
2014
2015
2016
Observation Well 101 - Aquifer 193 (7 year record)
Specific yield : 0.2 (0.02)
t.lin < 0.0113 (0.00113) days
t.crit < 3.5 (0.35) days
Amplitude = 1.42e-05 % (99.8 %)
Average h recession: NaN m
h recession [m / year]
Recession period (days)
4
5
7
h recession rate [m / year]
Jan
Mar
Apr
May
Jun
Jul
Aug
Sep
Oct
Nov
Month

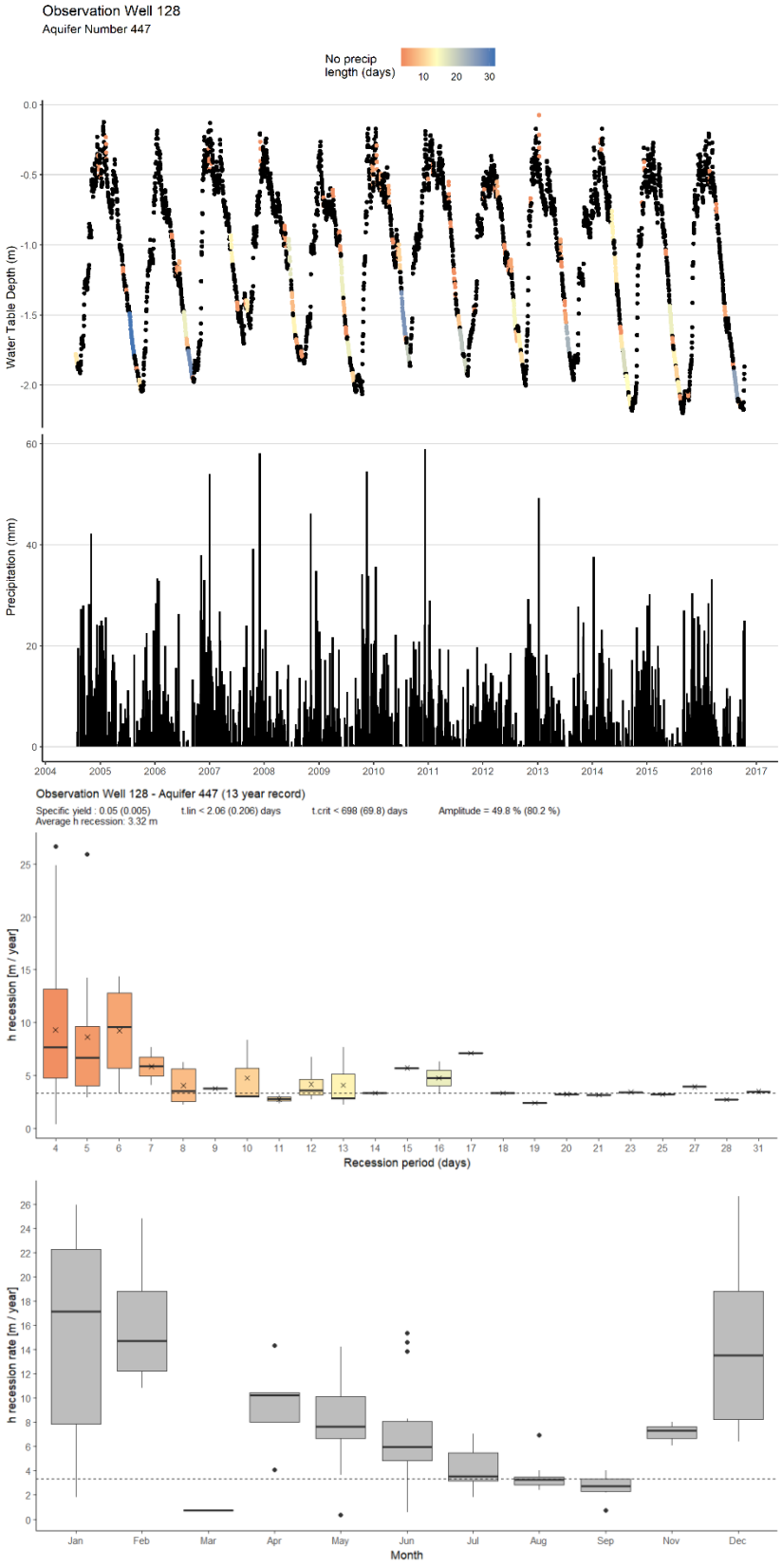
Observation Well 128
Aquifer Number 447
No precip length (days)
10
20
30
Water Table Depth (m)
0.0
-0.5
-1.0
-1.5
-2.0
Precipitation (mm)
60
40
20
0
2004
2005
2006
2007
2008
2009
2010
2011
2012
2013
2014
2015
2016
2017
Observation Well 128 - Aquifer 447 (13 year record)
Specific yield : 0.05 (0.005)
t.lin < 2.06 (0.206) days
t.crit < 698 (69.8) days
Amplitude = 49.8 % (80.2 %)
Average h recession: 3.32 m
h recession [m / year]
Recession period (days)
h recession rate [m / year]
Jan
Feb
Mar
Apr
May
Jun
Jul
Aug
Sep
Nov
Dec
Month

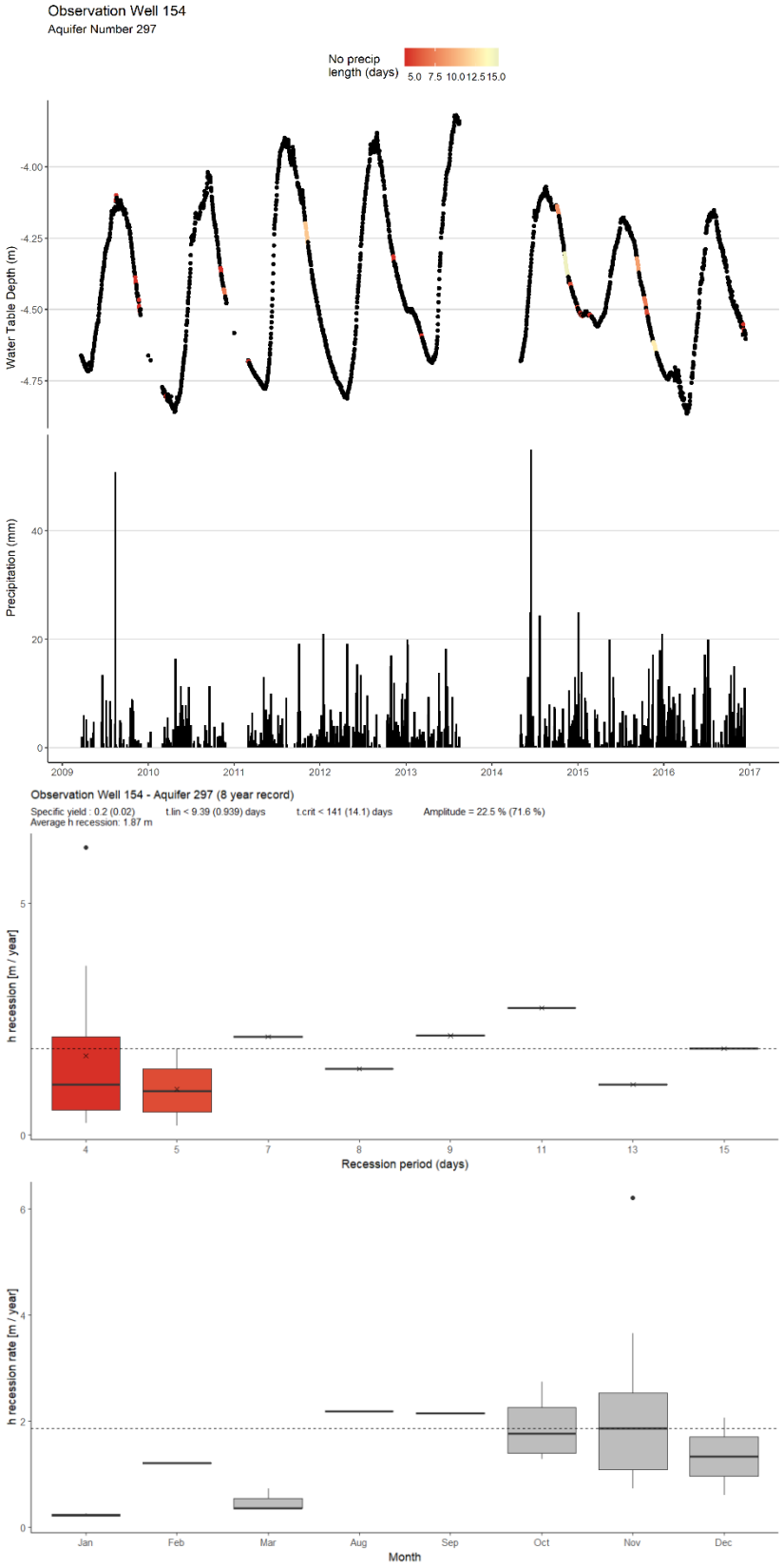
Observation Well 154
Aquifer Number 297
No precip length (days)
5.0 7.5 10.0 12.5 15.0
Water Table Depth (m)
-4.00
-4.25
-4.50
-4.75
Precipitation (mm)
40
20
0
2009
2010
2011
2012
2013
2014
2015
2016
2017
Observation Well 154 - Aquifer 297 (8 year record)
Specific yield : 0.2 (0.02)
t.lin < 9.39 (0.939) days
t.crit < 141 (14.1) days
Amplitude = 22.5 % (71.6 %)
Average h recession: 1.87 m
h recession [m / year]
5
0
4
5
7
8
9
11
13
15
Recession period (days)
h recession rate [m / year]
6
4
2
0
Jan
Feb
Mar
Aug
Sep
Oct
Nov
Dec
Month

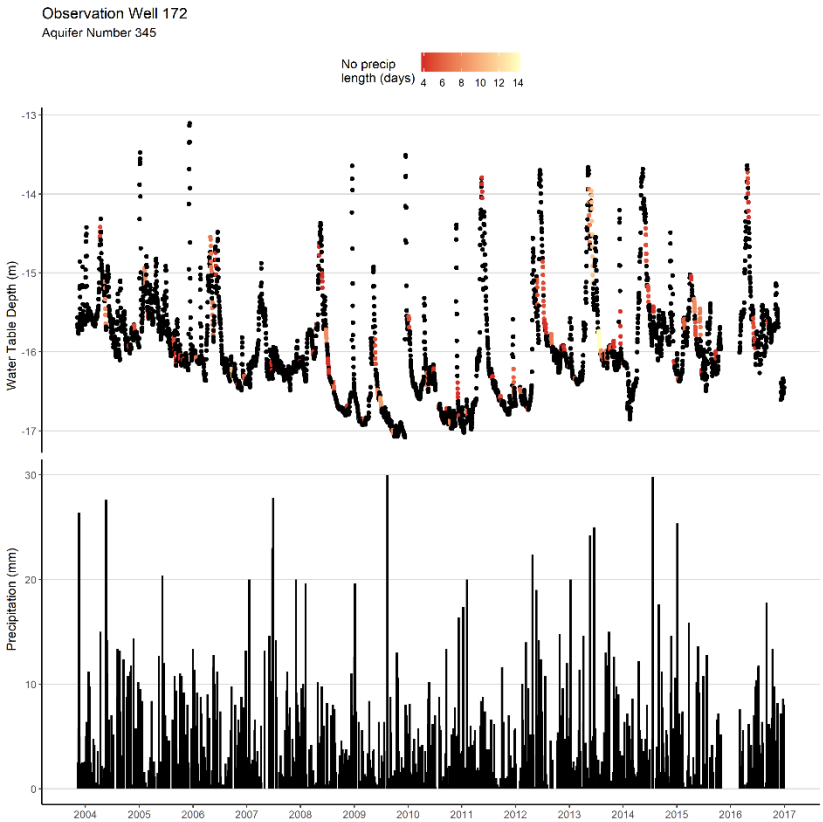
Observation Well 172
Aquifer Number 345
No precip length (days)
4 6 8 10 12 14
Water Table Depth (m)
-13
-14
-15
-16
-17
Precipitation (mm)
30
20
10
0
2004 2005 2006 2007 2008 2009 2010 2011 2012 2013 2014 2015 2016 2017

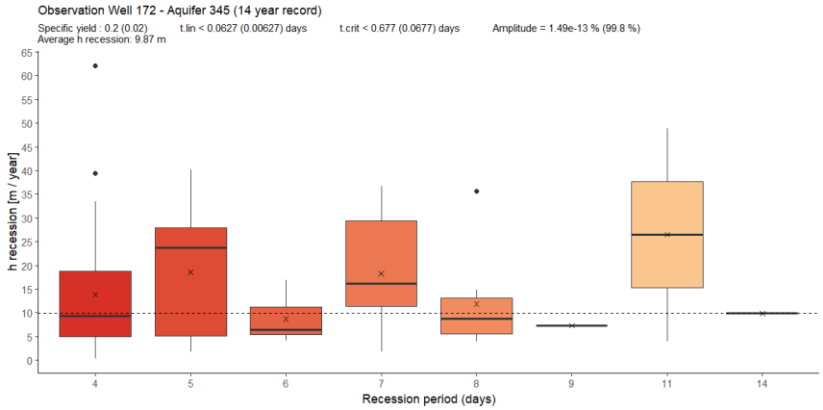
Observation Well 172 - Aquifer 345 (14 year record)
Specific yield : 0.2 (0.02)
t.lin < 0.0627 (0.00627) days
t.crit < 0.677 (0.0677) days
Amplitude = 1.49e-13 % (99.8 %)
Average h recession: 9.87 m
h recession [m / year]
Recession period (days)
4 5 6 7 8 9 11 14

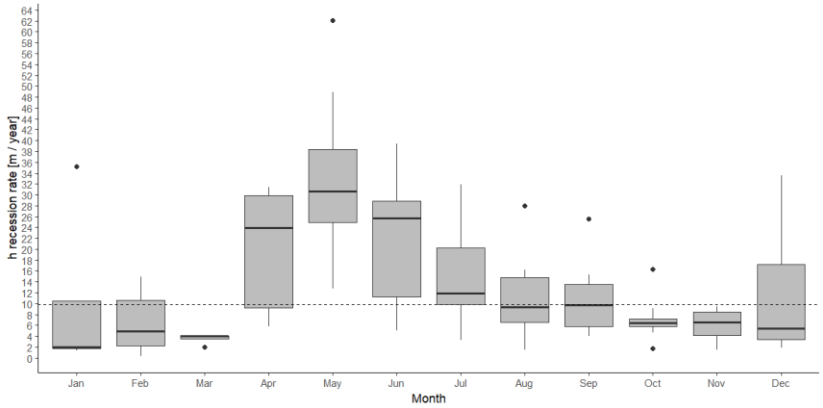
h recession rate [m / year]
Jan Feb Mar Apr May Jun Jul Aug Sep Oct Nov Dec
Month

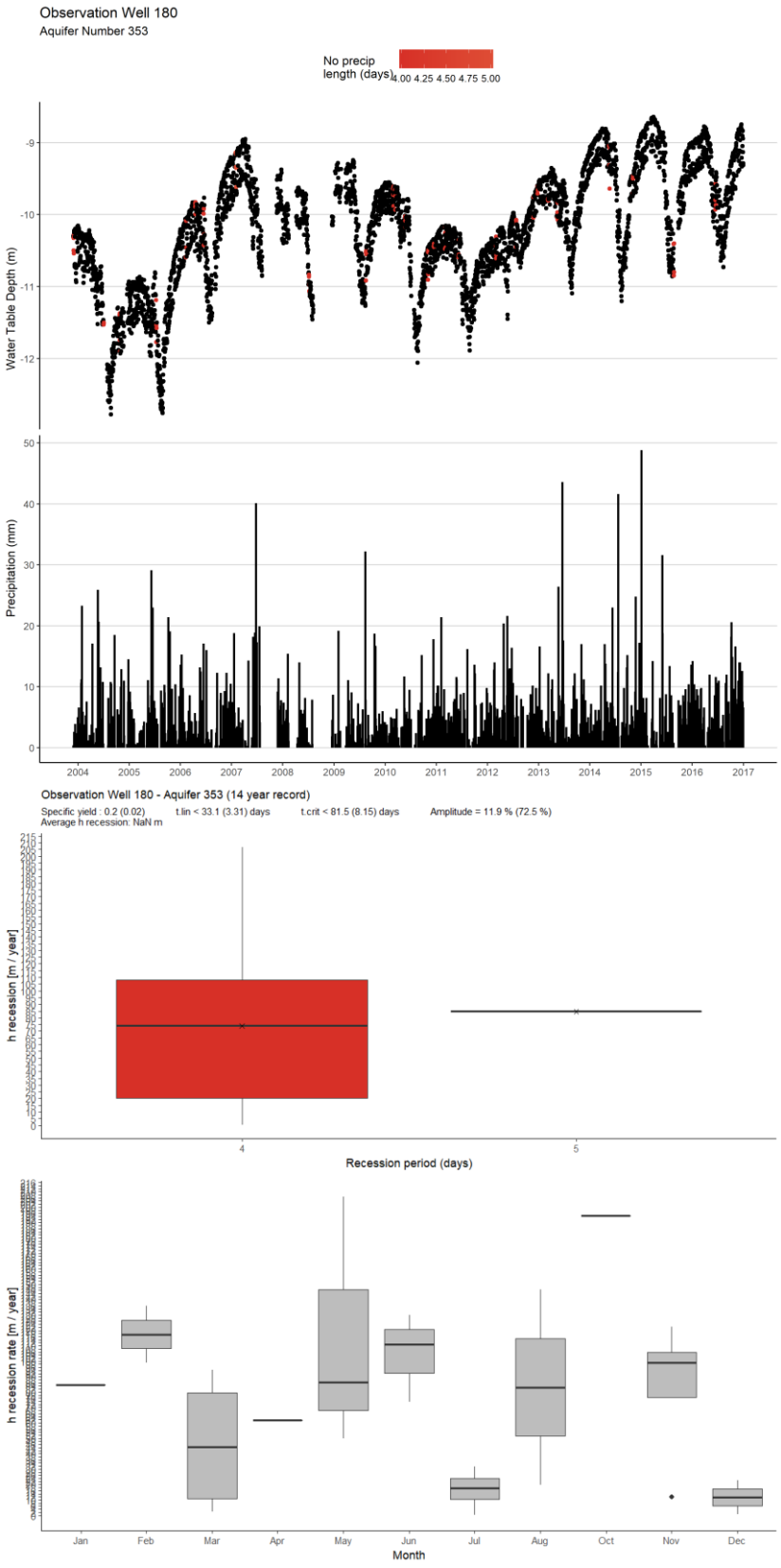
Observation Well 180
Aquifer Number 353
No precip length (days)
4.00 4.25 4.50 4.75 5.00
Water Table Depth (m)
-9
-10
-11
-12
Precipitation (mm)
50
40
30
20
10
0
2004
2005
2006
2007
2008
2009
2010
2011
2012
2013
2014
2015
2016
2017
Observation Well 180 - Aquifer 353 (14 year record)
Specific yield : 0.2 (0.02)
t.lin < 33.1 (3.31) days
t.crit < 81.5 (8.15) days
Amplitude = 11.9 % (72.5 %)
Average h recession: NaN m
h recession [m / year]
4
5
Recession period (days)
h recession rate [m / year]
Jan
Feb
Mar
Apr
May
Jun
Jul
Aug
Oct
Nov
Dec
Month

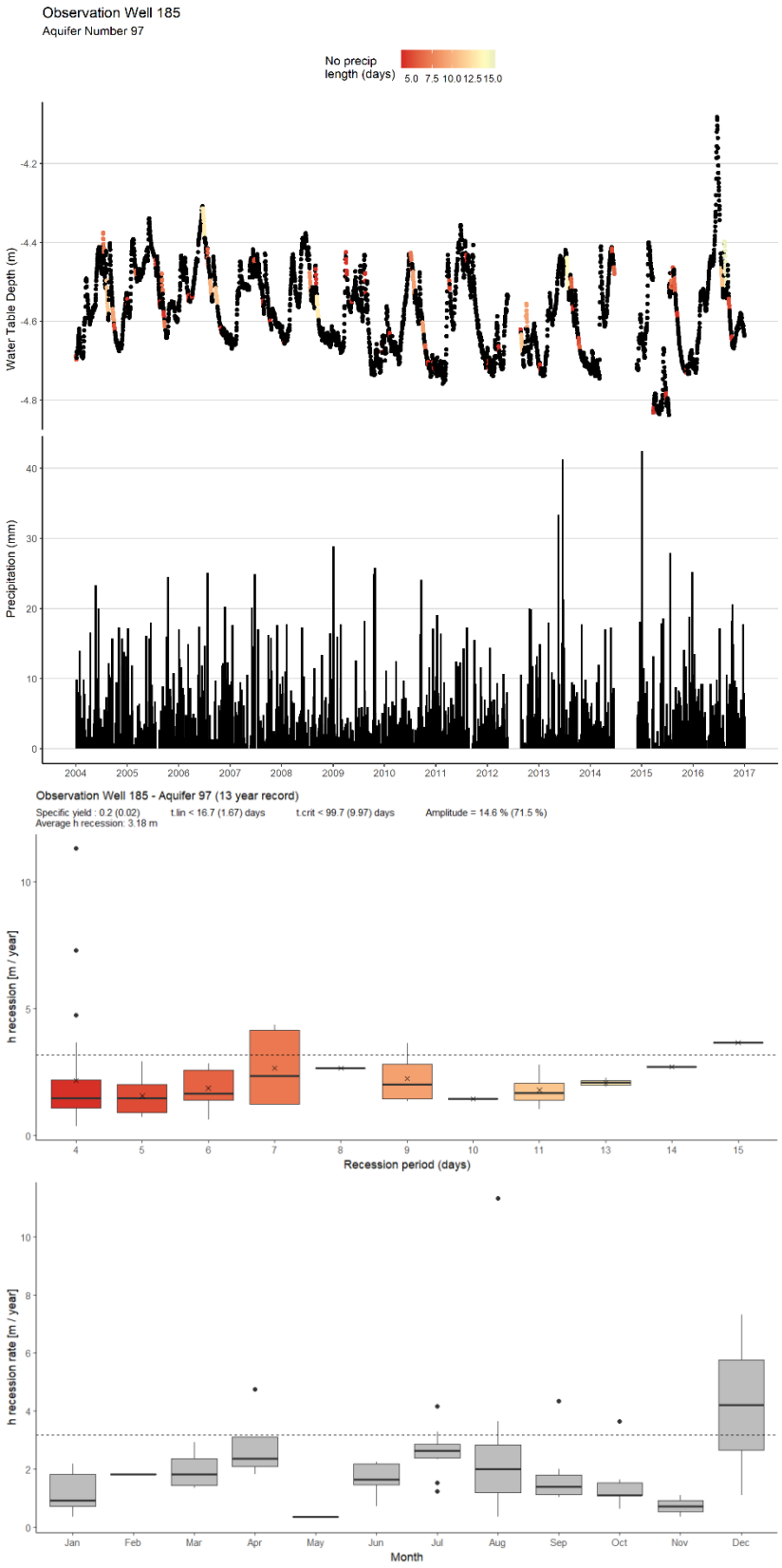
Observation Well 185
Aquifer Number 97
No precip length (days)
5.0 7.5 10.0 12.5 15.0
Water Table Depth (m)
-4.2
-4.4
-4.6
-4.8
Precipitation (mm)
40
30
20
10
0
2004 2005 2006 2007 2008 2009 2010 2011 2012 2013 2014 2015 2016 2017
Observation Well 185 - Aquifer 97 (13 year record)
Specific yield : 0.2 (0.02)
t.lin < 16.7 (1.67) days
t.crit < 99.7 (9.97) days
Amplitude = 14.6 % (71.5 %)
Average h recession: 3.18 m
h recession [m / year]
10
5
0
4 5 6 7 8 9 10 11 13 14 15
Recession period (days)
h recession rate [m / year]
10
8
6
4
2
0
Jan Feb Mar Apr May Jun Jul Aug Sep Oct Nov Dec
Month

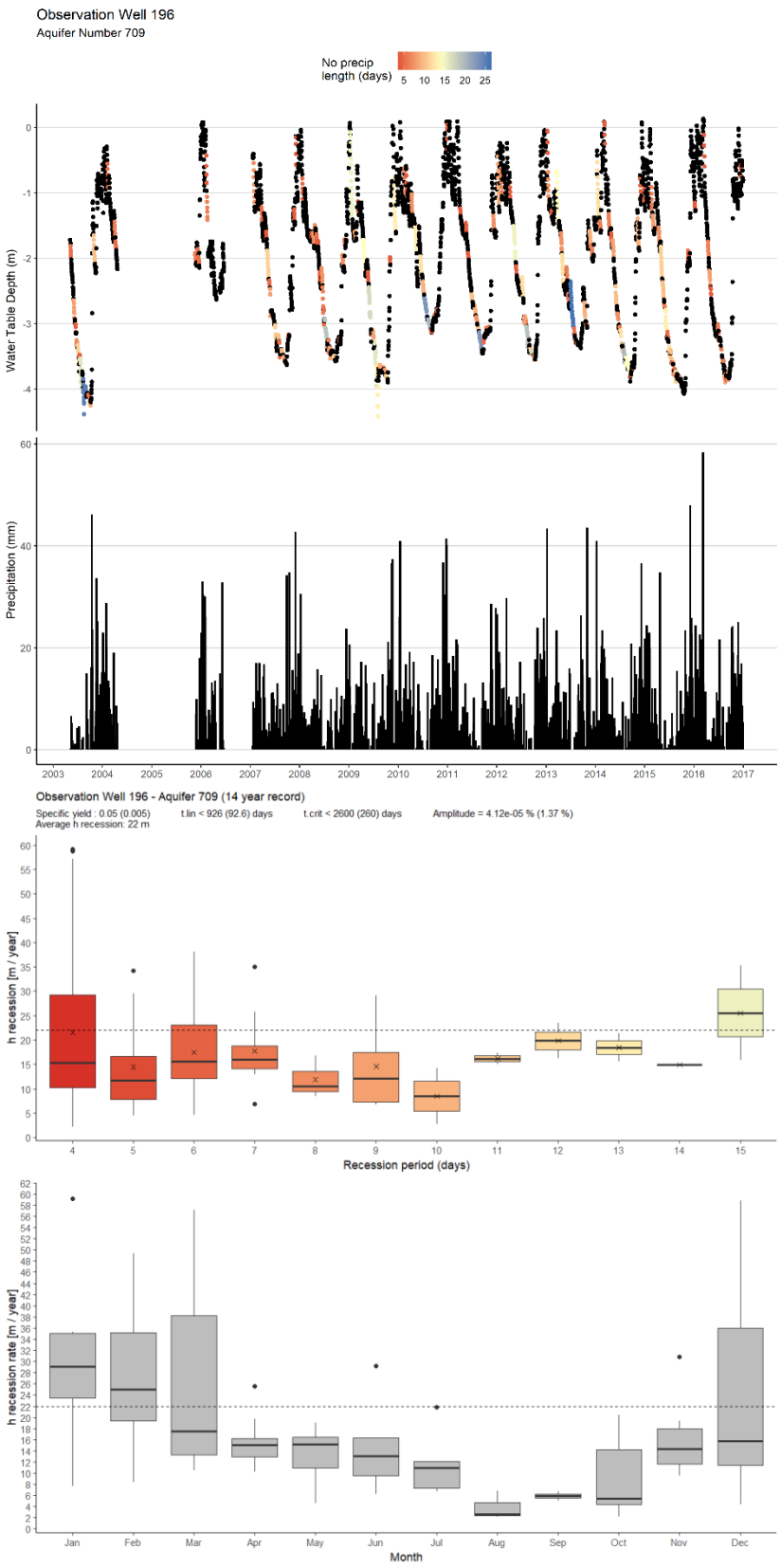
Observation Well 196
Aquifer Number 709
No precip length (days)
5 10 15 20 25
Water Table Depth (m)
Precipitation (mm)
2003 2004 2005 2006 2007 2008 2009 2010 2011 2012 2013 2014 2015 2016 2017
Observation Well 196 - Aquifer 709 (14 year record)
Specific yield : 0.05 (0.005)
Average h recession: 22 m
t.lin < 926 (92.6) days
t.crit < 2600 (260) days
Amplitude = 4.12e-05 % (1.37 %)
h recession [m / year]
Recession period (days)
h recession rate [m / year]
Jan Feb Mar Apr May Jun Jul Aug Sep Oct Nov Dec
Month

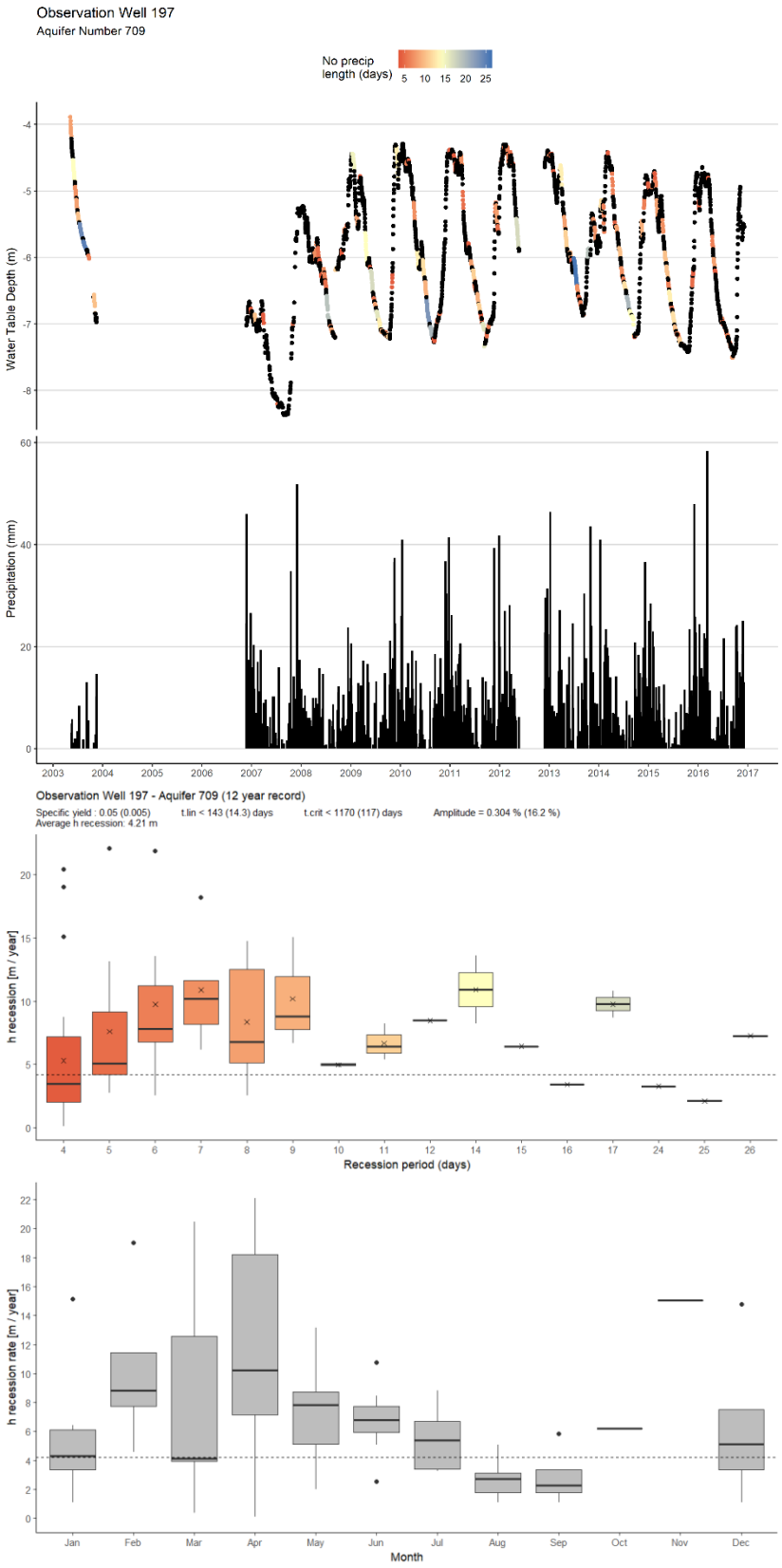
Observation Well 197
Aquifer Number 709
No precip length (days)
5 10 15 20 25
Water Table Depth (m)
-4
-5
-6
-7
-8
Precipitation (mm)
60
40
20
0
2003 2004 2005 2006 2007 2008 2009 2010 2011 2012 2013 2014 2015 2016 2017
Observation Well 197 - Aquifer 709 (12 year record)
Specific yield : 0.05 (0.005)
Average h recession: 4.21 m
t.lin < 143 (14.3) days
t.crit < 1170 (117) days
Amplitude = 0.304 % (16.2 %)
h recession [m / year]
20
15
10
5
0
4 5 6 7 8 9 10 11 12 14 15 16 17 24 25 26
Recession period (days)
h recession rate [m / year]
22
20
18
16
14
12
10
8
6
4
2
0
Jan Feb Mar Apr May Jun Jul Aug Sep Oct Nov Dec
Month

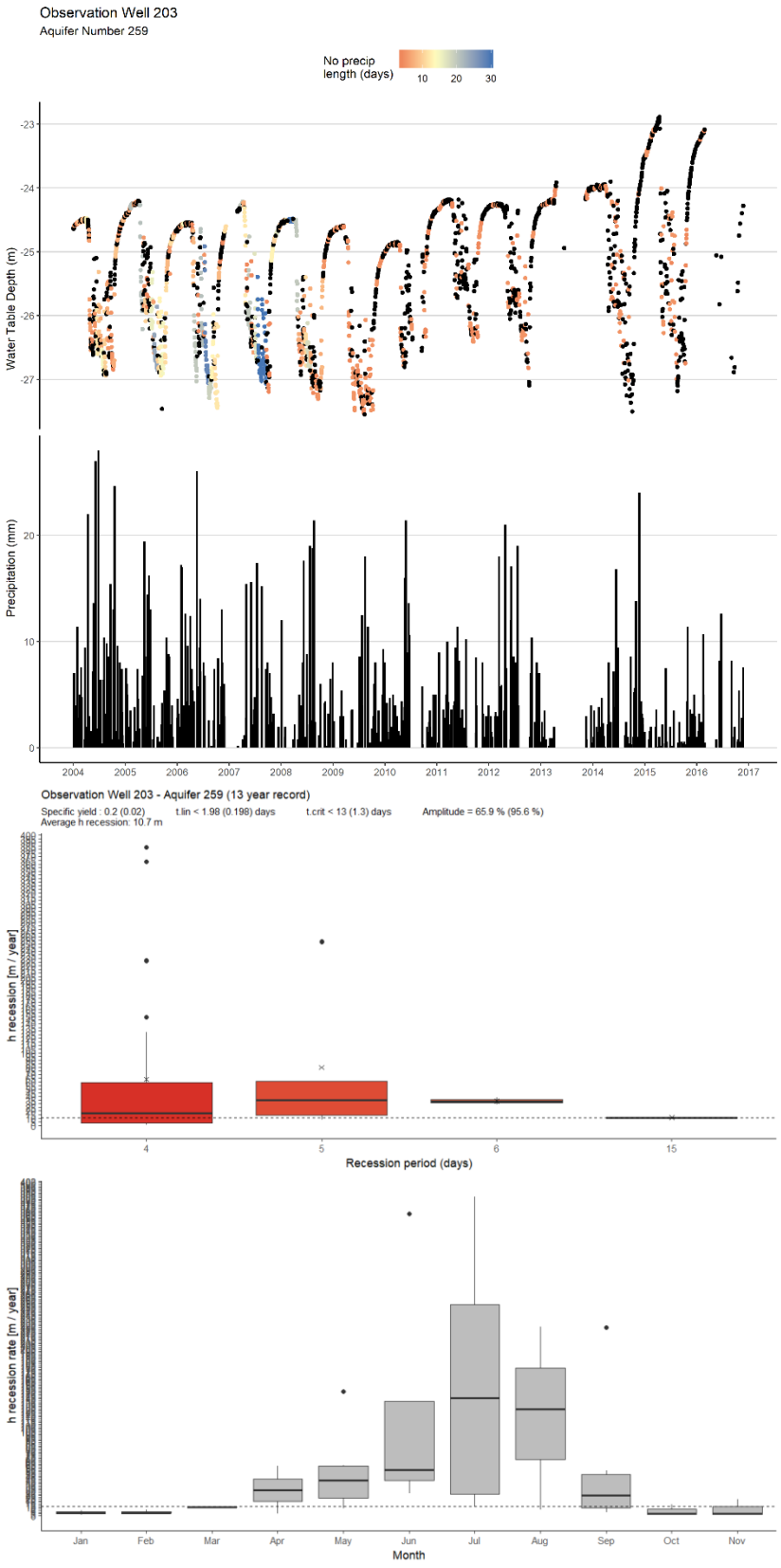
Observation Well 203
Aquifer Number 259
No precip length (days)
10
20
30
Water Table Depth (m)
-23
-24
-25
-26
-27
Precipitation (mm)
0
10
20
2004
2005
2006
2007
2008
2009
2010
2011
2012
2013
2014
2015
2016
2017
Observation Well 203 - Aquifer 259 (13 year record)
Specific yield : 0.2 (0.02)
t.lin < 1.98 (0.198) days
t.crit < 13 (1.3) days
Amplitude = 65.9 % (95.6 %)
Average h recession: 10.7 m
h recession [m / year]
4
5
6
15
Recession period (days)
h recession rate [m / year]
Jan
Feb
Mar
Apr
May
Jun
Jul
Aug
Sep
Oct
Nov
Month

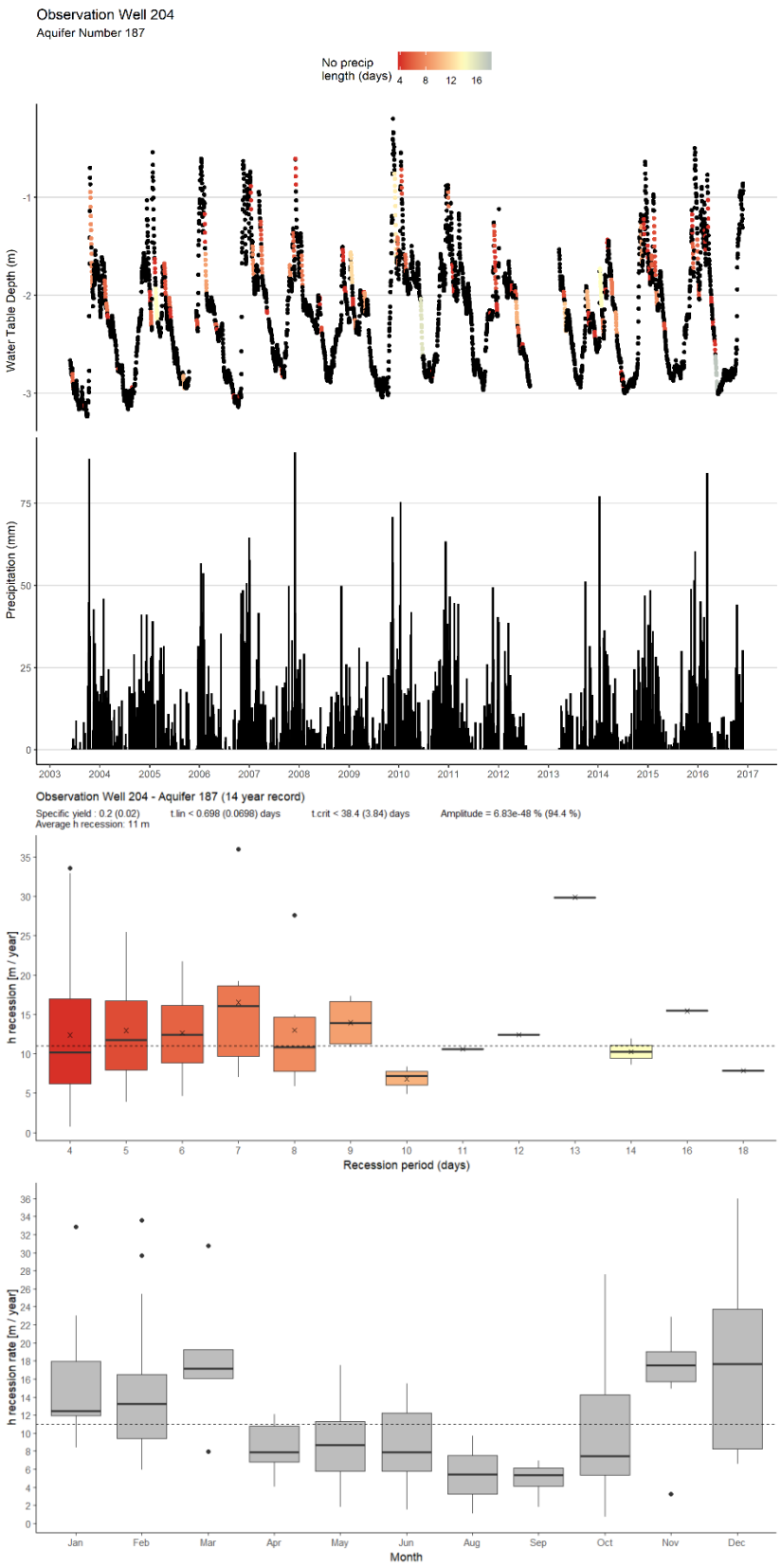
Observation Well 204
Aquifer Number 187
No precip length (days)
4
8
12
16
Water Table Depth (m)
-1
-2
-3
Precipitation (mm)
75
50
25
0
2003
2004
2005
2006
2007
2008
2009
2010
2011
2012
2013
2014
2015
2016
2017
Observation Well 204 - Aquifer 187 (14 year record)
Specific yield : 0.2 (0.02)
t.lin < 0.698 (0.0698) days
t.crit < 38.4 (3.84) days
Amplitude = 6.83e-48 % (94.4 %)
Average h recession: 11 m
h recession [m / year]
Recession period (days)
h recession rate [m / year]
Jan
Feb
Mar
Apr
May
Jun
Aug
Sep
Oct
Nov
Dec
Month

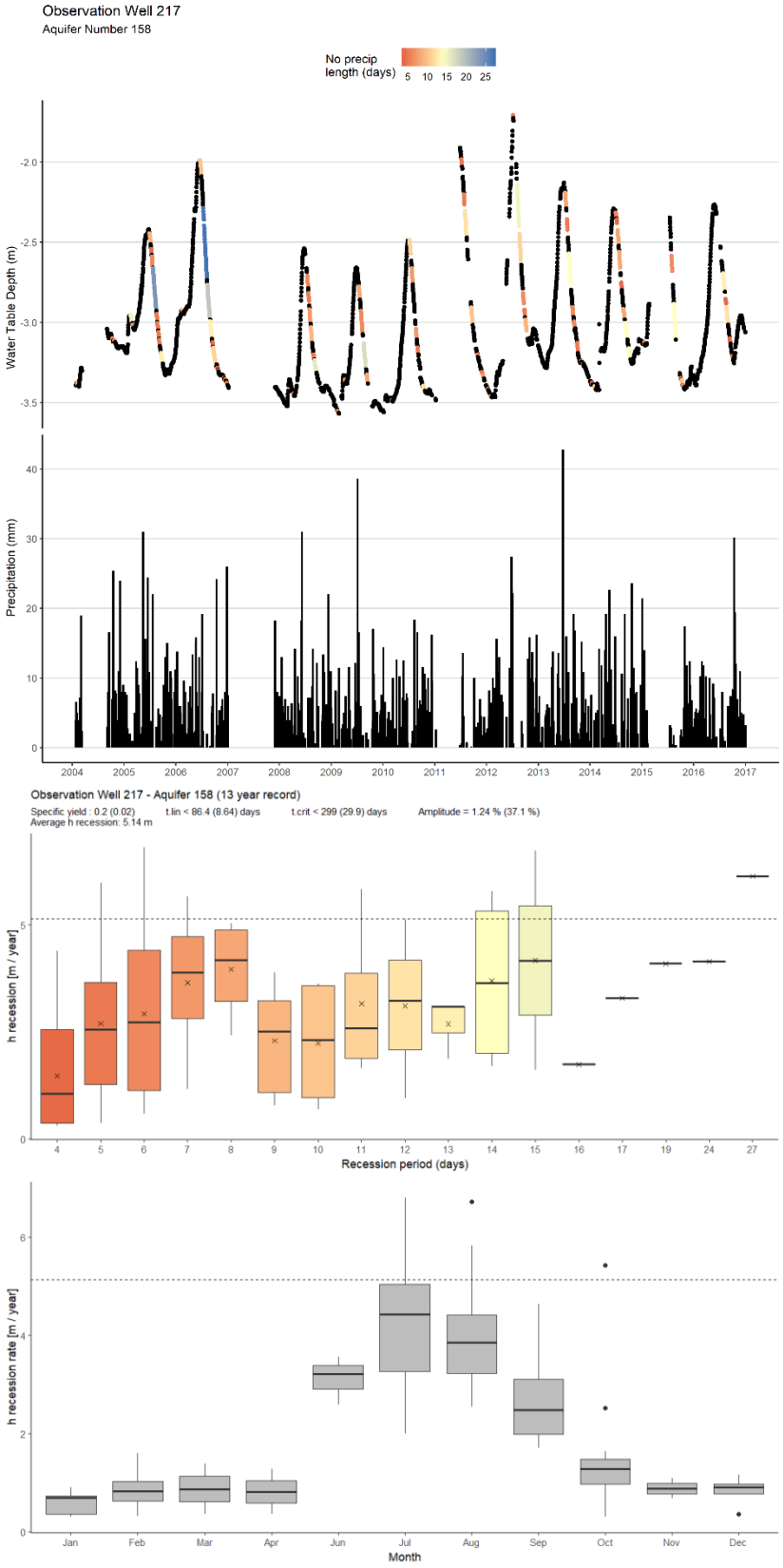
Observation Well 217
Aquifer Number 158
No precip length (days)
5 10 15 20 25
Water Table Depth (m)
-2.0
-2.5
-3.0
-3.5
Precipitation (mm)
40
30
20
10
0
2004 2005 2006 2007 2008 2009 2010 2011 2012 2013 2014 2015 2016 2017
Observation Well 217 - Aquifer 158 (13 year record)
Specific yield : 0.2 (0.02)
t.lin < 86.4 (8.64) days
t.crit < 299 (29.9) days
Amplitude = 1.24 % (37.1 %)
Average h recession: 5.14 m
h recession [m / year]
5
0
4 5 6 7 8 9 10 11 12 13 14 15 16 17 19 24 27
Recession period (days)
h recession rate [m / year]
6
4
2
0
Jan Feb Mar Apr Jun Jul Aug Sep Oct Nov Dec
Month

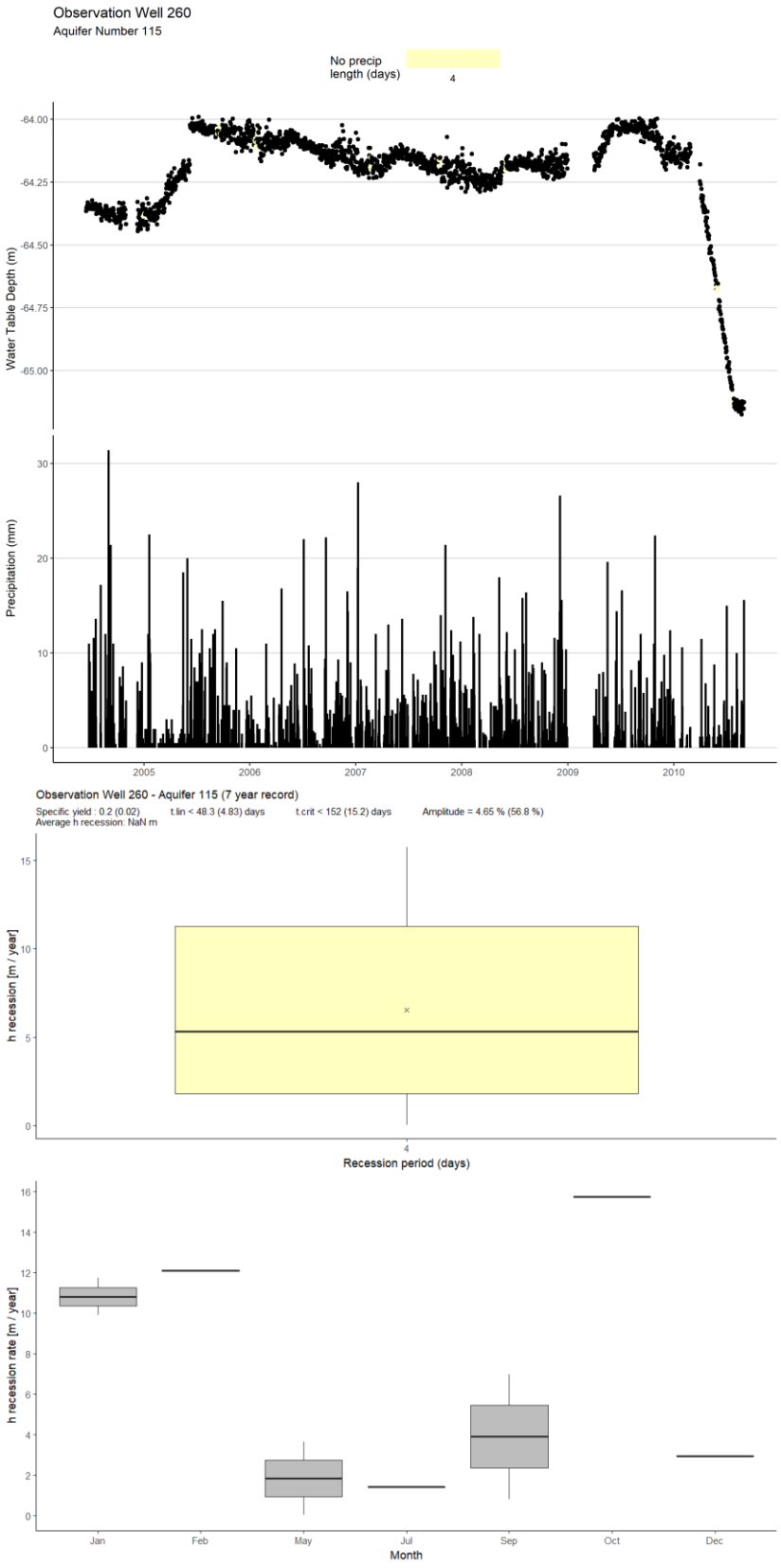
Observation Well 260
Aquifer Number 115
No precip length (days)
4
Water Table Depth (m)
-64.00
-64.25
-64.50
-64.75
-65.00
Precipitation (mm)
30
20
10
0
2005
2006
2007
2008
2009
2010
Observation Well 260 - Aquifer 115 (7 year record)
Specific yield : 0.2 (0.02)
t.lin < 48.3 (4.83) days
t.crit < 152 (15.2) days
Amplitude = 4.65 % (56.8 %)
Average h recession: NaN m
h recession [m / year]
15
10
5
0
4
Recession period (days)
h recession rate [m / year]
16
14
12
10
8
6
4
2
0
Jan
Feb
May
Jul
Sep
Oct
Dec
Month

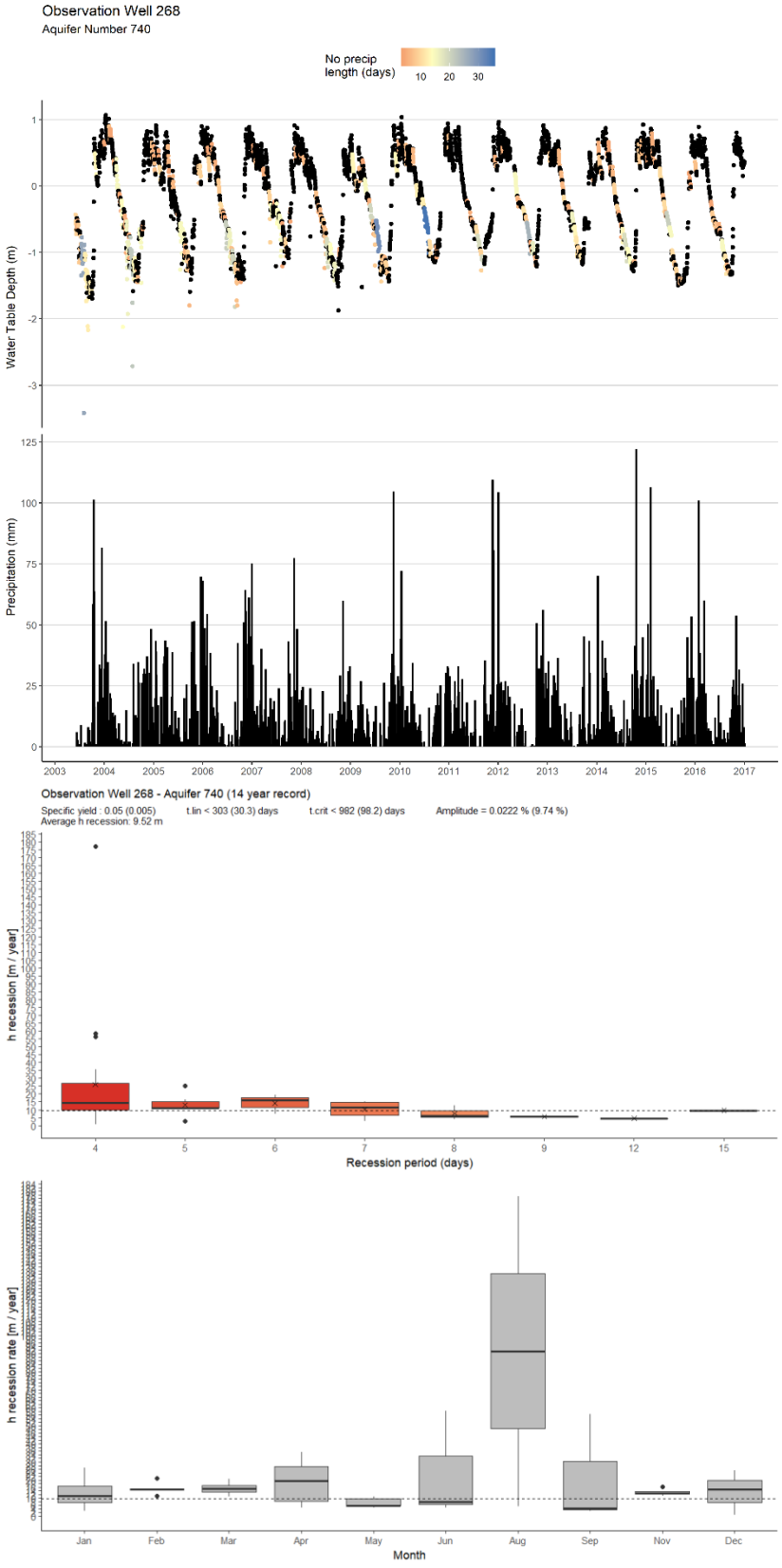
Observation Well 268
Aquifer Number 740
No precip length (days)
10
20
30
Water Table Depth (m)
Precipitation (mm)
2003
2004
2005
2006
2007
2008
2009
2010
2011
2012
2013
2014
2015
2016
2017
Observation Well 268 - Aquifer 740 (14 year record)
Specific yield : 0.05 (0.005)
Average h recession: 9.52 m
t.lin < 303 (30.3) days
t.crit < 982 (98.2) days
Amplitude = 0.0222 % (9.74 %)
h recession [m / year]
Recession period (days)
h recession rate [m / year]
Jan
Feb
Mar
Apr
May
Jun
Aug
Sep
Nov
Dec
Month

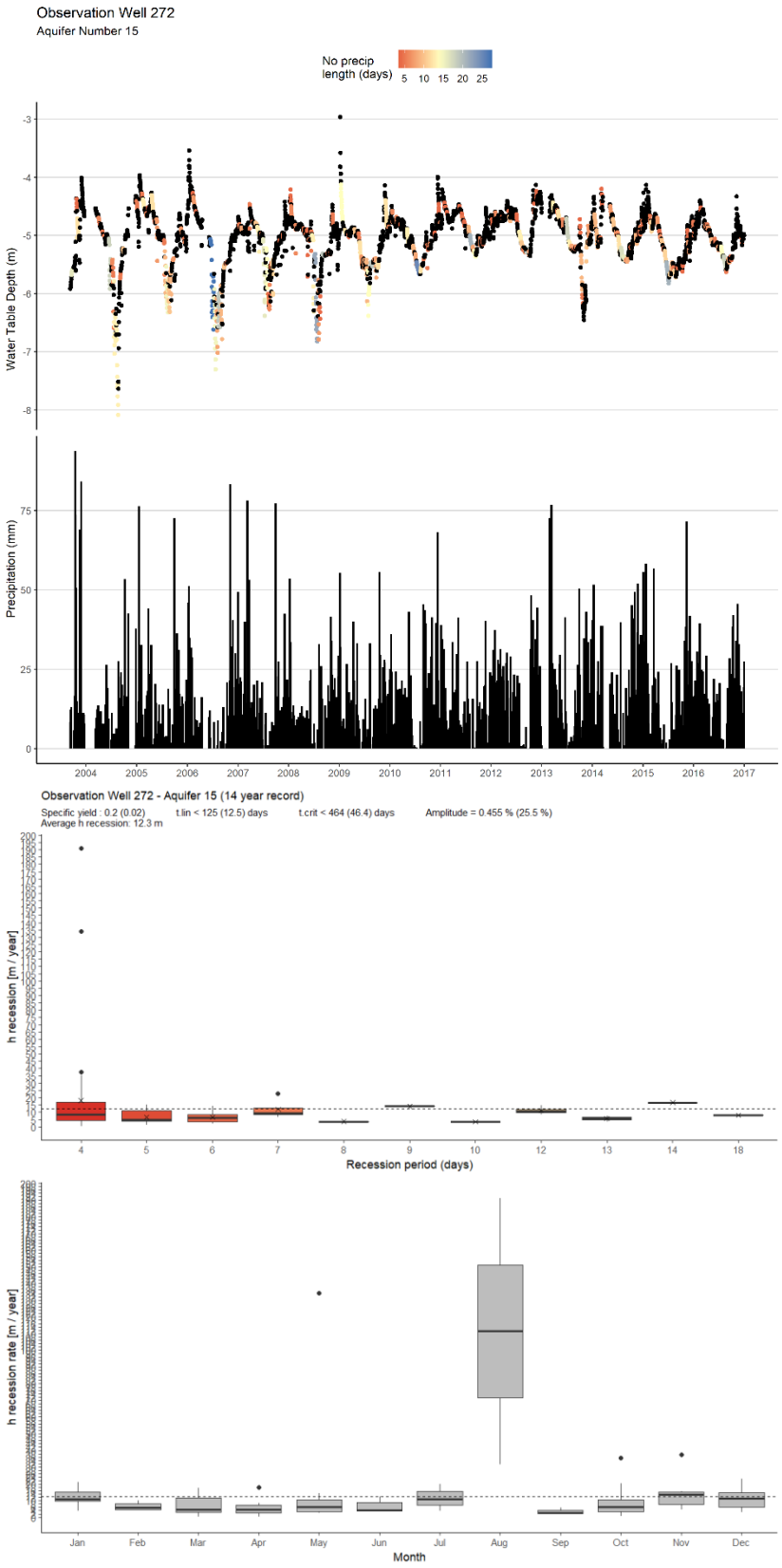
Observation Well 272
Aquifer Number 15
No precip length (days)
5 10 15 20 25
Water Table Depth (m)
-3
-4
-5
-6
-7
-8
Precipitation (mm)
75
50
25
0
2004 2005 2006 2007 2008 2009 2010 2011 2012 2013 2014 2015 2016 2017
Observation Well 272 - Aquifer 15 (14 year record)
Specific yield : 0.2 (0.02)
t.lin < 125 (12.5) days
t.crit < 464 (46.4) days
Amplitude = 0.455 % (25.5 %)
Average h recession: 12.3 m
h recession [m / year]
4 5 6 7 8 9 10 12 13 14 18
Recession period (days)
h recession rate [m / year]
Jan Feb Mar Apr May Jun Jul Aug Sep Oct Nov Dec
Month

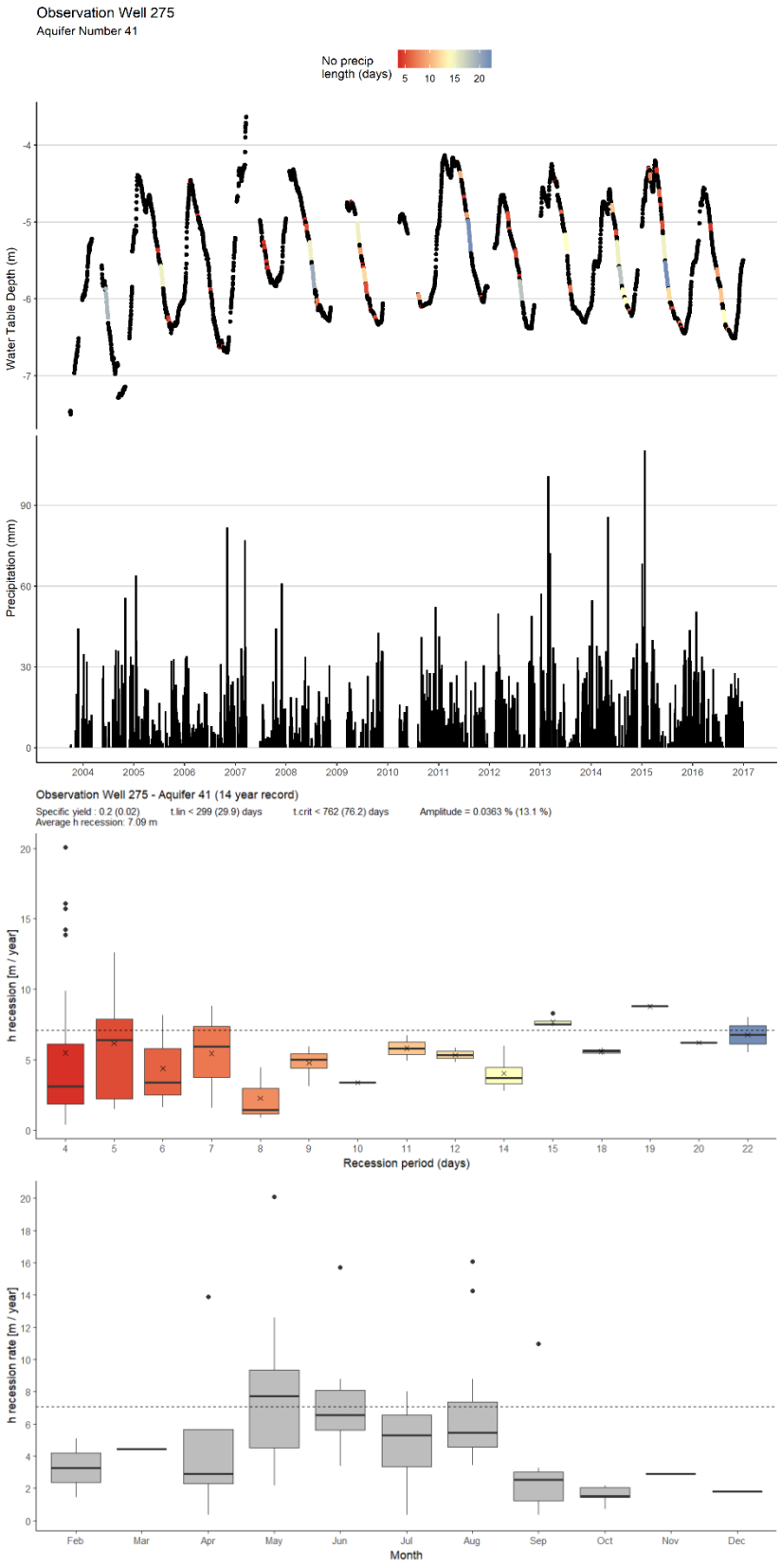
Observation Well 275
Aquifer Number 41
No precip length (days)
5
10
15
20
Water Table Depth (m)
-4
-5
-6
-7
Precipitation (mm)
90
60
30
0
2004
2005
2006
2007
2008
2009
2010
2011
2012
2013
2014
2015
2016
2017
Observation Well 275 - Aquifer 41 (14 year record)
Specific yield : 0.2 (0.02)
t.lin < 299 (29.9) days
t.crit < 762 (76.2) days
Amplitude = 0.0363 % (13.1 %)
Average h recession: 7.09 m
h recession [m / year]
Recession period (days)
4
5
6
7
8
9
10
11
12
14
15
18
19
20
22
h recession rate [m / year]
Feb
Mar
Apr
May
Jun
Jul
Aug
Sep
Oct
Nov
Dec
Month

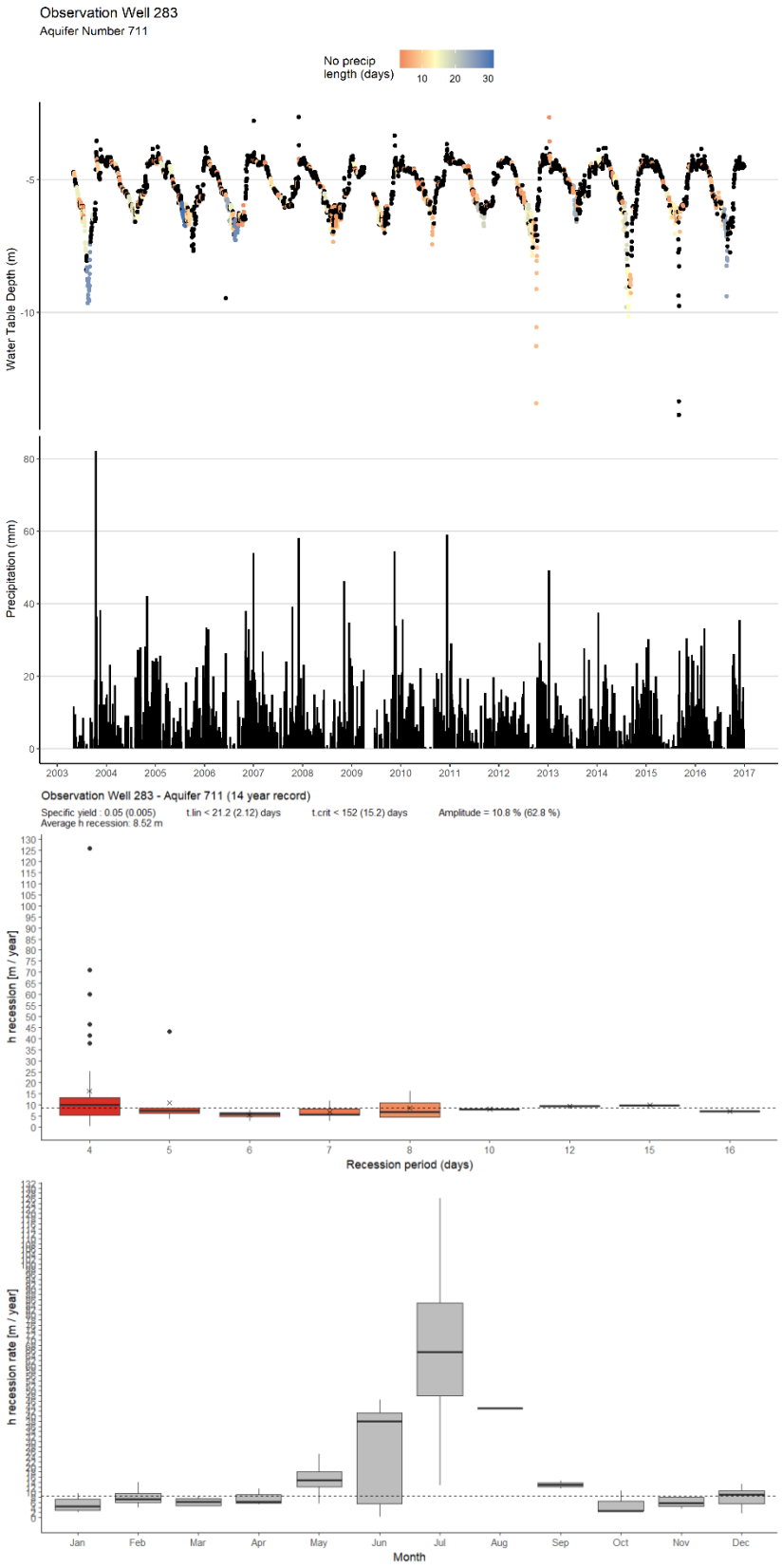
Observation Well 283
Aquifer Number 711
No precip length (days)
10
20
30
Water Table Depth (m)
-5
-10
Precipitation (mm)
80
60
40
20
0
2003
2004
2005
2006
2007
2008
2009
2010
2011
2012
2013
2014
2015
2016
2017
Observation Well 283 - Aquifer 711 (14 year record)
Specific yield : 0.05 (0.005)
Average h recession: 8.52 m
t.lin < 21.2 (2.12) days
t.crit < 152 (15.2) days
Amplitude = 10.8 % (62.8 %)
h recession [m / year]
Recession period (days)
4
5
6
7
8
10
12
15
16
h recession rate [m / year]
Jan
Feb
Mar
Apr
May
Jun
Jul
Aug
Sep
Oct
Nov
Dec
Month

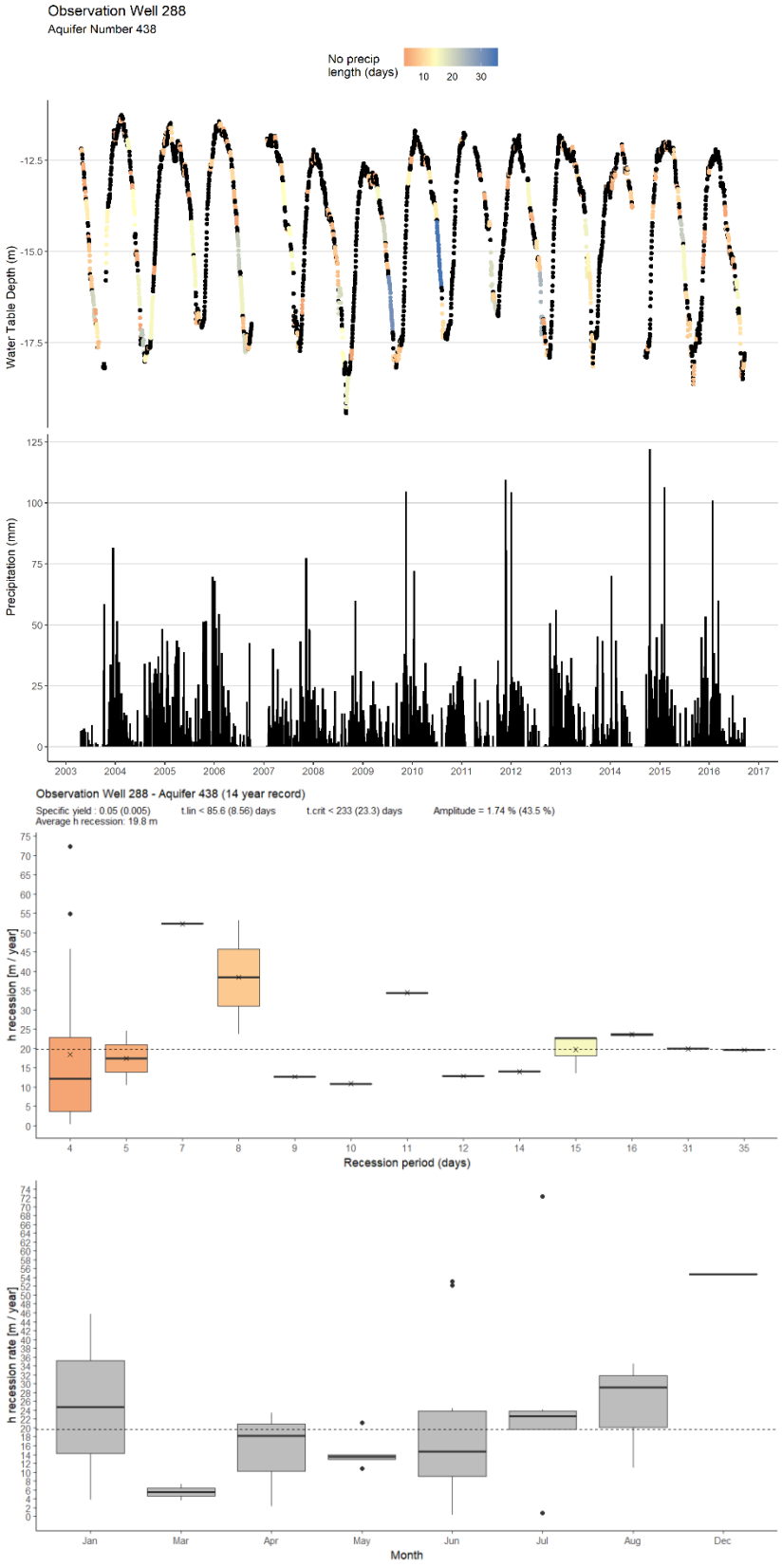
Observation Well 288
Aquifer Number 438
No precip length (days)
10
20
30
Water Table Depth (m)
-12.5
-15.0
-17.5
Precipitation (mm)
125
100
75
50
25
0
2003
2004
2005
2006
2007
2008
2009
2010
2011
2012
2013
2014
2015
2016
2017
Observation Well 288 - Aquifer 438 (14 year record)
Specific yield : 0.05 (0.005)
t.lin < 85.6 (8.56) days
t.crit < 233 (23.3) days
Amplitude = 1.74 % (43.5 %)
Average h recession: 19.8 m
h recession [m / year]
Recession period (days)
4
5
7
8
9
10
11
12
14
15
16
31
35
h recession rate [m / year]
Jan
Mar
Apr
May
Jun
Jul
Aug
Dec
Month

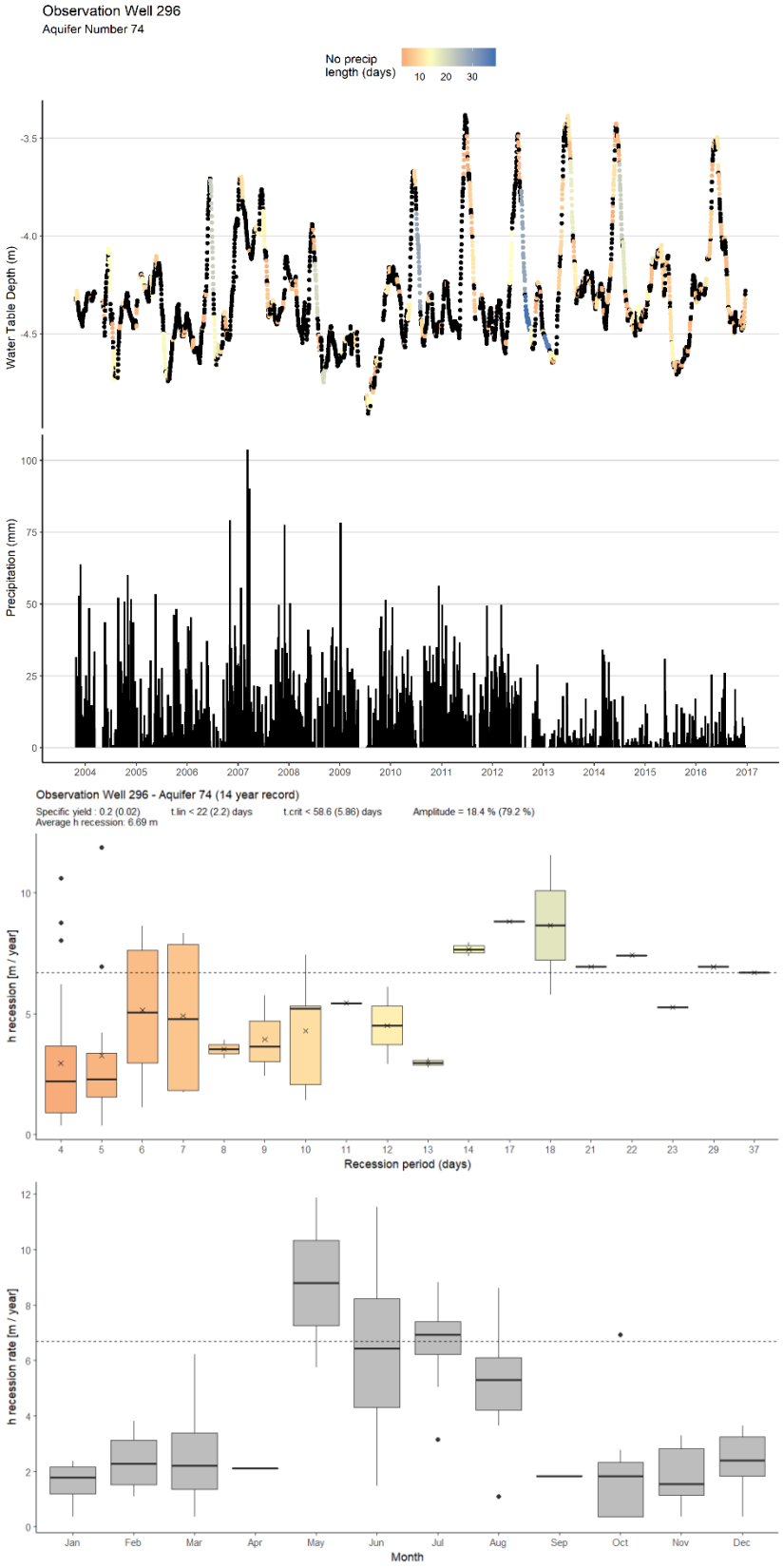
Observation Well 296
Aquifer Number 74
No precip length (days)
10
20
30
Water Table Depth (m)
-3.5
-4.0
-4.5
Precipitation (mm)
100
75
50
25
0
2004
2005
2006
2007
2008
2009
2010
2011
2012
2013
2014
2015
2016
2017
Observation Well 296 - Aquifer 74 (14 year record)
Specific yield : 0.2 (0.02)
t.lin < 22 (2.2) days
t.crit < 58.6 (5.86) days
Amplitude = 18.4 % (79.2 %)
Average h recession: 6.69 m
h recession [m / year]
Recession period (days)
4
5
6
7
8
9
10
11
12
13
14
17
18
21
22
23
29
37
h recession rate [m / year]
Month
Jan
Feb
Mar
Apr
May
Jun
Jul
Aug
Sep
Oct
Nov
Dec

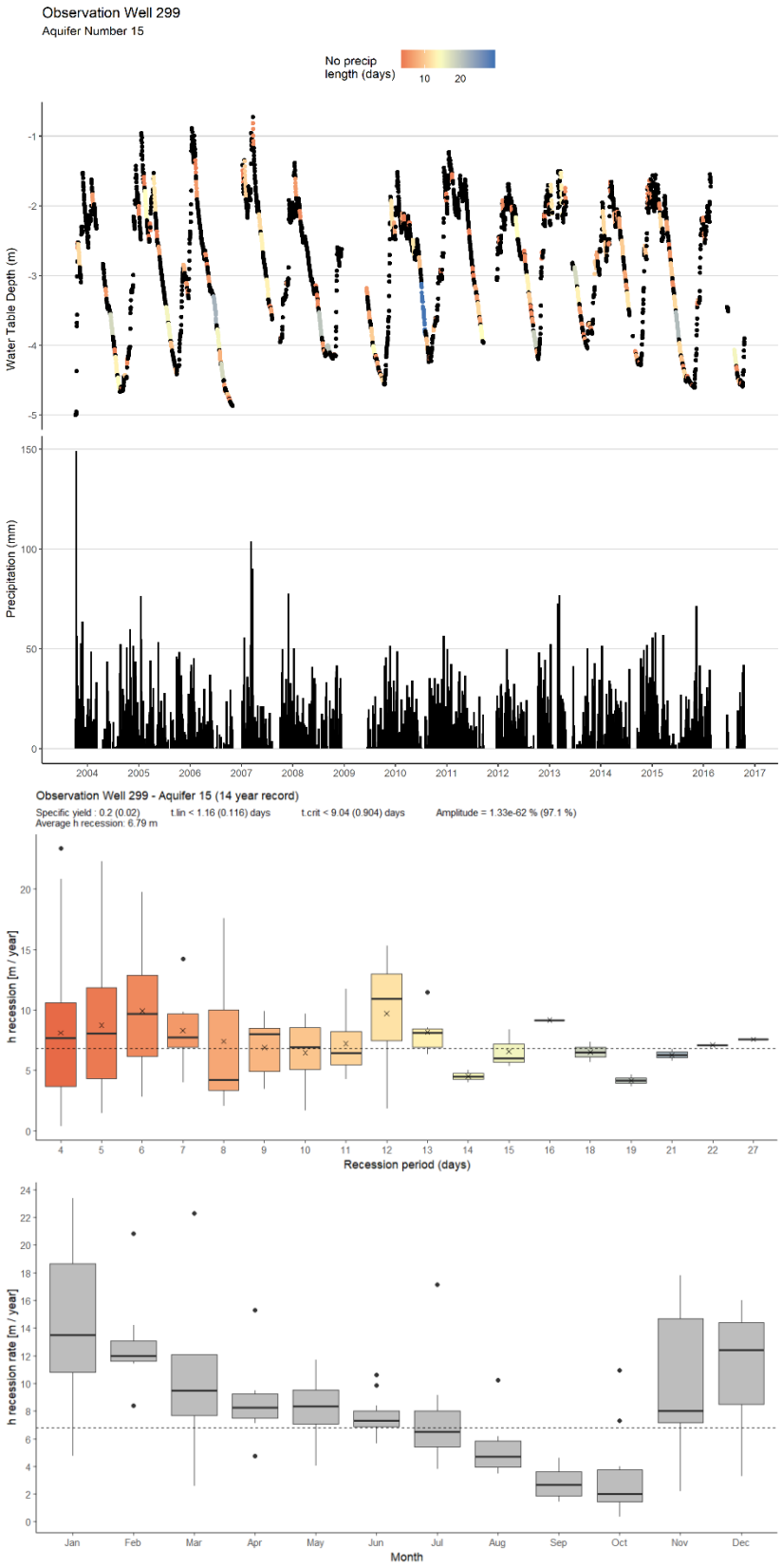
Observation Well 299
Aquifer Number 15
No precip length (days)
10
20
Water Table Depth (m)
-1
-2
-3
-4
-5
Precipitation (mm)
150
100
50
0
2004
2005
2006
2007
2008
2009
2010
2011
2012
2013
2014
2015
2016
2017
Observation Well 299 - Aquifer 15 (14 year record)
Specific yield : 0.2 (0.02)
t.lin < 1.16 (0.116) days
t.crit < 9.04 (0.904) days
Amplitude = 1.33e-62 % (97.1 %)
Average h recession: 6.79 m
h recession [m / year]
Recession period (days)
h recession rate [m / year]
Jan
Feb
Mar
Apr
May
Jun
Jul
Aug
Sep
Oct
Nov
Dec
Month

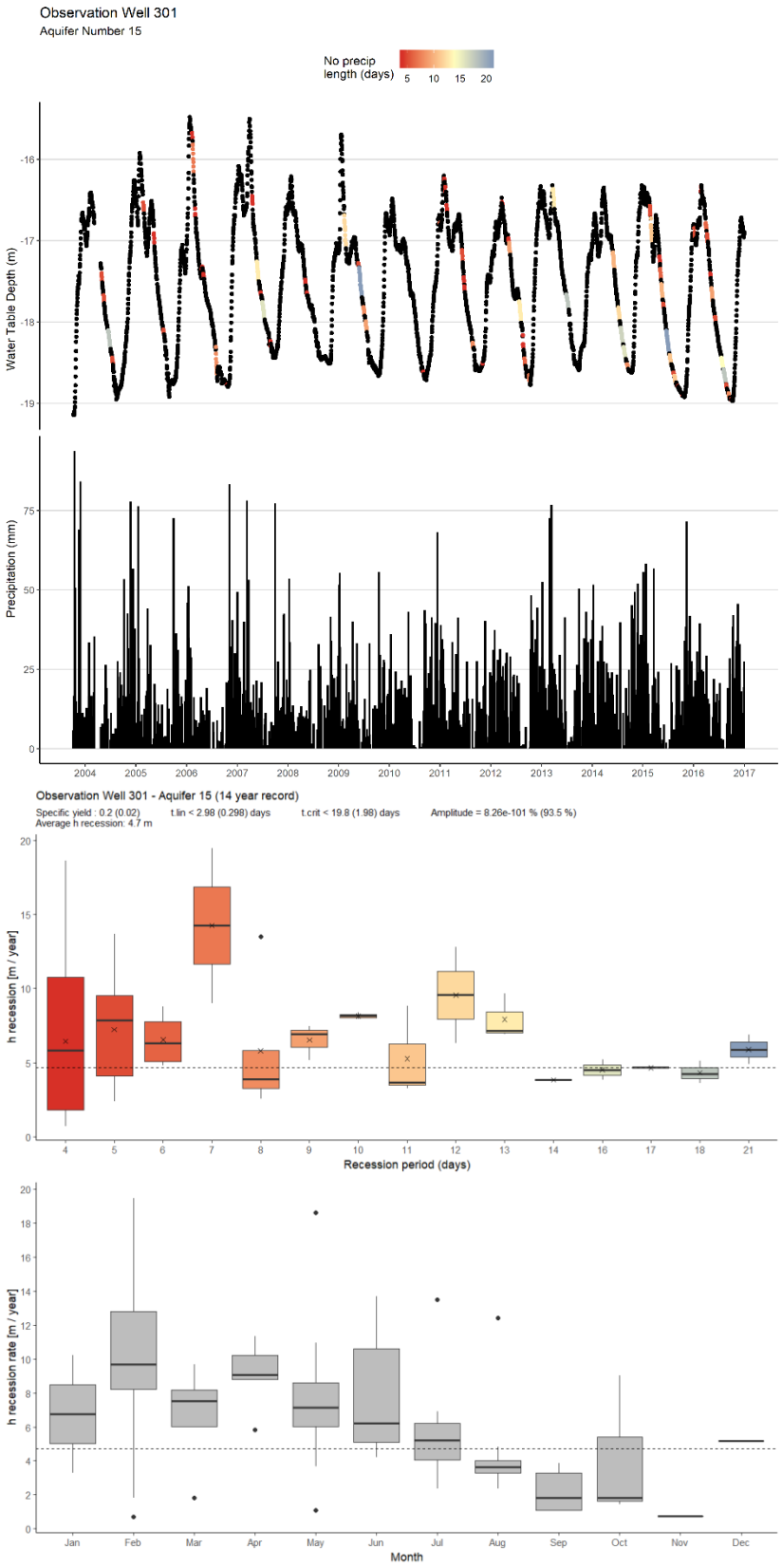
Observation Well 301
Aquifer Number 15
No precip length (days)
5
10
15
20
Water Table Depth (m)
-16
-17
-18
-19
Precipitation (mm)
75
50
25
0
2004
2005
2006
2007
2008
2009
2010
2011
2012
2013
2014
2015
2016
2017
Observation Well 301 - Aquifer 15 (14 year record)
Specific yield : 0.2 (0.02)
t.lin < 2.98 (0.298) days
t.crit < 19.8 (1.98) days
Amplitude = 8.26e-101 % (93.5 %)
Average h recession: 4.7 m
h recession [m / year]
Recession period (days)
h recession rate [m / year]
Jan
Feb
Mar
Apr
May
Jun
Jul
Aug
Sep
Oct
Nov
Dec
Month

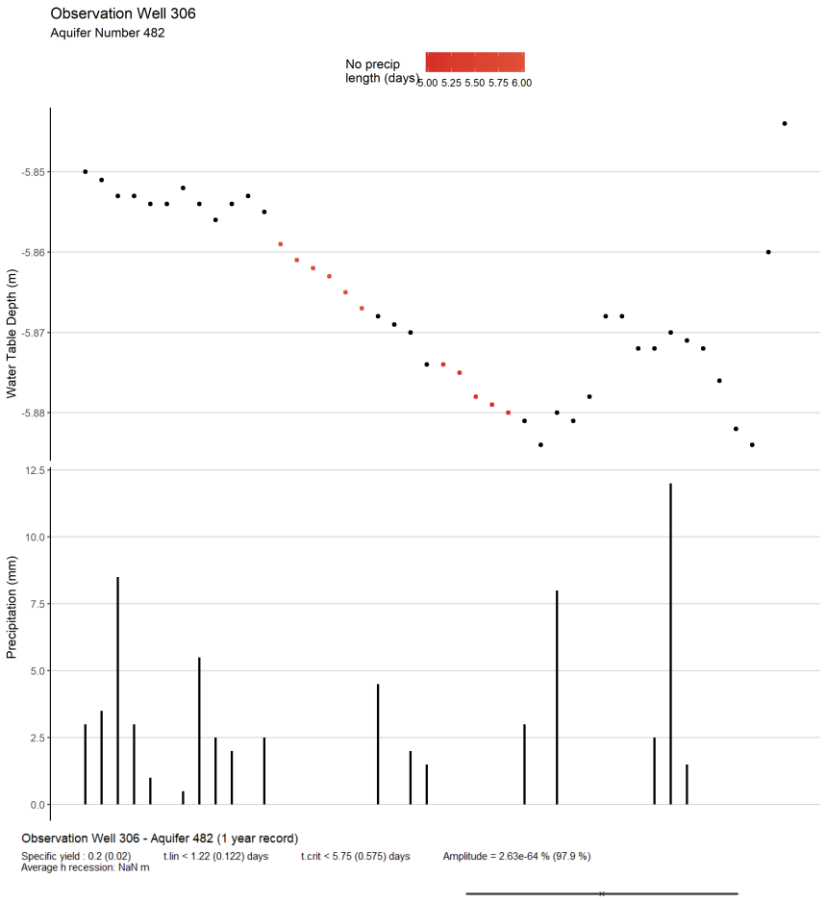
Observation Well 306
Aquifer Number 482
No precip length (days)
5.00 5.25 5.50 5.75 6.00
Water Table Depth (m)
-5.85
-5.86
-5.87
-5.88
Precipitation (mm)
12.5
10.0
7.5
5.0
2.5
0.0
Observation Well 306 - Aquifer 482 (1 year record)
Specific yield : 0.2 (0.02)
t.lin < 1.22 (0.122) days
t.crit < 5.75 (0.575) days
Amplitude = 2.63e-64 % (97.9 %)
Average h recession: NaN m

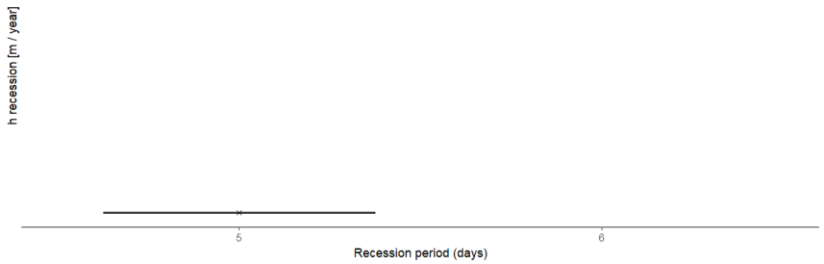
h recession [m / year]
5
6
Recession period (days)

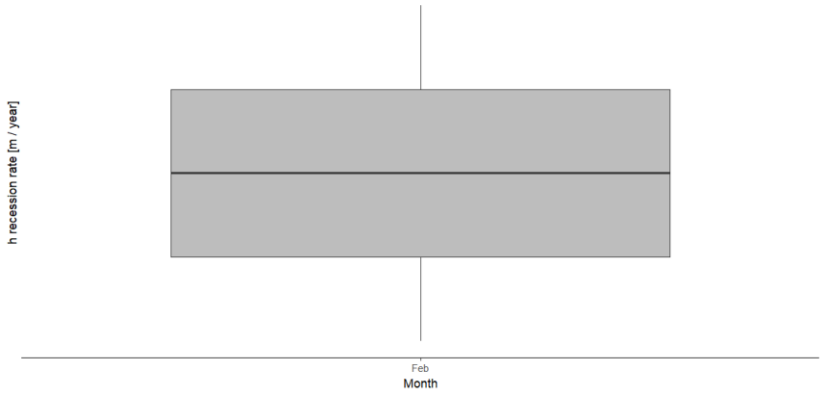
h recession rate [m / year]
Feb
Month

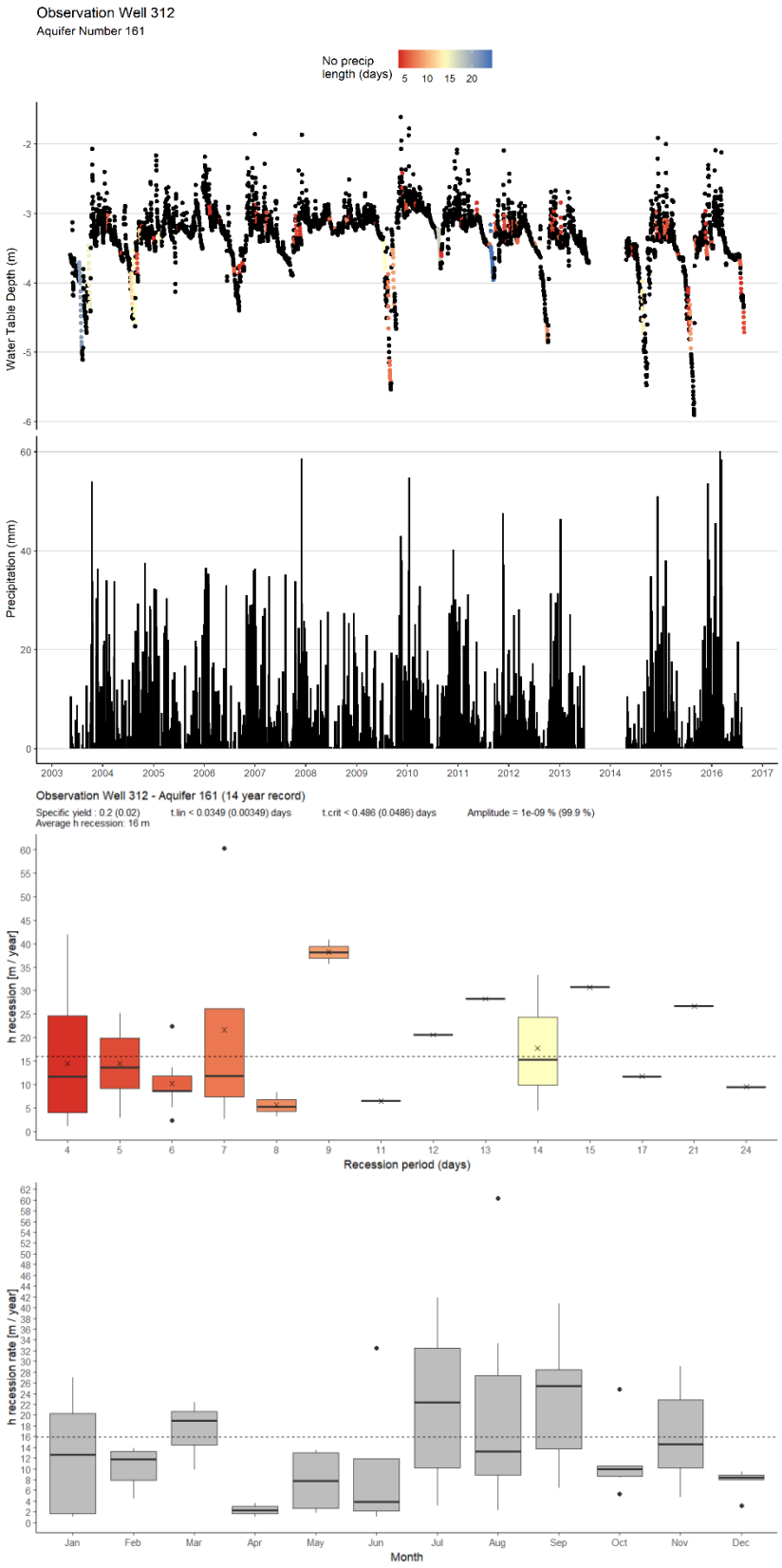
Observation Well 312
Aquifer Number 161
No precip length (days)
5 10 15 20
Water Table Depth (m)
-2
-3
-4
-5
-6
Precipitation (mm)
60
40
20
0
2003 2004 2005 2006 2007 2008 2009 2010 2011 2012 2013 2014 2015 2016 2017
Observation Well 312 - Aquifer 161 (14 year record)
Specific yield : 0.2 (0.02)
Average h recession: 16 m
t.lin < 0.0349 (0.00349) days
t.crit < 0.486 (0.0486) days
Amplitude = 1e-09 % (99.9 %)
h recession [m / year]
Recession period (days)
4 5 6 7 8 9 11 12 13 14 15 17 21 24
h recession rate [m / year]
Jan Feb Mar Apr May Jun Jul Aug Sep Oct Nov Dec
Month

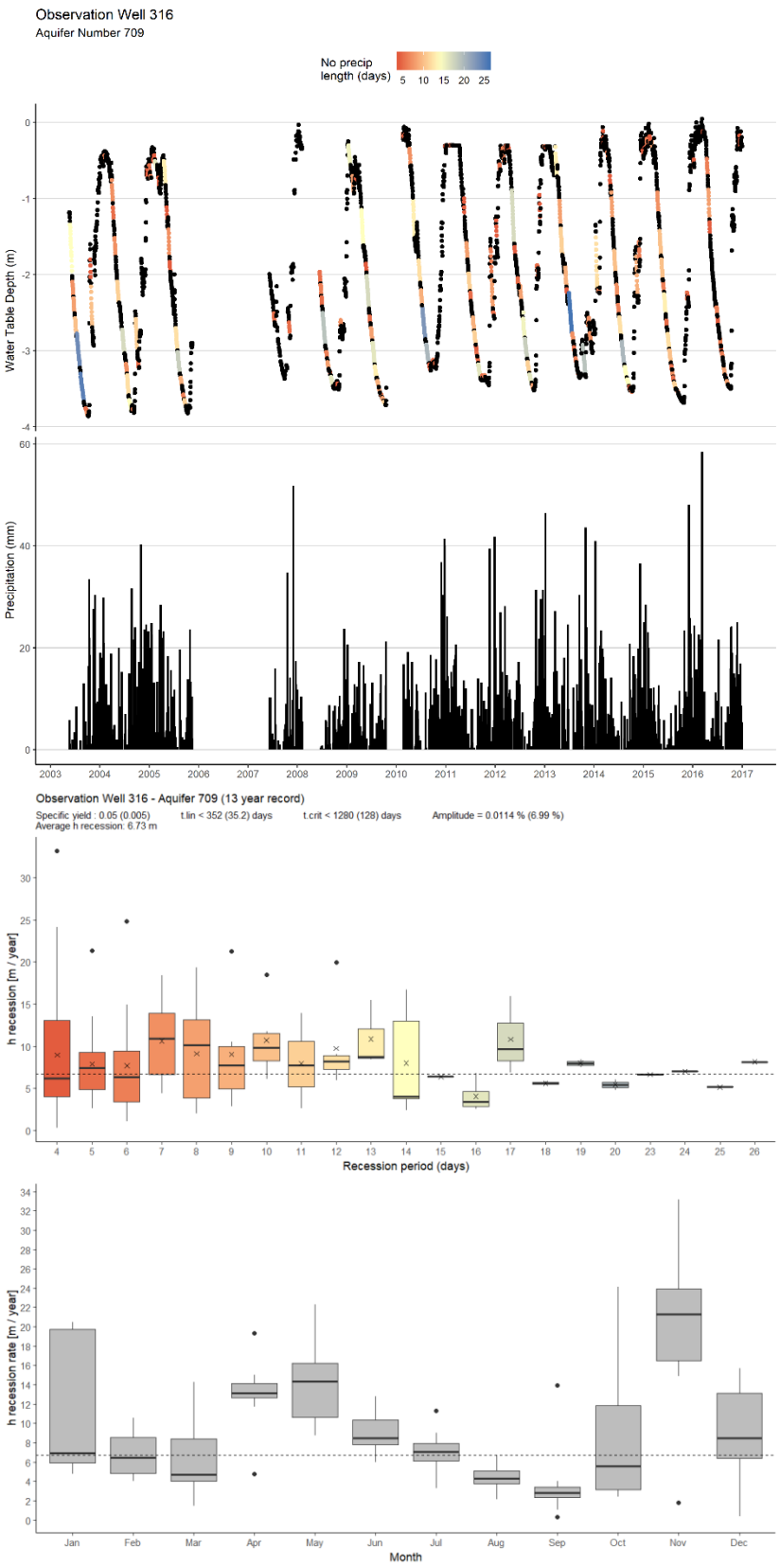
Observation Well 316
Aquifer Number 709
No precip length (days)
5 10 15 20 25
Water Table Depth (m)
Precipitation (mm)
2003 2004 2005 2006 2007 2008 2009 2010 2011 2012 2013 2014 2015 2016 2017
Observation Well 316 - Aquifer 709 (13 year record)
Specific yield : 0.05 (0.005)
t.lin < 352 (35.2) days
t.crit < 1280 (128) days
Amplitude = 0.0114 % (6.99 %)
Average h recession: 6.73 m
h recession [m / year]
Recession period (days)
h recession rate [m / year]
Jan Feb Mar Apr May Jun Jul Aug Sep Oct Nov Dec
Month

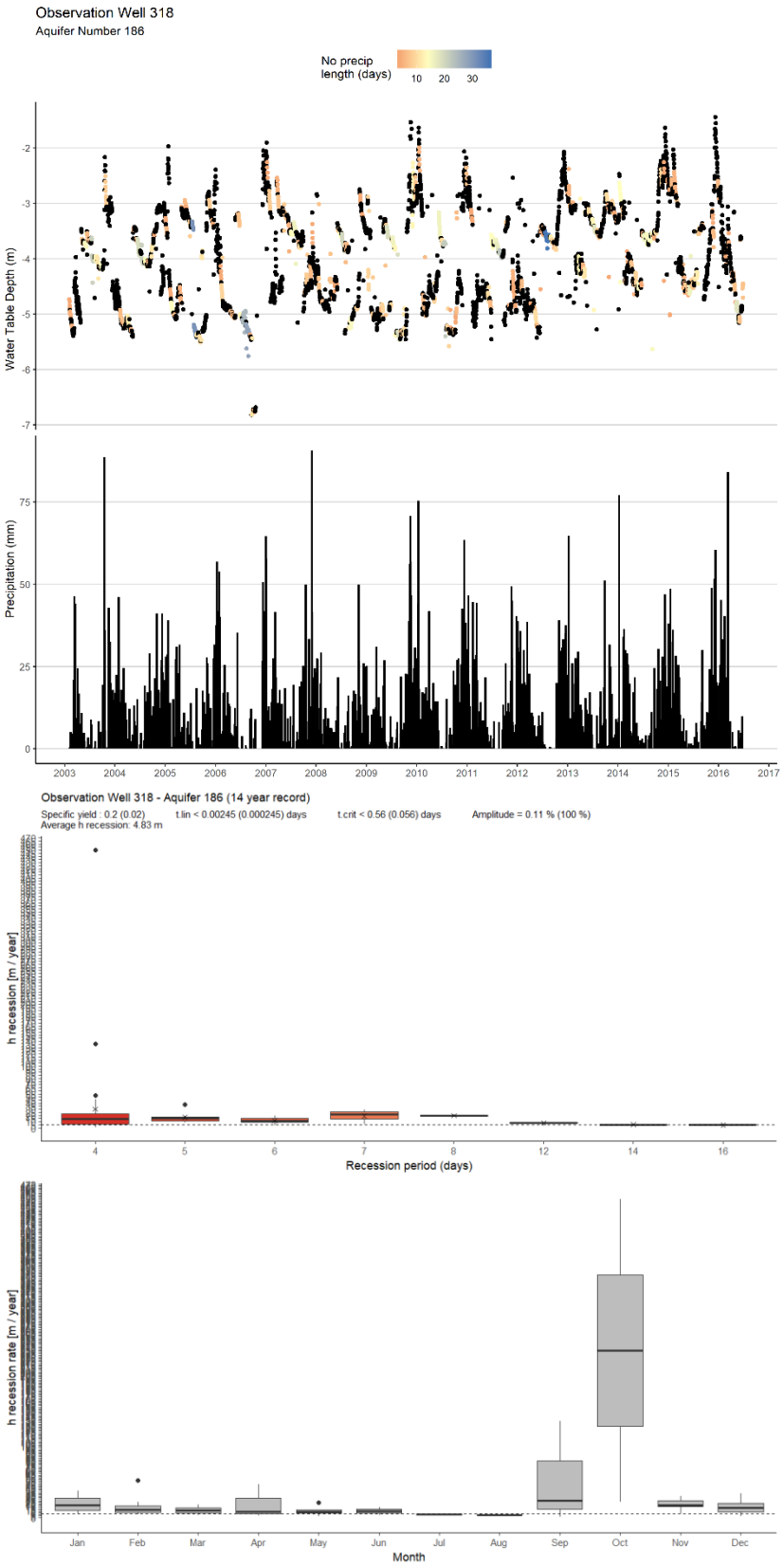
Observation Well 318
Aquifer Number 186
No precip length (days)
10 20 30
Water Table Depth (m)
-2
-3
-4
-5
-6
-7
Precipitation (mm)
75
50
25
0
2003 2004 2005 2006 2007 2008 2009 2010 2011 2012 2013 2014 2015 2016 2017
Observation Well 318 - Aquifer 186 (14 year record)
Specific yield : 0.2 (0.02)
t.lin < 0.00245 (0.000245) days
t.crit < 0.56 (0.056) days
Amplitude = 0.11 % (100 %)
Average h recession: 4.83 m
h recession [m / year]
4 5 6 7 8 12 14 16
Recession period (days)
h recession rate [m / year]
Jan Feb Mar Apr May Jun Jul Aug Sep Oct Nov Dec
Month

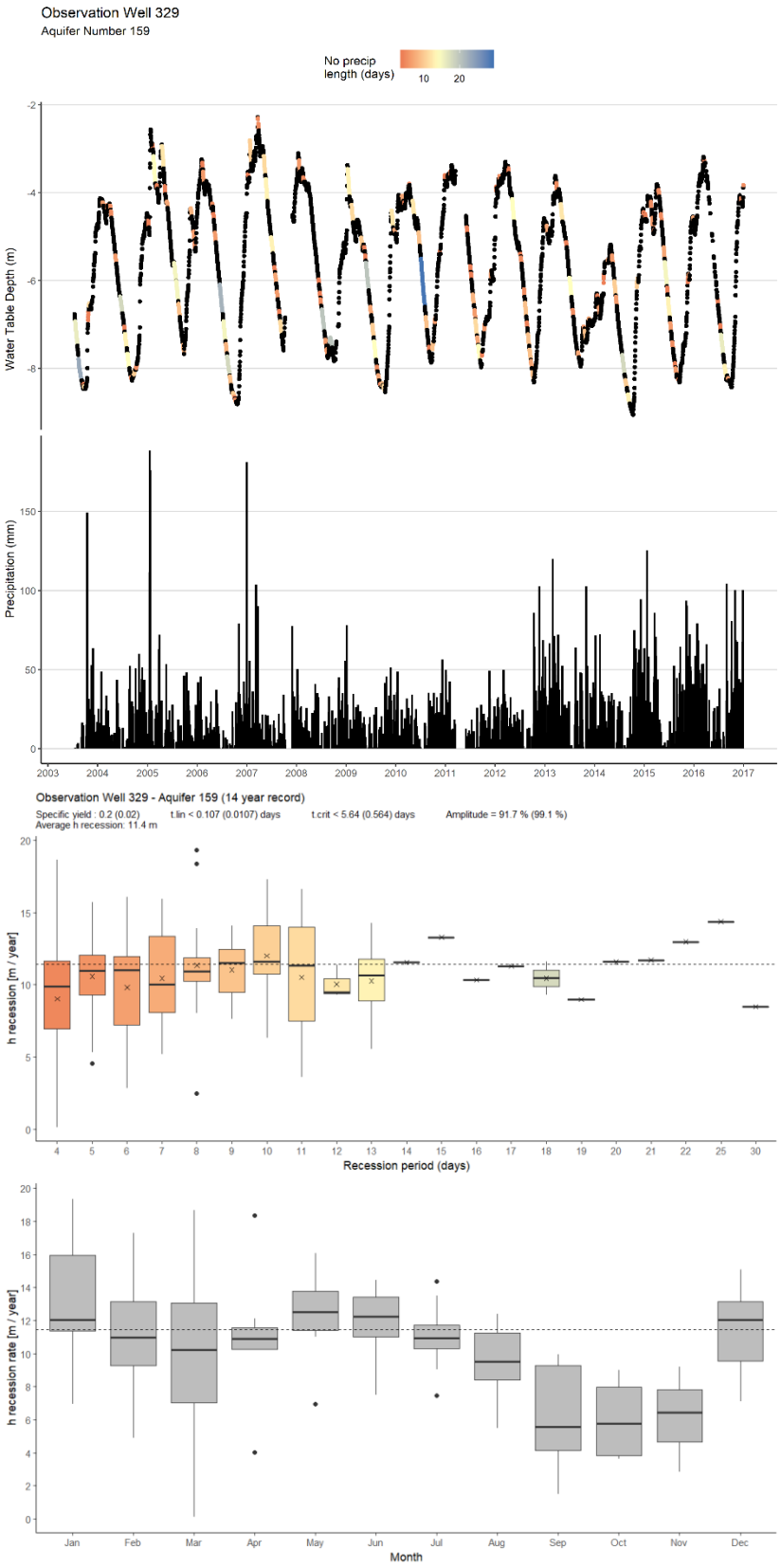
Observation Well 329
Aquifer Number 159
No precip length (days)
10
20
Water Table Depth (m)
-2
-4
-6
-8
Precipitation (mm)
150
100
50
0
2003
2004
2005
2006
2007
2008
2009
2010
2011
2012
2013
2014
2015
2016
2017
Observation Well 329 - Aquifer 159 (14 year record)
Specific yield : 0.2 (0.02)
t.lin < 0.107 (0.0107) days
t.crit < 5.64 (0.564) days
Amplitude = 91.7 % (99.1 %)
Average h recession: 11.4 m
h recession [m / year]
Recession period (days)
h recession rate [m / year]
Jan
Feb
Mar
Apr
May
Jun
Jul
Aug
Sep
Oct
Nov
Dec
Month

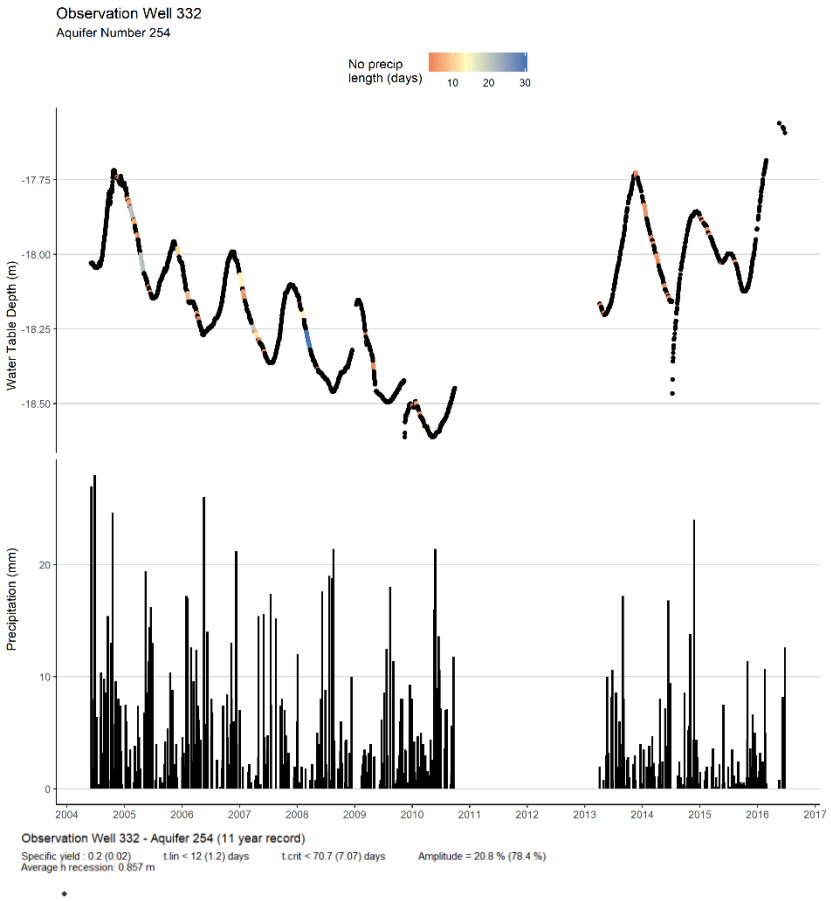
Observation Well 332
Aquifer Number 254
No precip length (days)
10
20
30
Water Table Depth (m)
-17.75
-18.00
-18.25
-18.50
Precipitation (mm)
0
10
20
2004
2005
2006
2007
2008
2009
2010
2011
2012
2013
2014
2015
2016
2017
Observation Well 332 - Aquifer 254 (11 year record)
Specific yield : 0.2 (0.02)
t.lin < 12 (1.2) days
t.crit < 70.7 (7.07) days
Amplitude = 20.8 % (78.4 %)
Average h recession: 0.857 m

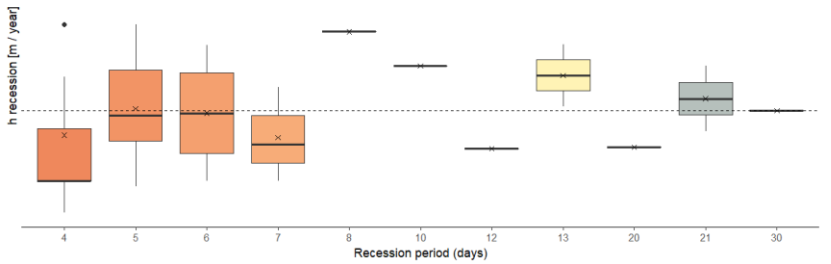
h recession [m / year]
4
5
6
7
8
10
12
13
20
21
30
Recession period (days)

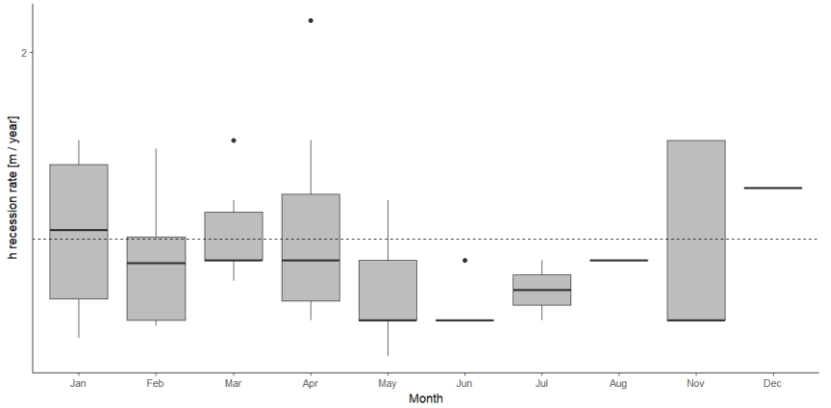
h recession rate [m / year]
2
Jan
Feb
Mar
Apr
May
Jun
Jul
Aug
Nov
Dec
Month

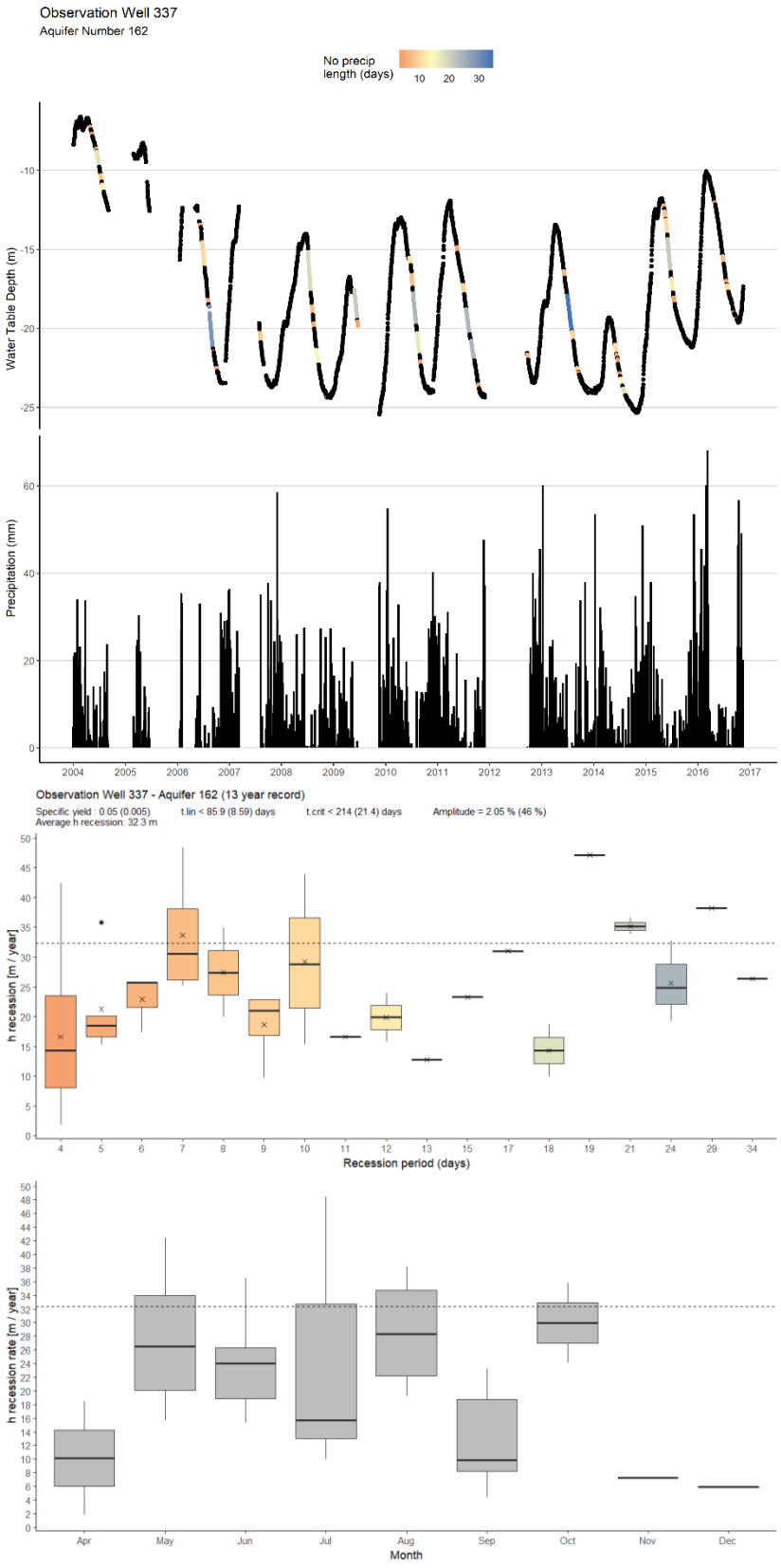
Observation Well 337
Aquifer Number 162
No precip length (days)
10
20
30
Water Table Depth (m)
-10
-15
-20
-25
Precipitation (mm)
60
40
20
0
2004
2005
2006
2007
2008
2009
2010
2011
2012
2013
2014
2015
2016
2017
Observation Well 337 - Aquifer 162 (13 year record)
Specific yield : 0.05 (0.005)
t.lin < 85.9 (8.59) days
t.crit < 214 (21.4) days
Amplitude = 2.05 % (46 %)
Average h recession: 32.3 m
h recession [m / year]
Recession period (days)
4
5
6
7
8
9
10
11
12
13
15
17
18
19
21
24
29
34
h recession rate [m / year]
Apr
May
Jun
Jul
Aug
Sep
Oct
Nov
Dec
Month

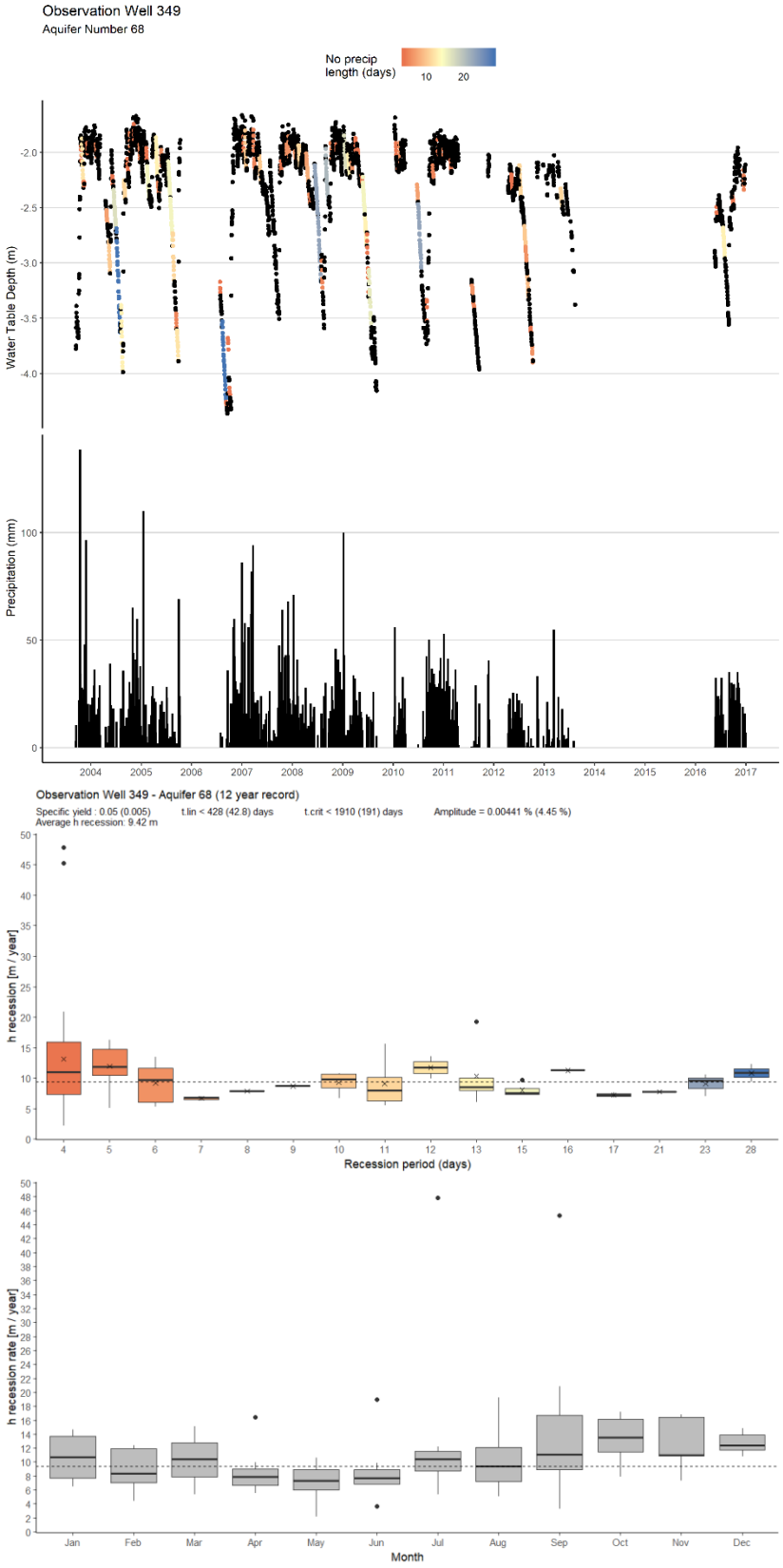
Observation Well 349
Aquifer Number 68
No precip length (days)
10
20
Water Table Depth (m)
-2.0
-2.5
-3.0
-3.5
-4.0
Precipitation (mm)
100
50
0
2004
2005
2006
2007
2008
2009
2010
2011
2012
2013
2014
2015
2016
2017
Observation Well 349 - Aquifer 68 (12 year record)
Specific yield : 0.05 (0.005)
t.lin < 428 (42.8) days
t.crit < 1910 (191) days
Amplitude = 0.00441 % (4.45 %)
Average h recession: 9.42 m
h recession [m / year]
Recession period (days)
4
5
6
7
8
9
10
11
12
13
15
16
17
21
23
28
h recession rate [m / year]
Jan
Feb
Mar
Apr
May
Jun
Jul
Aug
Sep
Oct
Nov
Dec
Month

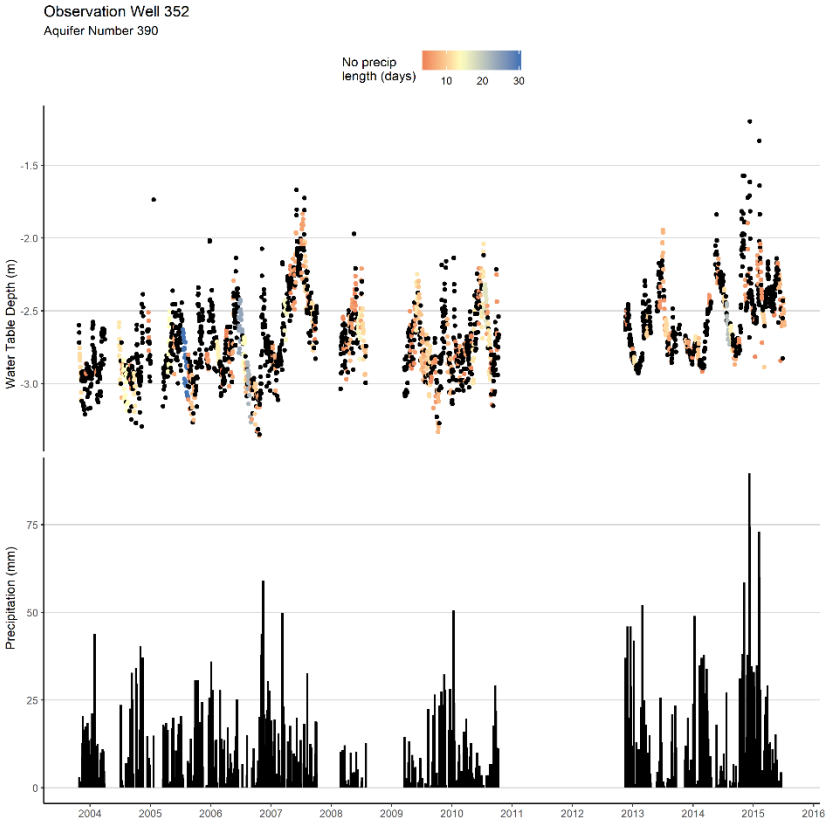
Observation Well 352
Aquifer Number 390
No precip length (days)
10
20
30
Water Table Depth (m)
-1.5
-2.0
-2.5
-3.0
Precipitation (mm)
75
50
25
0
2004
2005
2006
2007
2008
2009
2010
2011
2012
2013
2014
2015
2016

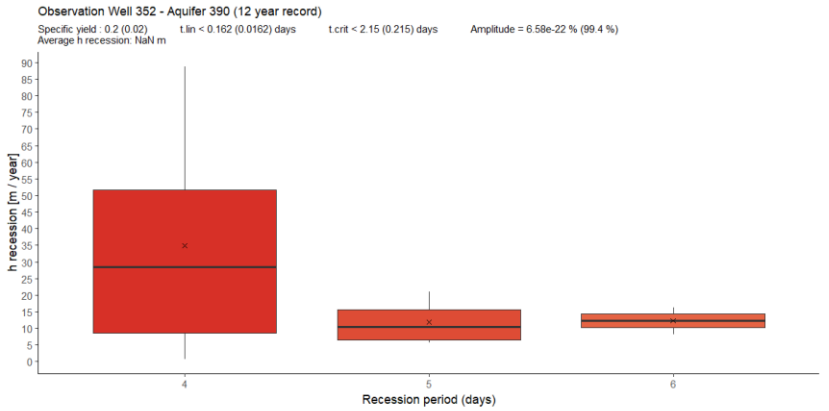
Observation Well 352 - Aquifer 390 (12 year record)
Specific yield : 0.2 (0.02)
t.lin < 0.162 (0.0162) days
t.crit < 2.15 (0.215) days
Amplitude = 6.58e-22 % (99.4 %)
Average h recession: NaN m
h recession [m / year]
Recession period (days)
4
5
6

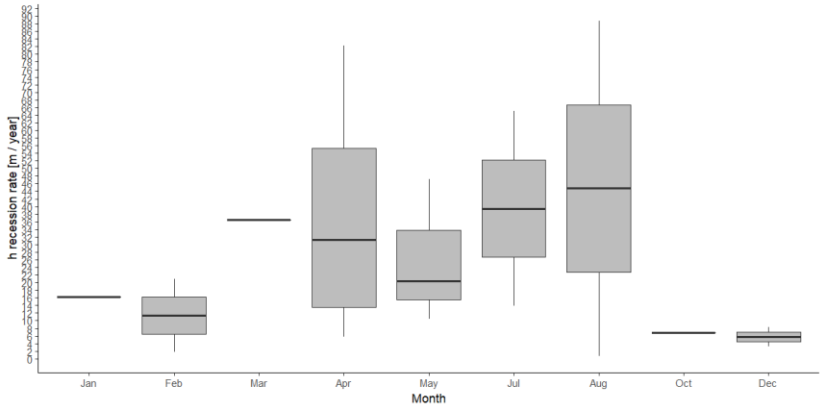
h recession rate [m / year]
Jan
Feb
Mar
Apr
May
Jul
Aug
Oct
Dec
Month

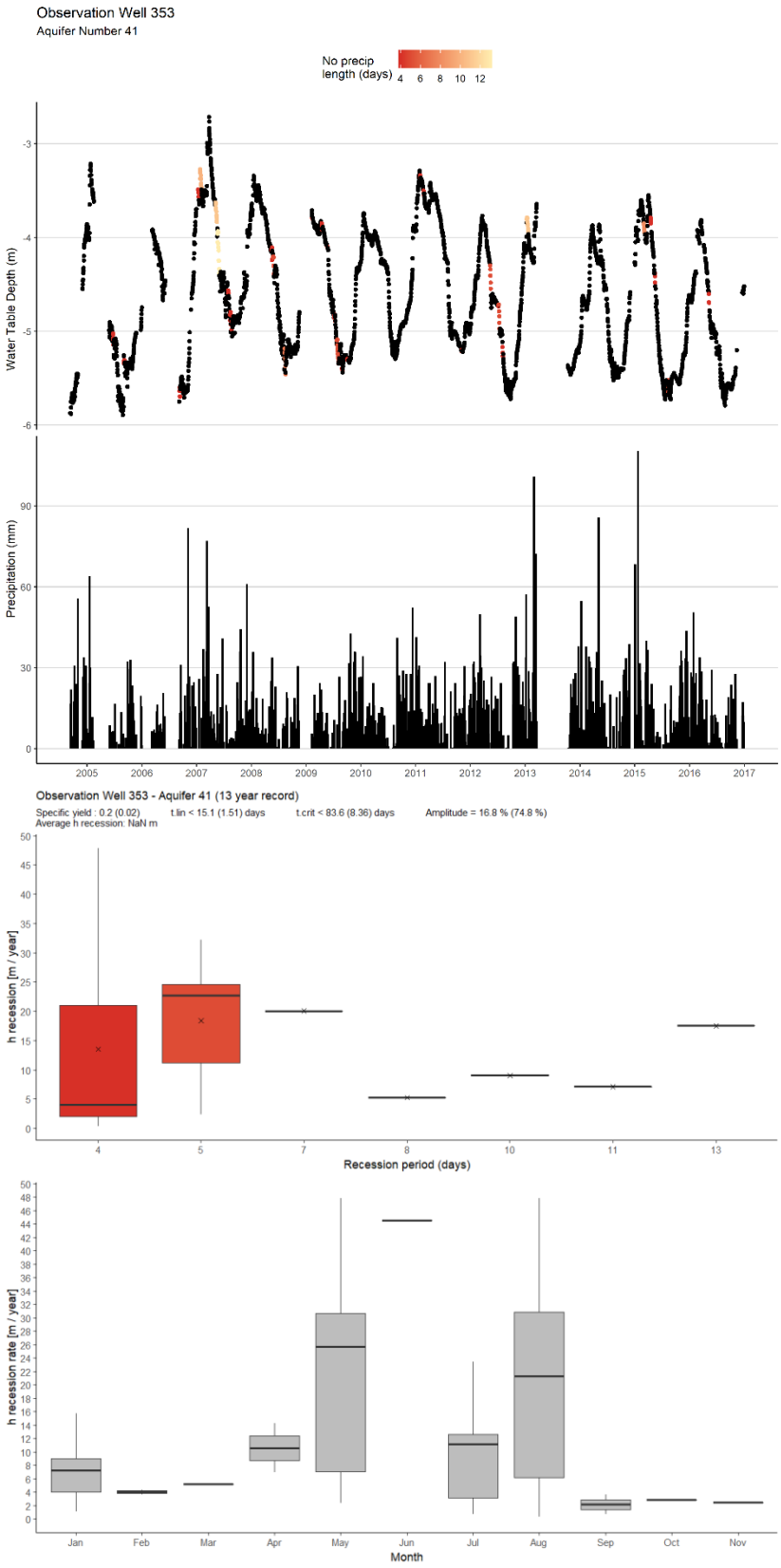
Observation Well 353
Aquifer Number 41
No precip length (days)
4 6 8 10 12
Water Table Depth (m)
-3
-4
-5
-6
Precipitation (mm)
90
60
30
0
2005 2006 2007 2008 2009 2010 2011 2012 2013 2014 2015 2016 2017
Observation Well 353 - Aquifer 41 (13 year record)
Specific yield : 0.2 (0.02)
t.lin < 15.1 (1.51) days
t.crit < 83.6 (8.36) days
Amplitude = 16.8 % (74.8 %)
Average h recession: NaN m
h recession [m / year]
50 45 40 35 30 25 20 15 10 5 0
4 5 7 8 10 11 13
Recession period (days)
h recession rate [m / year]
50 48 46 44 42 40 38 36 34 32 30 28 26 24 22 20 18 16 14 12 10 8 6 4 2 0
Jan Feb Mar Apr May Jun Jul Aug Sep Oct Nov
Month

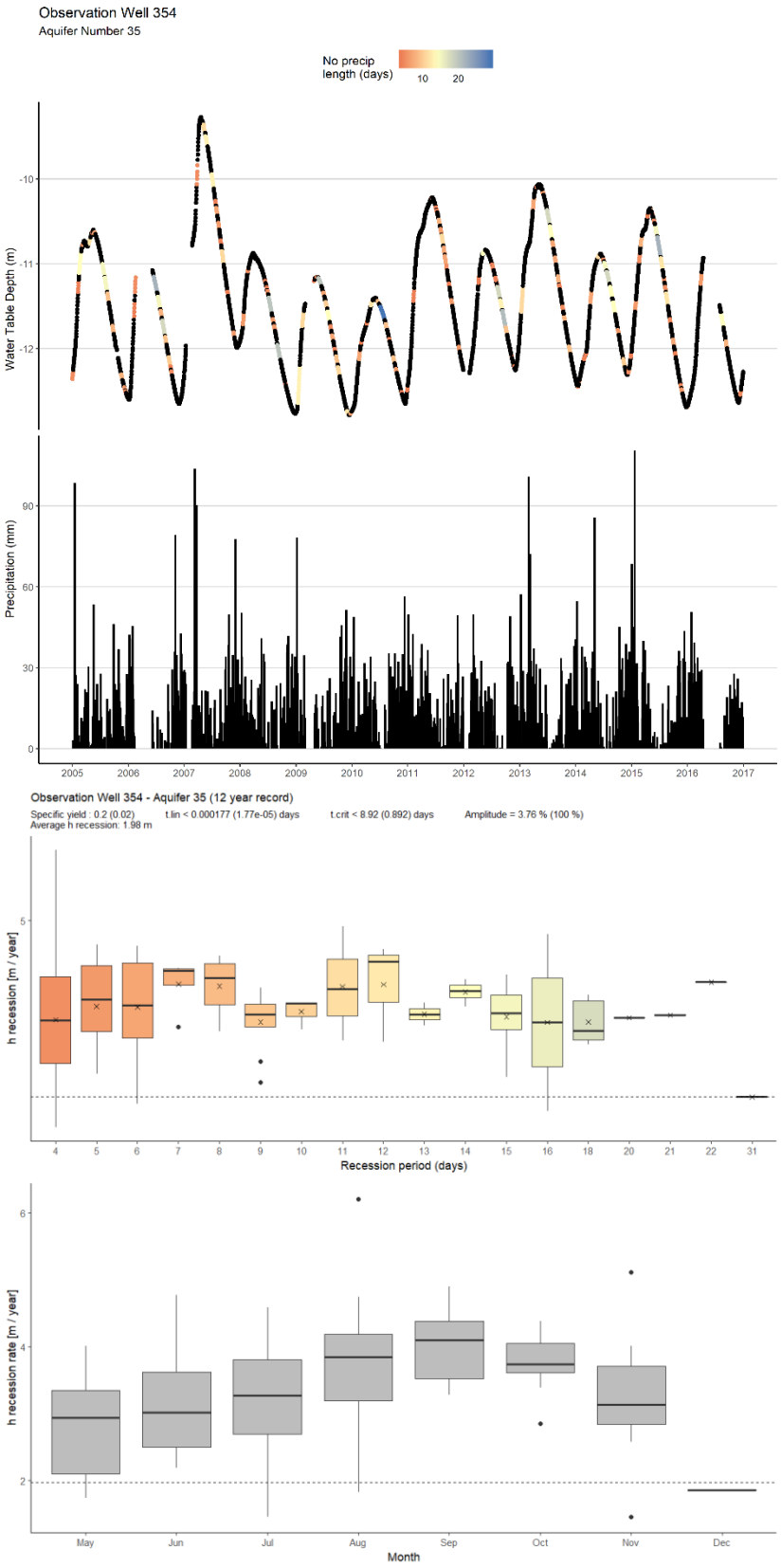
Observation Well 354
Aquifer Number 35
No precip length (days)
10
20
Water Table Depth (m)
-10
-11
-12
Precipitation (mm)
90
60
30
0
2005
2006
2007
2008
2009
2010
2011
2012
2013
2014
2015
2016
2017
Observation Well 354 - Aquifer 35 (12 year record)
Specific yield : 0.2 (0.02)
Average h recession: 1.98 m
t.lin < 0.000177 (1.77e-05) days
t.crit < 8.92 (0.892) days
Amplitude = 3.76 % (100 %)
h recession [m / year]
5
4
6
7
8
9
10
11
12
13
14
15
16
18
20
21
22
31
Recession period (days)
h recession rate [m / year]
6
4
2
May
Jun
Jul
Aug
Sep
Oct
Nov
Dec
Month

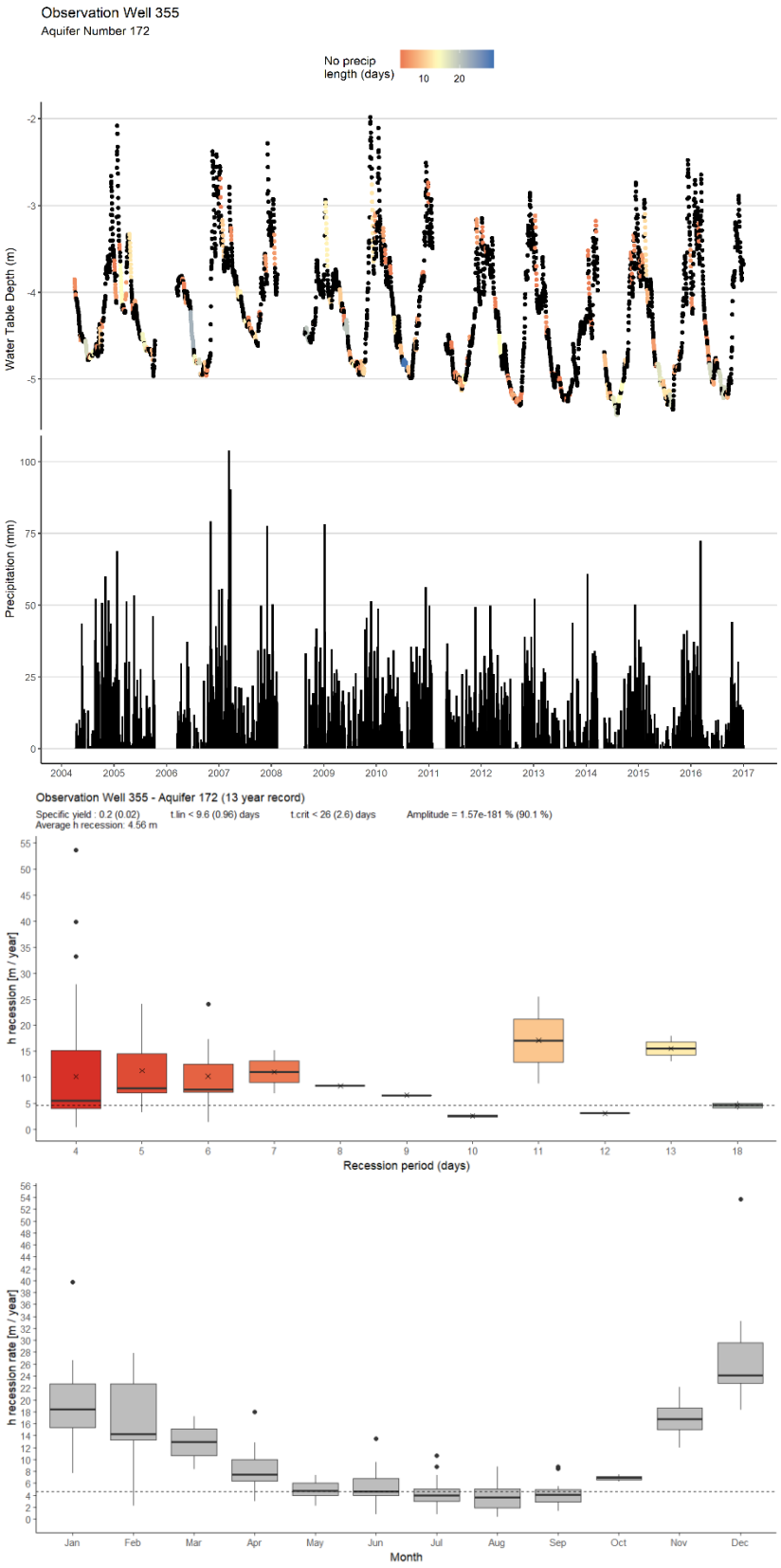
Observation Well 355
Aquifer Number 172
No precip length (days)
10
20
Water Table Depth (m)
-2
-3
-4
-5
Precipitation (mm)
100
75
50
25
0
2004
2005
2006
2007
2008
2009
2010
2011
2012
2013
2014
2015
2016
2017
Observation Well 355 - Aquifer 172 (13 year record)
Specific yield : 0.2 (0.02)
t.lin < 9.6 (0.96) days
t.crit < 26 (2.6) days
Amplitude = 1.57e-181 % (90.1 %)
Average h recession: 4.56 m
h recession [m / year]
Recession period (days)
4
5
6
7
8
9
10
11
12
13
18
h recession rate [m / year]
Jan
Feb
Mar
Apr
May
Jun
Jul
Aug
Sep
Oct
Nov
Dec
Month

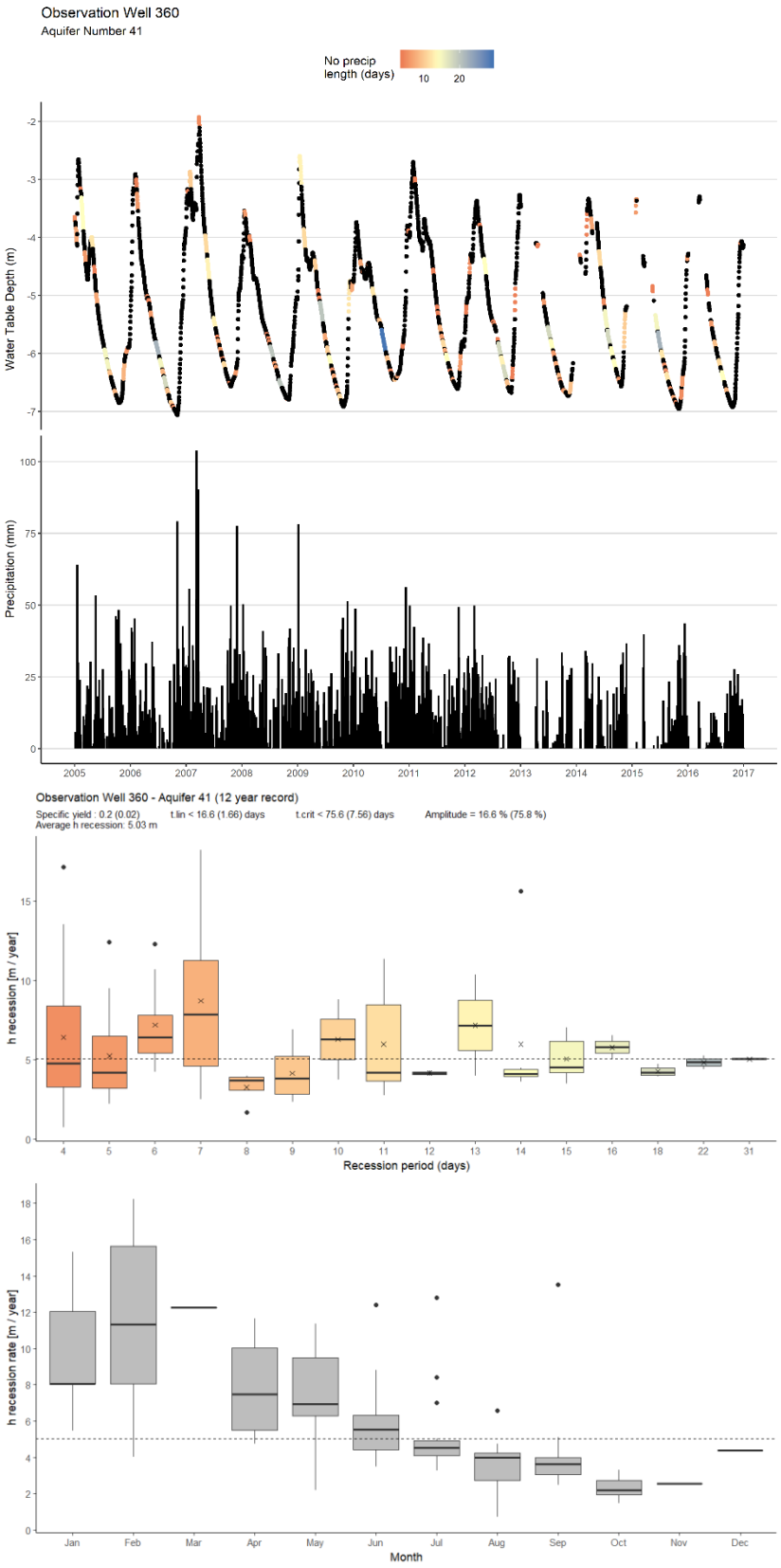
Observation Well 360
Aquifer Number 41
No precip length (days)
10
20
Water Table Depth (m)
-2
-3
-4
-5
-6
-7
Precipitation (mm)
100
75
50
25
0
2005
2006
2007
2008
2009
2010
2011
2012
2013
2014
2015
2016
2017
Observation Well 360 - Aquifer 41 (12 year record)
Specific yield : 0.2 (0.02)
t.lin < 16.6 (1.66) days
t.crit < 75.6 (7.56) days
Amplitude = 16.6 % (75.8 %)
Average h recession: 5.03 m
h recession [m / year]
15
10
5
0
4
5
6
7
8
9
10
11
12
13
14
15
16
18
22
31
Recession period (days)
h recession rate [m / year]
18
16
14
12
10
8
6
4
2
0
Jan
Feb
Mar
Apr
May
Jun
Jul
Aug
Sep
Oct
Nov
Dec
Month

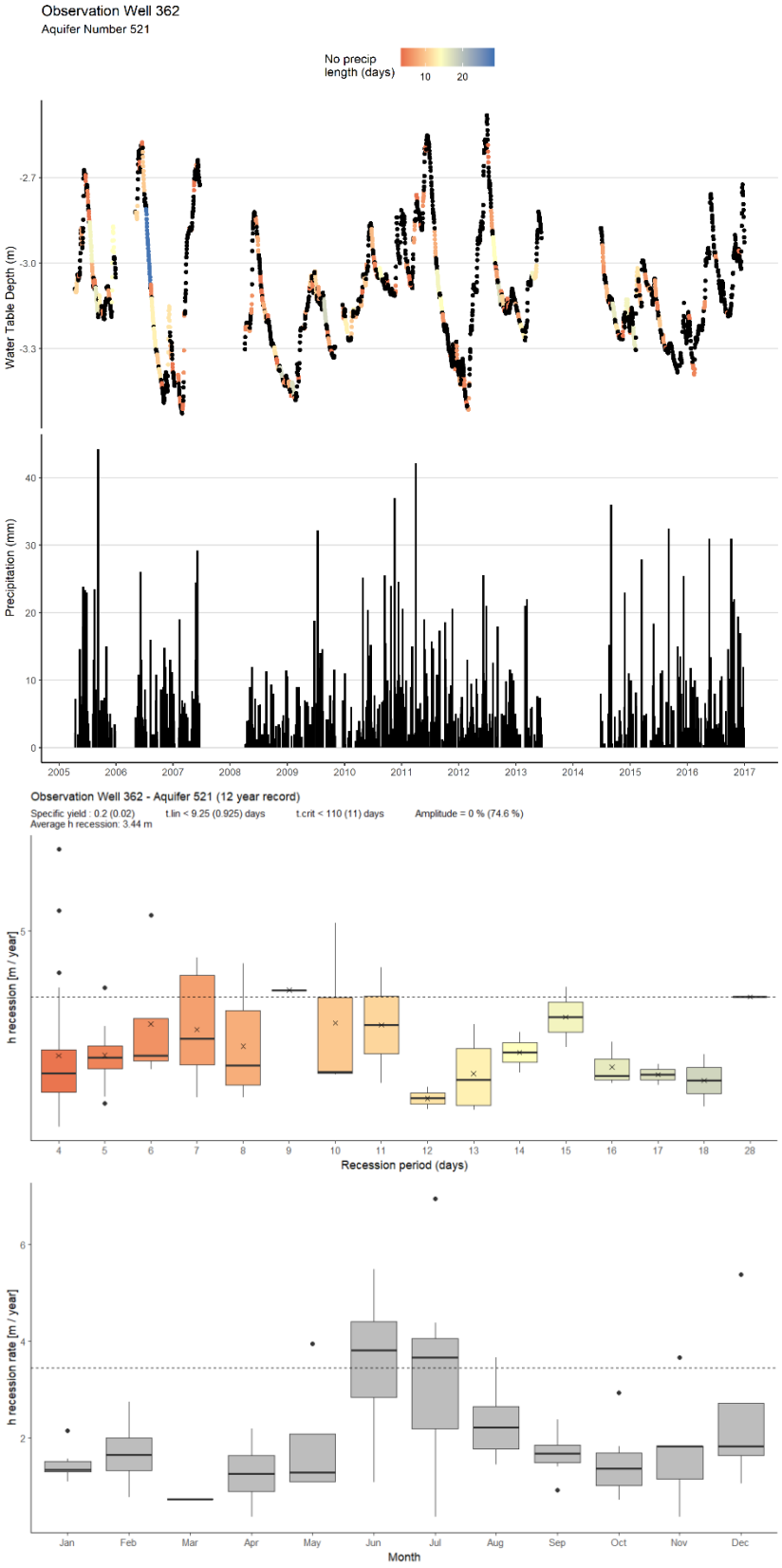
Observation Well 362
Aquifer Number 521
No precip length (days)
10
20
Water Table Depth (m)
-2.7
-3.0
-3.3
Precipitation (mm)
40
30
20
10
0
2005
2006
2007
2008
2009
2010
2011
2012
2013
2014
2015
2016
2017
Observation Well 362 - Aquifer 521 (12 year record)
Specific yield : 0.2 (0.02)
Average h recession: 3.44 m
t.lin < 9.25 (0.925) days
t.crit < 110 (11) days
Amplitude = 0 % (74.6 %)
h recession [m / year]
5
4
5
6
7
8
9
10
11
12
13
14
15
16
17
18
28
Recession period (days)
h recession rate [m / year]
6
4
2
Jan
Feb
Mar
Apr
May
Jun
Jul
Aug
Sep
Oct
Nov
Dec
Month

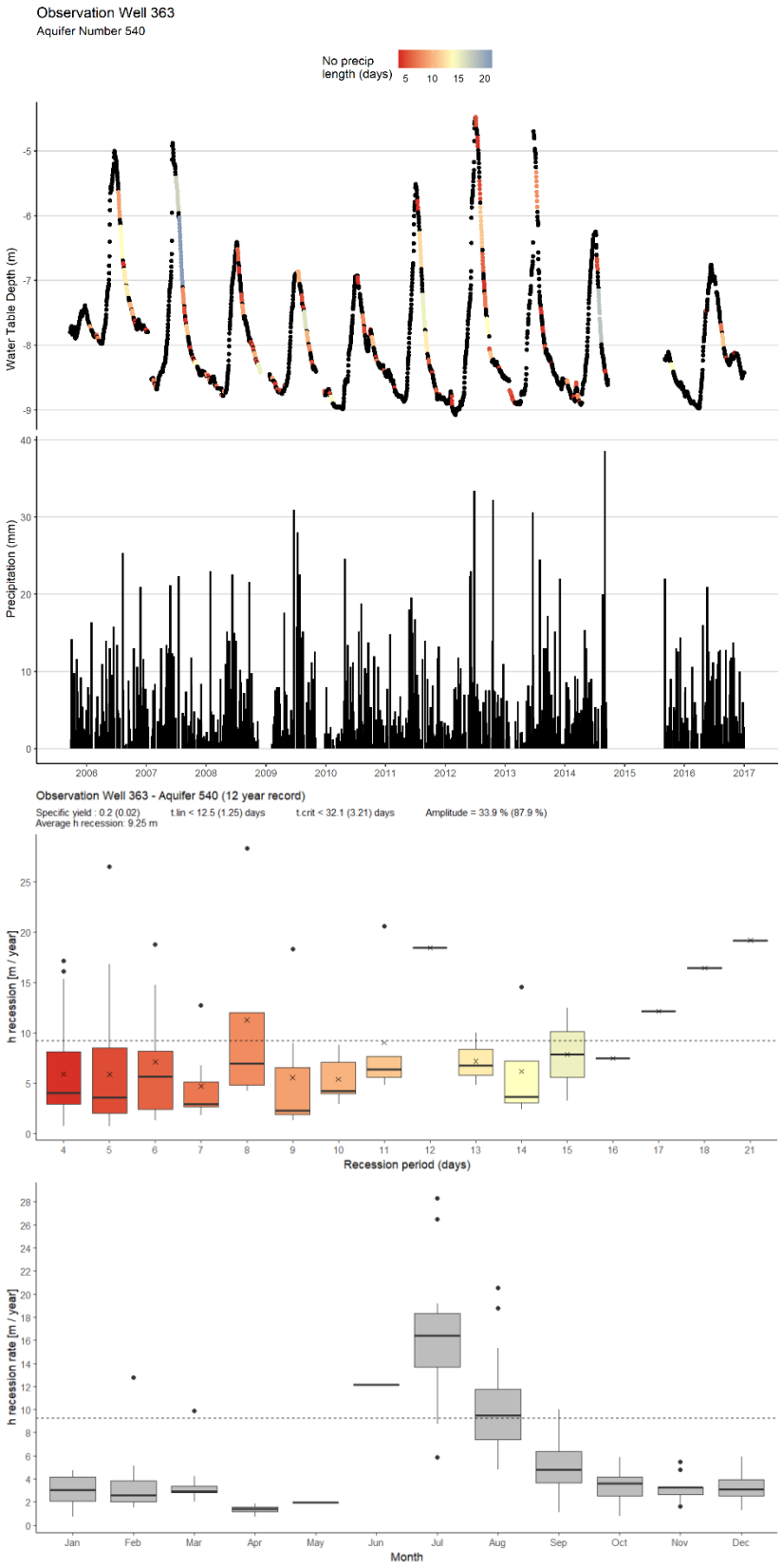
Observation Well 363
Aquifer Number 540
No precip length (days)
5
10
15
20
Water Table Depth (m)
-5
-6
-7
-8
-9
Precipitation (mm)
40
30
20
10
0
2006
2007
2008
2009
2010
2011
2012
2013
2014
2015
2016
2017
Observation Well 363 - Aquifer 540 (12 year record)
Specific yield : 0.2 (0.02)
t.lin < 12.5 (1.25) days
t.crit < 32.1 (3.21) days
Amplitude = 33.9 % (87.9 %)
Average h recession: 9.25 m
h recession [m / year]
25
20
15
10
5
0
4
5
6
7
8
9
10
11
12
13
14
15
16
17
18
21
Recession period (days)
h recession rate [m / year]
28
26
24
22
20
18
16
14
12
10
8
6
4
2
0
Jan
Feb
Mar
Apr
May
Jun
Jul
Aug
Sep
Oct
Nov
Dec
Month

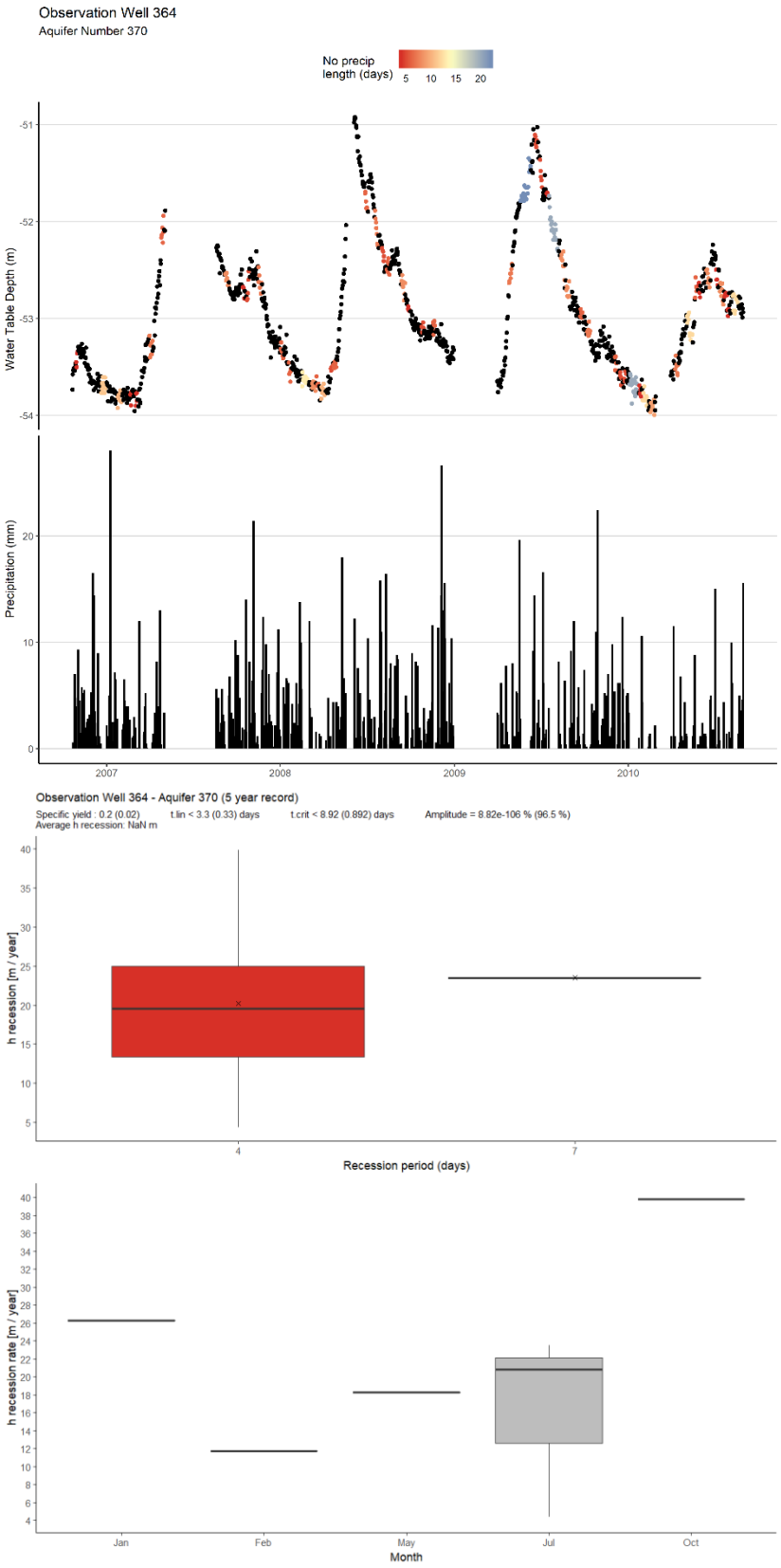
Observation Well 364
Aquifer Number 370
No precip length (days)
5
10
15
20
Water Table Depth (m)
-51
-52
-53
-54
Precipitation (mm)
0
10
20
2007
2008
2009
2010
Observation Well 364 - Aquifer 370 (5 year record)
Specific yield : 0.2 (0.02)
t.lin < 3.3 (0.33) days
t.crit < 8.92 (0.892) days
Amplitude = 8.82e-106 % (96.5 %)
Average h recession: NaN m
h recession [m / year]
Recession period (days)
4
7
h recession rate [m / year]
Jan
Feb
May
Jul
Oct
Month

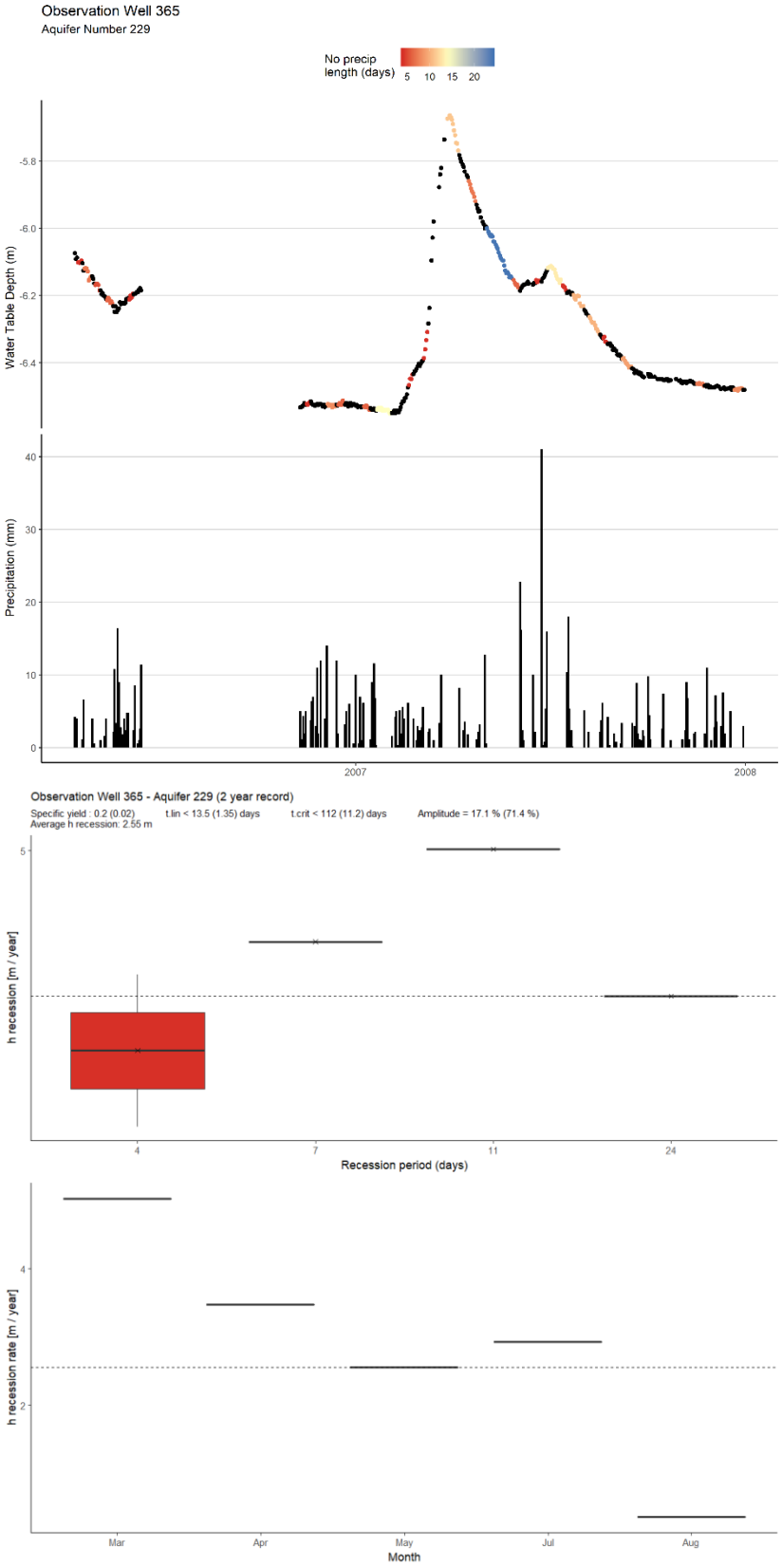
Observation Well 365
Aquifer Number 229
No precip length (days)
5
10
15
20
Water Table Depth (m)
-5.8
-6.0
-6.2
-6.4
Precipitation (mm)
40
30
20
10
0
2007
2008
Observation Well 365 - Aquifer 229 (2 year record)
Specific yield : 0.2 (0.02)
t.lin < 13.5 (1.35) days
t.crit < 112 (11.2) days
Amplitude = 17.1 % (71.4 %)
Average h recession: 2.55 m
h recession [m / year]
5
4
7
11
24
Recession period (days)
h recession rate [m / year]
4
2
Mar
Apr
May
Jul
Aug
Month

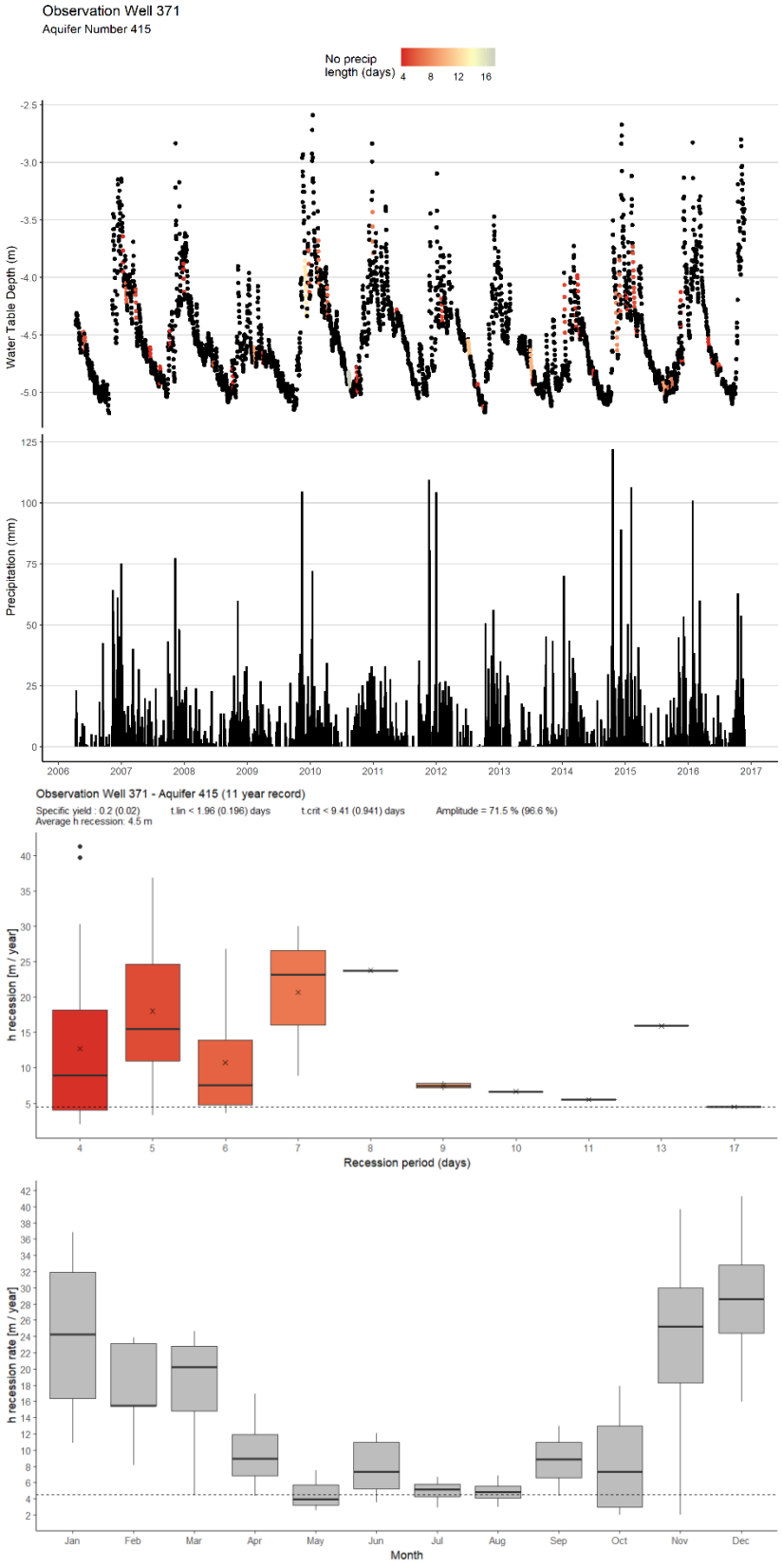
Observation Well 371
Aquifer Number 415
No precip length (days)
4
8
12
16
Water Table Depth (m)
-2.5
-3.0
-3.5
-4.0
-4.5
-5.0
Precipitation (mm)
125
100
75
50
25
0
2006
2007
2008
2009
2010
2011
2012
2013
2014
2015
2016
2017
Observation Well 371 - Aquifer 415 (11 year record)
Specific yield : 0.2 (0.02)
t.lin < 1.96 (0.196) days
t.crit < 9.41 (0.941) days
Amplitude = 71.5 % (96.6 %)
Average h recession: 4.5 m
h recession [m / year]
40
35
30
25
20
15
10
5
4
5
6
7
8
9
10
11
13
17
Recession period (days)
h recession rate [m / year]
42
40
38
36
34
32
30
28
26
24
22
20
18
16
14
12
10
8
6
4
2
Jan
Feb
Mar
Apr
May
Jun
Jul
Aug
Sep
Oct
Nov
Dec
Month

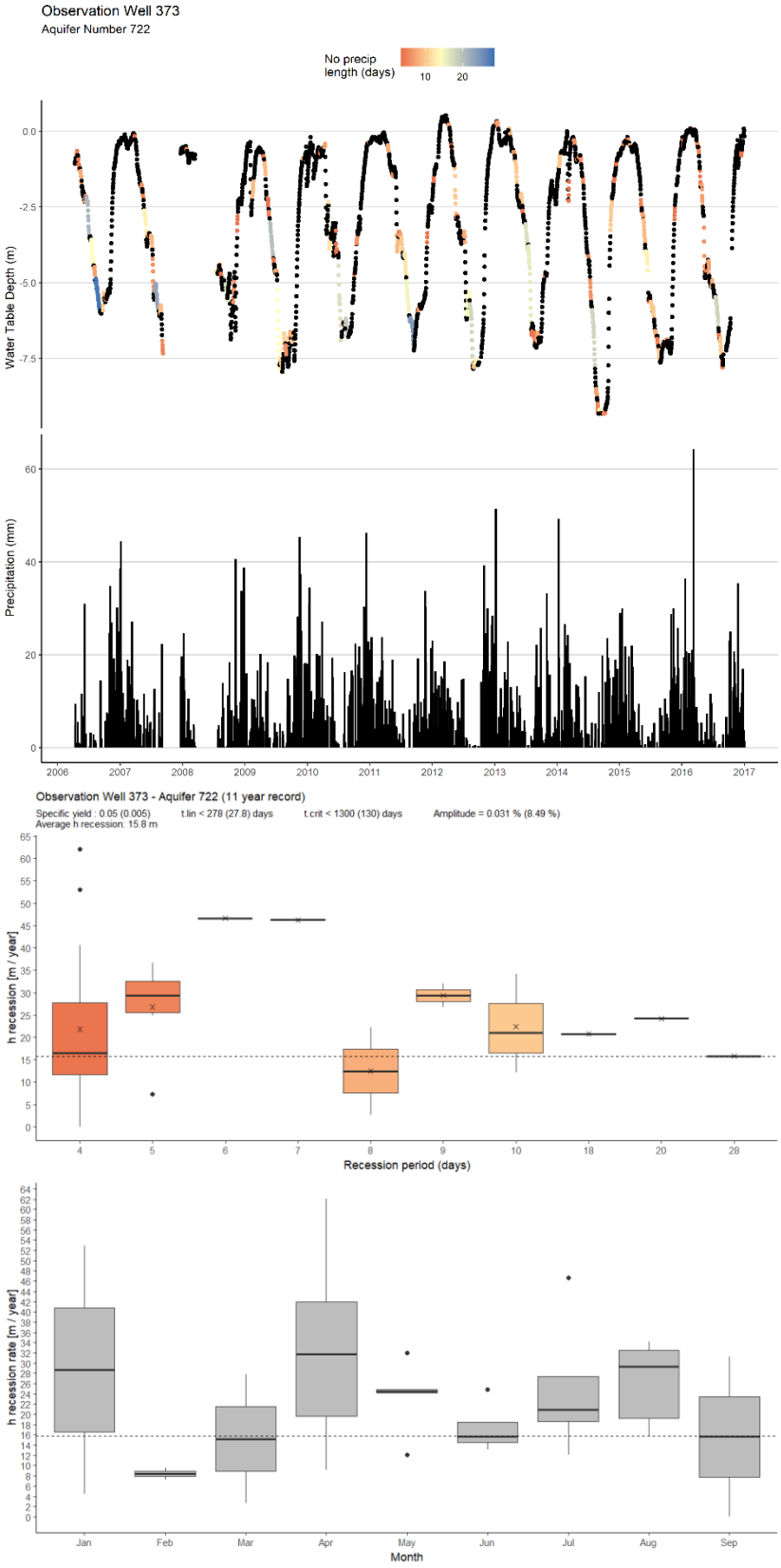
Observation Well 373
Aquifer Number 722
No precip length (days)
10
20
Water Table Depth (m)
0.0
-2.5
-5.0
-7.5
Precipitation (mm)
60
40
20
0
2006
2007
2008
2009
2010
2011
2012
2013
2014
2015
2016
2017
Observation Well 373 - Aquifer 722 (11 year record)
Specific yield : 0.05 (0.005)
t.lin < 278 (27.8) days
t.crit < 1300 (130) days
Amplitude = 0.031 % (8.49 %)
Average h recession: 15.8 m
h recession [m / year]
Recession period (days)
4
5
6
7
8
9
10
18
20
28
h recession rate [m / year]
Jan
Feb
Mar
Apr
May
Jun
Jul
Aug
Sep
Month

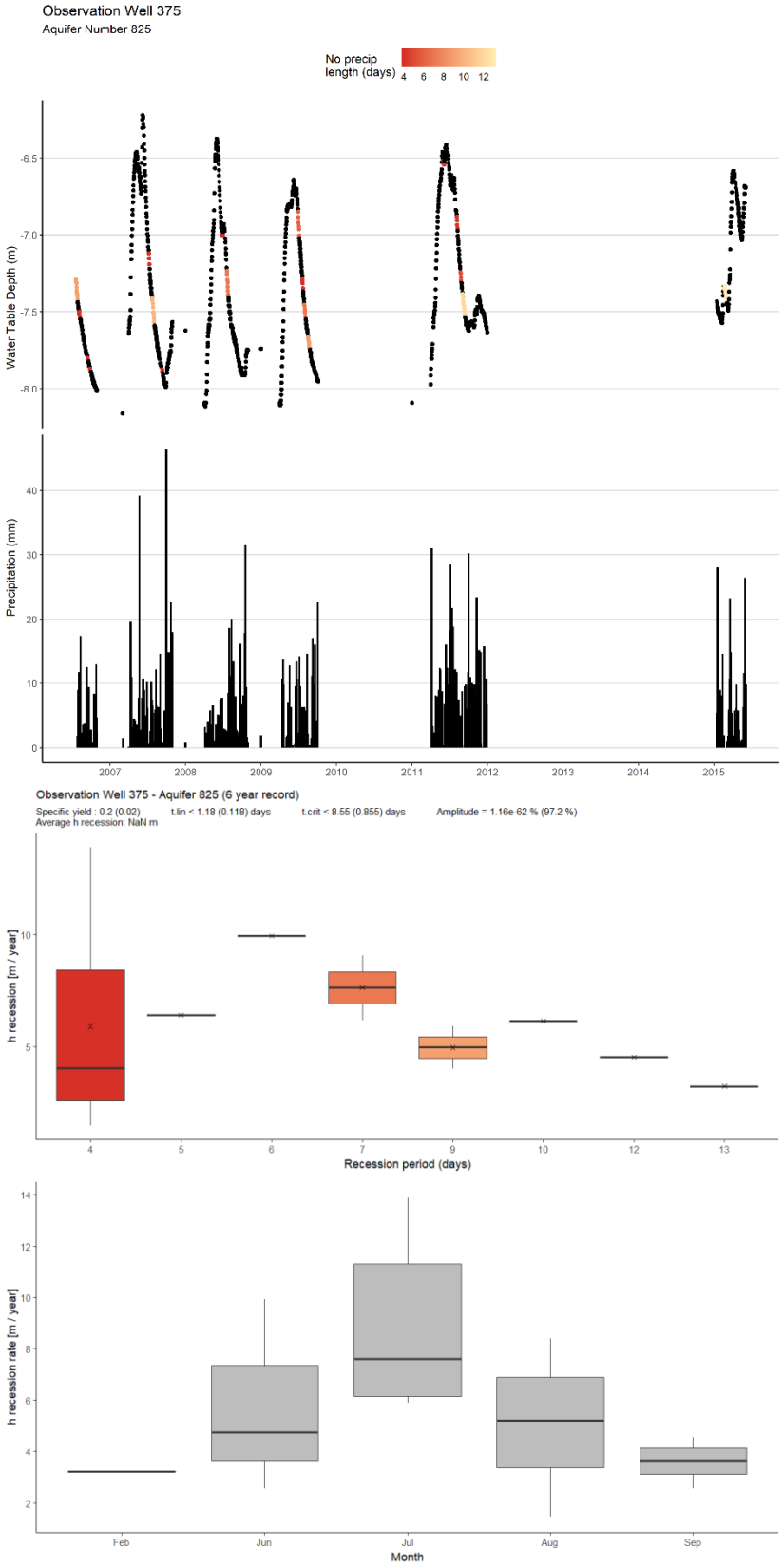
Observation Well 375
Aquifer Number 825
No precip length (days)
4 6 8 10 12
Water Table Depth (m)
-6.5
-7.0
-7.5
-8.0
Precipitation (mm)
40
30
20
10
0
2007
2008
2009
2010
2011
2012
2013
2014
2015
Observation Well 375 - Aquifer 825 (6 year record)
Specific yield : 0.2 (0.02)
t.lin < 1.18 (0.118) days
t.crit < 8.55 (0.855) days
Amplitude = 1.16e-62 % (97.2 %)
Average h recession: NaN m
h recession [m / year]
10
5
4
5
6
7
9
10
12
13
Recession period (days)
h recession rate [m / year]
14
12
10
8
6
4
2
Feb
Jun
Jul
Aug
Sep
Month

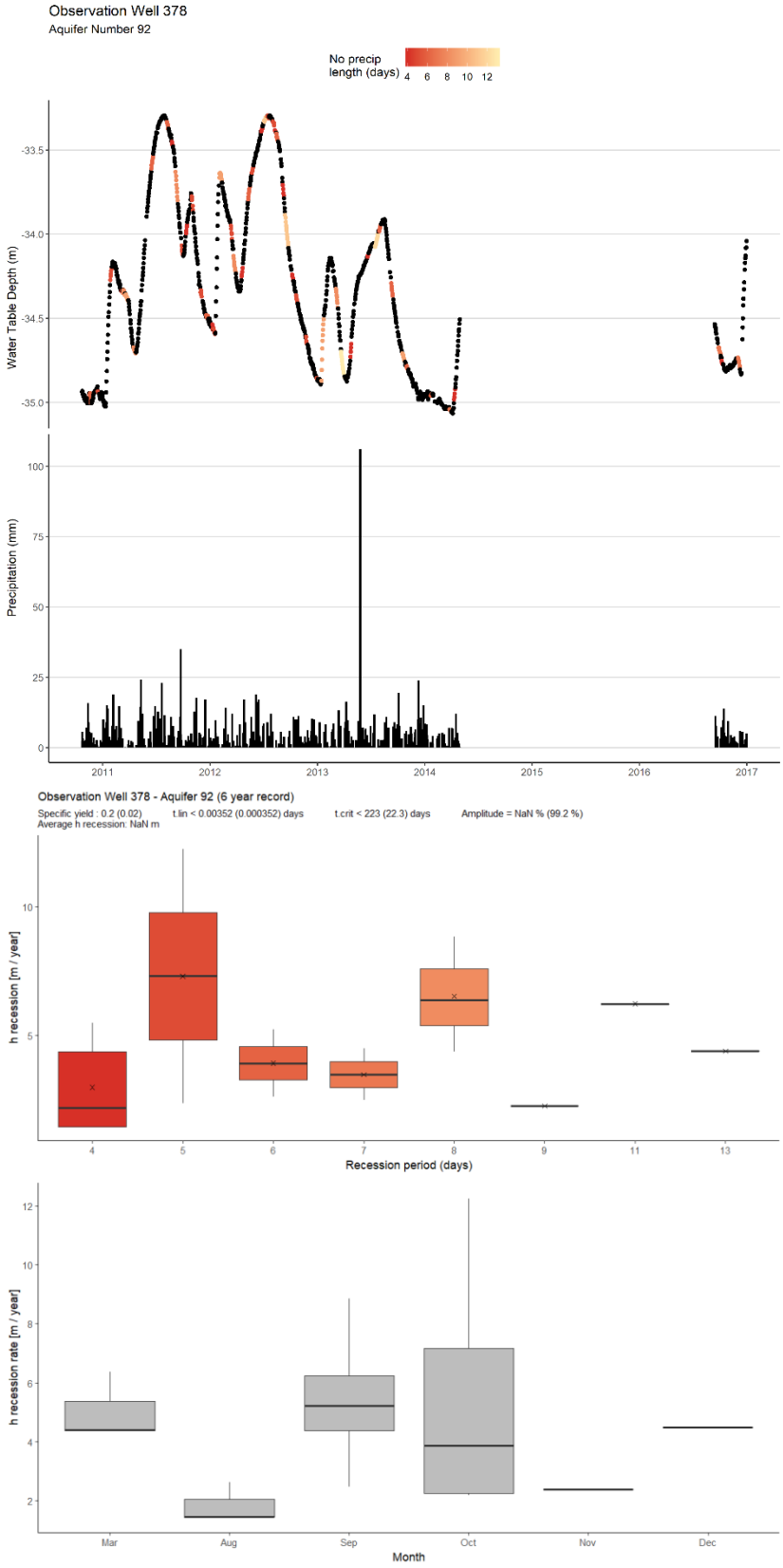
Observation Well 378
Aquifer Number 92
No precip length (days)
4 6 8 10 12
Water Table Depth (m)
-33.5
-34.0
-34.5
-35.0
Precipitation (mm)
100
75
50
25
0
2011
2012
2013
2014
2015
2016
2017
Observation Well 378 - Aquifer 92 (6 year record)
Specific yield : 0.2 (0.02)
t.lin < 0.00352 (0.000352) days
t.crit < 223 (22.3) days
Amplitude = NaN % (99.2 %)
Average h recession: NaN m
h recession [m / year]
10
5
4
5
6
7
8
9
11
13
Recession period (days)
h recession rate [m / year]
12
10
8
6
4
2
Mar
Aug
Sep
Oct
Nov
Dec
Month

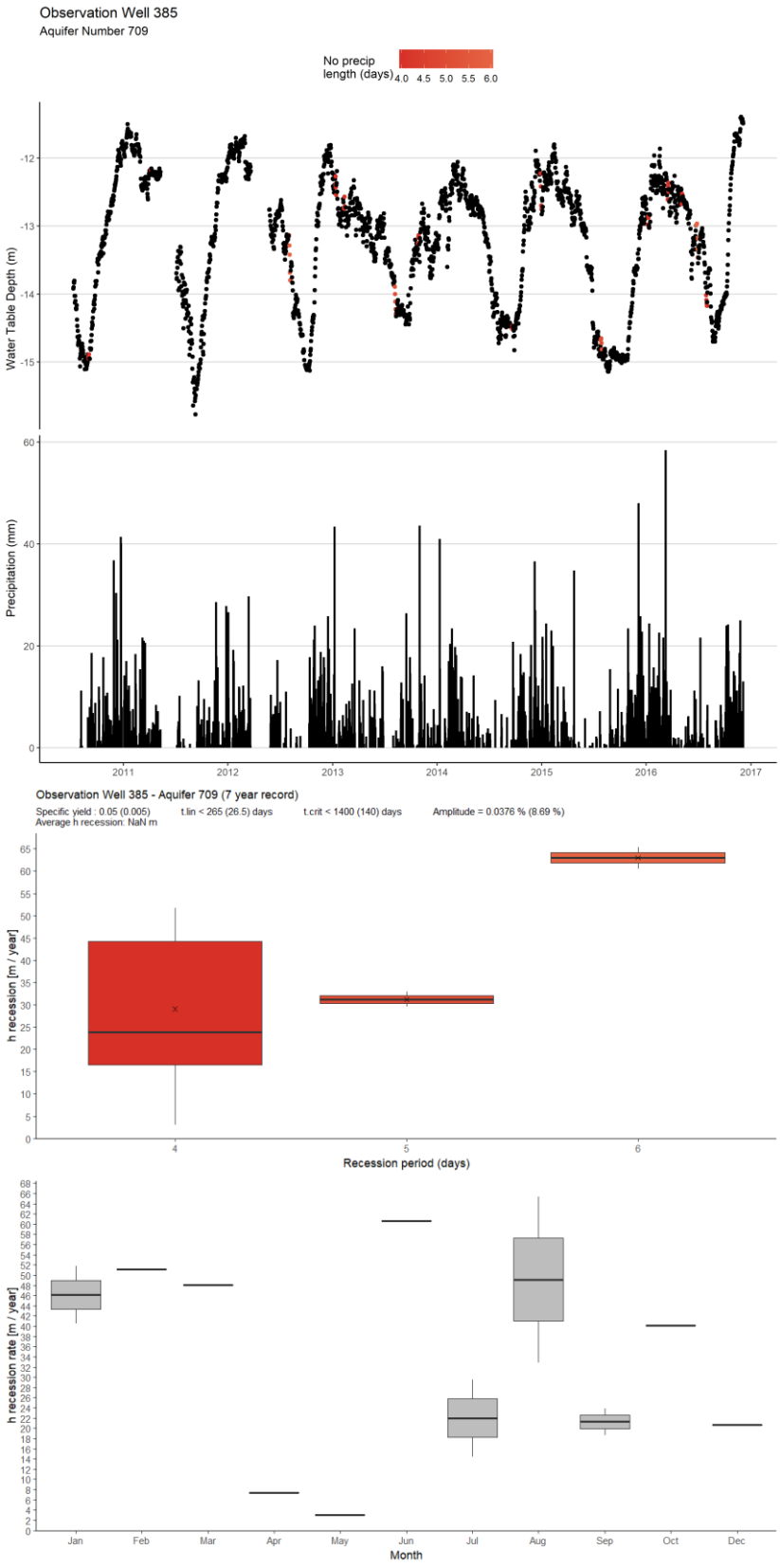
Observation Well 385
Aquifer Number 709
No precip length (days)
4.0 4.5 5.0 5.5 6.0
Water Table Depth (m)
-12
-13
-14
-15
Precipitation (mm)
60
40
20
0
2011
2012
2013
2014
2015
2016
2017
Observation Well 385 - Aquifer 709 (7 year record)
Specific yield : 0.05 (0.005)
t.lin < 265 (26.5) days
t.crit < 1400 (140) days
Amplitude = 0.0376 % (8.69 %)
Average h recession: NaN m
h recession [m / year]
Recession period (days)
h recession rate [m / year]
Jan
Feb
Mar
Apr
May
Jun
Jul
Aug
Sep
Oct
Dec
Month

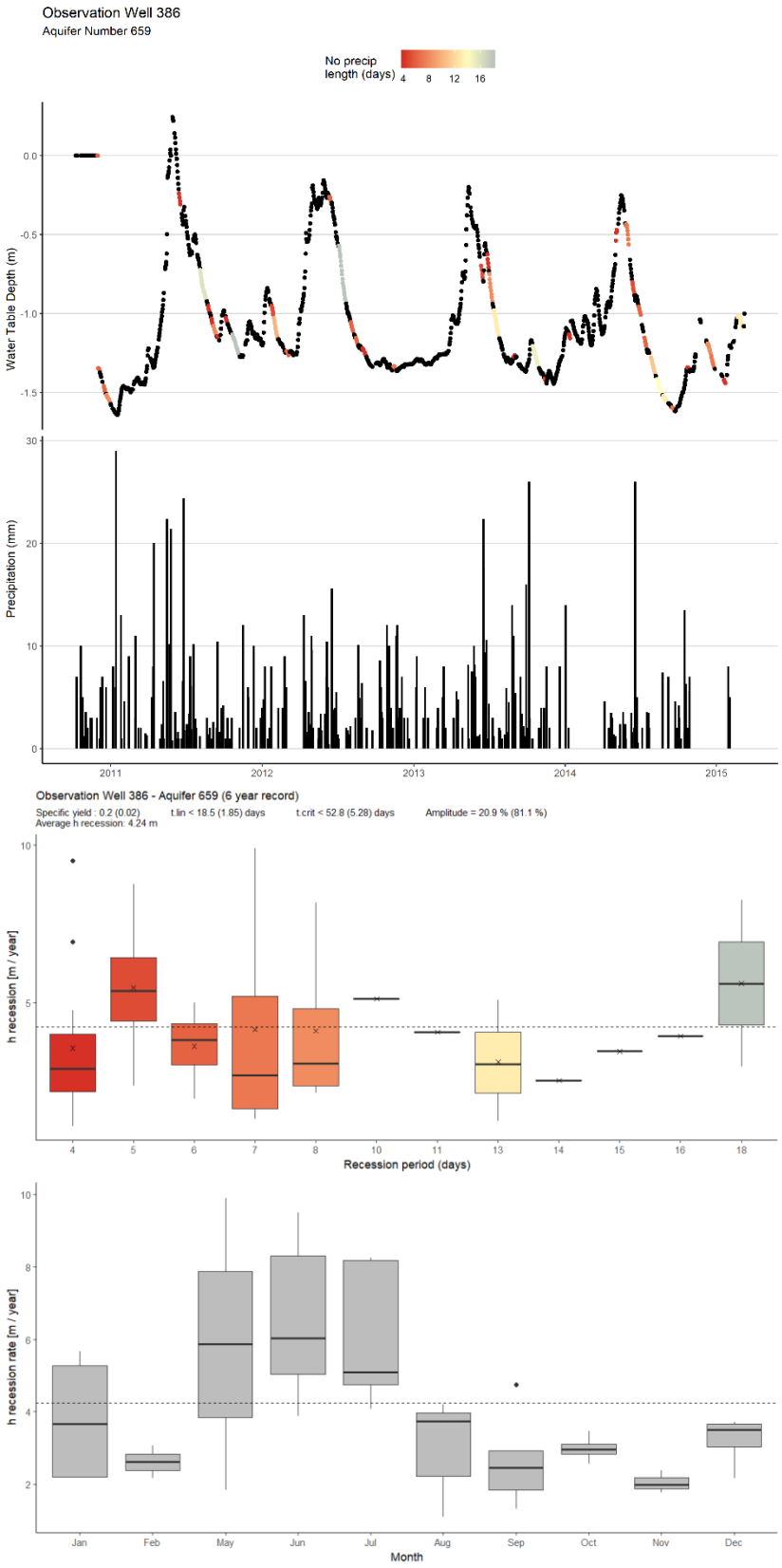
Observation Well 386
Aquifer Number 659
No precip length (days)
4
8
12
16
Water Table Depth (m)
0.0
-0.5
-1.0
-1.5
Precipitation (mm)
30
20
10
0
2011
2012
2013
2014
2015
Observation Well 386 - Aquifer 659 (6 year record)
Specific yield : 0.2 (0.02)
t.lin < 18.5 (1.85) days
t.crit < 52.8 (5.28) days
Amplitude = 20.9 % (81.1 %)
Average h recession: 4.24 m
h recession [m / year]
Recession period (days)
h recession rate [m / year]
Jan
Feb
May
Jun
Jul
Aug
Sep
Oct
Nov
Dec
Month

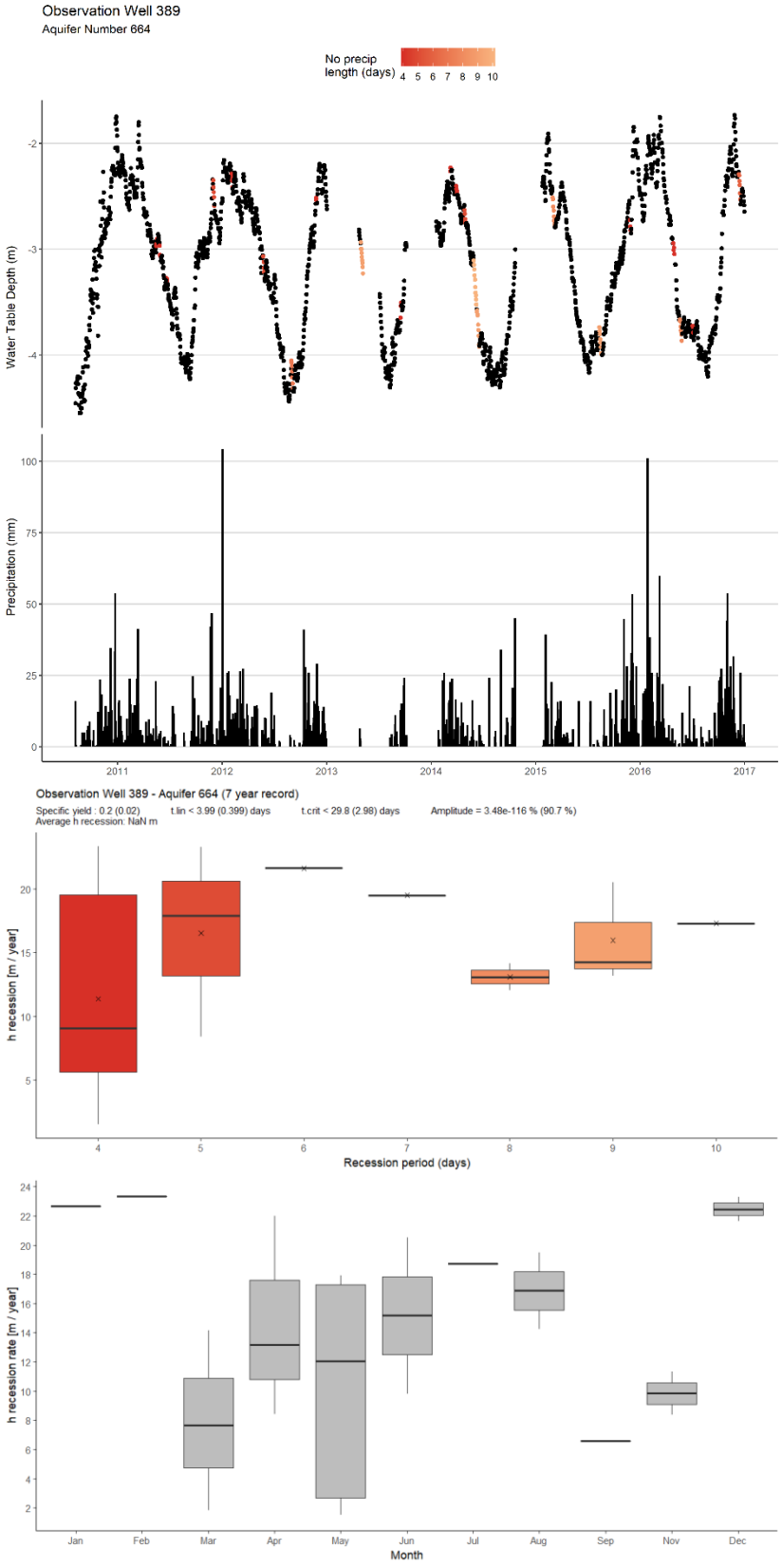
Observation Well 389
Aquifer Number 664
No precip length (days)
4 5 6 7 8 9 10
Water Table Depth (m)
-2
-3
-4
Precipitation (mm)
100
75
50
25
0
2011
2012
2013
2014
2015
2016
2017
Observation Well 389 - Aquifer 664 (7 year record)
Specific yield : 0.2 (0.02)
t.lin < 3.99 (0.399) days
t.crit < 29.8 (2.98) days
Amplitude = 3.48e-116 % (90.7 %)
Average h recession: NaN m
h recession [m / year]
20
15
10
5
4
5
6
7
8
9
10
Recession period (days)
h recession rate [m / year]
24
22
20
18
16
14
12
10
8
6
4
2
Jan
Feb
Mar
Apr
May
Jun
Jul
Aug
Sep
Nov
Dec
Month

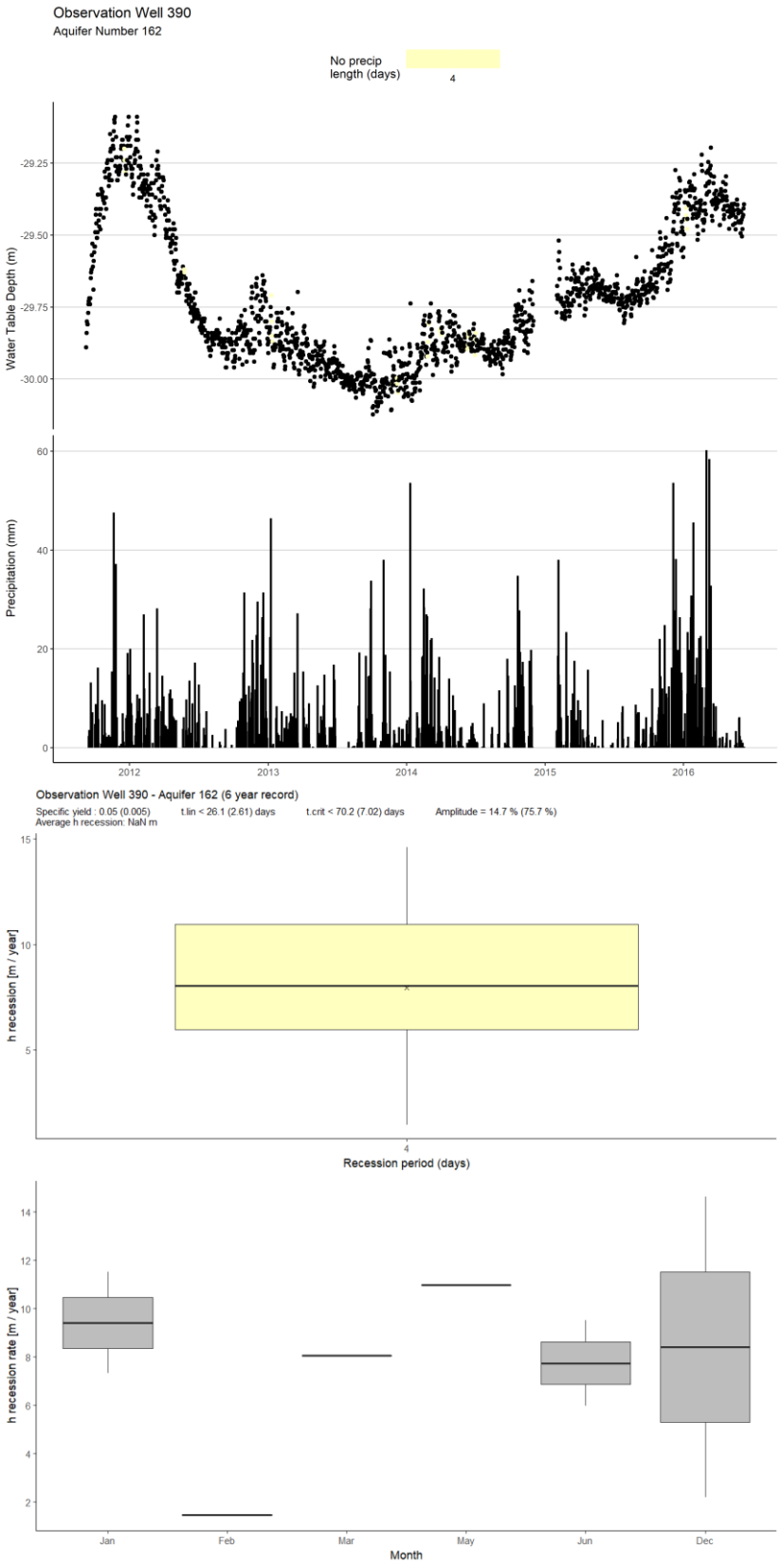
Observation Well 390
Aquifer Number 162
No precip length (days)
4
Water Table Depth (m)
-29.25
-29.50
-29.75
-30.00
Precipitation (mm)
60
40
20
0
2012
2013
2014
2015
2016
Observation Well 390 - Aquifer 162 (6 year record)
Specific yield : 0.05 (0.005)
t.lin < 26.1 (2.61) days
t.crit < 70.2 (7.02) days
Amplitude = 14.7 % (75.7 %)
Average h recession: NaN m
h recession [m / year]
15
10
5
4
Recession period (days)
h recession rate [m / year]
14
12
10
8
6
4
2
Jan
Feb
Mar
May
Jun
Dec
Month

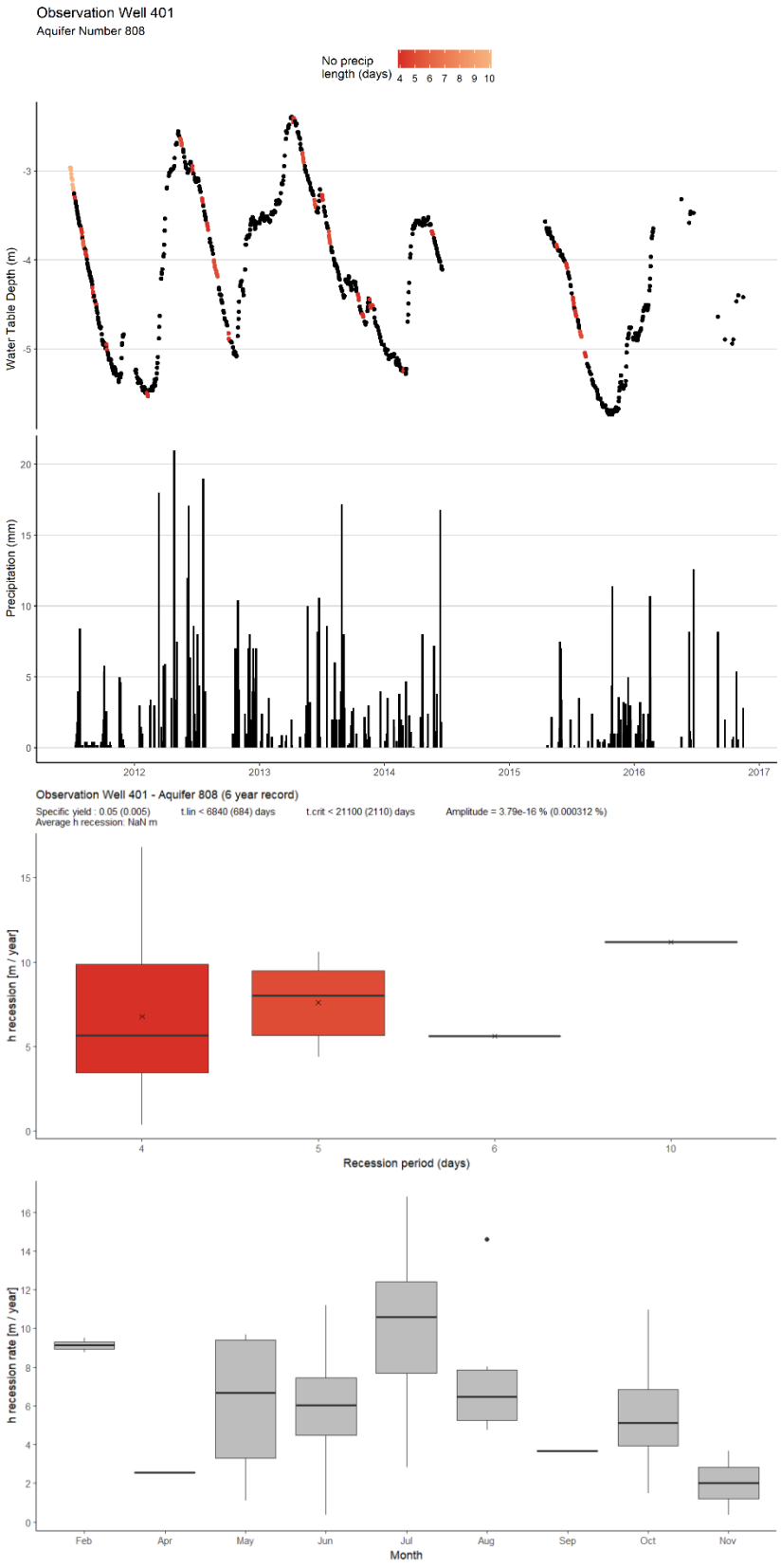
Observation Well 401
Aquifer Number 808
No precip length (days)
4 5 6 7 8 9 10
Water Table Depth (m)
-3
-4
-5
Precipitation (mm)
20
15
10
5
0
2012
2013
2014
2015
2016
2017
Observation Well 401 - Aquifer 808 (6 year record)
Specific yield : 0.05 (0.005)
t.lin < 6840 (684) days
t.crit < 21100 (2110) days
Amplitude = 3.79e-16 % (0.000312 %)
Average h recession: NaN m
h recession [m / year]
15
10
5
0
4
5
6
10
Recession period (days)
h recession rate [m / year]
16
14
12
10
8
6
4
2
0
Feb
Apr
May
Jun
Jul
Aug
Sep
Oct
Nov
Month

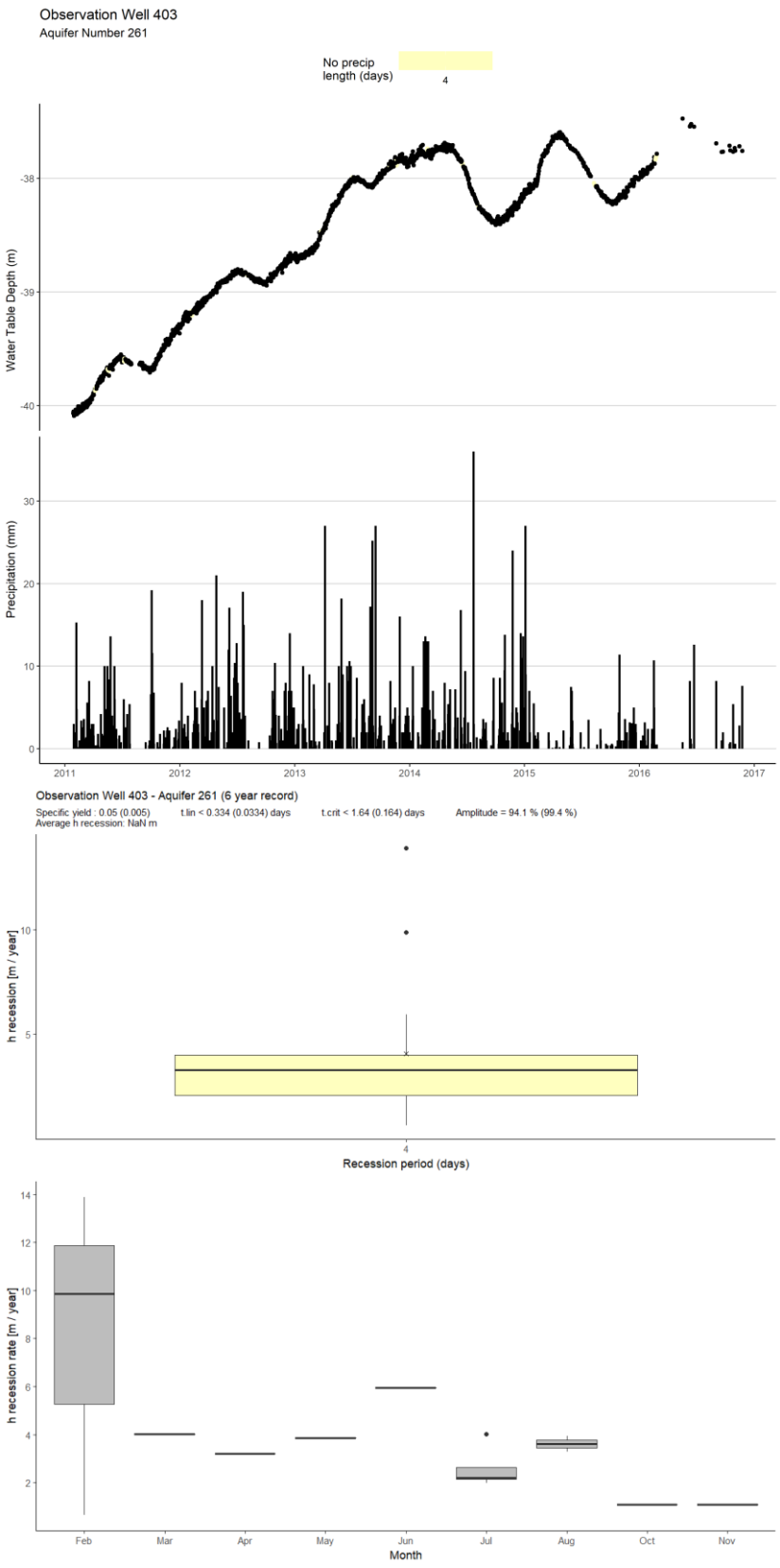
Observation Well 403
Aquifer Number 261
No precip length (days)
4
Water Table Depth (m)
-38
-39
-40
Precipitation (mm)
30
20
10
0
2011
2012
2013
2014
2015
2016
2017
Observation Well 403 - Aquifer 261 (6 year record)
Specific yield : 0.05 (0.005)
t.lin < 0.334 (0.0334) days
t.crit < 1.64 (0.164) days
Amplitude = 94.1 % (99.4 %)
Average h recession: NaN m
h recession [m / year]
10
5
4
Recession period (days)
h recession rate [m / year]
14
12
10
8
6
4
2
Feb
Mar
Apr
May
Jun
Jul
Aug
Oct
Nov
Month

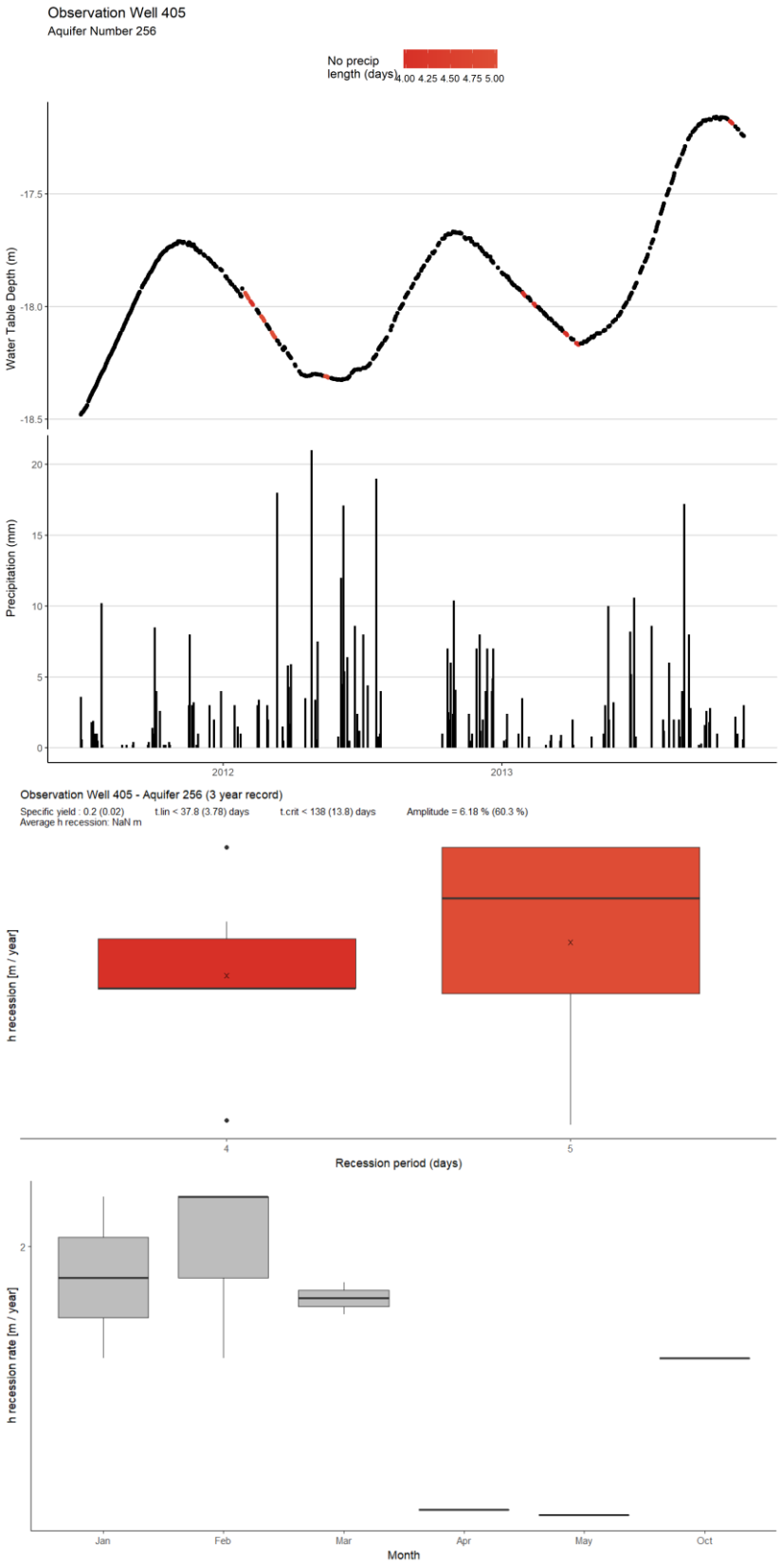
Observation Well 405
Aquifer Number 256
No precip length (days)
4.00 4.25 4.50 4.75 5.00
Water Table Depth (m)
-17.5
-18.0
-18.5
Precipitation (mm)
20
15
10
5
0
2012
2013
Observation Well 405 - Aquifer 256 (3 year record)
Specific yield : 0.2 (0.02)
t.lin < 37.8 (3.78) days
t.crit < 138 (13.8) days
Amplitude = 6.18 % (60.3 %)
Average h recession: NaN m
h recession [m / year]
4
5
Recession period (days)
h recession rate [m / year]
2
Jan
Feb
Mar
Apr
May
Oct
Month

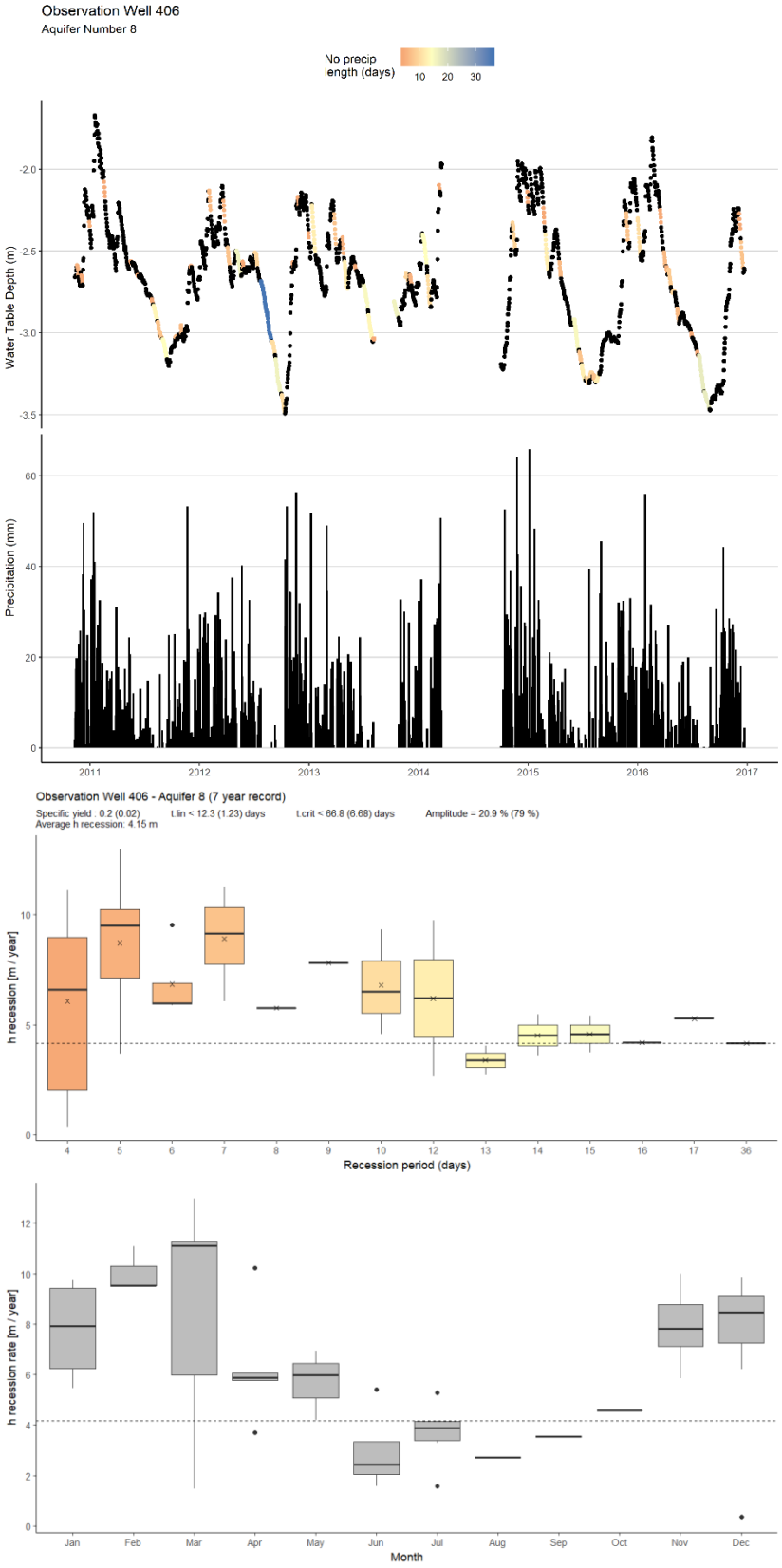
Observation Well 406
Aquifer Number 8
No precip length (days)
10
20
30
Water Table Depth (m)
-2.0
-2.5
-3.0
-3.5
Precipitation (mm)
60
40
20
0
2011
2012
2013
2014
2015
2016
2017
Observation Well 406 - Aquifer 8 (7 year record)
Specific yield : 0.2 (0.02)
t.lin < 12.3 (1.23) days
t.crit < 66.8 (6.68) days
Amplitude = 20.9 % (79 %)
Average h recession: 4.15 m
h recession [m / year]
Recession period (days)
4
5
6
7
8
9
10
12
13
14
15
16
17
36
h recession rate [m / year]
Jan
Feb
Mar
Apr
May
Jun
Jul
Aug
Sep
Oct
Nov
Dec
Month

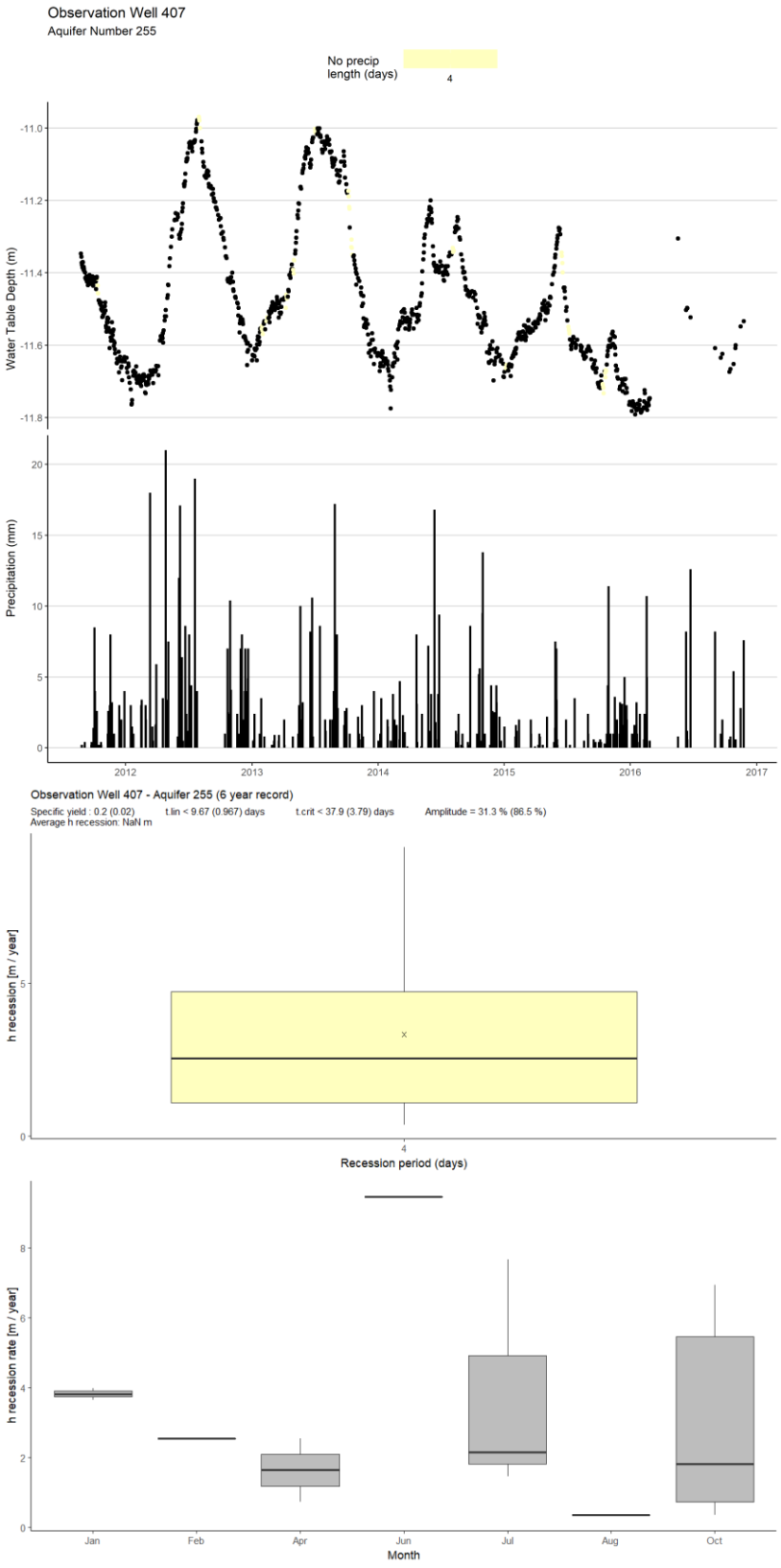
Observation Well 407
Aquifer Number 255
No precip length (days)
4
Water Table Depth (m)
-11.0
-11.2
-11.4
-11.6
-11.8
Precipitation (mm)
20
15
10
5
0
2012
2013
2014
2015
2016
2017
Observation Well 407 - Aquifer 255 (6 year record)
Specific yield : 0.2 (0.02)
t.lin < 9.67 (0.967) days
t.crit < 37.9 (3.79) days
Amplitude = 31.3 % (86.5 %)
Average h recession: NaN m
h recession [m / year]
5
0
4
Recession period (days)
h recession rate [m / year]
8
6
4
2
0
Jan
Feb
Apr
Jun
Jul
Aug
Oct
Month

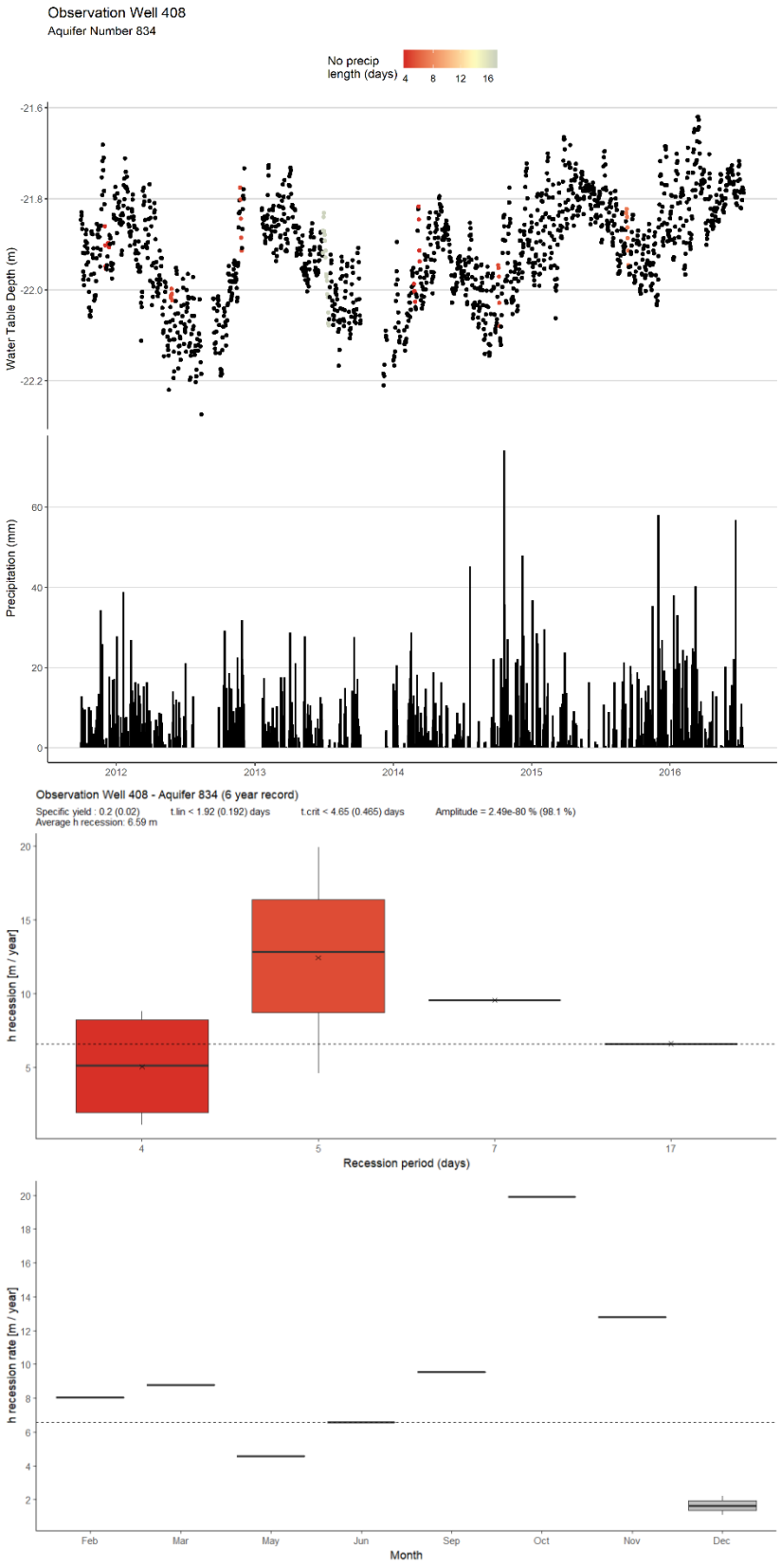
Observation Well 408
Aquifer Number 834
No precip length (days)
4
8
12
16
Water Table Depth (m)
-21.6
-21.8
-22.0
-22.2
Precipitation (mm)
60
40
20
0
2012
2013
2014
2015
2016
Observation Well 408 - Aquifer 834 (6 year record)
Specific yield : 0.2 (0.02)
t.lin < 1.92 (0.192) days
t.crit < 4.65 (0.465) days
Amplitude = 2.49e-80 % (98.1 %)
Average h recession: 6.59 m
h recession [m / year]
20
15
10
5
4
5
7
17
Recession period (days)
h recession rate [m / year]
20
18
16
14
12
10
8
6
4
2
Feb
Mar
May
Jun
Sep
Oct
Nov
Dec
Month

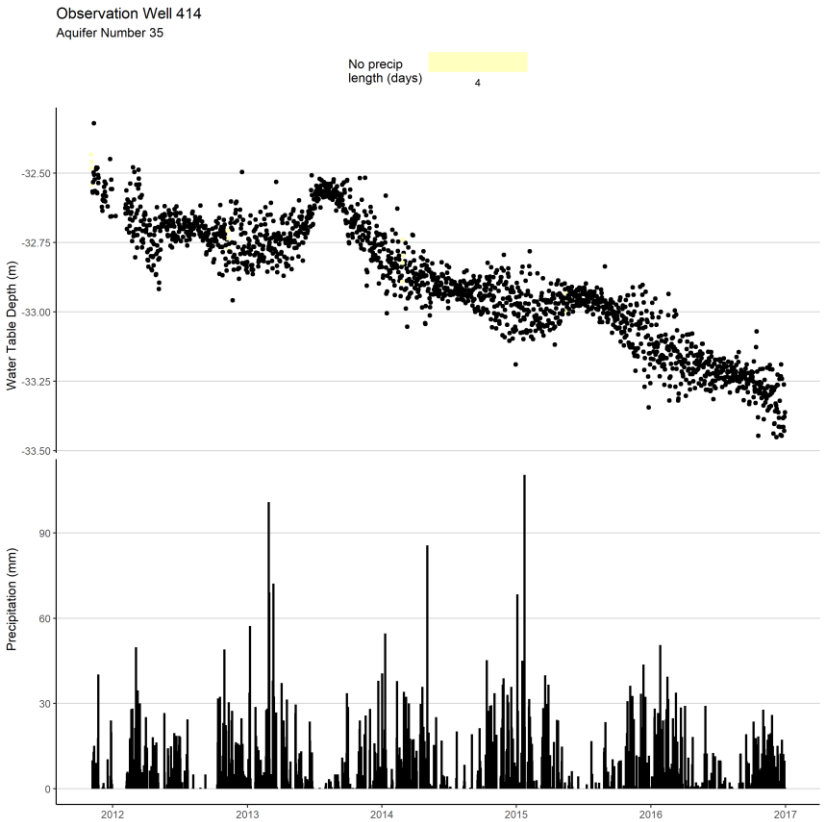
Observation Well 414
Aquifer Number 35
No precip length (days)
4
Water Table Depth (m)
-32.50
-32.75
-33.00
-33.25
-33.50
Precipitation (mm)
90
60
30
0
2012
2013
2014
2015
2016
2017

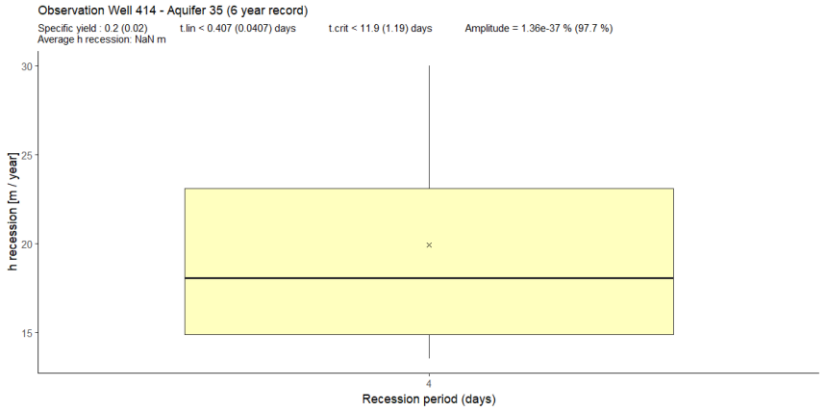
Observation Well 414 - Aquifer 35 (6 year record)
Specific yield : 0.2 (0.02)
t.lin < 0.407 (0.0407) days
t.crit < 11.9 (1.19) days
Amplitude = 1.36e-37 % (97.7 %)
Average h recession: NaN m
h recession [m / year]
30
25
20
15
4
Recession period (days)

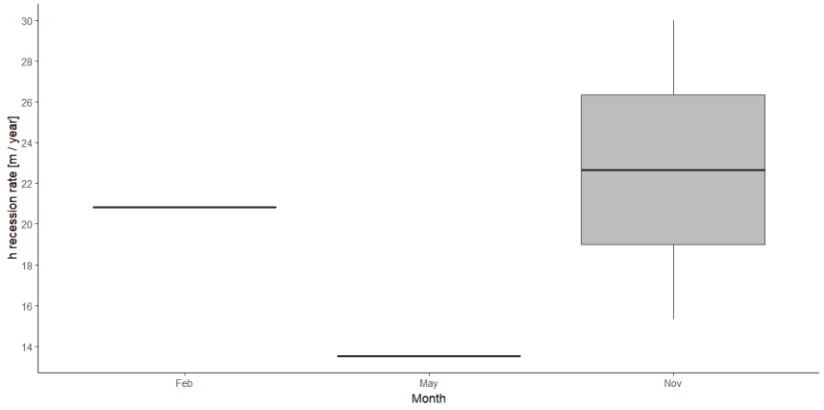
h recession rate [m / year]
30
28
26
24
22
20
18
16
14
Feb
May
Nov
Month

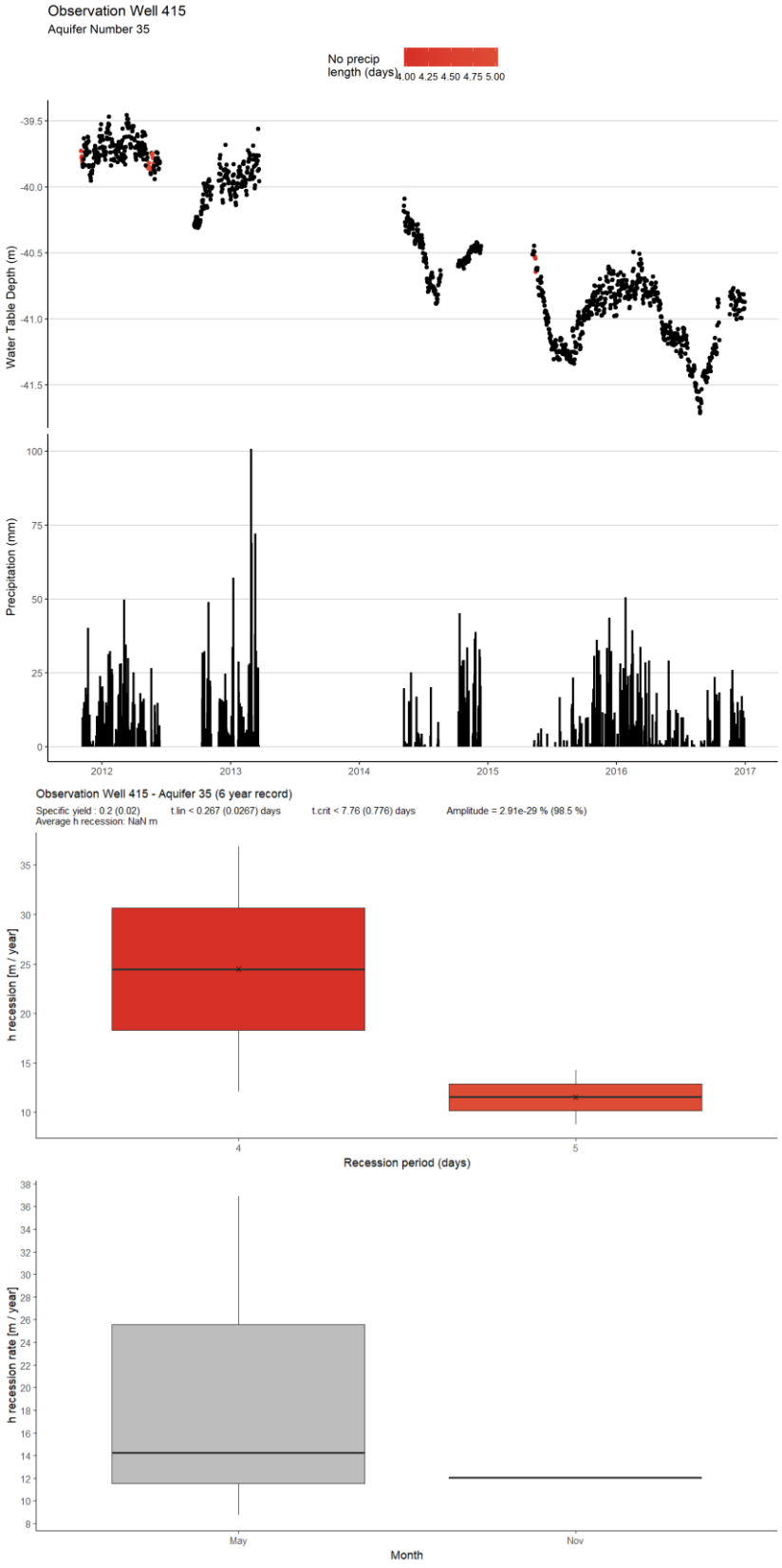
Observation Well 415
Aquifer Number 35
No precip length (days)
4.00 4.25 4.50 4.75 5.00
Water Table Depth (m)
-39.5
-40.0
-40.5
-41.0
-41.5
Precipitation (mm)
100
75
50
25
0
2012
2013
2014
2015
2016
2017
Observation Well 415 - Aquifer 35 (6 year record)
Specific yield : 0.2 (0.02)
t.lin < 0.267 (0.0267) days
t.crit < 7.76 (0.776) days
Amplitude = 2.91e-29 % (98.5 %)
Average h recession: NaN m
h recession [m / year]
35
30
25
20
15
10
4
5
Recession period (days)
h recession rate [m / year]
38
36
34
32
30
28
26
24
22
20
18
16
14
12
10
8
May
Nov
Month

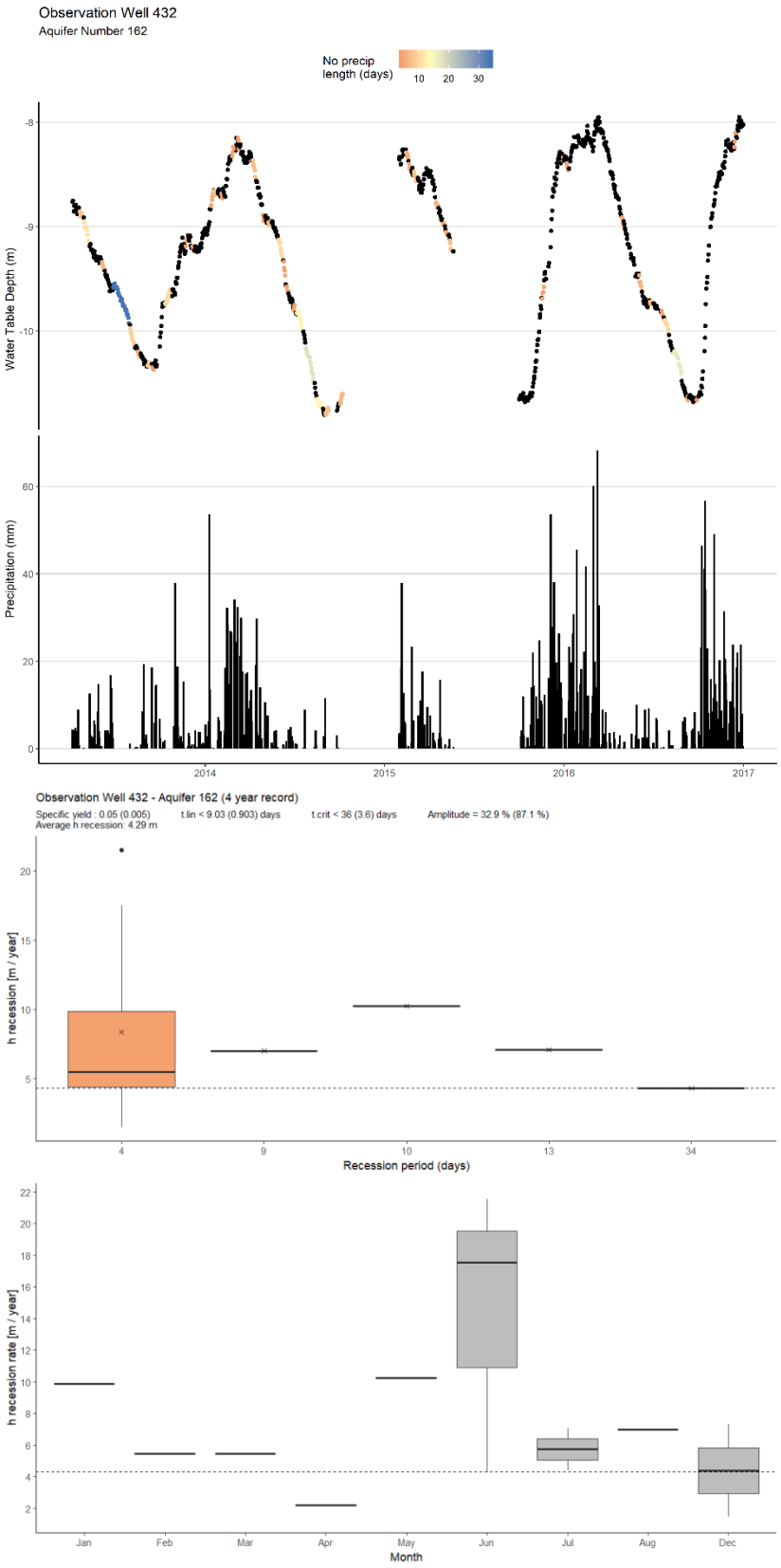
Observation Well 432
Aquifer Number 162
No precip length (days)
10
20
30
Water Table Depth (m)
-8
-9
-10
Precipitation (mm)
60
40
20
0
2014
2015
2016
2017
Observation Well 432 - Aquifer 162 (4 year record)
Specific yield : 0.05 (0.005)
t.lin < 9.03 (0.903) days
t.crit < 36 (3.6) days
Amplitude = 32.9 % (87.1 %)
Average h recession: 4.29 m
h recession [m / year]
20
15
10
5
4
9
10
13
34
Recession period (days)
h recession rate [m / year]
22
20
18
16
14
12
10
8
6
4
2
Jan
Feb
Mar
Apr
May
Jun
Jul
Aug
Dec
Month

APPENDIX C:
Chapter 4

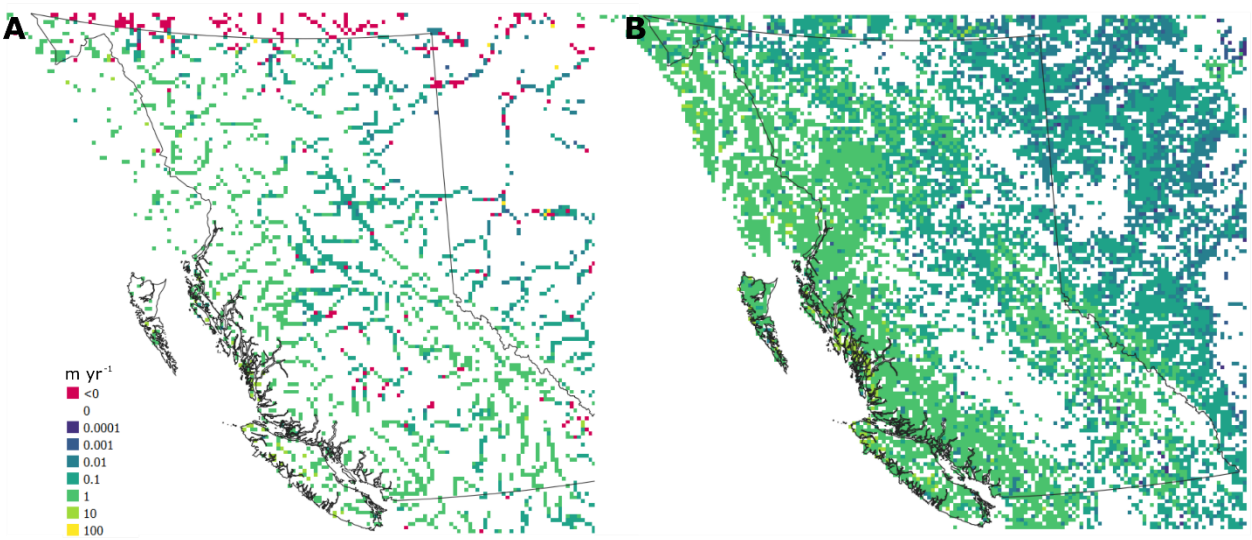

Figure S4.1 PCR-GLOBWB output for RIV (A) and DRN (B) in m yr^{-1}.

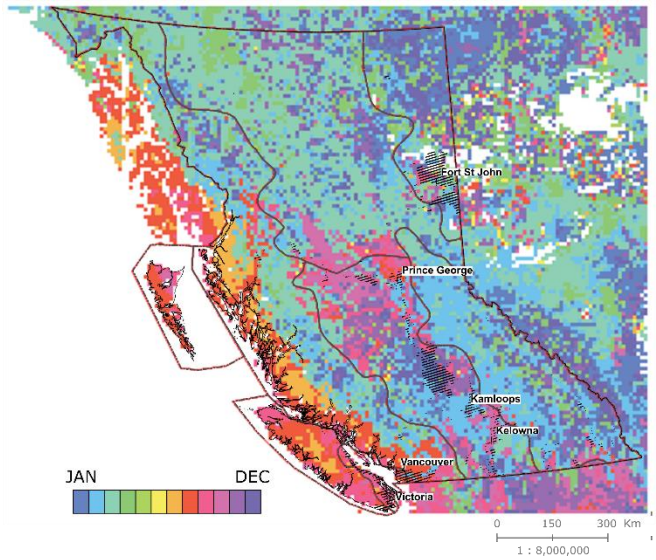

Figure S4.2 Index of representative month of MMF for extrapolation to annual flux.

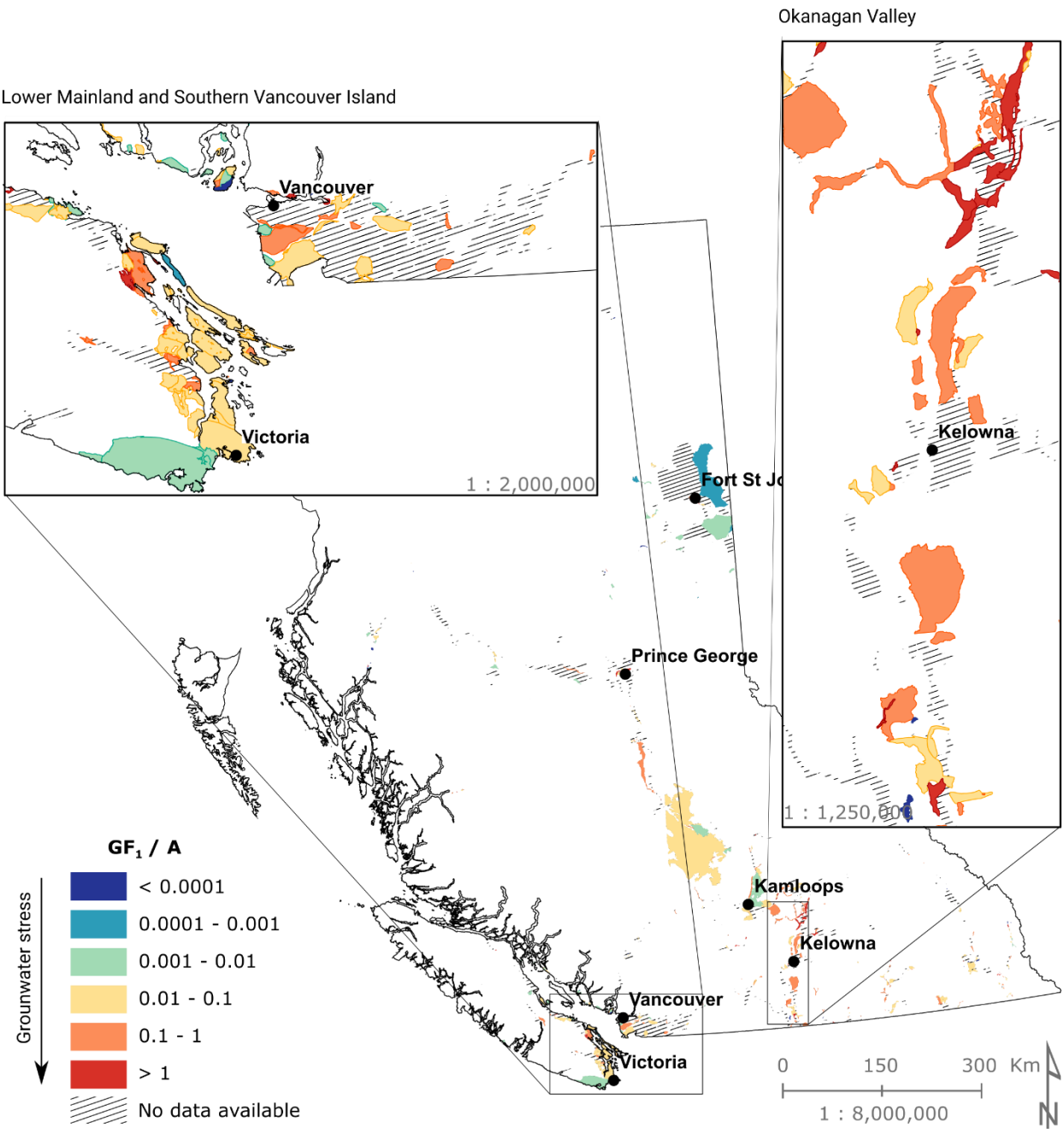

Figure S4.3 Resultant GF_1/A per aquifer in BC. GF/A was calculated using availability data from HELP and E_{PS}.

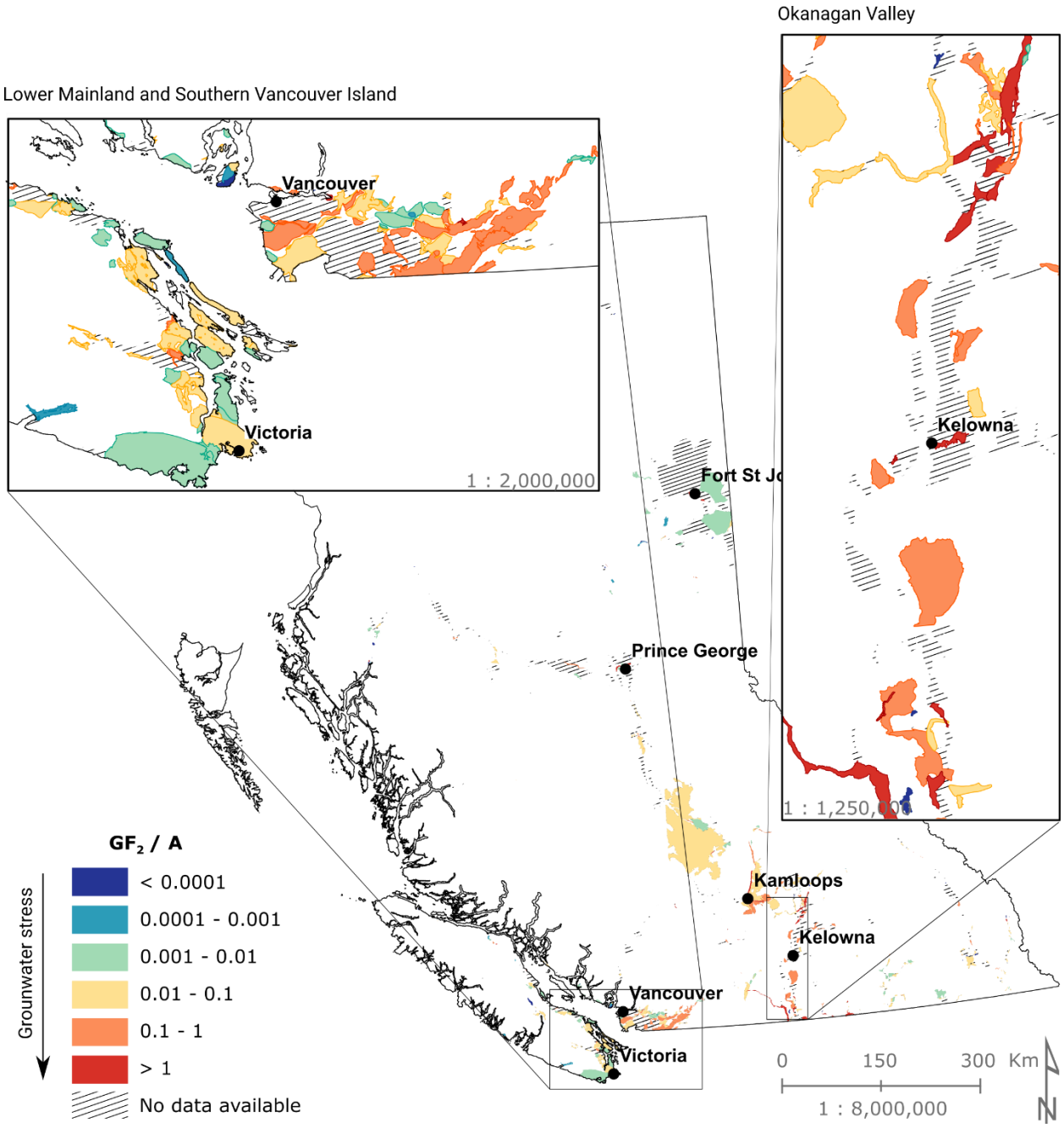

Figure S4.3b Resultant GF_2/A per aquifer in BC. GF/A was calculated using availability data from PCR-GLOBWB and E_{PS}.

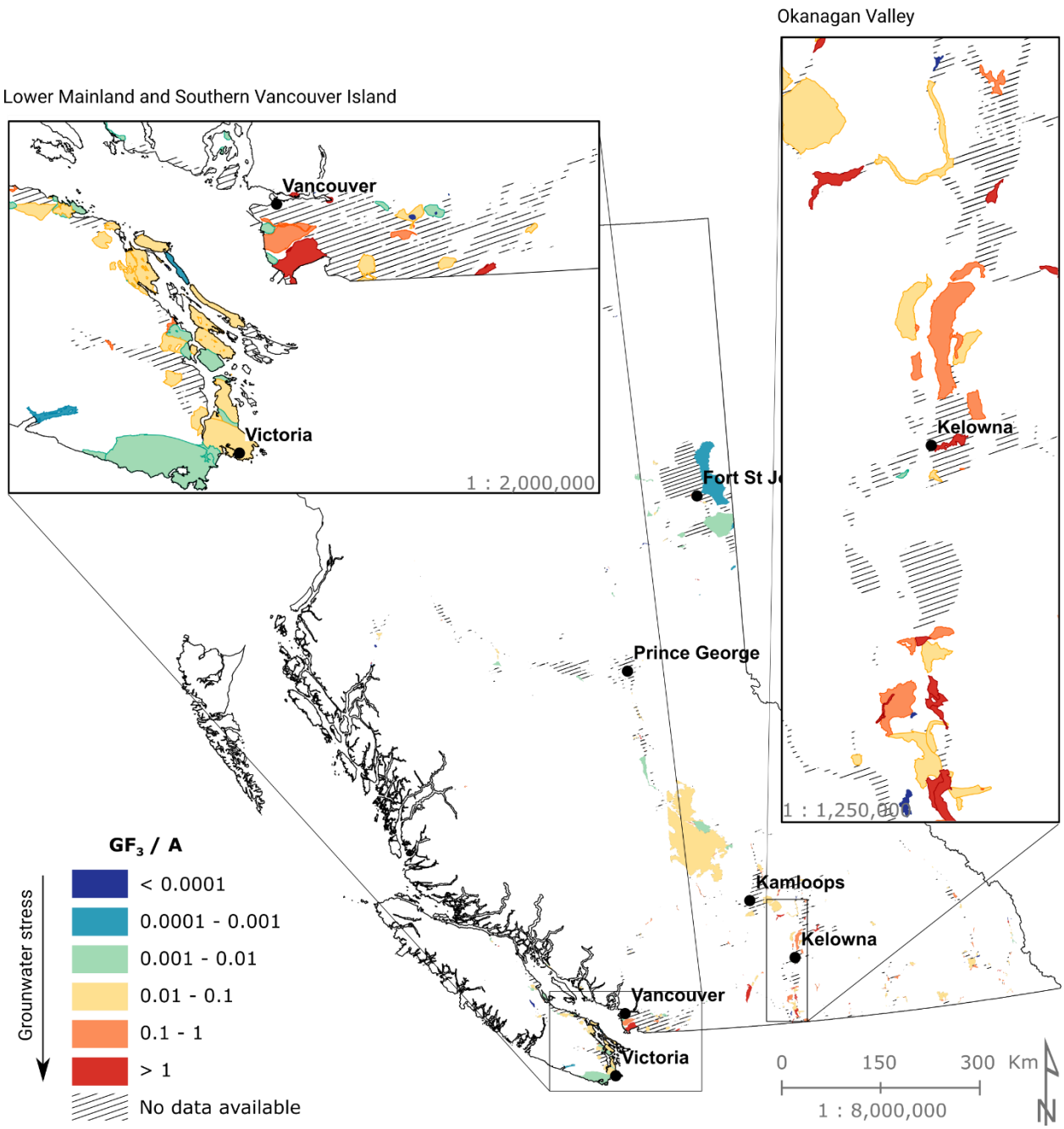

Figure S4.3c Resultant GF_3/A per aquifer in BC. GF/A was calculated using availability data from HELP and E_{LF}.

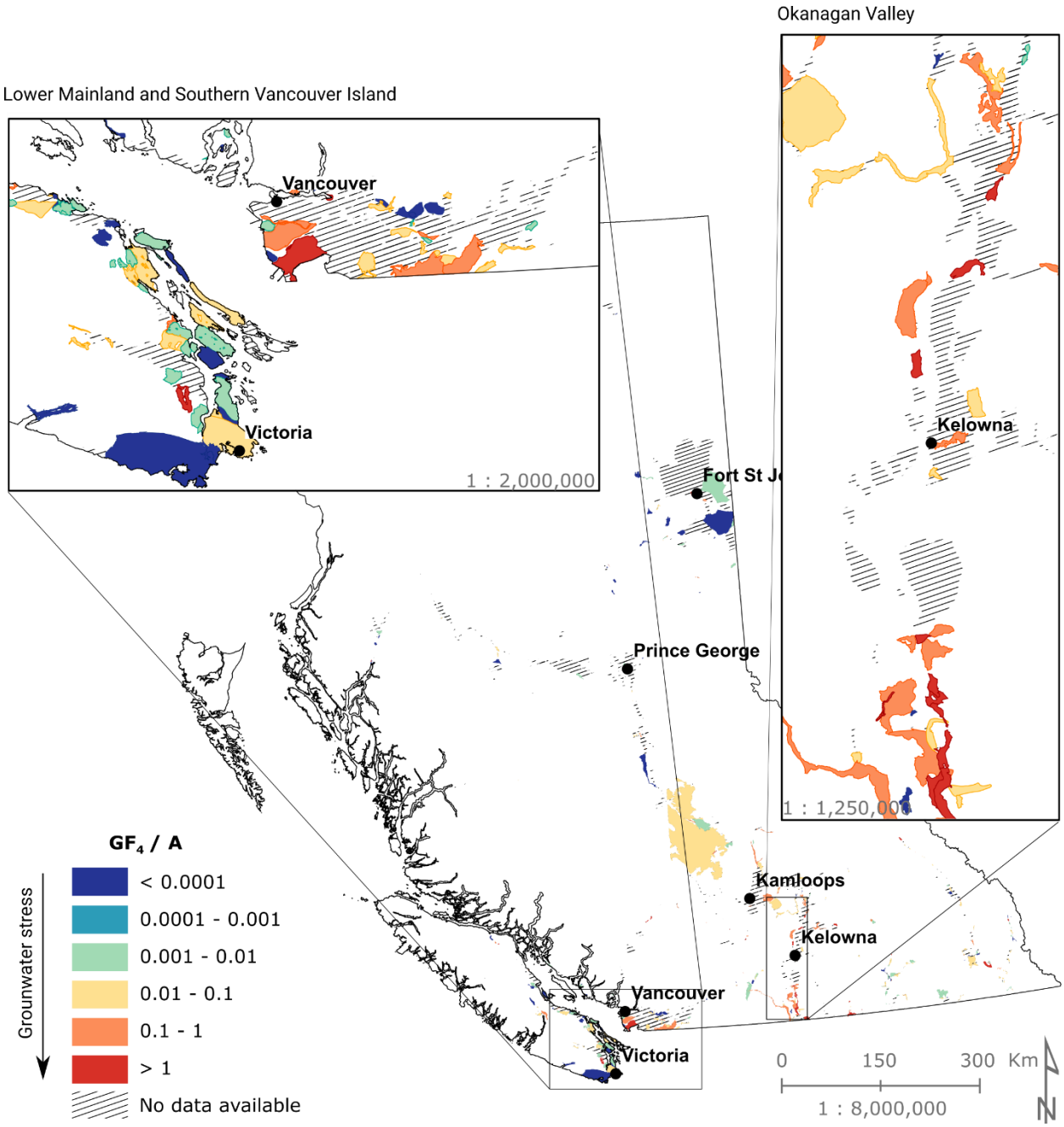

Figure S4.3d Resultant GF_4/A per aquifer in BC. GF/A was calculated using availability data from PCR-GLOBWB and E_{LF}.

S4.1 E_{LF} – R SCRIPTS

The following script calculates the groundwater's contribution to streamflow using stream sensitivities.

```
  setwd('Z:/2.active_projects/MoE_aquifer_stress/3.Working_Folder/Worki
ng/4. gwEFN/Working/1.Approach2_lowflow')

  #PACKAGES: raster & rgdal

  ##FUNCTIONS
    #creates index rasters for determining high, mod, low sensitivity
streamflow
  highsens <- function(x,y) {
    ifelse(x<0.1*y,
           ifelse(x>0,x,NA),
           NA)
    }
  modsens <- function(x,y) {
    ifelse(x>=0.1*y,
           ifelse(x <= 0.2*y,x,NA),
           NA)
    }
  lowsens <- function(x,y) {
    ifelse(x> 0.2*y, x, NA)
    }
    #creates stack of EFN for m3 yr-1 from m3 s-1
  hs.EFN.MMF <- function(x, na.rm=TRUE) {
    x*0.95*31536000
    }
  ms.EFN.MMF <- function(x, na.rm=TRUE) {
    x*0.9*31536000
  }
  ls.EFN.MMF <- function(x, na.rm=TRUE) {
    x*0.85*31536000
    }
    #combines E maps from high, mod, low sensitivity
  combineEFN <- function(h,m,l) {
    ifelse(!is.na(h), h,
           (ifelse(!is.na(m), m,
                   (ifelse(is.na(l), NA, l)))))
    }
    #creates a stack of upstream divided my MMF; percent of discharge
that comes from upstream [ x = upstream; y = monthly flow] defaults to
1 if >1
  pct.netcell <- function(x,y) {
    ifelse(x/y < 1, (1 - x/y), 1)
  }

  ##PROCESS FOR DERIVIN E2
```

```
 MAD.r <- raster("1.Data/MAD_NA.tif")        #load global mean annual
discharge [m3/s] (no GIS manipulation other than to save as .tif) data
from PCR-GLOBWB
 MMF.stack <- stack("1.Data/MMF_NA.tif")     #load global mean monthly
streamflow [m3/s] (same as above)
 months <- c("jan", "feb", "mar", "apr", "may", "jun", "jul" ,"aug",
"sep", "oct", "nov", "dec")
 names(MMF.stack) <- months                   #assigns months to stack
data
   #produces a geoTiff of highest annual flows in the high sensitivity
months
 hs.MMF <- overlay(MMF.stack, MAD.r, fun=highsens)
 ord.hs.MMF        <-        calc(hs.MMF,        fun=function(X,na.rm)
X[order(X,decreasing=T)])  #orders stack so that layer 1 has the max
value for cell from stack 1-12
 hs.EFN.m3yr                  <-                hs.EFN.MMF(ord.hs.MMF)
#applies high sens EFN 95% and converts m3/s to m3/year
 writeRaster(hs.EFN.m3yr[[1]],
filename="2.Analysis/R_output_rasters/hs_gwEFN_m3yr.tif",   format   =
"GTiff", overwrite=TRUE)
   #produces a geoTiff of lowest annual flows in the mod sensitivity
months
 ms.MMF <- overlay(MMF.stack, MAD.r,  fun=modsens)
 ord.ms.MMF <- calc(ms.MMF, fun=function(X,na.rm) X[order(X)])
 ms.EFN.m3yr <- ms.EFN.MMF(ord.ms.MMF)
 writeRaster(ms.EFN.m3yr[[1]],
filename="2.Analysis/R_output_rasters/ms_gwEFN_m3yr.tif",   format   =
"GTiff", overwrite=TRUE)
   # produces a geoTiff of lowest annual flows in the low sensitivity
months
 ls.MMF <- overlay(MMF.stack, MAD.r,  fun=lowsens)
 ord.ls.MMF <- calc(ls.MMF, fun=function(X,na.rm) X[order(X)])
 ls.EFN.m3yr <- ls.EFN.MMF(ord.ls.MMF)
 writeRaster(ls.EFN.m3yr[[1]],
filename="2.Analysis/R_output_rasters/ls_gwEFN_m3yr.tif",   format   =
"GTiff", overwrite=TRUE)
   #produces map of required annual flow per cell for BC; highest high
sens MMF; lowest mod sens MMF; lowest low sens MMF
 bc.E <- overlay(hs.EFN.m3yr[[1]], ms.EFN.m3yr[[1]], ls.EFN.m3yr[[1]],
fun = combineEFN)
 writeRaster(bc.E,
filename="2.Analysis/R_output_rasters/EFN_m3yr.tif", format = "GTiff",
overwrite=TRUE)
   # produces index map of which month is chosen for E2 (ie. highest of
high sens; lowest of mod and low sens)
 hs.index <- which.max(hs.MMF)
 ms.index <- which.min(ms.MMF)
 ls.index <- which.min(ls.MMF)
 gw.E.index <- overlay(hs.index, ms.index, ls.index, fun = combineEFN)
```

```
  writeRaster(gw.E.index,
filename="2.Analysis/R_output_rasters/E2_MMF_index.tif",    format    =
"GTiff", overwrite=TRUE)
    #produces index map of month with lowest MMF
  min.MMF.index <- which.min(MMF.stack)
  writeRaster(min.MMF.index,
filename="2.Analysis/R_output_rasters/min_MMF_index.tif",    format    =
"GTiff", overwrite=TRUE)

    #import monthly upstream values (m3/s)
  upstream.jan                                                        <-
raster("1.Data/UpstreamData/upstream_monthly/upstream_monthly/upstream
_jan_discharge.map")
  upstream.feb                                                        <-
raster("1.Data/UpstreamData/upstream_monthly/upstream_monthly/upstream
_feb_discharge.map")
  upstream.mar                                                        <-
raster("1.Data/UpstreamData/upstream_monthly/upstream_monthly/upstream
_maa_discharge.map")
  upstream.apr                                                        <-
raster("1.Data/UpstreamData/upstream_monthly/upstream_monthly/upstream
_apr_discharge.map")
  upstream.may                                                        <-
raster("1.Data/UpstreamData/upstream_monthly/upstream_monthly/upstream
_mei_discharge.map")
  upstream.jun                                                        <-
raster("1.Data/UpstreamData/upstream_monthly/upstream_monthly/upstream
_jun_discharge.map")
  upstream.jul                                                        <-
raster("1.Data/UpstreamData/upstream_monthly/upstream_monthly/upstream
_jul_discharge.map")
  upstream.aug                                                        <-
raster("1.Data/UpstreamData/upstream_monthly/upstream_monthly/upstream
_aug_discharge.map")
  upstream.sep                                                        <-
raster("1.Data/UpstreamData/upstream_monthly/upstream_monthly/upstream
_sep_discharge.map")
  upstream.oct                                                        <-
raster("1.Data/UpstreamData/upstream_monthly/upstream_monthly/upstream
_okt_discharge.map")
  upstream.nov                                                        <-
raster("1.Data/UpstreamData/upstream_monthly/upstream_monthly/upstream
_nov_discharge.map")
  upstream.dec                                                        <-
raster("1.Data/UpstreamData/upstream_monthly/upstream_monthly/upstream
_dec_discharge.map")
  upstream.stack <- stack(upstream.jan,
                          upstream.feb,
                          upstream.mar,
                          upstream.apr,
                          upstream.may,
```

```
                          upstream.jun,
                          upstream.jul,
                          upstream.aug,
                          upstream.sep,
                          upstream.oct,
                          upstream.nov,
                          upstream.dec)
  names(upstream.stack) <- months
  pctnetcell.stack      <-      overlay(upstream.stack,      MMF.stack,
fun=pct.netcell)     #output a stack of upstream/MMF for each cell per
month
  writeRaster(pctnetcell.stack,
filename="2.Analysis/R_output_rasters/pctnetcellstack.tif",   format   =
"GTiff", overwrite=TRUE)
  plot(pctnetcell.stack[[1]])
#double check values between 0-1
  pct_netcell   <-   stackSelect(pctnetcell.stack,   gw.E.index,   type
='index')
  plot(pct_netcell)
  E2_my3r <- overlay(pct_netcell, bc.E, fun= function(x,y) x*y)
  plot(E2_my3r)
  #the final product --> E2 = groundwater's contribution to environmental
flows
  writeRaster(E2_my3r,
filename="2.Analysis/R_output_rasters/E2_m3yr.tif",  format  =  "GTiff",
overwrite=TRUE)
#EXTRAS
    #produces map of index values of lowest MMF (1 = Jan; 12 = Dec)
  MMF.min.month.na <- which.min(MMF.stack)
writeRaster(MMF.min.month.na,
filename="2.Analysis/R_output_rasters/MMF_min_MMF_index.tif",  format  =
"GTiff", overwrite=TRUE)
```